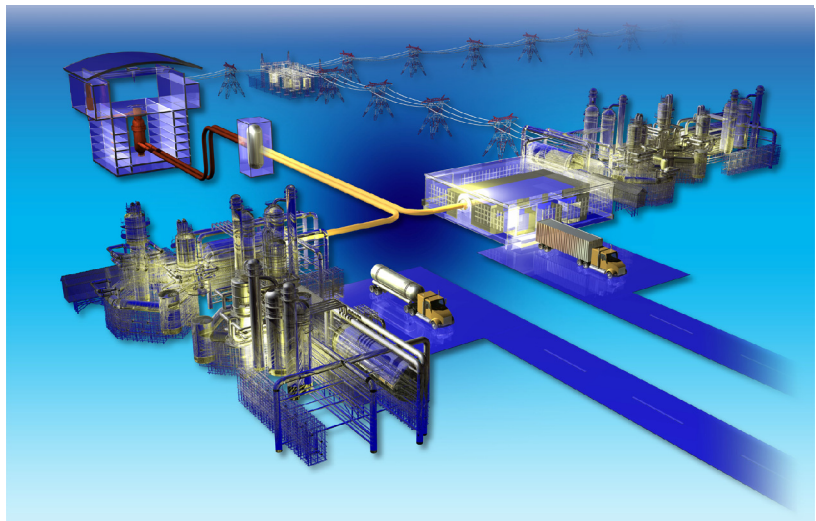


NGNP Conceptual Design Study: Composites R&D Technical Issues

Prepared by Westinghouse Electric Company, LLC for
the Next Generation Nuclear Plant Project

George O. Hayner

October 2008



The INL is a U.S. Department of Energy National Laboratory
operated by Battelle Energy Alliance.


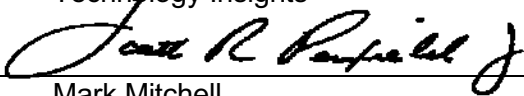


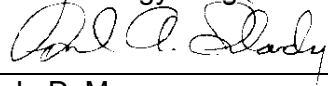

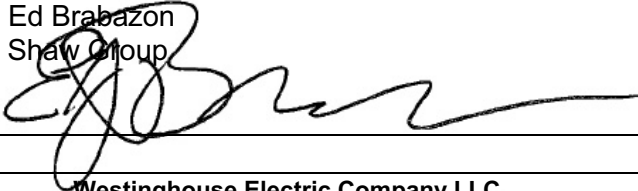


DISCLAIMER

This information was prepared as an account of work sponsored by Westinghouse Electric Company, LLC for an agency of the U.S. Government. Neither the U.S. Government nor any agency thereof, nor any of their employees, makes any warranty, expressed or implied, or assumes any legal liability or responsibility for the accuracy, completeness, or usefulness, of any information, apparatus, product, or process disclosed, or represents that its use would not infringe privately owned rights. References herein to any specific commercial product, process, or service by trade name, trade mark, manufacturer, or otherwise, does not necessarily constitute or imply its endorsement, recommendation, or favoring by the U.S. Government or any agency thereof. The views and opinions of authors expressed herein do not necessarily state or reflect those of the U.S. Government or any agency thereof.

NGNP Conceptual Design Study: Composites R&D Technical Issues

APPROVALS

Function	Printed Name and Signature	Date
Author	Name: George O. Hayner Company: Technology Insights 	10/29/08
Reviewer	Name: Scott R. Penfield, Jr., PE Company: Technology Insights 	31 OCT 2008
Reviewer	Name: Mark Mitchell Company: Pebble Bed Modular Reactor (Proprietary) Ltd. 	31 OCT 2008
Reviewer	Name: Michael Correia Company: Pebble Bed Modular Reactor (Proprietary) Ltd. 	31 OCT 2008
Reviewer	Name: Fred A. Silady Company: Technology Insights 	31 OCT 2008
Approval	Name: L. D. Mears Company: Technology Insights 	31 OCT 2008
Approval	Name: Ed Brabazon Company: Shaw Group 	31 OCT 2008

Westinghouse Electric Company LLC
Nuclear Power Plants
Post Office Box 355
Pittsburgh, PA 15230-0355

LIST OF CONTRIBUTORS

Name and Company	Date
George Hayner, Scott Penfield, Phil Rittenhouse, Fred Silady, and Dan Mears - Technology Insights Mark Mitchell, Steven Pieterse, Ruttie Nel, Shahed Fazluddin and Pieter Venter - Pebble Bed Modular Reactor (Proprietary) Ltd. Sten Caspersson, Alan Spring and Chris Hoffman – Westinghouse Electric Company Jan van Ravenswaay and Johan Markgraaff- M-Tech Industrial (Pty) Ltd.	31 October 2008

BACKGROUND INTELLECTUAL PROPERTY CONTENT

Section	Title	Description
None		

REVISION HISTORY
RECORD OF CHANGES

Revision No.	Revision Made by	Description	Date

DOCUMENT TRACEABILITY

Created to Support the Following Document(s)	Document Number	Revision

LIST OF TABLES

Table 1	Comparison of PBMR DPP and NGNP Key Operational Parameters ^a [1, 2].	19
Table 2	Properties of CFRC – Grade 2002 YR [8]	36
Table 3	Properties of CFRC - Grade 1502 YR [8]	41
Table 4	Helium Temperatures in the NGNP Piping Sections	48
Table 5	Hot Gas Duct System Materials for the PBMR DPP	49
Table 6	Selected Data Associated with the Reactivity Control System [14]	56
Table 7	Tentative PCDR RCS Metallic Materials for the PBMR NGNP	59
Table 8	Tentative IHX A and B Design Parameters	68
Table 9	Comparison of Three SiC Fibers Based on CY 2005 Information [3]	76
Table 10	Common Fiber Coatings for Interphase Layers in SiC/SiC Composites [3].	77
Table 11	Details of Manufacture, Elemental Composition and Approximate Cost of Three Generations of SiC Based Fibers [4]	78
Table 12	Typical Unirradiated Properties of Graphite and CFRC Materials at Room Temperature [8]	80
Table 13	Unirradiated Properties of High Performance SiC Fibers [10]	81
Table 14	Unirradiated Properties of Monolithic SiC and Selected SiC Composites [11], [12], [13], [14], [15]	81
Table 15	Influences of Neutron Irradiation on Dimensions and Swelling of FMI-222 Graphite Composite [28]	88
Table 16	Influence of Neutron Irradiation on Young’s Modulus and Flexural Strength of FMI-222 CFRC [28]	92
Table 17	Summary of Room Temperature Strength Data of Hi-Nicalon TM Type S Fiber, CVI SiC/SiC Composites [13]	94
Table 18	Crack Growth Resistance, R, of Selected Carbon Materials [33]	96
Table 19	Effects of Neutron Irradiation on the Fracture toughness of Graphite and CRFC Materials [35]	96
Table 20	CVD SiC Irradiation Creep Data from Bend Stress Relaxation Experiments [15]	97
Table 21	Selected Physical Properties of SGL NBC-07 Carbon Insulation Material [39]	100
Table 22	Selected Mechanical Properties of NBC-07 Baked Carbon Insulation Material [39]	102
Table 23	Selected Room Temperature Mechanical Properties of NBC-07 Baked Carbon Insulation Material Following Oxidation [39]	102
Table 24	Key Properties of ZYAROCK Rigid Ceramic Insulation [40]	103
Table 25	Key Properties of the OSC-2 Fused Quartz Insulation [41]	103
Table 26	Mean Thermal Conductivity (TC) Data Comparing Microtherm and Saffil Insulation Types	106
Table 27	Current ASTM Standards for the Mechanical evaluation of Fiber-reinforced Ceramic Matrix Composites]	119

LIST OF FIGURES

Figure 1	Layout of the Reactor Unit System in Relation to the PHTS, SHTS, SG and PCHX [3]	20
Figure 2	Vertical Schematic Section through the Reactor Unit [3].....	21
Figure 3	Horizontal Section through the RU without the Core Inlet and Outlet Pipes [3]	22
Figure 4	Helium Flow Path Configurations through the RU [3].....	22
Figure 5	Horizontal Section through the Side Reflector [4].....	24
Figure 6	Section Through the Central Reflector [3].....	24
Figure 7	Core Lateral Restraint Strap Positions [5]	25
Figure 8	Reactivity Control System Layout [3]	27
Figure 9	RSS Channel Interfaces	28
Figure 10	RSS Channel Interface Tubes Cross Section [5].....	29
Figure 11	Graphite Felt Insulation Used Adjacent to CFRC SAS Tube	29
Figure 12	HTS Coupling Concept [6]	30
Figure 13	HTS Operating Parameters [7].....	30
Figure 14	CFRC Design Methodology.....	32
Figure 15	Lateral Restraint Strap [5].....	35
Figure 16	Top Reflector Cross Section [11].....	39
Figure 17	Tie Rod Assembly Cutaway Looking From the Top [12]	40
Figure 18	Tie Rod Geometry [4]	40
Figure 19	Typical Core Outlet Connection Layout [13]	44
Figure 20	Detail of the Bottom Reflector Ring showing the location of the COC [4].....	44
Figure 21	Detail of the COC [5].....	45
Figure 22	DPP HGD Design Showing NGNP Temperatures	45
Figure 23	Schematic Layout of the Core Connection [13].....	47
Figure 24	Possible Passive Insulation Design for HGD.....	52
Figure 25	Positioning of the Reactivity Control System [8]	57
Figure 26	Reactivity Control System Control Rod Drive Mechanism [15].....	58
Figure 27	DPP Metallic Control Rod Articulated Connection [17]	61
Figure 28	Probable Location of Insulation in the NGNP Core [20].....	64
Figure 29	Bottom Reflector Horizontal Section Showing Typical Insulation Layers [4]	65
Figure 30	Option C Concepts of NGNP IHX A and B [6].....	67
Figure 31	Helium flow paths in IHX A Assuming Shell Side Coupling	67
Figure 32	Shell Side Coupling Option of IHX A and B [6].....	68
Figure 33	Heat Exchanger Flow Paths	68
Figure 34	Fibrillar Texture of a Carbonized PAN Fiber [2].....	74
Figure 35	Irradiation-Induced Dimensional Change of Selected Carbon Fiber Composites [24, 27]	84
Figure 36	Neutron Irradiation-Induced Dimensional Changes in GraphNOL N3M Graphite [25]	85

Figure 37	Microstructural Interpretation of Irradiation Induced Dimensional Changes in 1D CFRC composites [26].	85
Figure 38	Microstructural Interpretation of Irradiation Induced Dimensional Changes in 2D CFRC composites [26].	86
Figure 39	Dimensional Changes in 3D PAN CFRC [26].	86
Figure 40	Effect of Fiber Type and Graphitization Temperature on Irradiation Induced Dimensional Changes in 3D CFRCs [26].	88
Figure 41	Irradiation-induced Swelling of SiC as a Function of Irradiation Temperature and Fluence [15].	89
Figure 42	Irradiation-induced Swelling of Hi Nicalon Fiber SiC/SiC Composite Material as a Function of Irradiation Temperature and Fluence [55].	90
Figure 43	Irradiation-induced Swelling of Hi Nicalon Type S fiber SiC/SiC Composite Material as a Function of Irradiation Temperature and Fluence [55].	90
Figure 44	Neutron Irradiation-induced Strength Changes for GraphNOL N3M at Irradiation Temperatures 600 and 875°C [25].	91
Figure 45	Strength Change versus Fluence in CFRC Materials as a Function of Fiber Type, Architecture and Graphitization Temperature. [31].	92
Figure 46	The Irradiated-to-Non-irradiated Ultimate Strength Ratio ($S_U^{Irrad}/S_U^{Unirrad}$) Measured up to 8 dpa, Demonstrating the Irradiation Stability of Different SiC _f /SiC Composite Types Compared to Monolithic SiC [32].	93
Figure 47	Irradiation-induced Strength Changes of Hi Nicalon fiber SiC/SiC Composite Material as a Function of Irradiation Temperature and Fluence [55].	94
Figure 48	Irradiation-induced Strength Changes of Hi Nicalon Type S Fiber SiC/SiC Composite Material as a Function of Irradiation Temperature and Fluence [55].	95
Figure 49	Thermal Conductivity Changes in CFRC Material as a Function of Temperature for Irradiated and Unirradiated Material [37].	98
Figure 50	Ratio of Irradiated to Unirradiated Thermal Conductivity Values (K_{irr}/K_o) Measured at the Irradiation Temperature for High Purity CVD SiC and for Two Types of 2D SiC/SiC Composites [38].	99
Figure 51	Mean Coefficient of Thermal Expansion (CTE) Plot for NBC-07 Baked Carbon Insulation [39].	101
Figure 52	Thermal Conductivity of NBC-07 Baked Carbon Insulation [39].	101
Figure 53	Mean Thermal Conductivity Data for Microtherm Aerogel Silica Insulation Estimated for a 90 bar Helium Environment [43].	105
Figure 54	Summary of French He Test Data at 950°C and 813 Hours [48].	108
Figure 55	Ductile Fracture Behavior of Alloy 800 at 427°C [52].	110
Figure 56	Steps in the ASTM and ISO standards balloting processes	120

ACRONYMS

Abbreviation or Acronym	Definition
1/2/3D	1/2/3-Directional
AOO	Anticipated Operational Occurrence
ASME	American Society of Mechanical Engineers
ASTM	ASTM International
BR	Bottom Reflector
BPVC	Boiler and Pressure Vessel Code
CB	Core Barrel
CBA	Core Barrel Assembly
CBCS	Core Barrel Conditioning System
CEN	Comité Européen de Normalisation
CFRC	Carbon Fiber Reinforced Carbon
COC	Core Outlet Connection
CRDM	Control Rod Drive Mechanism
CSC	Core Structures Ceramics
CMC	Ceramic Matrix Composite
CR	Center Reflector
CTE	Coefficient of Thermal Expansion
CVD/CVI	Chemical Vapor Deposition/ Chemical Vapor Infiltration
DBA	Design Basis Accident
DBE	Design Basis Event
DDN	Design Data Need
DEGB	Double Ended Guillotine Break
DIN	Deutsches Institute fur Normung- German for German Institute for Standardization
DLOFC	Depressurized Loss of Forced Circulation
DOE	Department of Energy
dpa	Displacements per Atom
DPP	Demonstration Power Plant
EDN	Equivalent DIDO Nickel Fluence
EOL	End-of-Life
EPRI	Electric Power Research Institute
FEM	Finite Element Modeling
HGD	Hot Gas Duct
HPB	Helium Pressure Boundary

HPS	Hydrogen Production System
HTGR	High Temperature Gas-cooled Reactor
HTR	High Temperature Reactor
HSR/EPP	NASA High Speed Research/Enabling Propulsion Program
HTS	Heat Transport System
HTTR	High Temperature Test Reactor
IHX	Intermediate Heat Exchanger
ISO	International Organization for Standardization
ISR	Inner Side Reflector
KTA	Kerntechnischer Ausschuß (German Nuclear Safety Standards Commission)
LOC	Load Category
NASA	National Aeronautics and Space Administration
NGNP	Next Generation Nuclear Plant
NHSS	Nuclear Heat Supply System
NRC	Nuclear Regulatory Commission
NUREG	Nuclear Regulatory Commission Report
OCR	Outer Center Reflector
OSR	Outer Side Reflector
PAN	Polyacrylonitrile
Par	Parallel
PBMR	Pebble Bed Modular Reactor
PCDR	Preconceptual Design Report
PCHX	Process Coupling Heat Exchanger
PCS	Polycarbosilane (Precursor for SiC Fiber Production)
PCS	Power Conversion System
PEC	Petroleum Energy Center (Japan)
Per	Perpendicular
PHTS	Primary Heat Transport System
PLOFC	Pressurized Loss of Forced Circulation
PyC	Pryrolytic Carbon
QA	Quality Assurance
RCS	Reactivity Control System
RPS	Reactor Protection System
RPV	Reactor Pressure Vessel

RSS	Reserve Shutdown System
RT	Room Temperature
RU	Reactor Unit
SAS	Small Absorber Spheres
SG	Steam Generator
SHTS	Secondary Heat Transport System
SR	Side Reflector
SSC	Structures, Systems and Components
TR	Top Reflector
UK	United Kingdom
VHTR	Very High Temperature reactor

TABLE OF CONTENTS

<u>Section</u>	<u>Title</u>	
<u>Page</u>		
LIST OF TABLES.....		4
LIST OF FIGURES.....		5
ACRONYMS		7
TABLE OF CONTENTS.....		10
Summary and Conclusions.....		12
Introduction.....		18
Objectives and Scope		32
Organization of Report.....		33
1 IDENTIFICATION OF COMPONENTS.....		34
1.1 LATERAL RESTRAINT STRAP COMPONENTS		34
1.1.1 Identification of Components.....		34
1.1.2 Design Considerations.....		34
1.1.3 Surveillance, Inspection and Monitoring		35
1.1.4 Tolerance to irradiation Exposure		36
1.1.5 Range of Operating Temperature		36
1.1.6 Qualification of Components		37
1.2 UPPER REFLECTOR SUPPORT COMPONENTS		38
1.2.1 Identification of Components.....		38
1.2.2 Design Considerations.....		41
1.2.3 Surveillance, Inspection and Monitoring		41
1.2.4 Tolerance to irradiation Exposure		42
1.2.5 Range of Operating Temperature		42
1.2.6 Qualification of Components		42
1.3 HOT GAS DUCT COMPONENTS		42
1.3.1 Identification of Components.....		43
1.3.2 Design Considerations.....		46
1.3.2.1 Core Outlet Connection		46
1.3.2.2 Hot Gas Duct		48
1.3.3 Surveillance, Inspection and Monitoring		53
1.3.4 Tolerance to irradiation Exposure		53
1.3.5 Range of Operating Temperature		54
1.3.6 Qualification of Components		54
1.4 REACTIVITY CONTROL COMPONENTS		54
1.4.1 Identification of Components.....		55
1.4.2 Design Considerations.....		58

1.4.3	Tolerance to irradiation Exposure	61
1.4.4	Range of Operating Temperature	62
1.4.5	Qualification of Components	62
1.5	CORE SUPPORT/CORE BARREL INTERFACE INSULATION	62
1.5.1	Identification of Components	62
1.5.2	Design Considerations.....	63
1.5.3	Surveillance, Inspection and Monitoring	63
1.5.4	Tolerance to irradiation Exposure	63
1.5.5	Range of Operating Temperature	63
1.5.6	Qualification of Components	65
1.6	HIGH TEMPERATURE SECTION INSULATION.....	65
1.6.1	Identification of Components	66
1.6.2	Design Considerations.....	66
1.6.3	Range of Operating Temperature	66
1.6.4	Qualification of Components	66
1.7	LIST OF ASSUMPTIONS	69
1.8	REFERENCES.....	70
2	MATERIALS EVALUATIONS.....	71
2.1	CERAMIC MATRIX COMPOSITES (CMCs) INCLUDING CFRC AND SiC/SiC	71
2.1.1	Manufacturing	72
2.1.1.1	CFRC	72
2.1.1.2	SiC/SiC Composites	75
2.1.2	Properties.....	79
2.1.2.1	Irradiation Effects	82
2.2	STRUCTURAL CERAMICS.....	99
2.3	INSULATION PRODUCTS	99
2.4	EVALUATION OF METALLIC ALLOYS FOR THE RCS AND HGD LINER APPLICATIONS	106
2.5	SUMMARY	110
2.6	REFERENCES.....	112
3	DESIGN AND TECHNOLOGY DEVELOPMENT	115
3.1	DESIGN NEEDS.....	116
3.2	CODIFICATION APPROACH	117
3.3	DESIGN DATA NEEDS	123
	Bibliography	132
	Definitions.....	133
	Requirements.....	134
	List of Assumptions.....	135
	Appendix 1: 90% REVIEW VIEWGRAPHS	136

SUMMARY AND CONCLUSIONS

The objective of this study is to identify and evaluate the potential applications and design requirements for ceramics and ceramic composites in the NGNP Reactor and Primary Heat Transport System. In this context, ceramics and composites refer to non-graphite materials that serve structural functions, insulation functions or both. The study considers components for which ceramics/composites have already been selected for the PBMR Demonstration Power Plant (DPP), as well as other components for which the replacement of metallic materials with non-metallic materials might offer the potential for improved performance or longer design life. The composites evaluated have better high temperature properties above 1000°C than the metallic alloys evaluated, may have superior performance at high levels of neutron fluence and can be designed to provide optimal performance for specific applications. These factors are considered important for the components evaluated for the reasons discussed in the report.

The purpose of this study includes the following issues:

- Identify existing and potential applications for ceramics and ceramic composites in the High-Temperature Gas-Cooled Reactor (HTGR) primary system.
- Evaluate design requirements for the identified components, including both normal and off-normal operating conditions (i.e., stress, temperature, fluence, environmental conditions, etc.)
- Identify activities necessary to codify these materials (e.g., in American Society of Mechanical Engineers (ASME) and ASTM International (ASTM) codes
- Identify any additional work anticipated to be required to support NRC licensing of the Nuclear Heat Supply System (NHSS).
- The objective of initiating operation of Next Generation Nuclear Plant (NGNP) in 2018 shall be a factor in conducting this study

The following conclusions are apparent from the study:

Lateral Restraint Straps

1. The assembly that will be used in the DPP appears to be applicable for use in the NGNP. The design of this component is complete for the PBMR DPP.
2. This design uses Sigrabond Grade 2002 YR one dimensional (1D) carbon fiber reinforced composite (CFRC) material for the racetrack strap. However, the following additional items need to be addressed for the NGNP application:
 - a. The current design developed for the DPP needs to be reviewed for the NGNP and a determination made regarding possible changes to the design that may be required.
 - b. Modeling of the NGNP outer side reflector region needs to be performed to verify the estimate of fluence for the straps.
 - c. If the maximum calculated End of Life (EOL) fluence level is ≥ 0.2 dpa (carbon) or 3×10^{20} n/cm² (E>0.1 MeV), an irradiation program would be required for 1D CFRC material to be used in the straps (see DDN COMP 01-01). This is considered unlikely.
 - d. Modeling of the outer reflector region needs to be performed to determine the temperature environment for both normal and off-normal operating conditions.
 - e. The DPP procedures and qualification information for the core restraint strap material need to be reviewed; modified as required and validated for the NGNP design

Tie Rod Assembly

1. The Tie Rods that will be used in the DPP appear to be applicable for use in the NGNP. The design of this component is complete for the DPP.
2. This design uses Sigrabond Grade 1502 YR CFRC material (2D) for the tie rods. However, the following additional items need to be addressed for the NGNP application:
 - a. The current design developed for the DPP needs to be reviewed for the NGNP and a determination made regarding possible changes to the design that may be required.
 - b. Modeling of the NGNP upper reflector region needs to be performed to validate the estimate of fluence for the straps.
 - c. If the maximum calculated EOL fluence level is ≥ 0.5 dpa (carbon) or 5×10^{20} n/cm² ($E > 0.1$ MeV), an irradiation program would be required for the 2D CFRC material to be used in the tie rods (see DDN COMP 01-01). This is considered unlikely.
 - d. Modeling of the upper reflector region needs to be performed to validate the temperature environment for both normal and off-normal operating conditions.
 - e. The DPP procedures and qualification information for the tie rod material needs to be reviewed; modified as required and validated for the NGNP design

Core Outlet Connection (COC)

1. The Core Outlet Connection (COC) is being designed for the DPP and appears to be applicable to the NGNP Design.
2. The design being developed uses insulation systems and materials that may need to be modified for the NGNP as noted below:
 - a. Modeling of the NGNP needs to be performed to determine the temperatures seen by the metallic components of the COC.
 - b. A review, potential modification and validation of the COC design are required for the NGNP.
 - c. The materials design basis for the CFRC liner and the metallic components of the COC needs to be validated for the NGNP design. For the CFRC material selected, test data on specimens representative of the applications and the materials to be used is required (see DDN COMP 01-03).
 - d. Procedures for surveillance, inspection and monitoring of the COC need to be reviewed and modified as required for the NGNP.
 - e. Qualification procedures need to be developed for the NGNP COC.

Hot Gas Duct (HGD)

1. It is almost certain that the NGNP Hot Gas Duct (HGD) will require a liner with higher temperature capability than the Alloy 800H liner used in the DPP design.
2. It is recommended that the liner be fabricated using a Polyacrylonitrile (PAN) fiber-based CFRC material to ensure optimum performance for the life of the plant. For the CFRC material selected, test data on specimens representative of the applications and the materials to be used is required (see DDN COMP 01-03).

3. It is recommended that a high performance aerogel insulation system based on silica or alumina be considered for the HGD application (see DDN COMP 01-04).
4. Based on preliminary heat flow calculations performed by Microtherm, a 450mm radial thickness of aerogel insulation with a liner would result in a surface temperature of <100C on the outside of the HPB with no annulus cooling.
5. Other Hot Gas Duct design changes relative to the DPP design will likely be required for the NGNP due to the higher annulus cooling gas temperature, as noted below:
 - a. Modeling of the NGNP needs to be performed to determine the temperatures seen by the inner pressure pipe of the HGD
 - b. The materials basis for the piping design needs to be reviewed and potentially modified for the NGNP
 - c. An evaluation of the current Preliminary Conceptual Design Report (PCDR) piping design for the NGNP needs to be made to consider a specific off-normal event that has not been thoroughly evaluated. This off-normal event involves the loss of the secondary heat sink across Intermediate Heat Exchanger (IHX) A and B due to loss of function in the secondary system. One of the issues to be considered that could directly affect the current piping design is that helium cooling in the annulus from the circulator could increase in temperature up to some equilibrium level that could impact the integrity of the SA-533 pressure boundary piping.
 - d. Procedures for surveillance, inspection and monitoring of the HGD for the DPP need to be reviewed and modified as required for the NGNP
 - e. Qualification procedures need to be developed for the HGD.

Reactivity Control System (RCS)

1. The use of a composite would be more optimal for the Reactivity Control System (RCS) cladding, joint and secondary shock absorber; however, a redesign of the control rod segments would be required. This could represent a potential product improvement option for the DPP and could be required for the NGNP due to increased power and higher Depressurized Loss of Forced Circulation (DLOFC) temperatures.
2. If a CFRC or a SiC/SiC composite material was selected for this application, adequate pre-characterization test data and post-irradiation test data on specimens representative of the applications and the materials to be used is required. Irradiation test data for the specimens at a fluence $\geq 7 \times 10^{21} \text{ n/cm}^2$ ($E > 0.1 \text{ MeV}$) in increments of 3.5×10^{21} at irradiation temperatures of 750°C and 1000°C is required. It is anticipated that this effort would be expensive and require an extended schedule.
3. It is recommended that a SiC/SiC composite using a high performance Generation 3 [using Hi Nicalon Type S fibers and impregnated by chemical vapor deposition (CVD) or equivalent] design be used for this application (see DDN COMP 01-02). This recommendation is based primarily on the superior irradiation performance of this material compared to CFRC.

4. Other issues that need to be addressed are given below:
 - a. A review of the adequacy of the Alloy 800H material for the control rods is required for the NGNP application and a recommendation made for alternate materials to be used in the NGNP design, as noted above.
 - b. Modeling is required for the Inner Side Reflector (ISR) to determine the fluences seen by the control rods and chains for the NGNP application.
 - c. A modeling study to verify the temperature of the RCS control rods and chains needs to be performed for the NGNP design.
 - d. Qualification testing for RCS components has not been investigated for the NGNP design. Therefore, a study to determine qualification testing and procedures for these components is needed for the NGNP design after a material and design is selected for the high temperature, high fluence portion of the application.

Core Support/Core Barrel Interface Insulation

1. Enhanced insulation will likely be required in the lower layers of the Bottom Reflector (BR) assembly due to increased NGNP outlet temperature.
2. It is recommended that a fused quartz insulation product be used for this application, if required. The data requirements for the quartz insulation selected are the same as that obtained for the baked carbon given in Reference 39, Section 2 (see DDN COMP 01-04) except that limited irradiation testing should also be performed. Other issues that need to be addressed are given below:
 - a. A temperature analysis study that models the upper and lower reflector regions of the NGNP design is required to determine the insulation requirements that will be needed to protect metallic support components. Insulation for the upper reflector area is not planned for the DPP.
 - b. A modeling study of the NGNP is required to determine the radiation exposure expected for Layers 1, 2 and 3 of the Lower Reflector region of the CSC.
 - c. Qualification procedures for the fused or sintered quartz material will need to be developed, if required for the NGNP application.

High Temperature Section Insulation

1. It is recommended that a high performance aerogel insulation system, based on silica or alumina, be considered for the IHX applications (see DDN COMP 01-04). Other issues that need to be addressed are given below:
 - a. A design study of the IHX systems is needed to evaluate the insulation required and to provide a more detailed conceptual design of the IHX systems for the NGNP.
 - b. A modeling study is required to evaluate the temperature distributions in IHX A and B.
 - c. A qualification plan is required for the insulation to be used in IHX A and B.

Materials Evaluations

1. Materials evaluations have determined either specific materials or a general materials category (primarily CFRC) that are useable for the component applications noted.
2. Composites are several years from nuclear codification and can only be used in applications where design by test or analysis is appropriate for the application.
3. The composites evaluated have better high temperature properties above 1000°C than the metallic alloys evaluated. This could be important during off-normal events. While the properties of the highest temperature metallic alloys appear to be adequate for the RCS and liner applications at normal operating temperatures, these materials are not considered to be optimum.
4. The composites can be engineered for specific applications (such as the tie rods and the core lateral restraint straps).
5. The corrosive effects of helium impurities on the composites evaluated are unknown, because this issue has essentially not been investigated. The metallic alloys evaluated are either known to be subject to this type of attack to various degrees or it is suspected that they could be subject to this form of attack. This issue is important because all of the components evaluated must remain stable and able to perform their function over long time periods at elevated temperatures and it is known that this type of attack can potentially degrade the properties of the metallic alloys to various extents.
6. Pitch-based CFRC materials are better suited than PAN-based materials for use in components that are subjected to high neutron fluence; however, for components that have low or no neutron exposure, PAN-based CFRC composites have generally superior properties.
7. A primary issue for the application of CFRC components at higher levels of neutron exposure is swelling and eventual degradation of properties. This does not appear to be an issue for high performance SiC/SiC composite materials exposed to the same fluence level. This is important in the design of such a component to ensure that the function of the component could be maintained.
8. CFRC materials are more mature and versatile than high performance SiC/SiC composites. The only significant advantage that SiC/SiC composites have for the applications noted is higher resistance to neutron damage at higher fluence levels.
9. The use of baked carbon and or silica based insulation systems appears to be suitable for the lower reflector applications noted.
10. The use of high performance insulation material (as noted above) for the HGD and the IHX systems will be determined based on the evolution of design changes required for the HGD and the maturation of the IHX design. This study is limited to exploring potentially feasible concepts in these areas and a more extensive review to be performed during conceptual design will further define insulation and the associated design modifications required.
11. Alloy 230 appears to have adequate high temperature mechanical properties and helium corrosion resistance for the liner applications but, as noted above, is not considered optimum for these applications. This material is not suitable for the RCS application because this material appears to have poor post-irradiation properties.
12. Alloy 617 has the best overall strength at elevated temperature but is not suitable for either the liner applications or the RCS application because it has poor post-irradiation properties and contains a significant amount of cobalt.

13. Alloys X or XR are potentially viable for the liner applications because of their high resistance to helium corrosion and could represent a lower cost option, if needed. Post-irradiation properties may be unacceptable for the RCS application.
14. Alloy 800H may be a viable metallic alloy candidate for the RCS and liner applications; however, its mechanical properties near 1000°C and its resistance to corrosion from helium impurities at high temperature are issues that would require further evaluation if this material is selected.
15. If a high temperature metallic alloy was used for the liner or RCS applications, the existing DPP design would not require modification to accommodate these materials.

Composites Codification Approach

The following approach to codification of composites is recommended:

1. As an initial step, the approach should be based on the development of an ASME Code Case rather than development of a stand-alone section of the Code.
2. The approach used and the outline used for of the Code Case for composites should be similar to the approach used by the ASME Section III Subgroup on Nuclear Graphite for development of the nuclear graphite Code Case.
3. The approach taken should be similar to the initial tasks performed to strengthen ASME Section III, Subsection NH.
4. The development of a Code Case for composites is within the assigned charter for the Section III Subgroup.
5. Activities related to composites have been limited to date, due to lack of resources and the higher priority effort leading to the codification of graphite. An increased level of composites-related activity is expected after the graphite Code Case is drafted.
6. Key decisions that have been made within the ASME and ASTM have already initiated the composite codification effort.
7. The key factors required to further develop and simulate this effort are predictable funding and a consensus from stakeholders that this effort is required to further develop HTGRs.

INTRODUCTION

The Nuclear Heat Supply System (NHSS) of the Next Generation Nuclear Plant (NGNP) serves to heat the fluid in the Primary Heat Transport System (PHTS) by means of a nuclear reaction in the Reactor Unit (RU). The PHTS circulates the primary coolant from the Reactor Unit (RU) to the Intermediate Heat Exchanger (IHX), where the heat from the RU is transferred to the Secondary Heat Transport System (SHTS). The SHTS transports heat to the Hydrogen Production System (HPS) and the Power Conversion System (PCS), where the heat is either utilized or, in certain plant operating modes, rejected to the environment.

The NHSS design is based on the Pebble Bed Modular Reactor (PBMR) Demonstration Power Plant (DPP) reactor design, which uses the high-temperature gas-cooled reactor technology which was originally developed in Germany. This implies the use of spherical fuel elements, referred to as pebbles, which are in size and physical characteristics the same as the fuel which was developed for the German High-Temperature Reactor (HTR) programs. Similar to the German pebble bed reactors, the PBMR design uses an online refueling scheme.

The NHSS consists of the RU and all the support systems required for its operation and maintenance. The RU includes the following systems:

- Core Barrel Assembly
- Core Structure Ceramics
- Reactor Pressure Vessel
- Reactivity Control System
- Reserve Shutdown System
- In-Core Delivery System

For application in the NGNP project, the most significant change to the DPP reactor is an increase in the continuous power level from 400MWt to 500MWt. In addition, the reactor inlet/outlet temperatures are changed from 500°C/900°C to 350°C/950°C, while the reactor mass flow is decreased from 192kg/s to 160kg/s. A comparison of key operating parameters between the NGNP and the DPP is given in Table 1.

Another important change to the DPP reactor design for NGNP application is that the Core Barrel Conditioning System (CBCS) is not necessary, due to the lowering of the reactor inlet temperature. In the NGNP, the function of the CBCS is fulfilled by rerouting the flow path of the primary coolant, which is at a lower temperature than in the DPP. The change in the primary coolant flow path necessitates moving the PHTS cold pipe (reactor inlet) from the bottom (as it is on the DPP reactor) to the top of the Reactor Pressure Vessel (RPV).

While the PBMR DPP reactor functions as the heat source in a closed, recuperated Brayton power cycle, the NGNP NHSS uses the reactor to supply heat for hydrogen production and for steam generation in a conventional Rankine cycle. In the NGNP, there are two heat transport loops, the Primary Heat Transport System and the Secondary Heat Transport System. The PHTS consists of all PHTS ducting, the Primary Circulator for helium coolant and the Intermediate Heat Exchanger that transfers heat from the primary (nuclear) to the secondary (non-nuclear) heat transport loop. The SHTS also has a helium circulator, ducting and process heat exchangers that transfer heat to the Hydrogen Production System and the Power Conversion System.

Table 1 Comparison of PBMR DPP and NGNP Key Operational Parameters ^a [1, 2]

Parameter	Normal Operation		DLOFC		PLOFC ^{b,c}	
	NGNP	DPP	NGNP ^d	DPP ^b	NGNP	DPP
RIT (°C)	350	500	-	-	-	-
ROT (°C)	950	900	-	-	-	-
Tmax, CB (°C)	350 ^d	414 ^b	466-634	579 (48h)	565	482
Tmax, RPV (°C)	308 ^d	324 ^b	328-452	419 (56h)	401 (56h)	373 (48h)
He Mass Flow (kg.s ⁻¹)	160	192	-	-	-	-
Thermal Power (MW)	500	400	-	-	-	-

^a 25% increase in power level, hence 25% higher flux level assumed for NGNP compared to DPP

^b Based on Case 5, NGNP Special Study 20.2: Prototype Power Level Study, NGNP-20-RPT-002, 26-01-07 [1]

^c Indirect cycle NGNP design, hence operating pressure in system assumed to remain constant at 9 MPa

^d Reactor Parametric NGNP Special Study, NGNP-NHS 90 PAR, August 2008

Note: CB and RPV temperatures are only indicative and should not be used as absolute values

The RU in relation to the PHTS, SHTS, Steam Generator and Process Coupling Heat Exchanger (PCHX) is shown in Figure 1. A vertical and horizontal cross-section through the RU is shown in Figure 2 and Figure 3, respectively.

As illustrated in Figure 4, the inlet helium flow from the PHTS enters the RU at the top of the RPV. This flow then flows down between the CBA and RPV. This flow is used to maintain the RPV at temperatures within ASME Section III Code data for the RPV material. The flow then enters the riser channels in the Core Structures Ceramics (CSC) through openings in the Bottom Plate of the CBA. It flows up in the riser channels to the top of the core, then down through the fuel spheres and exits the RU through the bottom reflector.

Core Structures Ceramics

The CSC includes four major graphite components: (1) The Bottom Reflector (BR), (2) Side Reflector (SR), (3) Top Reflector (TR), and the (4) Center Reflector (CR). These components are constructed from individual graphite blocks that are arranged and interconnected so that they perform their required functions. The general arrangement and design principles that form the basis for the design

of the CSC are based on the German HTR designs. Insulation systems that will be used in the PBMR NGNP as part of the CSC will be discussed later in this report.

The NGNP Bottom and Center Reflectors are supported on a CFRC thermal expansion compensator that is doweled to the Bottom Support Plate of the CBA. This construction forms the base of the Core Structure by supporting the Side Reflector and core-level portions of the Center Reflector as well as the fuel core. The stability and the exact location of the Bottom Reflector are essential for this requirement.

The defuel chutes are located in the mid-radius of the fuel annulus and equally-spaced circumferentially at a pitch of 120°.

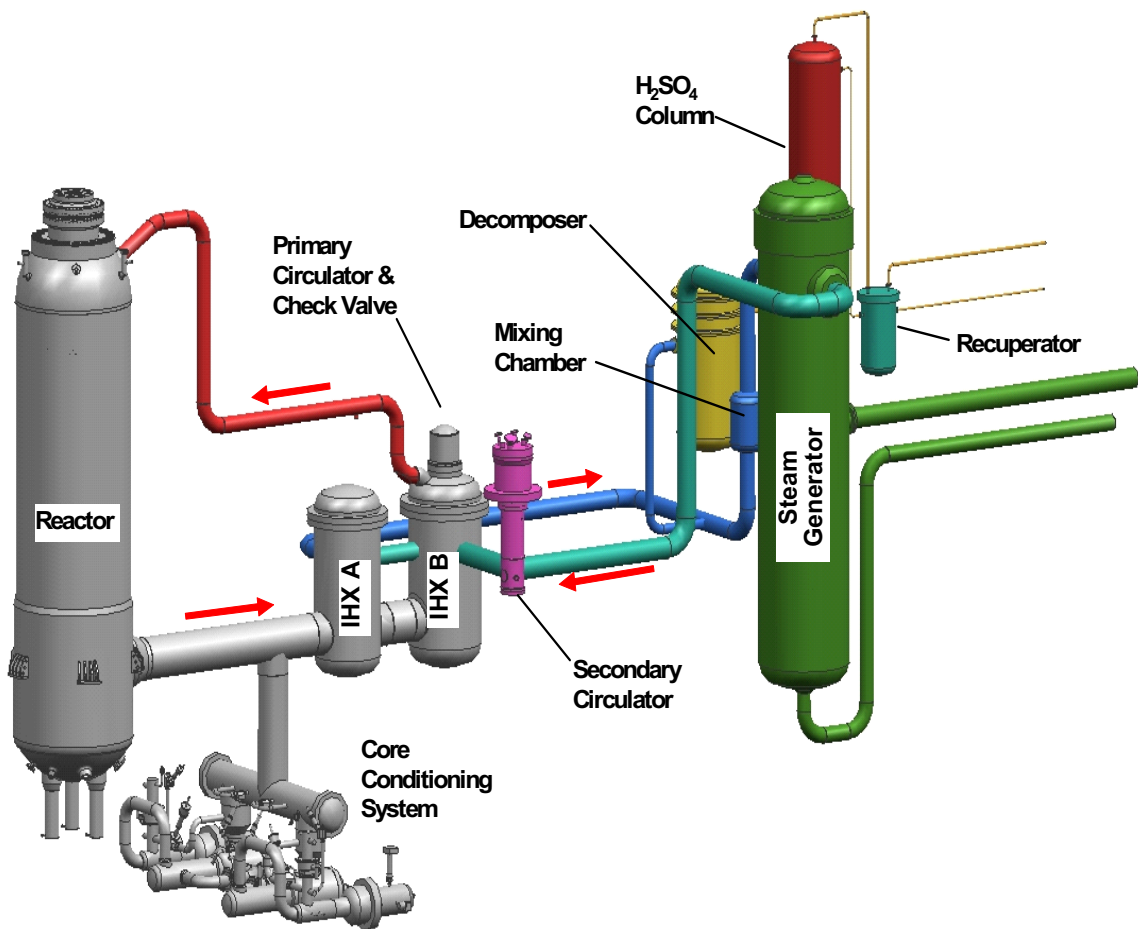


Figure 1 Layout of the Reactor Unit System in Relation to the PHTS, SHTS, SG and PCHX [3]

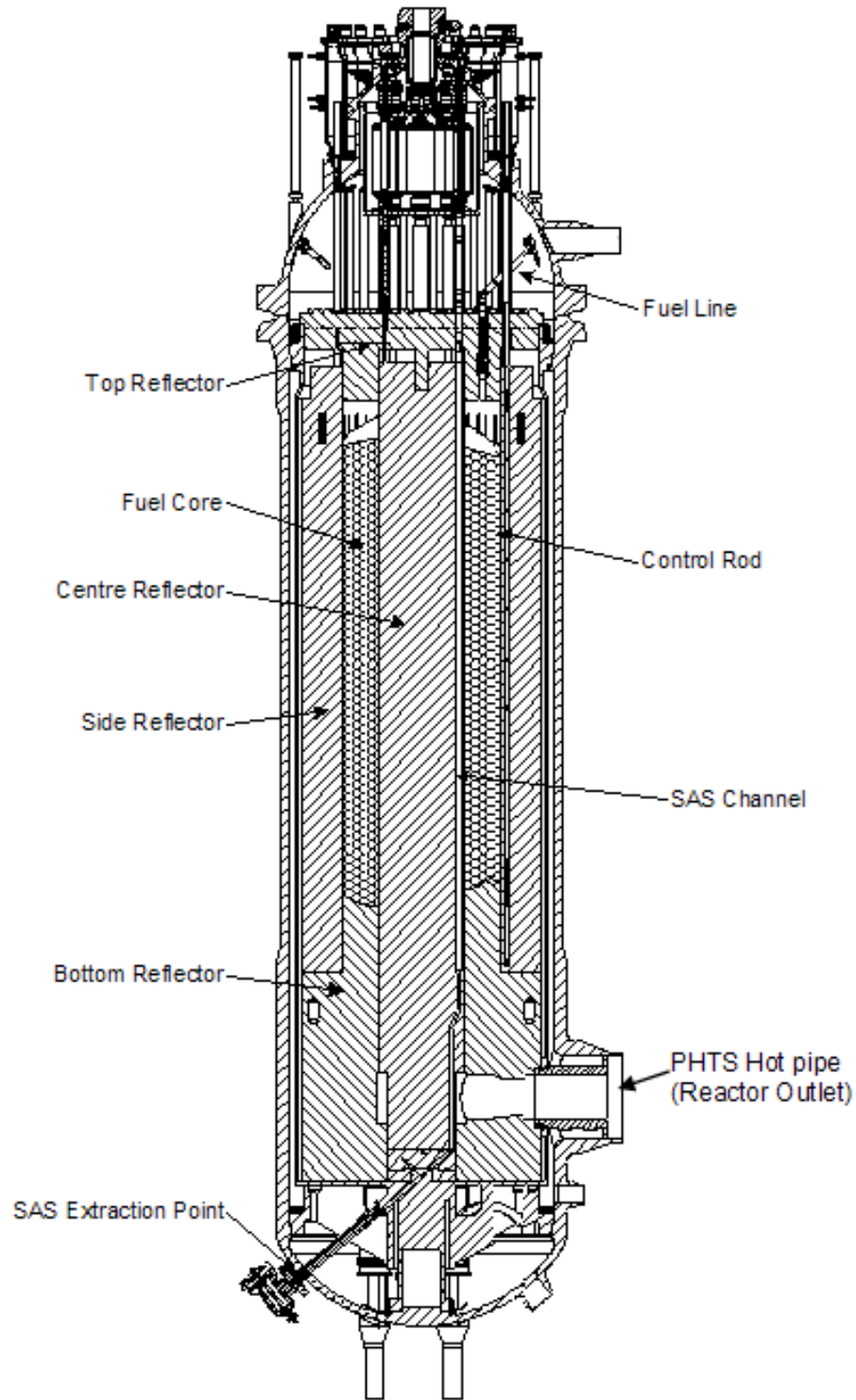


Figure 2 Vertical Schematic Section through the Reactor Unit [3]

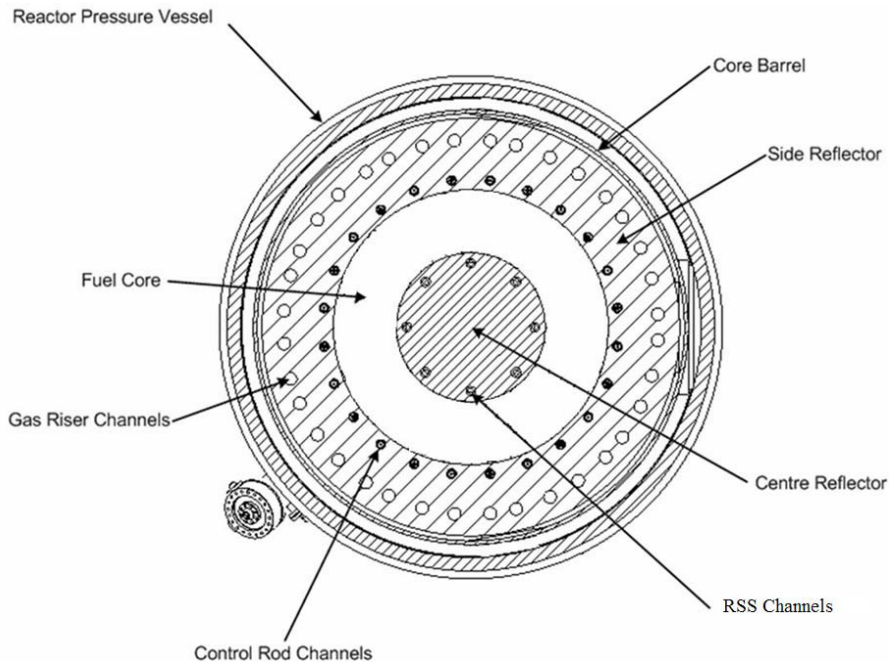


Figure 3 Horizontal Section through the RU without the Core Inlet and Outlet Pipes [3]

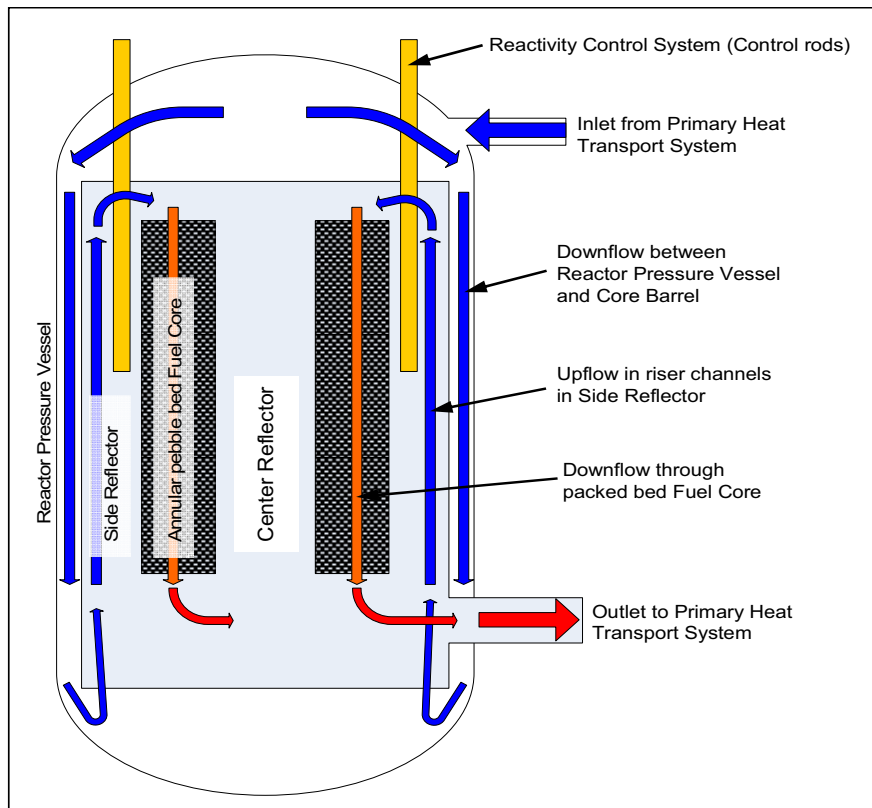


Figure 4 Helium Flow Path Configurations through the RU [3]

The side reflector is divided into the inner and outer side reflector. The outer side reflector (OSR) is constructed from eighteen 40° blocks, which are supported by the 40° bottom reflector outer blocks and form single columns to the top of the reactor.

The inner side reflector (ISR) is constructed from 24 blocks, 15° segments. Three of these ISR blocks are supported by a single bottom reflector block, which comprises a 45° segment. This configuration applies the single column principle in which any block is supported below by only one block. Application of this principle ensures that relative motion between the columns (due to temperature or irradiation induced dimensional changes) is accommodated without the generation of internal loads. A horizontal section through the side reflector is shown in Figure 5.

The Top Reflector is suspended from the Core Barrel Top Plate by means of Tie-Rods, manufactured from CFRC. The Top Reflector provides for neutron absorption and shielding above the core and also protects the top plate from high-temperature gas (particularly during accident conditions). The Top Reflector blocks are also staggered to prevent a direct path forming from the hot gas in the core to the top plate.

The structural integrity of the Top Reflector ensures that the interfaces, specifically for the RSS and RCS that pass through it, are ensured. The tie rods are designed to prevent the Top Reflector from dropping onto the pebble bed, even during Design Basis Accidents (DBAs). The top plate plug and the reflector suspended from it can be removed to provide access to the RU internals, notably the replaceable components of the Center and Side Reflectors.

The Central Reflector, which is manufactured from graphite blocks, comprises the Center Reflector Structural Spine and the Outer Center Reflector (OCR). The OCR protects the CR Structural Spine from the high levels of fast neutron irradiation. This ensures that the CR Structural Spine is dimensionally stable. The structural spine ensures the structural integrity of the Central Reflector. A section through the Central Reflector is shown in Figure 6.

As noted earlier (Figure 4), the helium flow is introduced into the Bottom Reflector of the Core Structure Ceramics, from where it is channeled to the top of the pebble bed in the gas riser channels, located in the Side Reflector. The gas then flows through the pebble bed from top to bottom, being heated in the process. At the bottom of the pebble bed, the gas is collected in the outlet plenum through flow slots between the blocks. The flow is then channeled from the outlet plenum into the Core Outlet Connection (COC) and the Hot Gas Duct (HGD).

Core circumferential support components, the Lateral Restraint Straps, surround and contribute to the support and stability of the Bottom and Side Reflectors of the CSC. The location of these straps is shown in Figure 7. These components, which were not shown in the PCDR, were developed for the PBMR DPP and will be used in the PBMR NGNP design.

Reactivity Control and Shutdown System

Reactivity Control System

The Reactivity Control System (RCS) is used to control the reactivity in the fuel core, to quickly shut the reactor down and to keep it in a shutdown mode. The RCS consists of 24 identical control rods. The control rods are grouped into one group of 12 control rods and another group of 12 shutdown rods. During normal operation, the control system moves each group alternatively so that the rods are inserted to an equal depth into the side reflector. The only difference between shutdown rods and normal operation control rods is the length of the chain, with the control rods only traveling in the top part of the

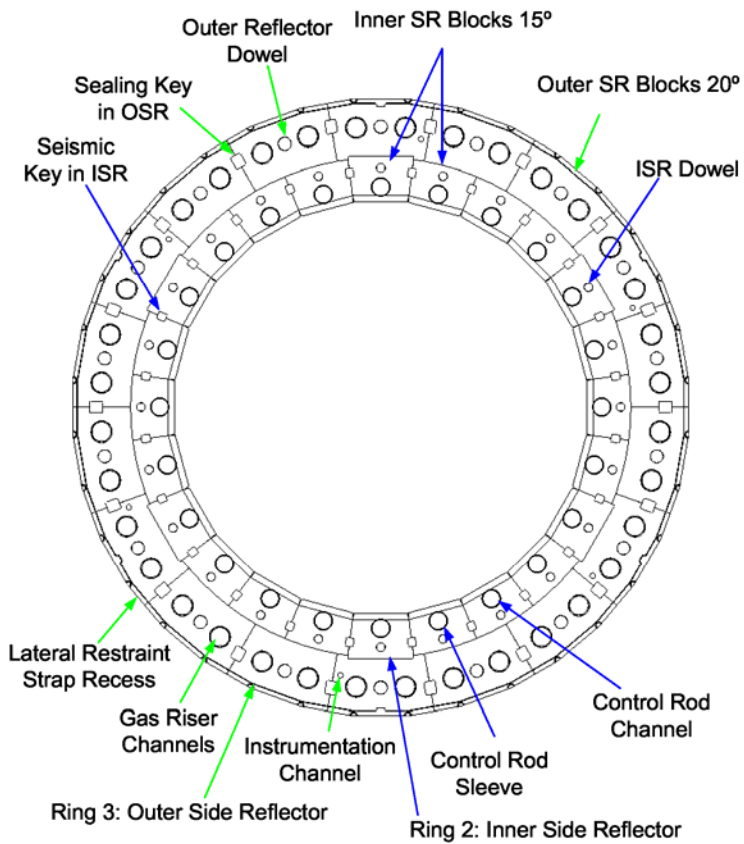


Figure 5 Horizontal Section through the Side Reflector [4]

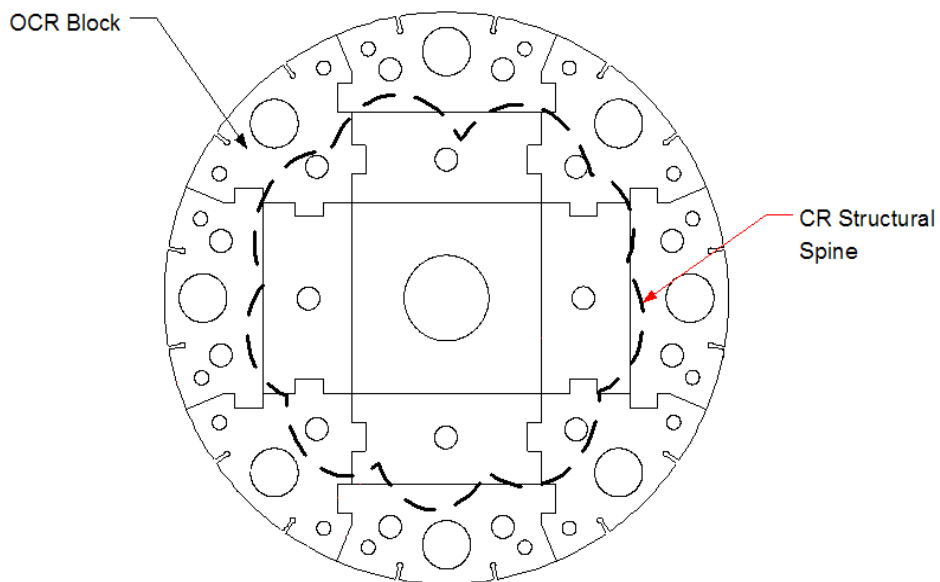


Figure 6 Section Through the Central Reflector [3]

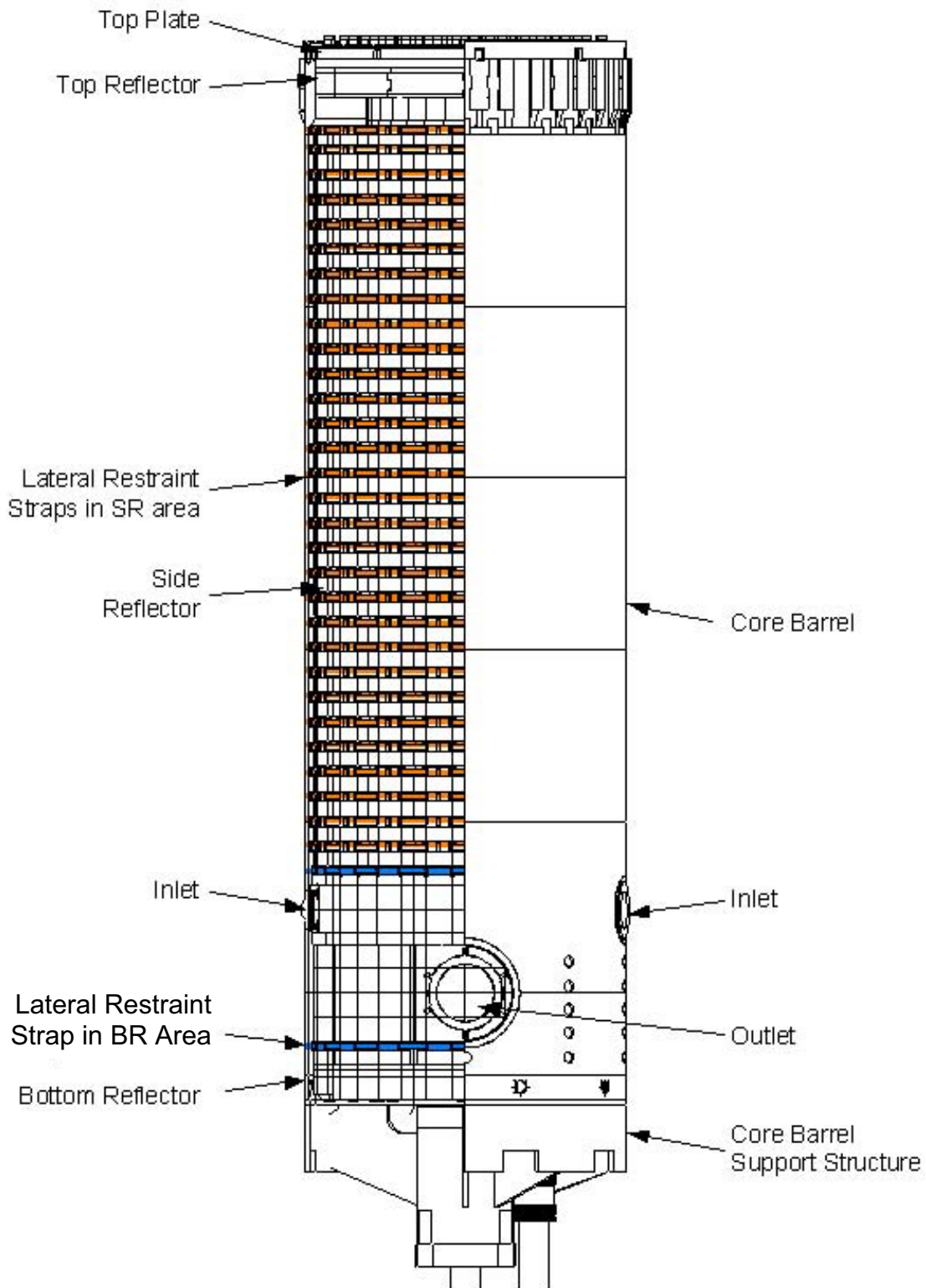


Figure 7 Core Lateral Restraint Strap Positions [5]

reflector, and the shutdown rods capable of traveling to the bottom part of the reflector. Each rod consists of six segments containing absorber material in the form of sintered B₄C rings between two coaxial cladding tubes. Gaps between the cladding tubes and B₄C rings prevent constraint forces from arising due to radiation-induced swelling of the B₄C. Pressure equalizing openings expose the B₄C to the coolant gas to avoid any pressure build-up.

The RCS consists of the following major subsystems/components:

- RCS Control Rod Drive Mechanism (CRDM) consisting of the chain drive, chain container and scram shock absorber which functions as the primary shock absorber. The purpose of the CRDM is to translate rotational movement into linear movement. Refer to the layout in Figure 8.
- Rod and chain, with the rods absorbing neutrons and the chain connects the chain drive to the control rod.
- RCS secondary shock absorber, which prevents damage to the control rod and the core structures ceramics in the event of a chain failure.
- RCS drive motor, which keep the control rod in position and move the control rod up and down. During a power failure the control rod will fall down the control rod channel under gravitational force.
- RCS control rod guide tubes connect the CRDM housing to the Core Structure and serve as a guide for the Control Rod.

During the anticipated operating modes of the Reactor Unit System, the RCS is required to raise and lower the control rods and hold them steady in any position over their entire range of travel. The control rod and shutdown rod positioning is commanded by the Operational Control System (OCS). Control- or shutdown rod insertion (scram) action is initiated by the Reactor Protection System (RPS), which overrides the OCS.

During full power operation, both banks of control rods (24) are inserted into the upper third of the core, as required for reactor regulation. For hot shutdown, both banks are moved simultaneously down to the middle third of the reactor. For cold shutdown, Bank 1 remains in the middle position, while Bank 2 is moved to the fully inserted position. Details of possible variations will be determined during the conceptual design phase.

When power is cut to the drive motors (scram activation), the rods are inserted by gravity. During this event, the drop velocity of the RCS units is limited to a pre-determined value.

This conceptual design study will consider the replacement of metallic components in the RCS with non-metallic components with the potential that the RCS could achieve a longer design life.

Reserve Shutdown System

Channels Interfaces for Small Absorber Spheres (SAS) are provided at 8 positions in the Top and Center Reflectors, as indicated in Figure 9. The SAS are 10mm in diameter and consist of B₄C impregnated graphite. These spheres are normally inserted to ensure cold shutdown during all maintenance operations. The Channel Interfaces provide a path for the absorber spheres through the Top Plate, the Top Reflector and into the Center Reflector, even if there is up to 50mm of misalignment between the Top Reflector and the Center Reflector, as noted in Figure 10. A portion of the path for the

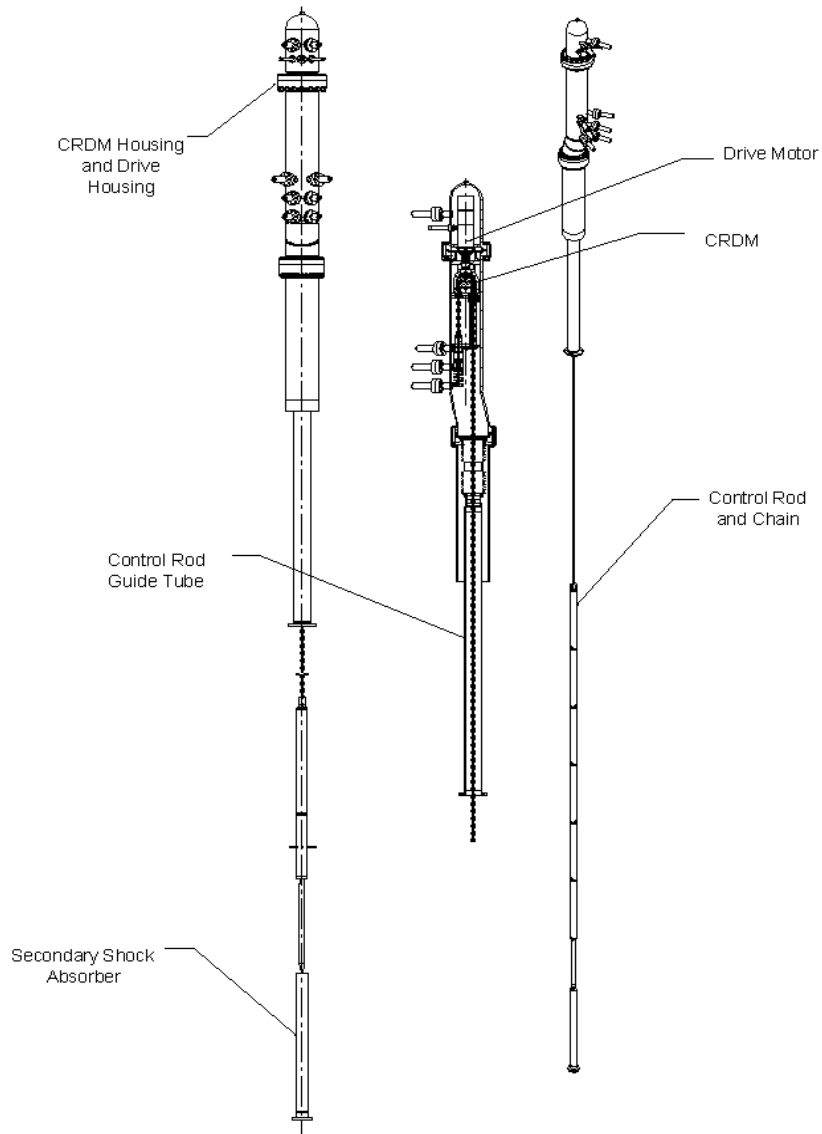


Figure 8 Reactivity Control System Layout [3]

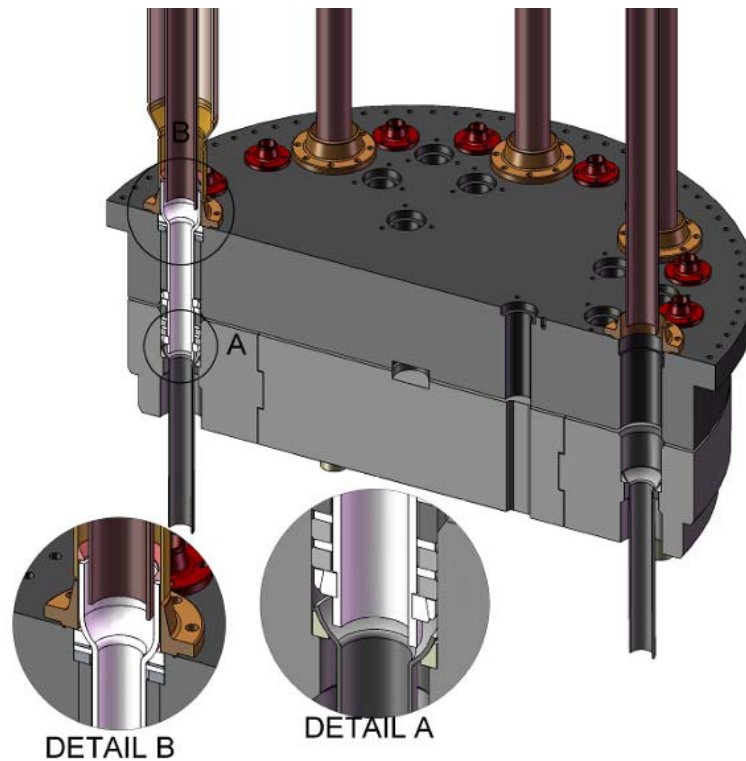


Figure 9 RSS Channel Interfaces

spheres is fabricated from SGL SIGRABOND 1502 YRCFRC tubes. SGRATHERM RFA-FF rigid graphite felt insulation is used adjacent to the tubes in the RSS Interface between the Top and Center Reflector to protect against high temperature helium streaming (Figure 11). Provision is made for the removal of the spheres following the completion of maintenance. These components are applicable for the NNGP design and require no qualification testing.

Heat Transport System

The HTS is comprised of a primary helium heat transport loop, the PHTS, and a secondary helium heat transport loop, the SHTS. The basic concepts of these two circuits are shown schematically in Figure 12. Operating conditions are shown in Figure 13. The PHTS (components shown in red in Figure 12) includes the primary circuit piping, including internal ducts, insulation and external supports, the Intermediate Heat Exchanger (IHX), including the IHX vessel and associated internal and external supports and insulation, plus the primary circulator. The IHX is arranged in two sections, IHX A and IHX B, which are differentiated by their operating temperatures and choice of materials. The heat transfer core of IHX A, the higher temperature section, is expected to be replaced within the plant lifetime and is designed for ease of access. IHX B, which operates at lower temperatures, is designed as a plant lifetime component. The SHTS (components shown in green in Figure 12) includes the secondary circuit piping, along with its internal ducts, insulation and external supports, the secondary circulator, plus a fixed orifice and a helium-mixing chamber that are included in the NNGP Demonstration Plant, but not required in the NNGP Commercial Plant. Also shown in the figure are the delivery interfaces from the SHTS to the Process Coupling Heat Exchanger (PCHX) of the Hydrogen Production System (HPS) and

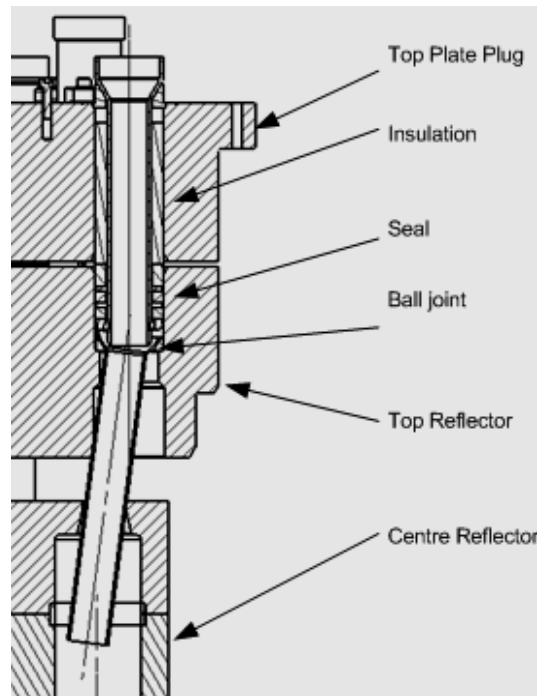


Figure 10 RSS Channel Interface Tubes Cross Section [5]

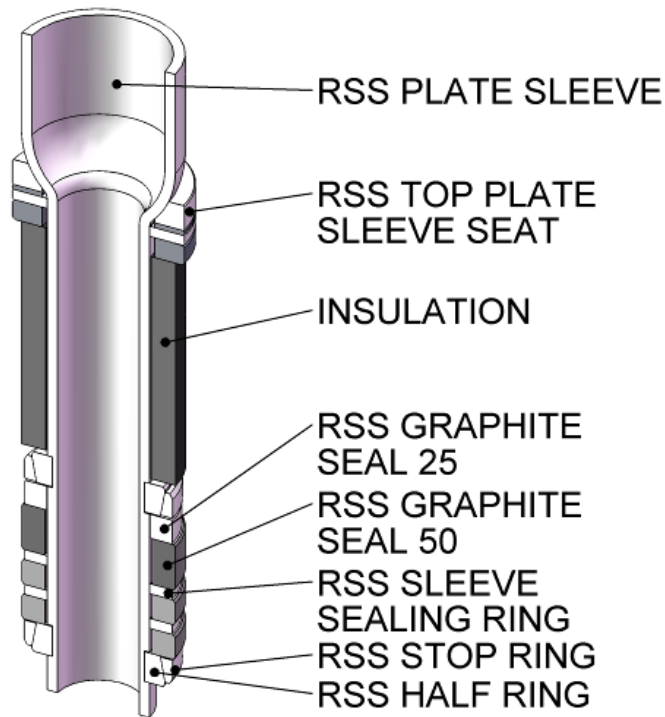


Figure 11 Graphite Felt Insulation Used Adjacent to CFRC SAS Tube

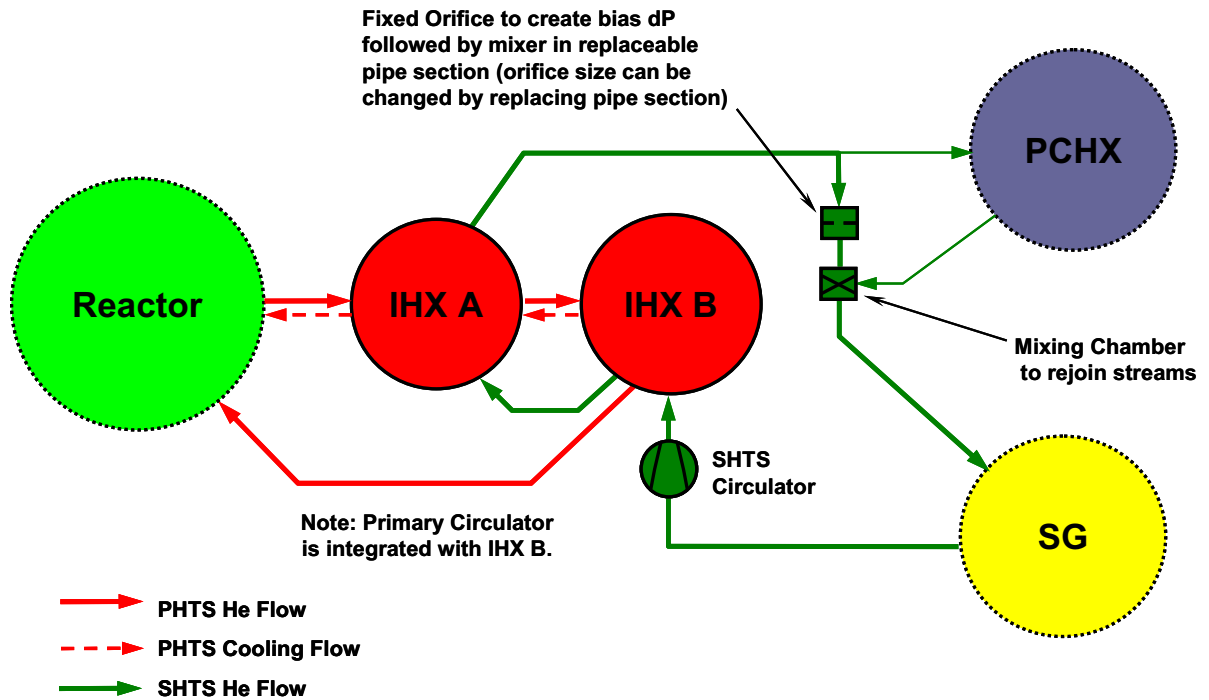


Figure 12 HTS Coupling Concept [6]

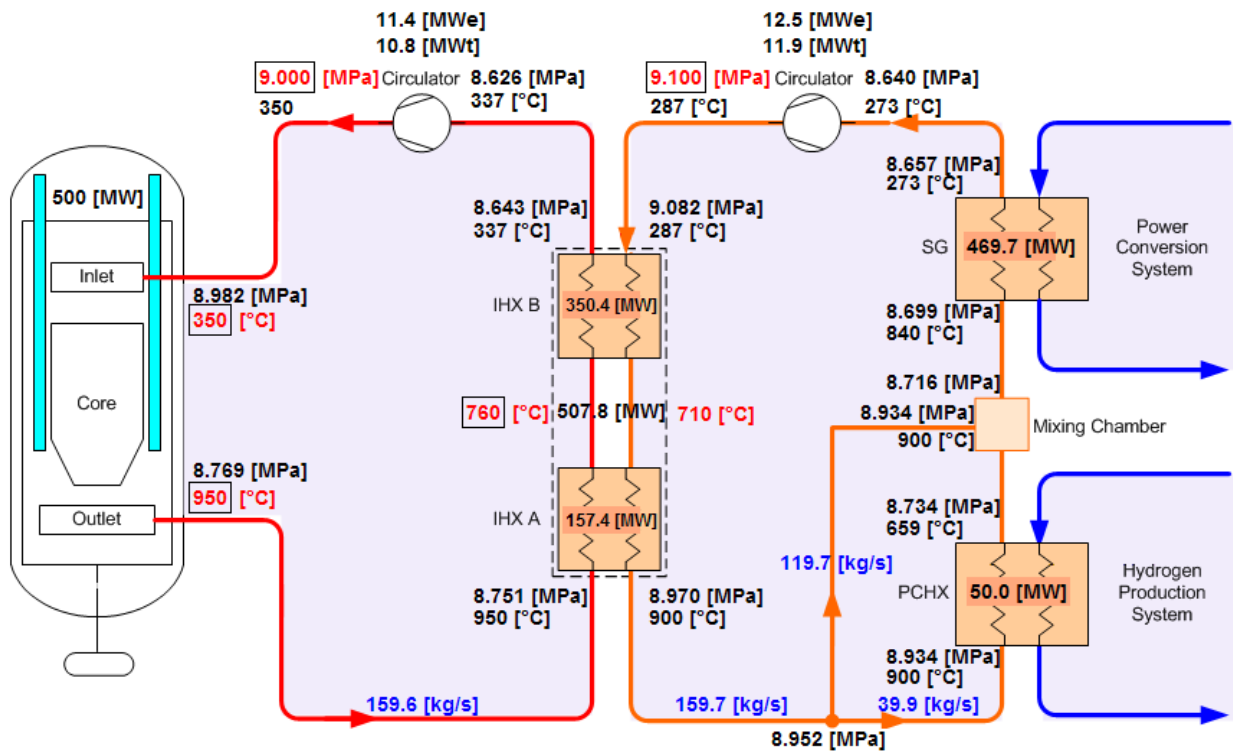


Figure 13 HTS Operating Parameters [7]

Steam Generator (SG) of the Power Conversion System (PCS). Insulation systems and the interface of the Hot Gas Duct with the RU will be considered in this study.

Composites

This study considers the design of composite components for various applications. The design of composite components using CFRC should adhere to the following general guidelines because these materials are not ASME Code materials with associated design rules.

- **Avoid use in highly irradiated condition**

The irradiation exposure for CFRC parts should be limited to regions of stability as discussed in Section 2 of the study. The irradiation performance of the CFRC component must be verified for the specific material and design to be used for the component. Specific SiC/SiC composites; however, appear to be applicable for use in components that will be exposed to a significant end of life (EOL) neutron fluence.

- **Design with high margin**

Uncertainties introduced due to the application of the part are countered by building in margin considered on a case by case basis in combination with redundancy and application of the part.

- **Design for redundancy**

The design of a CFRC part should be such that in the event of a failure of the loaded single CFRC part, the load must safely transfer to the neighboring parts without adversely affecting their performance or result in the failure of function of the parts assembly.

- **Design for inspection and replacement**

Replaceable CFRC parts should be inspectable. If a CFRC part is not inspectable, the CFRC part must have a high design margin and be designed for the life of the plant.

- **Use of Commercial Grade Material**

CFRC parts should be designed from commercial grade materials.

Two design routes are available for CFRC parts; Design-by-Testing and Design-by-Analysis (see Figure 14). The decision on which route to choose is based on the design input data. If a part meets the following criteria the part can be designed by analysis. In all other instances, design-by-testing should be applied:

- The parts have simple geometry
- The part material properties are simple and well understood
- The loading on the part is simple.
- The design margin on the part is high.

Test data should be analyzed by applying a suitable statistical treatment to the test results. Based on this information, the designer can determine the final design size for the part.

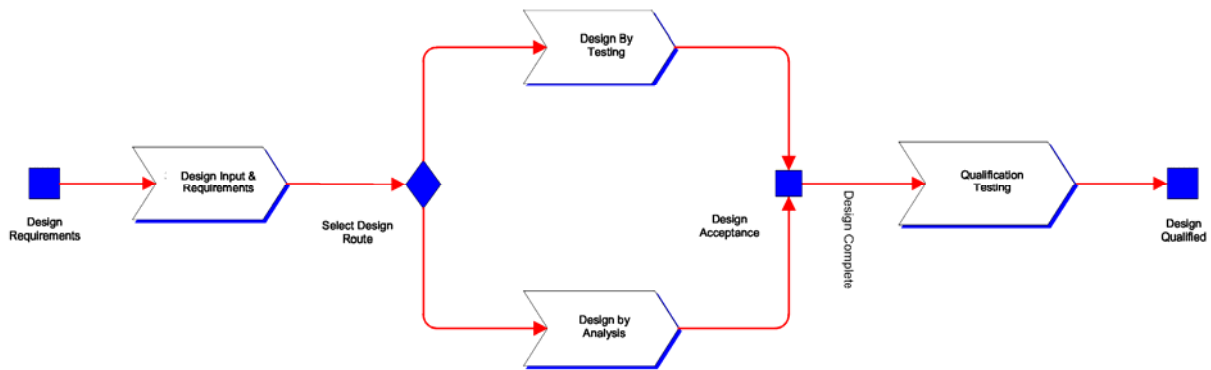


Figure 14 CFRC Design Methodology

Design by analysis may be applied to CFRC parts that have well understood geometry, material and loads. The analysis of these parts can be done using existing FEM packages and models or the analysis can be carried out with hand calculations. Based on the analysis results, the design size can be determined and qualification testing on the part can be carried out.

OBJECTIVES AND SCOPE

This study identifies the potential applications of and design requirements for ceramic and ceramic composites (non-graphite materials) in the PBMR-based NNGP primary system. Key elements of the objectives and scope are:

- Identify structural and thermal insulator components that are anticipated to be fabricated from ceramic or ceramic composites for use in the PBMR NNGP primary system
- Evaluate ceramic and ceramic composite materials with the required material properties for each component identified
- Evaluate the feasibility, issues, estimated costs and schedule associated with component fabrication for the materials identified, considering the NNGP target for initial operation in 2018
- Identify the operating conditions for normal and off-normal conditions, including estimated stress, temperature, fluence, environmental conditions and other important conditions for the components identified in the PBMR NNGP
- Identify activities necessary to codify these materials (e.g. in ASME and ASTM codes)
- Identify any additional work (development requirements in the form of Design Data Needs (DDNs)) anticipated to be required to support codification and NRC licensing of the NHSS associated with the components and materials identified
- Identify committed or planned work in support of the DPP associated with the components and materials evaluated.

The actual components evaluated in the study are given below:

- Core Circumferential Support Components
 - Lateral Restraint Strap Assembly with CFRC Components
- Upper Reflector Support Components
 - CFRC Tie Rods; RSS Channel Interface Tubes
- Hot Gas Duct Components
 - Hot Gas Duct, Including Liner and Insulation
 - Core Outlet Connection (COC) CFRC Liner
- Reactivity Control Components
 - Control Rods, Cladding Tubes and Joints; RCS Secondary Shock Absorber
- Core Support/Core Barrel Interface Insulation
 - Bottom Reflector Insulation; RSS Interface Insulation
- High Temperature Section Insulation
 - IHX A and B Insulation

ORGANIZATION OF REPORT

The report is organized along the lines of the three technical tasks within the statement of work:

- Subtask 1 – Identification of Components (Section 1)
- Subtask 2 – Materials Evaluations (Section 2)
- Subtask 3 – Technology Development Plan (Section 3)

1 IDENTIFICATION OF COMPONENTS

Structural and thermal insulating components are identified for which the selection of ceramic and/or composite materials might provide significant advantage in the NGNP Reactor System and PHTS.

1.1 Lateral Restraint Strap Components

The Lateral Restraint Straps (Figure 7) surround and contribute to the support and stability of the Bottom and Side Reflectors of the CSC, providing circumferential support to the enclosed graphite reflector assemblies. They interface with the CBA, which in turn transmits lateral loads to the RPV. These circumferential supports must expand to maintain the same inner diameter as the outer diameter of the reflector assembly and, therefore, it is essential that they have effective rates of thermal expansion that are similar to those of the reflector assembly that they enclose. This is in order to minimize gaps in the reflector and associated leakage flow and to reduce loads in the reflector assembly during thermal cycling. These components also assist in limiting the movement of the core during a seismic event. These components are being developed for the PBMR DPP and are applicable to the PBMR NGNP. Because this is a well developed design, no alternatives will be discussed in this study. Discussion includes the following factors:

- Identification of components
- Design considerations for the use of composites and/or ceramics
- Surveillance, inspection and monitoring
- Tolerance to irradiation exposure
- Range of operating temperature
- Qualification of components

1.1.1 Identification of Components

The restraint strap design that supports the OSR is shown in Figure 15.

1.1.2 Design Considerations

The Lateral Restraint Straps are closed segmented rings that surround and support the Bottom and Side Reflectors of the CSC. Lateral support is provided to the reflectors by the interface of the Straps with the Core Barrel Assembly, which, in turn, transmits lateral loads to the RPV. The Straps also provide circumferential support to the enclosed reflector assemblies, effectively serving a function that is similar to hoops on a barrel. In this latter capacity, the Lateral Restraint Straps are designed to have the same effective rate of thermal expansion as the outer diameter of Bottom and Side Reflectors contained within. This is achieved by utilizing two materials, CFRC and Type 316 Stainless Steel, with specified relative lengths in the design of the Straps.

Matching the relative thermal expansion of the Lateral Restraint Straps and CSC minimizes the formation of gaps in the reflector and associated leakage flow. It further reduces “breathing loads” (caused by increases and decreases in the diameter at the Reflector/Pebble Core interface) during thermal cycling. The Lateral Restraint Straps also allow for relative vertical movements between the columns by means of sliding, thereby accommodating relative vertical movements of the individual columns due to temperature differences.

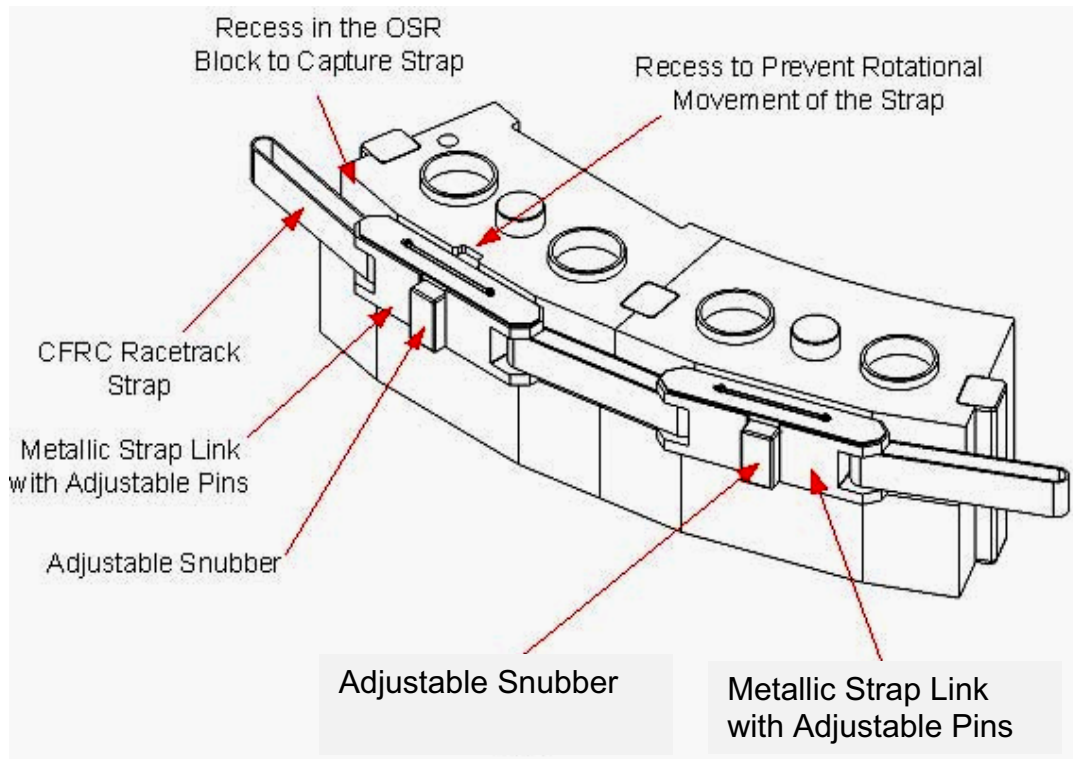


Figure 15 Lateral Restraint Strap [5]

Protrusions from the metallic portions of the straps provide for load transfer between the CSC and the CB during a seismic event. These protrusions will make contact with the CB as the reflectors move during a seismic event, thereby limiting the movement of the core. There are recesses in the OSR every 60° where the metal strap protrudes into the OSR blocks. This prevents the Lateral Restraint Strap from rotating around the OSR. The BR Lateral Restraint Strap is identical to the SR straps (see Design Task A1, Section 3).

The CFRC Racetrack Straps will be fabricated using SGL Sigrabond 2002 YR polyacrylonitrile (PAN) Fiber that is wound unidirectionally in a racetrack layup in the loading direction. The 2002 YR material is impregnated with Coal Tar Pitch. The properties of the Grade 2002 YR material are given in Table 2 for orientations both perpendicular (Per) and parallel (Par) to the fibers. All other strap components are fabricated from Type 316 stainless steel. PBMR has a completed design for the Straps for the DPP and a testing program will be performed on the Straps prior to installation. The CFRC straps are designed for flexural strength and slightly negative thermal expansion properties. The existing PBMR DPP design for the core lateral circumferential support straps appears to be adequate for the NNGP design.

1.1.3 Surveillance, Inspection and Monitoring

The core restraint straps have been designed with large margins and redundancy. Presently, there are no plans for monitoring, inspection or surveillance.

Table 2 Properties of CFRC – Grade 2002 YR [8]

Property	Unit	Value
Density	kg/m ³	1340 ± 30
Thermal Conductivity (RT)	W/mK	Per 3.8 ± 0.17 Par 66.0 ± 6.1
CTE (20 °C to 200 °C)	10 ⁻⁶ /K	Par -0.03 ±0.17
Compressive Strength	MPa	Per 3.73 ± 0.5
Flexural Strength (3-point)	MPa	Par 207.7 ± 0.5
Flexural Elastic Modulus	GPa	Par 154.4 ± 0.4
Inter-laminar Shear Strength	MPa	Par 5.93 ± 0.65

1.1.4 Tolerance to irradiation Exposure

The peak fluence estimated for the straps is 2×10^{20} n/cm² ($E > 0.1$ MeV) for the PBMR NGNP design at 60 years (0.1 dpa, carbon). The NGNP fluence estimate is based on DPP fluence+25% (power correction) multiplied by 1.5 (design life correction). Under these conditions, the material is considered to be exposed to only low level irradiation. Modeling needs to be performed to verify the fluence estimate (see Design Task A2, Section 3). If the estimated fluence is shown to be a significant underestimate based on future modeling, a limited irradiation program needs to be performed on the specific material selected for the race track strap to verify the effect of the actual irradiation exposure on the material selected (see DDN COMP 01-01, Section 3). The proper function of the CFRC Racetrack Strap in the NGNP design requires that the neutron fluence remains low. The indicated fluence levels are not significant for the metallic components of the Lateral Restraint Straps.

1.1.5 Range of Operating Temperature

The maximum operating temperature for the strap is estimated to be 400-450°C during normal operation. The estimate is based on DPP temperature plus 50°C for NGNP temperature. The maximum estimated temperature for the strap during a worst case DBE is 750°C. The temperature limit for the metallic components in the strap is 816°C [8]. The design and qualification of the 316 stainless steel components are based on ASME Section III, Division 1, Subsection NG, which is approved for the design and manufacture of core support structure components at design temperatures up to 427 C (for austenitic materials). However, this design temperature limit is projected to be exceeded for the strap components. ASME Code Case N-201-4 (Class CS Components in Elevated Temperature Service, Section III Division 1) provides for the use of Type 316 for in-core support structure applications at temperatures up to 816°C. Therefore, based on temperature estimates, the straps appear to be adequate for the application.

Adequate modeling needs to be performed for the outer reflector region to validate the temperature environment for both normal and off-normal operating conditions during the life of the NGNP (see Design Task A3, Section 3).

1.1.6 Qualification of Components

Material qualification of the strap material (SIGRABOND 2002YR) and CFRC plate material (SIGRABOND 1502YR) used for other applications (tie rods) are similar and will be discussed in this section. Irradiation and oxidation effects are considered insignificant for these applications. Elemental purity of the composites will be monitored during qualification and fabrication. Sampling is based on required statistical reliability, load category and plant event category.

Plant events and load cases are identified and categorized in accordance with the PBMR DPP Integrated Design Process as noted below:

- Event Category A is associated with normal operation, which is defined as when the plant is operated within the limits of the plant operating technical specification. The requirement for this category is that the specified service function of the SSC must be achieved for its total design life.
- Event Category P is associated with test and inspection conditions, and requires that tests and inspections that have to be performed outside the normal operating envelope of the SSC must be considered in the design.
- Event Category B is associated with Anticipated Operational Occurrences (AOOs), which are defined as any deviation from normal conditions anticipated to occur often enough that the design should include a capability to withstand these conditions without operational impairment.
- Event Category C is associated with emergency conditions. Emergency conditions include deviations from normal conditions, which requires shutdown for correction of the condition(s) or repair of damage. Such events have a low probability of occurrence, but are included to provide assurance that no gross loss of structural integrity will result as an associated effect of any damage developed in the system. The design requirement for this category is that after the occurrence of such an event, it must be possible to return the plant to service, thus, the investment must be preserved. This means that plastic deformations in areas of geometrical discontinuities will be acceptable, provided that the affected SSC can be inspected, repaired or replaced, if required.
- Event Category D is associated with faulted conditions. Faulted conditions are any of those combinations of conditions associated with extremely low-probability events whose consequences are such that the integrity of the SSC may be impaired to the degree that it could not be returned to service. The investment may be lost, but nuclear safety must be preserved. Thus, radioactive releases are not allowed to exceed the regulatory limits. Plastic deformations or damage to components in larger areas will, therefore, be acceptable.

The Designer for the DPP classifies the load cases into Load Categories. The determination of the loading condition must take place as part of a structural analysis. Load Categories (LOC) are assigned to events as noted below:

- LOC A corresponds to Event Categories A,P and B
- LOC B corresponds to Event Categories C and D

. After an event has occurred with loads corresponding to the loading Category B, further reactor operation is not permitted unless a stress analysis or a suitable examination after the removal of the load shows that the reactor internals are undamaged. If necessary, the damaged part(s) must be replaced.

The strength of the respective components is assessed by statistical testing. The following loading limits are defined:

- LOC A: Strength corresponding to a probability of failure (POF) of 10^{-4}
- LOC B: Strength corresponding to a POF of 10^{-3}

It was concluded for the lateral restraint strap CFRC segments that component properties could not be reliably obtained by the extraction of test samples from the fabricated racetrack segments, because these samples would not be sufficiently representative of the component strength, given its geometry. For this reason, testing will be done using actual components.

The number of test specimens to be tested for each property is based on the minimum number of specimens required per batch for material qualification in accordance with MIL-Handbook-17-5, Part C: Testing [9]. The specified test specimen numbers either comply with, or exceed the minimum recommended number in accordance with Reference 10.

The qualification procedures for the strap components have not been specifically developed for the NGNP design; however, it is expected that the procedures developed for the DPP design will be adequate for the NGNP design. Therefore, the DPP procedures and qualification information need to be reviewed; modified as required and validated for the NGNP design (see Design Task A4, Section 3).

1.2 Upper Reflector Support Components

The function of the Upper Reflector is to provide neutron reflection and radiation shielding to the area above the top plate, as well as to thermally insulate the CB top plate from the core. The Top Reflector blocks are suspended from the CB Top Plate by means of support components in the PBMR NGNP design. Because these components are subject to static and potentially dynamic tensile loading at the operating temperature range of the upper reflector, redundancy and margin are important considerations in the design. These components have been developed for the PBMR DPP and are applicable to the PBMR NGNP. Because this is a well developed design, no alternatives will be discussed. Discussion includes the following factors:

- Identification of Components
- Design considerations for the use of composites and/or ceramics
- Surveillance, inspection and monitoring
- Tolerance to irradiation exposure
- Range of operating temperature
- Qualification of components

1.2.1 Identification of Components

The function of the Top Reflector is to provide neutron reflection and radiation shielding to the Top Plate and the area above the top plate, as well as to thermally insulate the Core Barrel Top Plate from the core. The Top Reflector blocks will be suspended from the CB Top Plate by means of CFRC Tie Rods. A cross section showing the Top Reflector design is given in Figure 16. (Note: There is actually a gap between the Top Reflector and the Side Reflector that is not shown in the sketch.) A cutaway of the Tie

Rod Assembly is given in Figure 17. (Note that the Top Plate is not Shown in this figure.) The Tie Rod geometry is given in Figure 18.

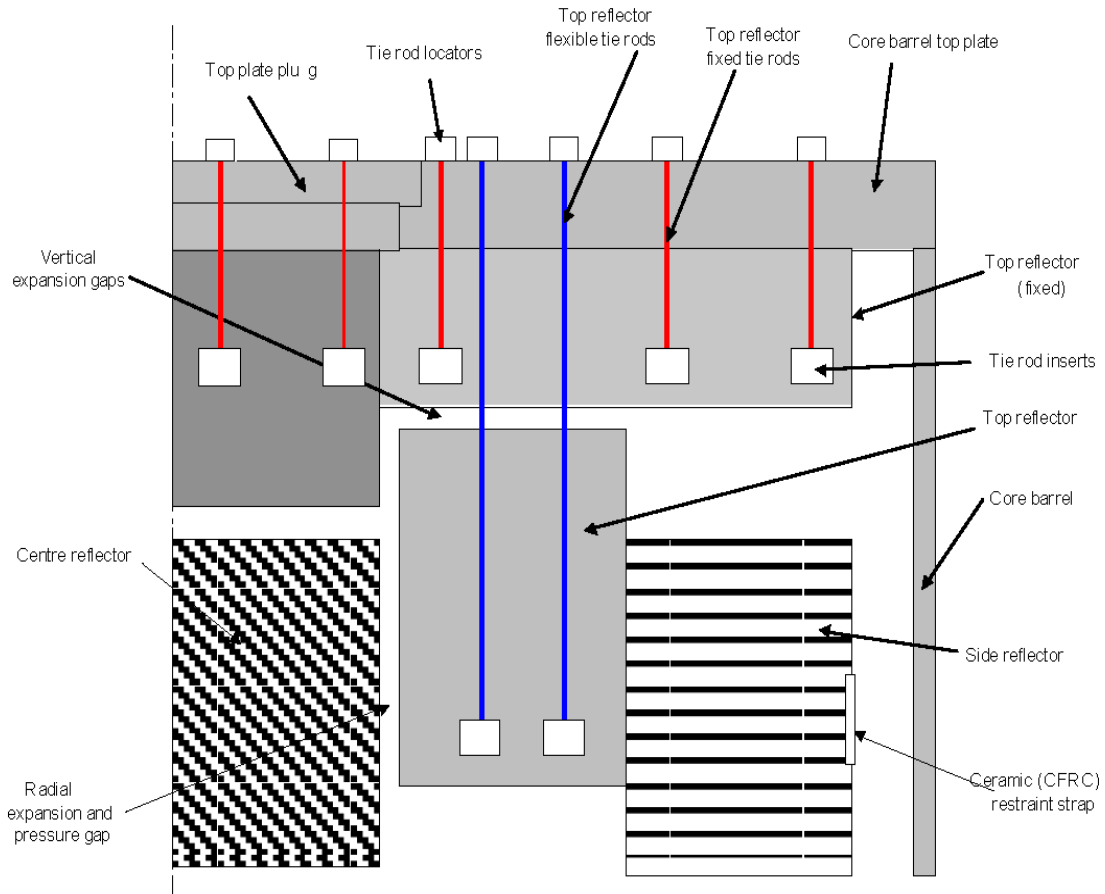


Figure 16 Top Reflector Cross Section [11]

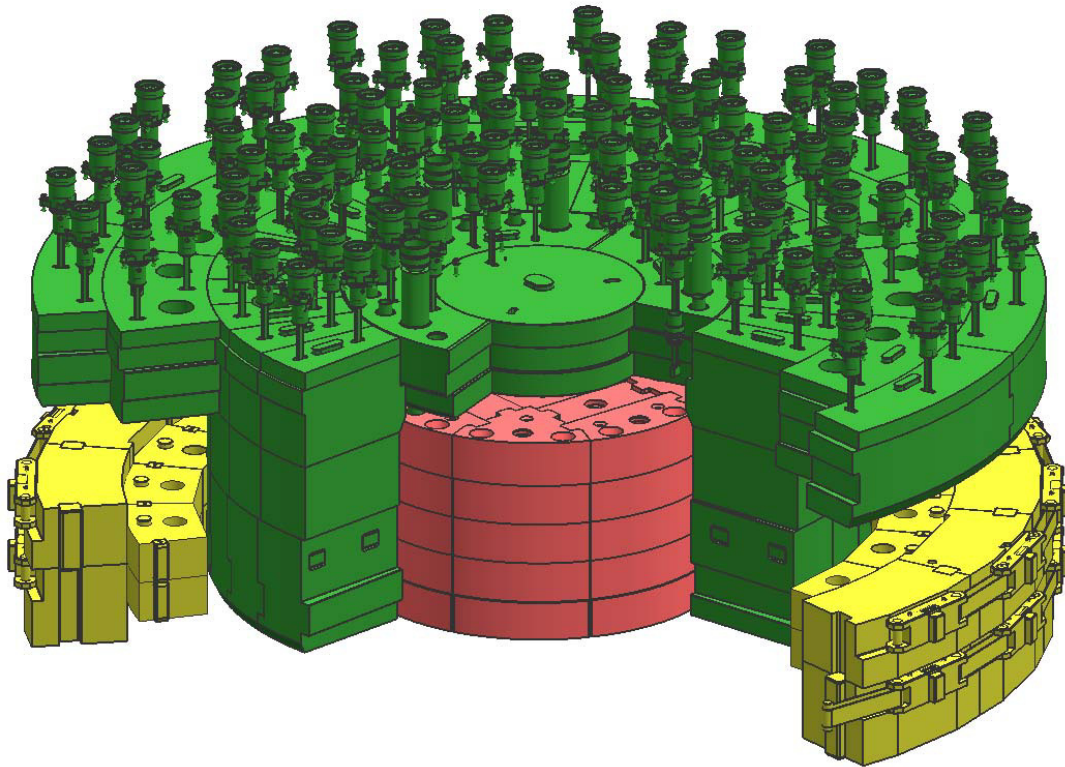


Figure 17 Tie Rod Assembly Cutaway Looking From the Top [12]

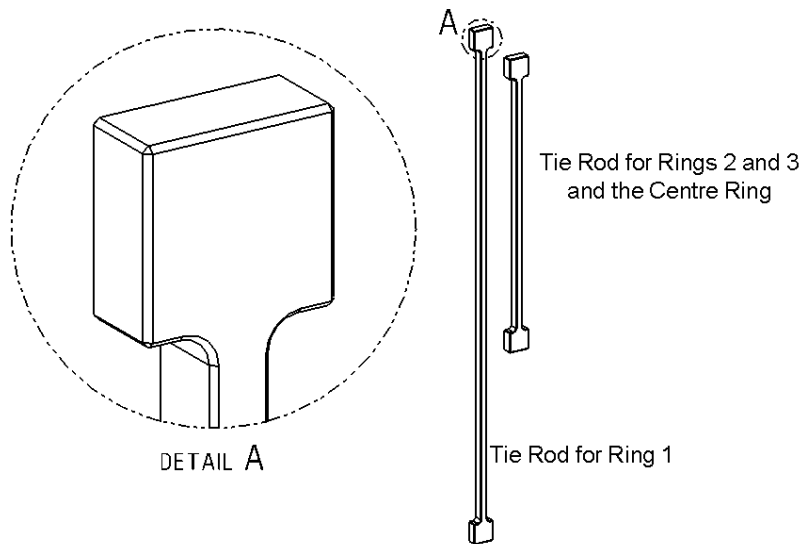


Figure 18 Tie Rod Geometry [4]

1.2.2 Design Considerations

The design described in the following paragraphs has been applied to the PBMR DPP; however, this or a similar design could be applied to the PBMR NGNP. CFRC was selected for this application because thermal creep could not be ruled out using an ASME Section III Code approved metallic alloy.

The Tie Rods are cut from flat CFRC plate (laminated, 2D woven fabric lay-up). There are 60 long Tie Rods (called flexible tie rods in Figure 16) and 72 short Tie Rods (called fixed Tie Rods in Figure 16) used to suspend the Outer Top Reflector, Rings 2 and 3, and a further 20 short Tie Rods used to suspend the Top Reflector Plug also called the Center Ring. Both ends of the Tie Rods are T-shaped. The bottom of the Tie Rod fits into slots in the Top Reflector.

The Tie Rods will be fabricated from a laminated CFRC plate material (SGL SIGRABOND 1502 YR). The Tie Rods will be fabricated using 2D woven polyacrylonitrile (PAN) fiber mat and impregnated with Coal Tar Pitch into a plate form. The important properties of this material are given in Table 3. The Tie Rod design was developed for the DPP and the current design of the Tie Rods needs to be reviewed to determine if changes to the design are required for the NGNP (see Design Task B1, Section 3).

Table 3 Properties of CFRC - Grade 1502 YR [8]

Property	Unit	Value
Density	kg/m ³	1560 ± 20
Thermal Conductivity	W/mK	Per 7.6 ± 1.7 Par 58.5 ± 1.7
CTE (20 °C to 200 °C)	10 ⁻⁶ /K	Per 8.14 ± 0.10 Par -0.26 ± 0.05
Compressive Strength	MPa	Per 253.2 ± 14.1
Tensile Strength	MPa	Par 488.8 ± 23.5
Tensile Young's Modulus	GPa	Par 108.3 ± 1.6
Inter-laminar Shear Strength	MPa	Par 7.4 ± 0.6
Thermal Creep		Insignificant

1.2.3 Surveillance, Inspection and Monitoring

The following surveillance, inspection and monitoring has been proposed for the detection of tie-rod failures in the DPP:

- Monitor CB strain gauges, CB temperatures, the amount of spheres entering the reactor, the position of the control rods, axial neutron flux profile around the core, pressure differential in the core and top of pebble bed (visual) to detect modification core geometry
- Perform control rod and/or SAS insertion tests to detect changes in reflector geometry

- Monitor CB heat rejection, CB temperatures, CB strain gauges, CBCS inlet temperature, CBCS mass flow and in-core pressures to detect changes in the gas flow path

The surveillance, monitoring and inspection procedures developed for the DPP need to be reviewed for the NNGP design (see Design Task B2, Section 3). For example, there is no CBCS in the NNGP.

1.2.4 Tolerance to irradiation Exposure

The peak fluence expected for this material is estimated to be 2×10^{20} n/cm² ($E > 0.1$ MeV) (0.1 dpa, carbon) at 60 years for the PBMR NNGP design. The NNGP fluence estimate is based on the DPP fluence +25% (power correction) multiplied by 1.5 (design life correction). Under these conditions, the material is considered to be exposed to only low level irradiation. Adequate modeling needs to be performed for the top reflector region to validate the fluence environment during the life of the NNGP (see Design Task B3, Section 3). If the estimated fluence given is shown to be a significant underestimate based on modeling, a limited irradiation program needs to be performed on the specific material selected for the race track strap to verify the effect of the actual irradiation exposure on the material selected (see DDN COMP 01-01, Section 3).

1.2.5 Range of Operating Temperature

The maximum operating temperature for the Tie Rods is estimated to be 550°C during normal operation. The estimate is based on DPP temperature plus 50°C for NNGP temperature. The maximum estimated temperature for the Tie Rods during a worst case DBE is 650°C. There should be no issues associated with the use of this material in this temperature range.

Adequate modeling needs to be performed for the top reflector region to validate the temperature environment for both normal and off-normal operating conditions during the life of the NNGP (see Design Task B4, Section 3). Currently, the operating environment in these areas is estimated to be higher than the DPP design based on informal modeling and projections but this has not been validated.

1.2.6 Qualification of Components

This information is given in Section 1.1.6.

The qualification procedures for the Tie Rod components have not been specifically developed for the NNGP design; however, it is expected that the procedures developed for the DPP design will be adequate for the NNGP design. Therefore, the DPP procedures need to be reviewed, modified as required and validated for the NNGP design (see Design Task B5, Section 3).

1.3 Hot Gas Duct Components

The Hot Gas Duct (HGD) interfaces with the outlet plenum opening in the BR of the PBMR NNGP and channels high-temperature (950°C) helium to the IHX. The Hot Gas Duct in the DPP design is a complex multilayered system that is enclosed within a part of the primary helium pressure boundary. The high-temperature elements (the liner and the insulation) of the HGD are non-load bearing components that are designed to shield and insulate the pressure boundary piping and to resist high temperature and high flow conditions, including abrasion from entrained particles. Most of these components are being developed for the PBMR DPP and are potentially applicable to the PBMR NNGP; however, several issues need to be considered:

- The higher reactor outlet temperature of 950°C and the impact on the liner creep fatigue

- The higher temperature (350°C) of the helium flow from the circulator outlet that is used to cool piping components in the outer annulus, compared to the DPP design
- Potential transients affecting the NNGP Helium Pressure Boundary (HPB) that are not present in the DPP design
- The need for replacement or further qualification of the Alloy 800H liner because the outlet helium temperature for the NNGP design is higher than that of the DPP design
- The need for an alternate inner pressure pipe material and/or an alternate insulation material to protect the inner pressure pipe from excessive temperature exposure
- The possibility of a less complicated and/or expensive hot duct piping design

Discussion regarding the hot gas duct components includes the following factors for both the alternatives and the PBMR design being developed:

- Identification of components
- Design considerations for the use of composites and/or ceramics
- Surveillance, inspection and monitoring
- Tolerance to irradiation exposure
- Range of operating temperature
- Qualification of components

1.3.1 Identification of Components

The Core Outlet Connection (COC) (Figure 19) provides the interface between the opening in the core outlet plenum of the BR and the remainder of the Hot Gas Duct. A vertical section through the RU showing the core outlet is given in Figure 2. The location of the COC in the BR is shown in Figure 20. A detail of the COC is given in Figure 21.

Two different PHTS piping designs, depending on their location in the main coolant loop, are currently noted in the PCDR. The piping between the reactor vessel outlet and IHX A and between IHX A and IHX B will be a straight “rigid” design. More specifically, the pipes that form the pressure boundary will be allowed to expand freely and to move the IHX A and IHX B vessels on sliding supports and the Reactor Pressure Vessel is fixed. This concept, which is typical of support systems used in LWRs, allows the use of relatively short, straight pipes. Actual flow of the 950°C helium from the reactor outlet to IHX A and the 760°C helium from IHX A to IHX B occurs in the HGD, comprising internal concentric ducts separated by a layer of insulation, as shown in Figure 22. The inner, highest surface temperature, portion of this concentric duct arrangement (the liner) will be free-floating axially and has no pressure retaining function; the inner pressure pipe that surrounds it will use bellows or other means to accommodate thermal expansion. The insulation between the liner and the inner helium pressure pipe provides for minimization of heat loss and minimization of the temperature of the inner pressure pipe material. A flow of cooler return PHTS helium (350°C), diverted from the circulator outlet, will be directed through the annulus between the helium pressure boundary and the inner pressure pipe. This high-temperature piping design is similar to that applied in the PBMR DPP; however, both the reactor outlet gas temperature and cooling gas temperature are higher in the PBMR NNGP design. For this reason, changes to the design shown in Figure 22 are likely to be required.

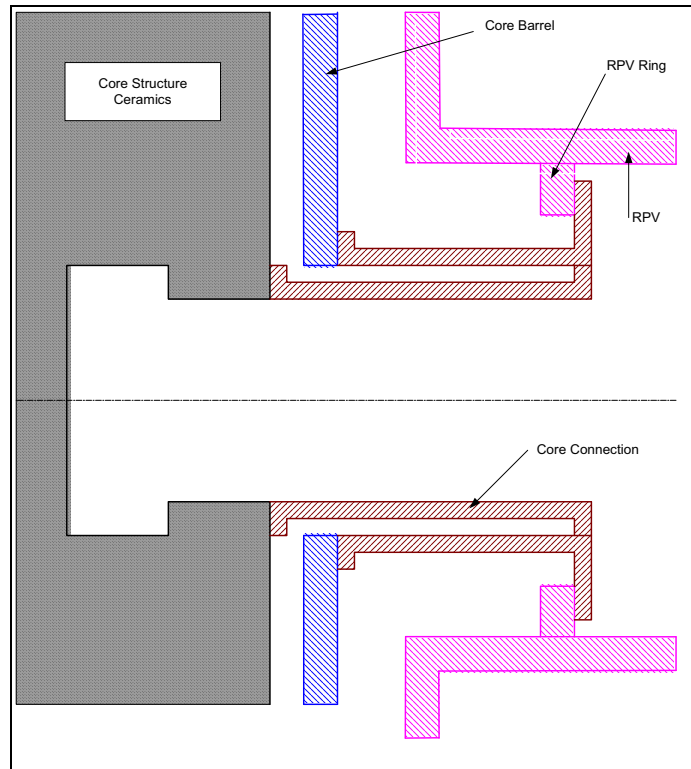


Figure 19 Typical Core Outlet Connection Layout [13]

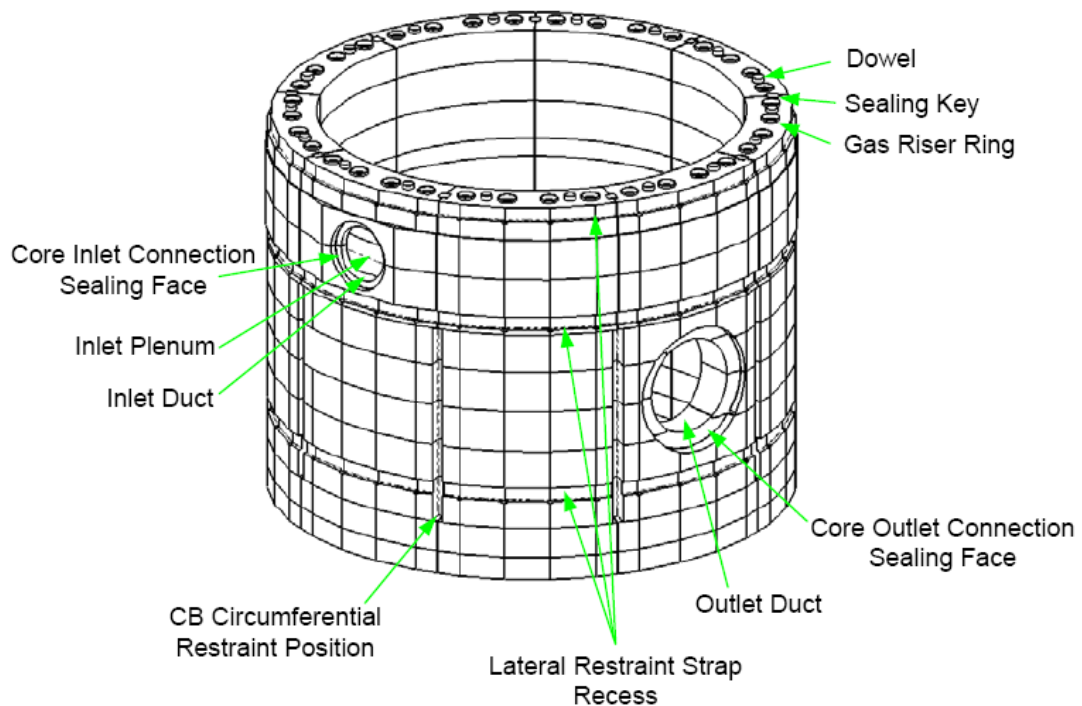


Figure 20 Detail of the Bottom Reflector Ring showing the location of the COC [4]

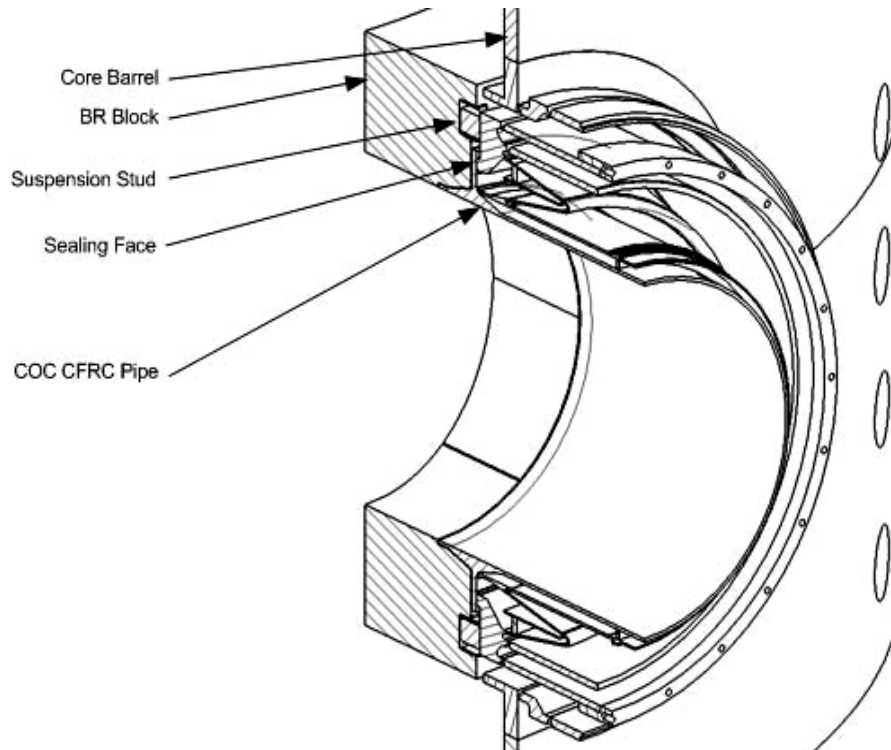


Figure 21 Detail of the COC [5]

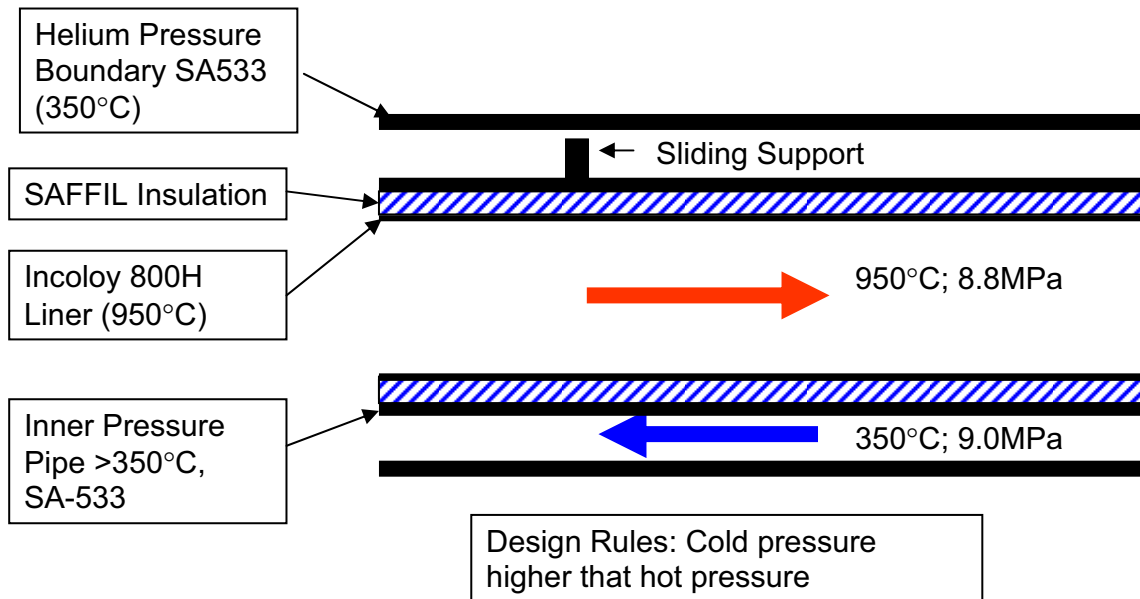


Figure 22 DPP HGD Design Showing NGNP Temperatures

1.3.2 Design Considerations

1.3.2.1 Core Outlet Connection

The Core Outlet Connection (COC) is being designed for the DPP and appears to be applicable to the NGNP Design; however, some modification may be required. The COC directly connects to the Hot Gas Duct Piping and contains a CFRC Inner Pipe (Liner) as the first barrier for the 900 C helium outlet in the DPP. The liner was selected for the COC DPP application due to thermal mixing issues. This liner will almost certainly be required to contain the 950°C helium outlet flow in the NGNP Design. Specifics regarding material are not available for the liner at this point. PBMR has a basic design for the COC for the DPP and a contract for detail design is being negotiated. As noted, the design of the COC was developed for the DPP and a review, potential modification and validation of this design is required for the NGNP (see Design Task C1 and DDN COMP 01-03, Section 3).

The CSC, CB and RPV move independently of each other. Sealing between these components is provided by the COC. The COC is fixed to an inner ring inside the RPV and fixed to the CB. Figure 19 shows a schematic layout of a typical assembly that consists of the CSC, COC and RPV.

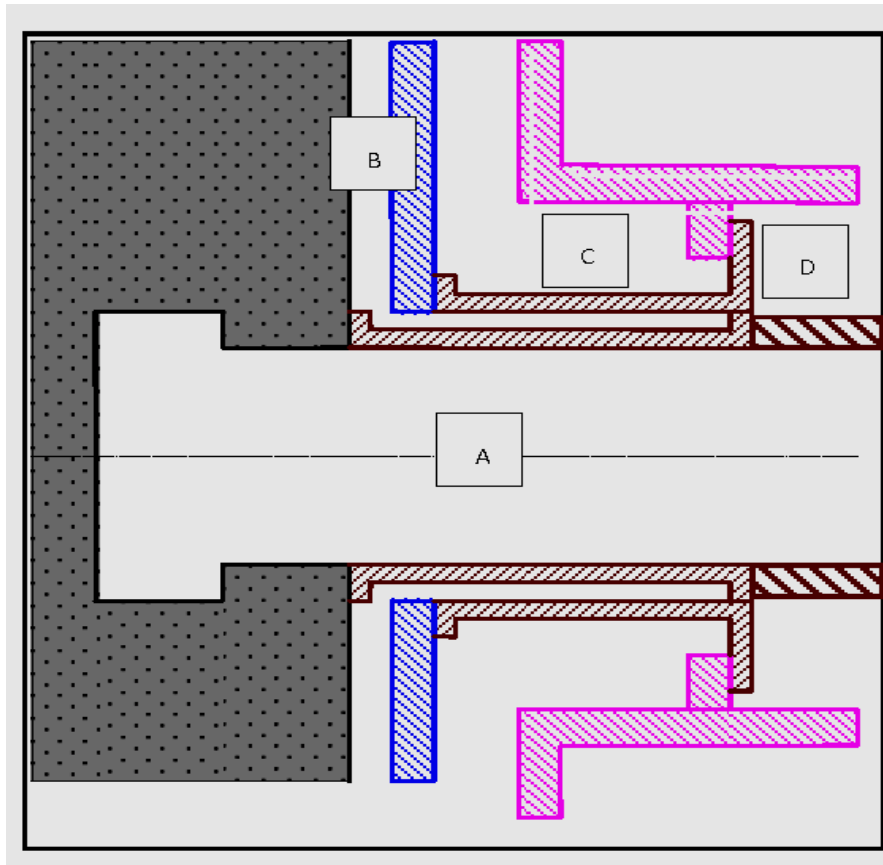
The functions of the COC are as follows (refer to Figure 23):

- To compensate for movement between the RPV and CB.
- To compensate for movement between the RPV and CSC.
- To minimize leakage between the inside of the CB and the Core Outlet (B to A).
- To minimize leakage from the outside of the CB to the inside of the CB (C to B).
- To provide a flow path for the helium that exits the core

During normal operation, there is a possibility of leakage across the Sealing Face. In that event, helium at 500°C in the DPP design would mix with the hot helium at the Core Outlet which will be at 900°C in the DPP design. This would cause a temperature gradient across the liner and would limit the lifetime of a metallic liner. Therefore, a CFRC liner is included to protect the metal components from the temperature gradient. The CFRC liner is more resistant to temperature gradients because of relatively low thermal expansion and contraction properties compared to Alloy 800H. The CFRC liner has currently been developed only for the DPP COC and CFRC is not otherwise used in the DPP Hot Gas Duct. The NGNP preconceptual design did not include detailed consideration of the Hot Gas Duct or the possible use of a CRFC liner. The potential for replacing the current Alloy 800H liner in the NGNP will be discussed later in this report.

The COC is designed to endure the entire plant service life, which is 40 years for the DPP. The COC will be designed in such a way that no maintenance will be required. Should the COC or any part of it fail, the complete system would need to be replaced.

The existing PBMR DPP COC design appears to be adequate for the PBMR NGNP design based on available information. However, the current design of this component was developed for the DPP and needs to be validated for the NGNP. Also, the materials design basis for the CFRC liner needs to be validated for the NGNP design. This includes further investigation of the metallic components of the COC that will be subjected to temperatures greater than 850°C (see Design Task C2, Section 3).



Note: D indicates the annulus between the Hot Gas Duct and the Pressure Boundary.

Figure 23 Schematic Layout of the Core Connection [13]

1.3.2.2 Hot Gas Duct

The HTS piping provides the path for transport of hot helium gas between various components of the HTS. The operating conditions for the NNGP are shown in Figure 13 and temperatures in the various sections of the PHTS and SHTS piping are summarized in Table 4.

Table 4 Helium Temperatures in the NNGP Piping Sections

Piping Location	Temperature (°C)*
Primary Heat Transport System	
RPV to IHX A	950
IHX A to IHX B	760
IHX B to Circulator	337
Circulator to RPV	350
Secondary Heat Transport System	
IHX A to PCHX	900
IHX A to Mixing Chamber	900
Mixing Chamber to SG	840
PCHX to Mixing Chamber	659
SG to Circulator	273
Circulator to IHX B	287
IHX B to IHX A	700
*Initial studies indicate that transient temperatures are only very slightly higher than these.	

The sections of pipe providing for transport of high-temperature helium gas within the PBMR DPP are dual circuit pipes (Figure 22). Their design is based on developments within the German HTR program. In the dual circuit design, the high-temperature helium is contained within an inner circuit (the HGD) and isolated from the HPB. Active cooling is provided in the annulus between the HPB and HGDs. This design limits temperatures seen by the HPB and permits the use of a conventional material for the HPB (SA-533, Grade B, Class 1 or 2) that is maintained within established ASME Code conditions.

As shown in Figure 22, each HGD consists of two layers. The inner layer is a non-pressure-retaining liner that actually channels the high-temperature helium flow. The outer layer is an inner pressure pipe. The inner pressure pipe is designed for the maximum differential pressures that will be seen during normal operation and transients, including DBEs. In all cases where flow is present, the higher pressure

is on the outside of the pressure pipe, tending to leak from the low-temperature to the high-temperature regions. Insulation is provided between the liner and the inner pressure pipes. Supports (not shown) between the inner pressure pipe and the liner are designed to reduce stresses and to restrict convective flow of helium within the insulating layer.

The HGDs are completely enclosed within the piping of the HPB. The design is such that the driving force for the cooling flow in the annulus remains under external pressure for all conditions in which there is forced circulation within the HGD. During events in which forced circulation is lost (pressurized or depressurized conditions), the pressure external to the pressure pipe will rapidly decline to equilibrium with the outlet helium flow.

The pressure pipe and the HPB are designed in accordance with ASME Section III, Subsection NC. Transient conditions within the licensing basis typically result in reduced flow and collapse of the differential pressure across the pressure pipe, thus reducing loads.

The design of the DPP HGD was developed on a first principles basis, using the materials identified in Table 5. The design process utilizes the data provided for Alloy 800H in draft KTA Standard 3221.1, issued by the Kerntechnische Ausschuß (the Nuclear Technical Committee of the German Nuclear Safety Standards Commission). A potential alternative is ASME Section III, Subsection NH for the intermediate temperature pipes.

Table 5 Hot Gas Duct System Materials for the PBMR DPP

Component	Material	Applicable ASME Design Code	Qualification Approach
Core Outlet/CCS Inlet Pressure Pipe	SA-672 Grade J90 (Made from SA-533 Type B, Cl 2 plate)	Section III, Subsection NC	Use NRC-accepted ASME Specification
Core Outlet/CCS Inlet Liner (950 C)	SB-409 Alloy 800H	Not applicable	Design by analysis, based on KTA 3221, supported by appropriate test data
Insulation	Al ₂ O ₃ and SiO ₂ (Saffil)	Not applicable	TBD

While Alloy 800H is incorporated into a number of ASME Code and German DIN standards, the ASME Code does not presently provide for its application at temperatures above 760°C. Alloy 800H is presently covered in draft KTA 3221.1 at temperatures up to 1100°C; hence the selection of this German standard as the basis of the analyses of the liner; however, the lifetime of an Alloy 800H component would become progressively shorter at higher temperatures because of reduced creep strength, reduced effectiveness of the protective oxide film, and microstructural changes within the component.

As a future consideration, it should be noted that an ongoing cooperative initiative between ASME and DOE is presently developing data to support the use of Alloy 800H within the framework of Section III, Subsection NH to 900°C; however, the use of Alloy 800H at 950°C for the liner application will not be addressed in this initiative. Therefore, there is a significant incentive to select and qualify alternate materials for the NNGP liner application.

As noted earlier, the design and materials of choice for the HGDs are based on prior developments within the German HTR program. As part of that development, the HGD design underwent successful qualification testing in Germany at 900°C to 950°C for periods up to 15,000 h. The velocity limit applied in the PBMR DPP design is consistent with that earlier testing. Wind tunnel testing was also used in the course of design verification to evaluate flow-induced loads on the liner.

Finally, there is virtually no exposure to high radiation of any of the components (HPB and inner pressure pipe, liner, or insulation) of the HGDs. Therefore, limit curves for irradiation are not applicable for these components.

PBMR considered materials other than Alloy 800H for use as the HGD Liner. Among these were Ni-base alloys Hastelloy X and Alloy 625 and CFRC. However, Alloy 800H was the choice based on a combination of factors, including lower cost, sufficient strength and environmental compatibility, real life service experience, and the German HTR design and testing work. Alloy 800H has the following advantages as a liner material for the HGD of the DPP:

- Adequate high-temperature strength and creep resistance
- Extensive fabrication experience in large diameter pipe sections
- Extensively tested as liner material for qualification of the insulated “hot pipe” design in the German HTR program.

Limitations of Alloy 800H for the NNGP PBMR HGD design include the following factors:

- Marginal creep strength at temperatures > 900°C.
- Marginal resistance to impure helium at temperatures > 900°C.
- Sensitivity to internal oxidation, with a consequent reduction in strength

Merits of a CFRC liner material for the NNGP PBMR HGD design as a substitute liner material are:

- High-temperature strength, and creep resistance
- Fabrication is possible by fiber-winding large diameter pipe sections to make up the liner.
- Low thermal conductivity perpendicular to fiber orientation helps to limit temperatures of the outer ferritic steel boundary of the hot duct.

The principal disadvantage for the use of CFRC material for the HGD liner application involves details associated with the construction of the pipe. The piping system detailed design is proprietary; however, PBMR believes that the use of a CFRC liner is potentially feasible for the NNGP design and is currently investigating this issue. Also, the use of a higher temperature metallic alloy, such as Alloys 230, X or XR, as a substitute for Alloy 800H should be feasible using current German based pipe construction methods if the use of a CFRC liner is determined not to be feasible, or as an alternative to the Alloy 800H material currently used.

The DPP design uses ~110°C helium in the pipe annulus from the high pressure compressor outlet; however, the NNGP design uses 350°C helium from the primary heat transfer system (PHTS) circulator outlet in this annulus. Helium cooling gas supplied to the cooling annulus and cooling flow are inherently linked in the DPP design and the cooling gas is supplied at the highest pressure in the Brayton Cycle. Loss of cooling in the annulus inherently shuts down circulation in the Brayton Cycle, which causes a

loss of circulation in the pipe and allows an equilibrium temperature in the pipe to develop. This temperature is believed to be $<371^{\circ}\text{C}$, so that the integrity of the SA 533 steel pipes will not be affected. However, circulation and HGD cooling are not inherently linked in the NNGP PCDR design, and the potential exists for a high temperature PHTS transient associated with a loss of heat transfer through the intermediate heat exchanger and a failure to trip the PHTS circulator. The equilibrium temperature in the pipe under these conditions is believed to be high enough to affect the integrity of the pipes. Therefore, because of this issue and the difference in temperatures for the annulus cooling flow and the helium outlet temperature, a HGD design modification will probably be required. Without modification, the Inner Pressure Pipe will probably exceed the normal operational limit of 371°C for SA 533 in the NNGP design. The Helium Pressure Boundary Pipe is also SA 533 and will be close to the 371°C limit for normal operation.

A HGD design for the NNGP should address the following issues:

- Protect the HPB from excessive temperatures
- Retain the use of SA-533 steel for the HPB
- Reduce the HPB external temperatures to a reasonable temperature (e.g., $\leq 100^{\circ}\text{C}$)
- Avoid excessive heat losses
- Eliminate transient concerns noted above
- Easy to manufacture and install
- Less expensive to manufacture
- Make repair to the pipe conceptually possible

A possible design that could achieve these objectives is given in Figure 24. This design could utilize a 2D CFRC liner with a low radial thermal conductivity perpendicular to the fibers and high performance insulation of the type that will be discussed later in the report. Based on preliminary heat flow calculations performed by Microtherm (an insulation vendor), a 450mm radial thickness of aerogel silica based insulation between the liner and the HPB would result in a surface temperature on the exterior of the HPB of $<100^{\circ}\text{C}$ and eliminate the need for annulus cooling, which would eliminate the transient concerns noted above. The thickness of insulation noted would conceptually allow the same exterior pipe dimension and the same radial interior dimension for the high temperature helium flow path inside the liner. The example given in Figure 24 is only one of several alternative designs possible.

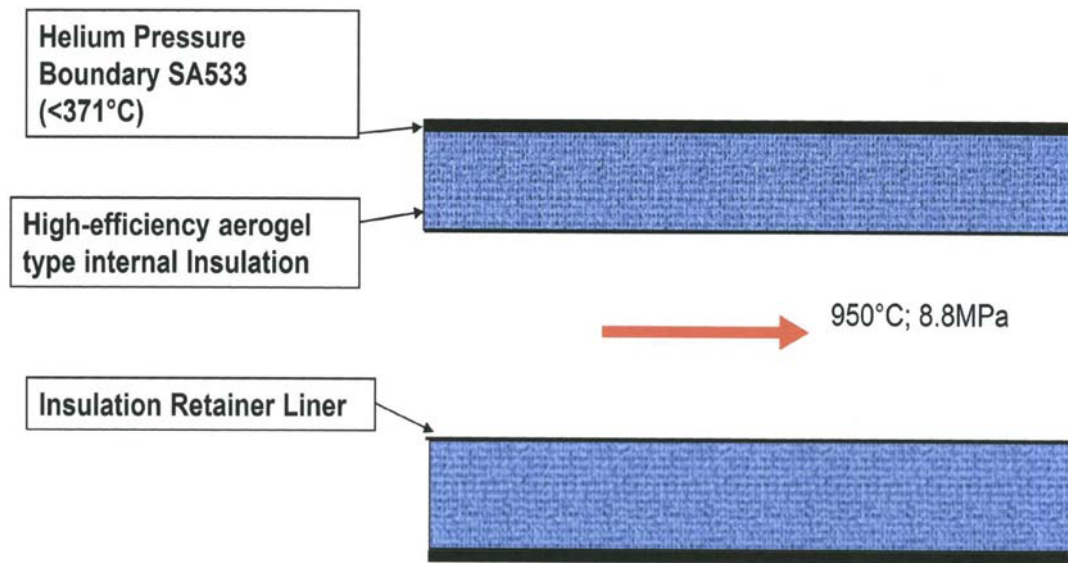


Figure 24 Possible Passive Insulation Design for HGD

Changes made to the DPP design need to be carefully considered because the DPP design has been extensively evaluated for postulated events and validated over many years during the German HTGR program development. The design noted in Figure 24 and other possible designs have not been similarly evaluated and validation of a new design for postulated events could require an extensive effort. Other issues, noted below, also require consideration:

- The properties of the aerogel type insulation in a high temperature helium environment have been estimated and these estimates have been incorporated into the conceptual design noted, but empirical data based on required laboratory testing have not been performed (see DDN COMP 01-04). Therefore, testing will be required to confirm the feasibility and economic desirability of any alternative design.
- Sole reliance for protecting the HPB against hot gas impingement is placed on the passive insulation and the liner because the annulus cooling in the present HGD design would be eliminated in the alternative design noted.
- If comparable reliability of the HPB cannot be assured, an alternate design may require additional reactor building design to protect against a double ended guillotine break (DEGB) postulated pipe failure scenario. On-line monitoring or in-service inspection of the insulation and liner condition may mitigate concern, but these possibilities have not been evaluated at this point.

The conceptual passive HGD design could provide the following benefits:

- Eliminates transient concerns
- Easy to manufacture and install
- Less Expensive
- Repairs to pipe conceptually possible

- Based on preliminary heat flow calculations performed by Microtherm, 450mm radial thickness of aerogel insulation with a liner would result in a surface temperature of < 100C on the outside of the HPB with no annulus cooling
- The passive design is potentially applicable for other HGD sections in the PHTS and SHTS

Whether the concentric design is needed for all of the HGD sections in the PHTS and SHTS still needs to be finalized. It is likely that a SA 533 B single wall design with a layer of internal insulation would be sufficiently conservative for those sections containing helium at <350°C. These are IHX B to the circulator and circulator to the RPV in the PHTS and the SG to circulator and circulator to IHX B in the SHTS, as noted in Table 5. It is almost certain that the NGNP Hot Gas Duct and probably other piping also will require a CFRC liner or an alternate metallic material rather than the Alloy 800H liner used in the DPP design. The materials issues involved are discussed in more detail in Section 2 of this report. It is almost certain, as noted above, that the DPP piping will need some redesign for the NGNP and several issues need to be considered:

- Can the piping be redesigned so that the helium cooling is not required?
- If the above redesign is not feasible, then either the piping will require more efficient internal insulation or the inner pressure pipe and/or the HPB may need to be an alternate material that would allow normal operation at a higher temperature.
- It would; however, be desirable to not replace the HPB material for the piping because this would cause additional complications in joining the alternate material selected to the HPB of the reactor.

The conceptual basis for alternate designs has been investigated in this report; however, a more detailed investigation of the issues involved needs to be performed. Because the piping systems were developed for the DPP, the piping system design needs to be reviewed and potentially modified for the NGNP (see Design Task C3). Also, the materials basis for the piping design needs to be reviewed and potentially modified for the NGNP (see Design Task C4).

1.3.3 Surveillance, Inspection and Monitoring

In general, the HGD System components are not easily replaceable and will be designed for the full lifetime of the plant.

The approach to condition monitoring of the COC and the HGD has not yet been determined for the DPP design.

The monitoring of selected parameters and analysis of data will be used to justify the postponement of remedial actions or the anticipation of scheduled maintenance. Procedures for surveillance, inspection and monitoring of the COC and HGD for the DPP will need to be reviewed and modified as required for the NGNP (see Design Task C5, Section 3).

1.3.4 Tolerance to irradiation Exposure

The COC would be exposed to very low irradiation fluence (about 10^{10} n/cm², E>0.1 MeV) for the life of the plant. There is essentially no exposure to high radiation for any of the piping components (HPB, inner pressure pipe, liner, or insulation). Therefore, irradiation exposure is not an issue for these components.

1.3.5 Range of Operating Temperature

The range of operating temperatures in the HTS piping is indicated in Figure 13 and Table 4. The reactor outlet HGD liner would be exposed to 950°C helium flow. Temperatures seen by other metallic components of the HGD during normal and abnormal operations for the PBMR NGNP design have not been evaluated. Modeling needs to be performed for the NGNP to determine the exposure temperature for the inner pressure pipe for the current design and the metallic components in the COC potentially exposed to temperatures over 850°C (see Design Task C6, Section 3). An evaluation of the current PCDR piping design for the NGNP needs to be made to consider a specific off-normal event that has not been thoroughly evaluated. This off-normal event involves the loss of the secondary heat sink across IHX A and B due to loss of function in the secondary system. One of the issues to be considered that could directly affect the current piping design is that helium cooling in the annulus from the circulator could increase in temperature up to some equilibrium level that could impact the integrity of the SA-533 pressure boundary piping (see Design Task C8 and DDN-COMP 01-02, Section 3).

1.3.6 Qualification of Components

As far as possible, qualification testing of the COC for the DPP will be done at the assembly or component level. Where functions cannot be carried out without interaction with other subsystems, tests will either be carried out at a system level, or test rigs will be used to simulate the interface with other subsystems.

Fabrication of the HGDs for the DPP will be in accordance with ASME Section III, Subsection NC (Pressure Pipes) and design by analysis (liners). Quality control provisions will be employed during the manufacturing, installation, and commissioning processes to ensure that the HGDS functions as per the design.

Efforts to extend appropriate ASME Code sections to include stress allowables for Alloy 800H up to 900°C are presently underway as a cooperative effort between ASME and DOE. It would be desirable to extend the present temperature range to at least 950°C. This would benefit both the design and licensing processes.

The HGD for the DPP will be subjected to qualification testing using representative test sections at appropriate conditions. This is in addition to the qualification testing of the HGD design performed in the German HTR program.

Qualification procedures for the NGNP COC and HGDS need to be developed for the NGNP design (see Design Task C7, Section 3).

1.4 Reactivity Control Components

In the PBMR DPP design, the RCS safety function of ensuring normal hot shutdown relies on the insertion of control rods into the channels provided in the ISR. The RCS is designed to be able to transition the reactor to the zero-power and subcritical condition under all operating conditions and AOOs, and to keep the reactor subcritical in the hot shutdown condition. The power is also limited in the upper region of the core by the control rods that are partially inserted in the ISR during full load operation. In the DPP design, graphite sleeves are used to line the control rod channel openings in the ISR blocks. These sleeves are fabricated from reflector graphite and subjected to high fluence levels at high temperatures. The sleeves are used to ensure that, even in the event of cracking in the ISR blocks, the channels remain clear.

In the DPP design, each control rod consists of six segments containing boron carbide absorber material in the form of rings between two cladding tubes. The segments are held together by articulated joints and suspended to form a complete rod. In the DPP design, each control rod (except the boron carbide) is fabricated using metallic components; therefore, the control rod assembly may have a lifetime less than the life of the reactor and require replacement at some point.

For the NNGP PBMR reactor design, replacement of all or a portion of the metallic components in the control rods with composite materials or alternate metallic materials to extend the lifetime and the temperature range will be considered. Discussion includes the following issues:

- Identification of Components
- Design considerations for the use of composites and/or ceramics
- Tolerance to high irradiation exposure
- Range of operating temperature
- Qualification of components

These RCS components are subject to relatively high temperatures, high radiation fluences and low stresses. The primary design issues are long term stability and continued function under the conditions of exposure. Alternate materials to be considered for this application are limited to composites (either CFRC or SiC/SiC) or alternate high temperature metallic alloys. SiC/C is not considered due to a lack of irradiation data for this material. A primary factor for selecting these materials will be relative cost and availability. SiC/SiC composites are expensive, less available compared to the other material options and have high resistance to radiation damage and high stability; however, CFRC may be adequate for this application. All of these materials can be fabricated in a wide range of complex shapes.

1.4.1 Identification of Components

The RCS consists of both control rods and shutdown rods. The configuration for both the control rods and the shutdown rods is identical, except with regard to chain length. The control rods form a bank consisting of 12 identical rods and the shutdown rods form a second bank of 12 identical rods. These two banks are arranged with alternating rods above the control rod channels in the ISR.

The rods are freely suspended in the ISR column by chains. Guides are not necessary between the CSC and the rods. A large annular gap (25 mm) exists between the control rod and the sleeve to avoid jamming of the rods. The rods are cooled inside and outside by a stream of cold gas to remove the heat generated in the absorber.

The chains link the control rods to the Control Rod Drive Mechanism (CRDM) that is used to raise and lower the control rods in the control rod channels and to hold them at any position in their travel range. The CRDMs are installed above the core and are integrated into the RPV head. The essential parts of the drive mechanisms are given below:

- A link chain to connect the drive mechanism and absorber. When the rod is raised, the chain is stored in a loose pile in a container, and it is drawn out of this container when the rod is lowered.
- An electric motor drive, which holds the control rod in position or moves the rods up or down.
- A gearbox, with a reducing bevel gear and spur gear between the chain sprocket and drive motor.
- An eddy current brake with permanent magnets on the motor shaft to limit drop velocity in case of a SCRAM.

- A shock absorber to absorb the kinetic energy of the falling rod and the rotating masses (installed at the drive-side end of the link chain) in case of a SCRAM.
- A rod position indicator with a resolver as well as proximity sensors for the upper and lower limit positions to indicate rod full-in and full-out positions.

The construction of the control rods and their drive mechanisms is apparent from Figure 8, Figure 25 and Figure 26. Selected data associated with the RCS is given in Table 6.

Table 6 Selected Data Associated with the Reactivity Control System [14]

Parameter	Value
Control rod absorber length	6500 mm
Control rod absorber diameter	100 mm
Control rod maximum travel	Approx. 6500 mm (control rods) Approx 10200 mm (shutdown rods)
Control rod normal speed	1 cm/s
Chain material	Inconel 625
Rod cladding tubes	Incoloy 800H
Rod absorber material	B ₄ C rings
Secondary shock absorber	Incoloy 800H

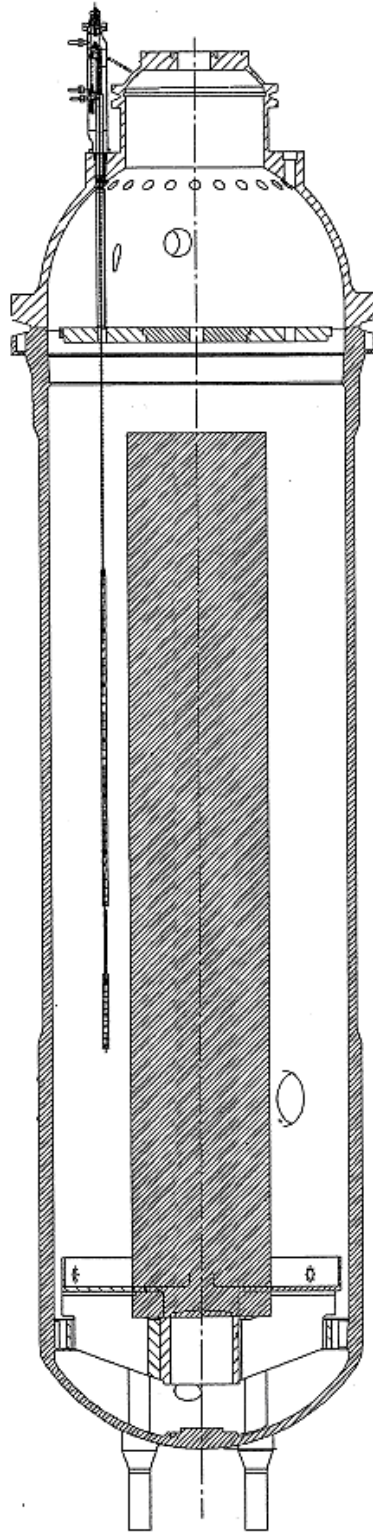


Figure 25 Positioning of the Reactivity Control System [8]

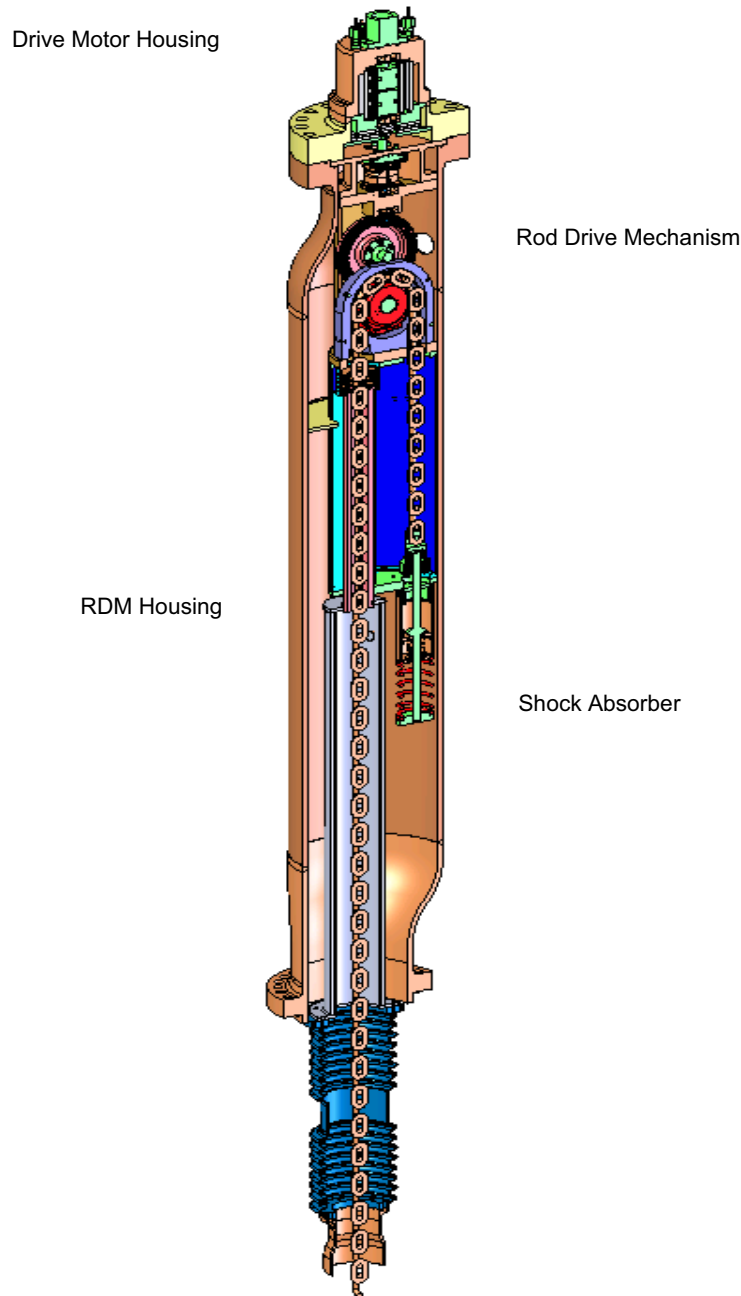


Figure 26 Reactivity Control System Control Rod Drive Mechanism [15]

1.4.2 Design Considerations

The primary function of the RCS during normal operation is reactivity control. It is also used for hot shutdown, fine reactor outlet temperature adjustment, and trimming. Twenty-four rods, 12 for control and 12 for shutdown, are employed in the RCS. Each of the 24 rods consists of six segments containing

absorber material in the form of sintered B₄C rings between two coaxial Alloy 800H tubes in the DPP design, with the annulus containing the absorber being closed at both ends. Small openings are provided in the containers to avoid any significant pressure differentials. The individual segments are held together by articulated joints and suspended from one another to form a complete rod. All of the rods are freely suspended within graphite ISR sleeves on Inconel Alloy 625 chains, attached to the control rod drive mechanism. Shock absorbers are provided on the end of each chain to absorb the kinetic energy of the falling rod in the event of a SCRAM. Finally, 316H stainless steel Guide Tubes are provided to guide the control and shutdown rods into the ISR during all movements of the rods. The metallic materials for components described above are given in Table 7, along with relevant ASME Specifications.

Table 7 Tentative PCDR RCS Metallic Materials for the PBMR NGENP

Component	Materials	Applicable ASME Design Code	Qualification Approach
RCS Chain	SB-446 Alloy 625	Not applicable	Design by analysis, supported by appropriate test data
RCS Absorber Cladding Tubes	SB-407 Alloy 800H	Not applicable	Design by analysis, based on KTA 3221, supported by appropriate test data
RCS Shock Absorber	SB-408 Alloy 800H	Not applicable	Design by analysis, based on KTA 3221, supported by appropriate test data
RCS Guide Tubes	SA-182 F316H SA-312 Gr 316H	Section III, Subsection NG (Tubes)	Use NRC-accepted ASME Specification + EJEMA8 (Bellows)

The individual segments are held together by articulated joints and suspended from one another to form a complete rod. This minimizes torsion caused by asymmetric temperature profiles. Each segment joint is held in place by mechanical stops.

The Alloy 800H cladding tubes of the control rods in the DPP design will be designed by analysis from first principles, supported by appropriate test data. Design criteria to be adhered to include <0.4% creep strain during full-life under normal operation and <0.1% strain during all off-normal events (taking into account the effects of irradiation on tensile ductility). Materials data utilized come from KTA standards, suppliers' data, extrapolations from ASME data, and additional testing, if necessary.

The Alloy 625 chain will nominally operate at 500°C for the DPP design, but may reach temperatures up to 800°C for DBEs. Alloy 625 was chosen as the chain material rather than Alloy 800H, because of its greater high temperature strength. Alloy 625 is incorporated in ASME Section II, Parts B and D. As with the Alloy 800H components, the qualification approach for the Alloy 625 chains is design by analysis, supported by appropriate test data.

No replacement of the control rods is planned but access for and means of replacement exist. Another challenge for the control rods is associated with DBEs involving passive heat removal. In this instance, temperatures up to 1000°C might be experienced. This is a potential driver in consideration of CFRC or SiC/SiC for RCS application in the DPP or NGNP.

Since the early 1980s, consideration and study has been given to the use of CFRC or SiC/SiC materials for control rods [16]. Such materials can have advantages over metallic alloys in terms of mechanical, physical, and thermal properties and can be tailored during manufacture to optimize one or more properties. Use of CFRC material for control rods would minimize any concerns associated with corrosion (normal operation and DBA conditions) or high temperature strength during DBAs. There has been concern that very high temperatures during DBAs could cause failure of the metallic control rod structure by mechanisms such as slumping or creep-collapse. Although such events would not compromise safety, they would have many other significant negative consequences.

The use of composites for the high temperature RCS components would eliminate any concerns relative to control rod failure or damage due to very high temperatures during DBAs. If there is a “weak link” associated with this application for CFRC, it is almost certainly that of its response to irradiation in terms of dimensional stability. Studies of such effects have been performed with CFRC materials with several fiber architectures and fiber materials [16]. These studies have covered irradiation temperatures to 800°C and fluences to 10 dpa with the following general results:

- The complexity of the CFRC architecture appears to improve dimensional stability during irradiation, those composites with 1D architecture are the least stable dimensionally and those with 3D architecture have the greatest dimensional stability.
- 3D composites based on pitch fibers show much greater dimensional stability under irradiation than do those composites with PAN fibers. Recent preliminary data for 800°C, 10 dpa irradiated CFRC showed that, while some shrinkage was observed, it retained strength and did not enter into a swelling regime. This is certainly encouraging in terms of the potential use of CFRC materials as RCS components.

CFRC products are generally commercially available as sheets, plates, pipes, and rods but not with 3D architectures. The latter normally requires hand lay-up at high cost.

SiC/SiC composites show essentially no degradation in mechanical properties up to 1500°C without neutron irradiation during short term tests (excluding oxygen effects). The mechanical properties are nearly unchanged from room temperature values. These types of composites have relatively less maturity for manufacture compared to CFRCs with less design flexibility, higher manufacturing cost and less availability. This material has more stability than CFRCs under high levels of neutron irradiation.

Figure 27 indicates the current design of the DPP design control rod cladding and joint. This design would need to be changed if composites were used to replace Alloy 800H for this part of the RCS assembly. PBMR has initiated a study to investigate the feasibility of a design and materials change for this component in support of both the DPP and NGNP designs. While acceptable for the DPP, the use of Alloy 800H in the high temperature and high fluence areas of the RCS does not appear to be adequate for the NGNP design, based on available information. This issue will be discussed further in Section 2 of this study. Discussion of alternate materials for this component for the NGNP application are given in this study; however, a review of the adequacy of the Alloy 800H material is required for the NGNP application and a recommendation made for alternate materials to be used in the NGNP design, if required (see Design Study D1, Section 3).

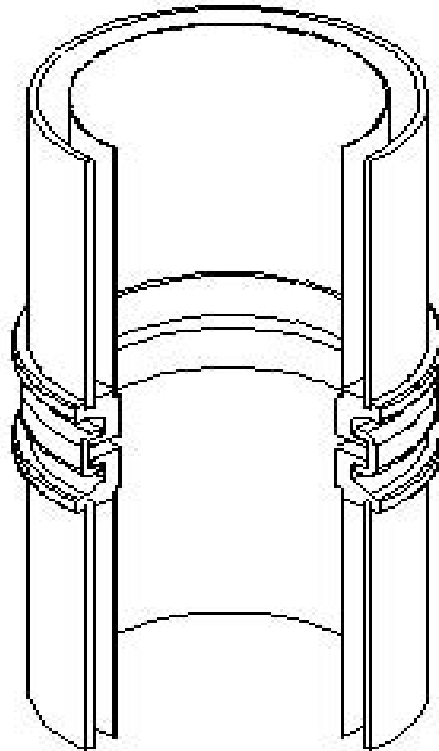


Figure 27 DPP Metallic Control Rod Articulated Connection [17]

1.4.3 Tolerance to irradiation Exposure

The RCS cladding and joints are estimated to be exposed to a neutron fluence of up to 5×10^{21} n/cm² ($E > 0.1$ MeV) (about 3.6dpa, carbon or about 7 dpa SiC) for the NGNP design at 60 years. The estimate is based on DPP fluence+25% (power correction) multiplied by 1.5 (design life correction) for NGNP fluence. A significant amount of irradiation data for Alloy 800H has been collected in the German HTR program. Some of their early results were published in Reference 18. Considerably more irradiation data on Alloy 800H has been generated by Forschungszentrum Jülich in Germany. Examination of the existing radiation hardening (strength increase and ductility decrease) data for Alloy 800H indicates that its EOL ductility may be adequate to meet the criteria for the NGNP design. Further, these Alloy 800H components can be replaced, if necessary, in both the DPP and NGNP designs. Section 2 contains a discussion of irradiation exposure to materials applicable to the RCS application. Modeling is required for the ISR to determine the fluence of the control rods and chains for the NGNP application (see Design Task D2, Section 3). If a CFRC material was selected for this application, an irradiation program would be required to determine post-irradiation properties of the specific material to be used (see DDN COMP 01-03, Section 3)

The situation of Alloy 625 with regard to radiation effects is also very similar to that for Alloy 800H, but irradiation levels should be lower. The chains can be replaced, but the likelihood of replacement being required is even less than for the control rods.

1.4.4 Range of Operating Temperature

The maximum temperature of the control rods during normal operation for the NGNP design is estimated to be 750°C. The estimate is based on DPP temperature plus 50°C for NGNP temperature. Temperatures up to 1000°C are projected for certain DBAs involving passive heat removal. The temperature exposure is the limiting issue for the continued use of Alloy 800H for this application. The shock absorber temperature will mimic that of the bottom sections of the control rods. The Alloy 625 chain will operate nominally at 500°C, but could reach temperatures up to 800°C in the case of DBEs/DBAs. The approach for qualifying these components is design by analysis, supported by appropriate test data.

A modeling study to verify the temperature of the RCS control rods and chains needs to be performed for the NGNP design (see Design Task D3, Section 3).

1.4.5 Qualification of Components

Qualification testing for RCS components has not been investigated for the NGNP design. Therefore, a study to determine qualification testing and procedures for these components is needed for the NGNP design (see Design Task D4, Section 3).

1.5 Core Support/Core Barrel Interface Insulation

Insulation components are used in the bottom reflector region of the PBMR NGNP CSC design to reduce the temperature exposure of metallic load-bearing components. Discussion will include the following areas:

- Identification of components
- Design considerations for the use of specific ceramics
- Tolerance to irradiation exposure
- Range of operating temperature
- Qualification of components

These components are subjected to compressive stresses and are fabricated in the form of carbon blocks, fused ceramic forms or plate material that can be fabricated into complex shapes. The key properties needed for this type of application are low thermal conductivity, material stability under compressive loading and fabricability for the specific application. Material choices include baked carbon or fused silica insulation materials, based on investigations that have been performed for the DPP design. These materials can be fabricated into a wide range of forms. Resistance to radiation damage is not a primary consideration because these components are used in an area of fairly low fluence.

1.5.1 Identification of Components

Layers 1, 2 and 3 in the DPP Bottom Reflector will be insulation layers of SGL Baked Carbon Type NBC-07 in the DPP design. The plan for the NGNP is to utilize baked carbon for these layers unless a layer of fused quartz is required. The layer of fused quartz may be required because fused quartz has better insulation properties than the baked carbon. The need for a material with enhanced insulation properties will be determined after an analysis to establish the insulation requirements of the NGNP CSC has been completed. Baked carbon is preferred for use as an insulator in this area because its neutronic properties are similar to the core graphite. It is also probable that one or more thin layers of CFRC will be used as thermal expansion compensators in the NGNP design. Based on current information, it is unlikely that insulation will be required near the top reflector or other locations in the CSC.

The insulation and CFRC layers will extend across the full cross-section of the bottom reflector structure and are shown in Figure 28. A horizontal section of the insulation layers below the BR showing the insulation segments is shown in Figure 29.

1.5.2 Design Considerations

The key properties of the insulation materials proposed for use as a primary or alternate material are given in Section 2.

The NBC-07 carbon to be used for this application is the non-graphitized precursor to NBG-18 graphite used for both the DPP and NGNP CSC graphite material. The NBC-07 material is impregnated once and re-baked at a nominal temperature of 1100°C following impregnation. Grade NBC-07 carbon is a vibration molded carbon where the “against grain” orientation is the direction parallel to the pressing of the billet during forming and “with grain” orientation is the direction perpendicular to the pressing direction. Grade NBG-18 graphite exhibits slight anisotropy in properties; however, the combination of isotropic filler coke and vibration molding render the NBC-07 material essentially isotropic.

The analysis of the CSC for insulation requirements for the NGNP was not completed during pre-conceptual design. Therefore, a temperature analysis study of the upper and lower reflector regions for the NGNP is required to determine the insulation requirements that will be required to protect metallic support components (see Design Task E1, Section 3).

1.5.3 Surveillance, Inspection and Monitoring

Surveillance, inspection and monitoring procedures for insulation in the CSC are not required because these components will be designed for the reactor lifetime.

1.5.4 Tolerance to irradiation Exposure

Based on available information, baked carbon insulation and fused quartz are used in an area of the core that is not exposed to significant fast neutron irradiation; however, a specific analysis has not been performed for the NGNP. Therefore, a modeling study is required be performed for the NGNP to determine the radiation exposure expected for Layers 1, 2 and 3 of the Lower Reflector region of the CSC (see Design Task E2 and DDN-4, Section 3).

1.5.5 Range of Operating Temperature

It is estimated based on available information that the maximum temperature exposure for the layers of insulation is 700°C. The range of operating temperature for fused quartz insulation is up to 1050°C under normal conditions; however, a practical limit, based on projected reactor operational temperature cycles, is probably in the 900-950°C range. Baked carbon has an operating range up to 1000°C. Therefore, these materials should be adequate for this application.

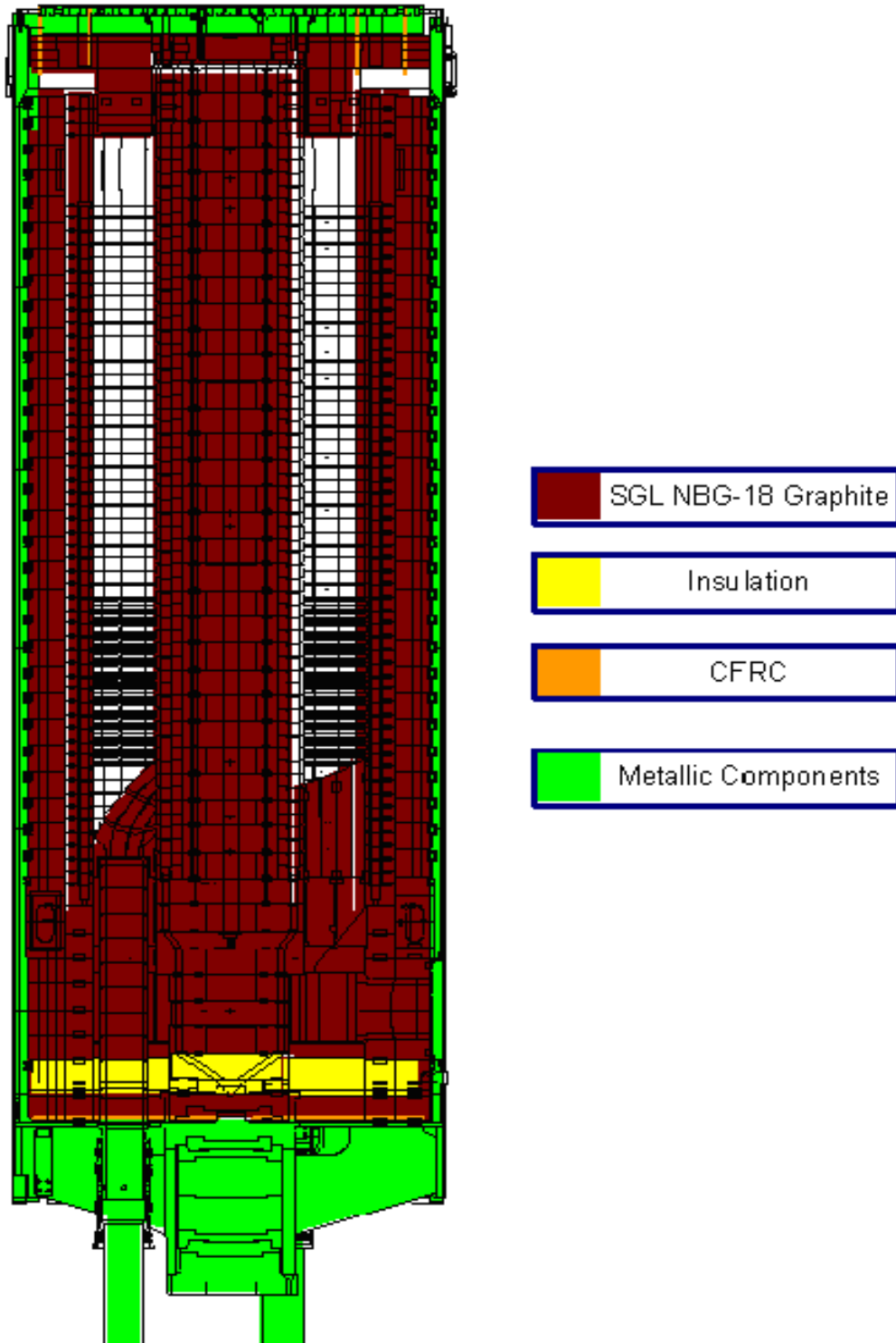


Figure 28 Probable Location of Insulation in the NGNP Core [20]

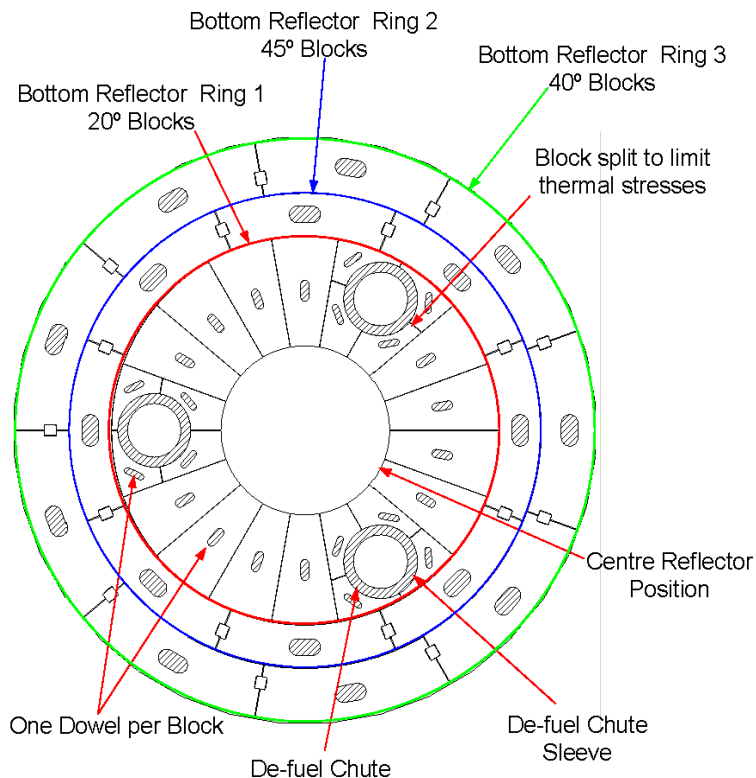


Figure 29 Bottom Reflector Horizontal Section Showing Typical Insulation Layers [4]

1.5.6 Qualification of Components

The qualification procedures for the baked carbon are discussed in Reference 19 and will be discussed in Section 2 because the qualification activities essentially involve a full characterization of the material applicable for the application. Qualification procedures for the fused quartz material will need to be developed if required for the NNGP application (see Design Task E3, Section 3).

1.6 High Temperature Section Insulation

Insulation components are required within the IHX itself to limit heat loss and to protect the metallic piping and IHX pressure vessel from excessive temperature exposure. Similar requirements are found in the secondary piping from the IHX to the process coupling heat exchanger and/or steam generator. In the case of the latter, it is desirable to consider the use of passive insulation in specific areas of the secondary system piping rather than the complex actively-cooled piping design of the type used for the primary system piping. Discussion will include the following areas:

- Identification of components
- Design considerations for the use of specific insulation materials
- Range of operating temperature
- Qualification of components

The insulation associated with these components is non-load bearing. These insulation components would normally be fabricated in the form of felts, batts, woven tubular products or fused ceramic insulation products that can be fabricated into complex shapes. The key properties needed for this type of application are low thermal conductivity, material stability and fabricability for the specific application. Material choices would include silica, alumina or zirconia based insulation material which can be fabricated in a wide range of forms. Resistance to radiation damage is not a consideration because these components are used in areas of essentially no radiation exposure.

IHX assumptions used to evaluate the insulation required for IHX A and B are given in Section 1.7.

1.6.1 Identification of Components

An IHX concept, designated Option C, was selected as the basis for further work on the NGNP Intermediate Heat Exchanger (IHX) in Reference 7. Insulation internal to the IHX units was not a part of the Reference 7 study but is considered within this study. Sketches of the IHX concepts NGNP IHX B (left) and IHX A (right) based on Option C are shown in Figure 30. IHX A connects directly to the NGNP core outlet via the COC and the HGD and has an inlet temperature of 950°C and an estimated outlet temperature of 760°C. IHX B connects directly to the outlet of IHX A and has an estimated outlet temperature of 337°C. The HPB for each unit is fabricated from SA-533B carbon steel that needs to be maintained at less than 371°C during normal operation. IHX A has a cooling annulus (not shown in Figure 30) with 350°C helium flow from the circulator. Therefore, internal insulation is required to maintain the HPB for both IHX A and B below the operational maximum temperature noted. It is assumed that components internal to the HPB will not require insulation except the baffle shown as light green. The baffle will also require insulation to reduce parasitic heat losses. Components internal to the HPB will be fabricated from metallic components suitable for the temperature environment.

The flow path in IHX A is shown in Figure 31. The secondary flow path is shown in yellow and the primary flow path is shown in red. The flow path given assumes a shell side coupling option for IHX A and B shown in Figure 32. Note that IHX A is on the left and is directly connected to the Reactor Outlet Pipe. The flow paths within the individual Plate Fin Heat Exchangers (PFHE) assumed to be used in the Option C design is given in Figure 33. Selected IHX A and B design parameters are given in Table 8.

1.6.2 Design Considerations

There is currently no information associated with insulation design of the IHX; however, it is clear that a design study of the IHX systems will be required to evaluate the insulation required and to provide a more detailed conceptual design of the IHX systems for the NGNP (see Design Task F1 and DDN-4, Section 3).

1.6.3 Range of Operating Temperature

IHX A will operate in the range from about 950°C to 760°C. IHX B will operate in the range from about 760°C to 337°C. A modeling study is required to evaluate the temperature distributions in IHX A and B (see Design Task F2, Section 3).

1.6.4 Qualification of Components

No information is currently available for the qualification of IHX A and B. Therefore, a qualification plan is required for these systems (see Design Task F3, Section 3).

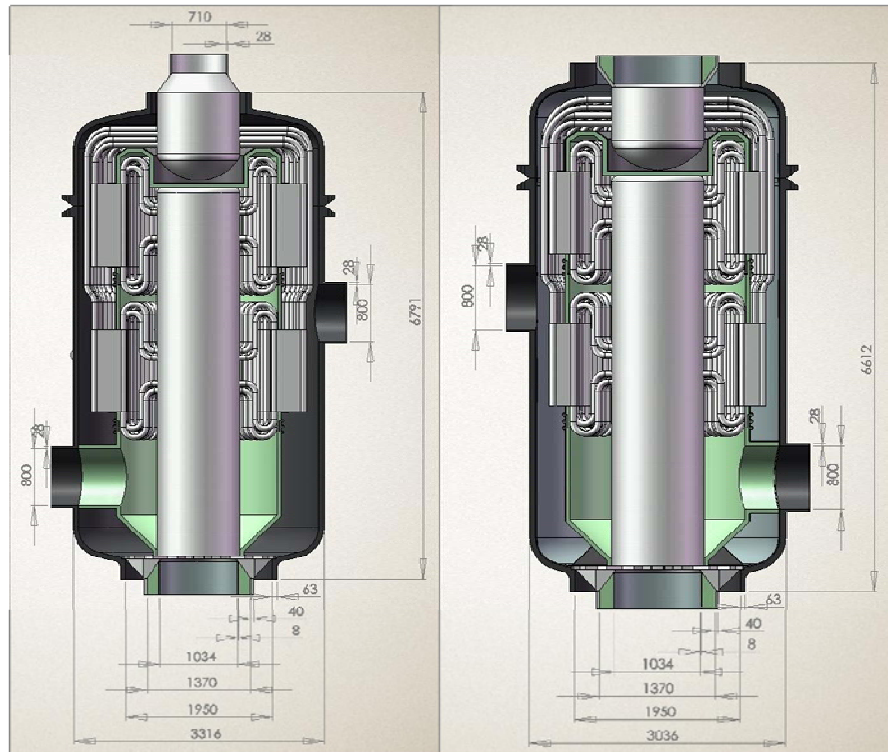


Figure 30 Option C Concepts of NGNP IHX A and B [6]

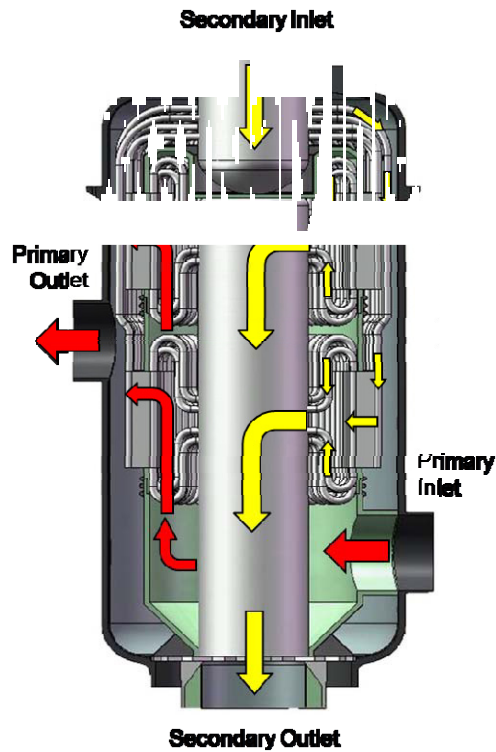


Figure 31 Helium flow paths in IHX A Assuming Shell Side Coupling

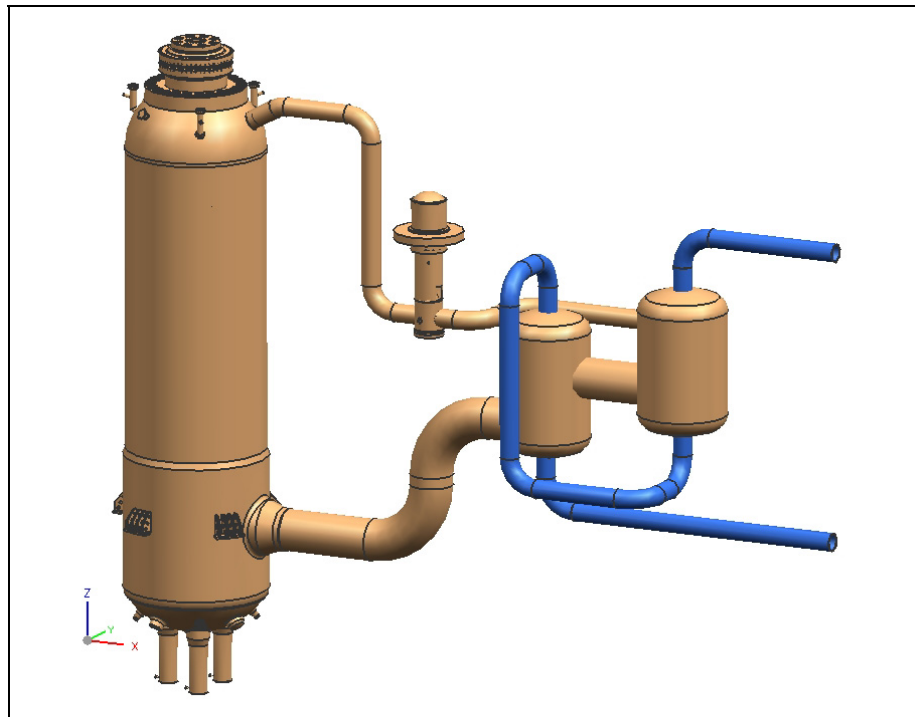


Figure 32 Shell Side Coupling Option of IHX A and B [6]

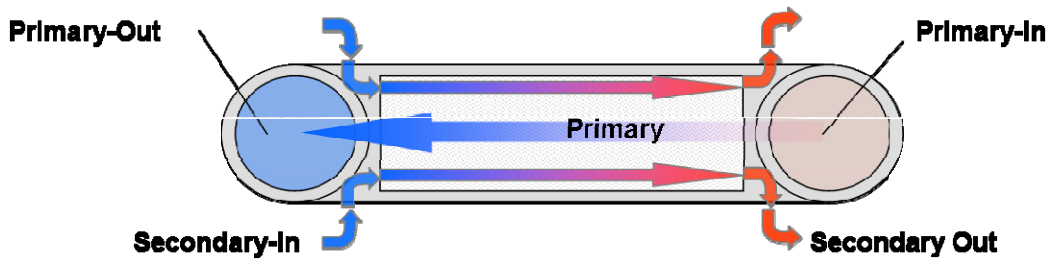


Figure 33 Heat Exchanger Flow Paths

Table 8 Tentative IHX A and B Design Parameters

Feature	IHX A	IHX B
Number of Cores	138	170
Vessel OD, m	3.0	3.3
Vessel Height, m	6.6	6.8
Total Weight, kg	11,000	

1.7 LIST OF ASSUMPTIONS

Piping assumptions used to evaluate the applicability of the DPP design for the NGNP application are given below:

- The primary outlet helium flow and pressure is 160kg/s and 8.8Mpa
- The ID of the liner pipe is 1000mm
- The liner has a wall thickness of 10mm, is not pressure retaining and allows high pressure helium to access the insulation
- The wall thickness of the inner pressure pipes is 50mm
- The radial distance across the cooling annulus is 240mm
- The radial distance across the insulation is 200mm
- The OD of the HPB needs to be maintained $<100^{\circ}\text{C}$
- The inner pressure pipe and the HPB need to be maintained $\leq 371^{\circ}\text{C}$
- The temperature of the annulus cooling flow is 350°C and has adequate flow to remove dissipated heat
- The length of the HGD piping [from the reactor to IHX A] is 10m
- Radiation, convection and conduction needs to be considered
- ASME Code thermal conductivity data for SA 533 steel is used. Data is contained ASME Code Section II, Part D, Table TCD, Material Group B

IHX assumptions used to evaluate the insulation required for IHX A and B are given below:

- Insulation is required on the ID surface of the IHX A inner pressure vessel
- Insulation is required on the ID surface of the IHX B HPB
- The temperature of the annulus cooling flow in IHX A is 350°C and has adequate flow to remove dissipated heat
- The inner pressure structure and the HPB need to be maintained $\leq 371^{\circ}\text{C}$
- The wall thickness of the pressure retaining IHX structures is 50mm
- Insulation is required to protect against parasitic losses within IHX A and B. Losses need to be reduced to the lowest reasonable extent possible. This probably involves insulation of the baffle on the OD surface
- Other piping within the HPB does not require insulation
- The OD of the HPB needs to be maintained $<100^{\circ}\text{C}$
- Adequate radial distance within the HPB is available for the thickness of insulation required
- Radiation, convection and conduction needs to be considered
- ASME Code thermal conductivity data for SA 533 steel should be used as noted above

1.8 References

1. NNGP Special Study 20.2: Prototype Power Level Study, NNGP-20-RPT-002, January 26, 2007
2. Reactor Parametric NNGP Special Study, NNGP-NHS 90 PAR, August 2008
3. NNGP PCDR, Section 4, Nuclear Heat Supply System, Revision 0, NNGP-04-RPT-01, May 2007
4. Core Structure Ceramics Design Description, Document 026224, Revision C (draft), 6/05, Proprietary Class 2
5. Core Structure Ceramics Design Report, PBMR Document Number 015908, Revision D (Draft), July 2008
6. NNGP PCDR, Section 6, Heat Transport System, Revision 0, NNGP-06-RPT-01, May 2007
7. NNGP Conceptual Design Study, IHX and Heat Transport System, NNGP-HTS-RPT, TI001, Rev. 0, April 2008
8. PBMR Demonstration Plant Safety and Analysis Report, Document Number 001929, Revision 2, Chapter 4, August 2006
9. Military Handbook 17-5, US DOD, Volume 5, June 2002
10. PBMR Material Qualification Plan ,Carbon Fiber Reinforced Carbon Strap, Document 031327 (draft), 8/05
11. Technical Description of the PBMR Demonstration Plant, Doc 016956, Rev 4, February 2006
12. Brief Description of the PBMR Design as Applied to the NNGP, Presentation by Mark Mitchell, Idaho Falls, ID April 2007
13. PBMR Gas Cycle Pipes System, Core Connection Development Specification, Document Number 031975, Revision 1 Approved, May 2006
14. PBMR Demonstration Plant Safety Analysis Report, Document Number, 001929-4 Rev 2B (Draft), Chapter 4, Reactor Unit and Fuel, 09/07
15. US Design Certification, High Temperature Materials- Metallics, Document Number 089723, Rev. 1, April 2008
16. "Evaluation of Materials Issues in the PBMR and GT-MHR", EPRI, Palo Alto, CA: 2002, 1007505
17. The Use of Advanced Materials in VHTRs, Shahed Fazluddin, et al, 2nd International Topical Meeting on High temperature Reactor technology, Paper E06, Beijing, China, September 22-24, 2004
18. 'Irradiation Behavior of High-Temperature Alloys for High-Temperature Gas-Cooled Reactor Service', Nuclear Technology, Vol. 66, No. 3, September 1984.
19. NBC-07 Baked Carbon Material Datasheet, PBMR Document Number 022141, Rev. 3, June 2008
20. Presentation, Design and Materials Aspects of PBMR, Mark Mitchell et al Anaheim ANS Meeting 2008

2 MATERIALS EVALUATIONS

This section addresses the potential materials identified for the components described in Section 1. This section will document the review of materials data from U.S. National Labs and other sources, including NASA. Most information given in this section was not documented in the PCDR. The anticipated operating environment for each material and the associated components will be characterized, as allowed by the present state of design development. Where the state of the design does not provide complete information, reasonable estimates are provided, based on scoping estimates and/or engineering judgment. Based on Section 1, the material properties of the candidate ceramic, composite or metallic alloys potentially applicable for these components will be defined. The evaluation will summarize material properties such as thermal stability, thermal conductivity, strength values, creep, and other factors required to assess the viability of the materials for normal operating conditions, anticipated transients, abnormal events and design basis events. The summary of materials properties will cover at least the range of conditions identified in the NNGP PCDR. The activities necessary to codify the selected materials (e.g., in the ASME and ASTM codes) and any additional work needed to support NRC licensing of the plant will be evaluated. None of the applications for composite materials identified in Section 1 for the NNGP are ASME Code applications. Therefore, this evaluation will summarize which activities are likely to be required for NRC approval, including testing development, determination of required material properties, and codification activities. An estimated timeline and costs for these activities has been developed; however, because of the extended times and the significant scope involved with these activities, the estimates and timelines should be viewed as a best guess only.

2.1 Ceramic Matrix Composites (CMCs) including CFRC and SiC/SiC

Carbon fiber reinforced carbon (CFRC) materials are high strength composites consisting of a carbon or graphite matrix with carbon fiber reinforcement. Characteristic properties without considering irradiation include: [1]

- High specific strength and rigidity at elevated temperatures
- Low density and open porosity
- Low thermal expansion
- Extremely high resistance to thermal shock
- Electrical conductivity
- Anisotropy. In materials with aligned fibers, selected properties including the flexural and tensile strength, electrical and thermal conductivity have different values for different fiber orientations (parallel or perpendicular to the fiber or layer)
- Excellent resistance to alternating loads, even at high temperatures
- Pseudoplastic fracture behavior
- Corrosion resistance
- Tailorable physical and mechanical properties

SiC/SiC composites are high strength composite materials consisting of a SiC matrix with SiC fiber reinforcement. Characteristic properties without considering irradiation include:

- High specific strength and rigidity at elevated temperatures

- Low density and open porosity. Specific SiC/SiC composite materials can be manufactured to have a low helium permeability
- Low thermal expansion
- Pseudoplastic fracture behavior
- General chemical inertness
- Predictable fracture mode
- Tailorable physical and mechanical properties

The key differences in these materials are:

- With specific fiber types, SiC/SiC composites show little swelling or volume expansion under irradiation up to 10dpa compared to CFRC
- CFRC starts to show indications of degradation at low irradiation doses. In general as irradiation continues, dimensional changes, increases in strength and decreases in thermal conductivity continues to turnaround. Following turnaround, the properties rapidly deteriorate.
- SiC/SiC composites are less available, more expensive, less mature and less versatile as engineering materials compared to CFRC materials or high temperature metallic alloys.

The CFRC components to be used in the PBMR DPP design in areas with little or no irradiation exposure are based on PAN (polyacrylonitrile) fibers. The CFRC matrix material is a carbonized phenolic resin. Different grades of CFRCs have been selected for the NNGP strap and tie rod applications based on their respective functions and requirements. The main difference between the two grades is the fiber architecture. The materials to be used in the NNGP for these applications were selected primarily for their high temperature strength, creep resistance and low thermal expansion properties. However, it should be noted that the fluence levels associated with these applications is only an estimate for the NNGP and the actual fluence levels that are obtained following NNGP modeling studies may require incremental testing relative to the DPP.

2.1.1 Manufacturing

2.1.1.1 CFRC

CFRC materials are comprised of two components, highly ordered carbon fibers and a carbon matrix. They are most commonly made by gradually building up a carbon matrix on a fiber preform through a series of impregnation and pyrolysis steps. Although more expensive than graphites, they are considerably stronger and tougher than graphites and retain the many desirable attributes of graphite, including high thermal conductivity and low thermal expansion [2]. CFRC materials are typically described as being unidirectional (1D), two-directional (2D), or three-directional (3D). This indicates the number of fiber bundle directions that the composite possesses. In 2D CFRC, the fibers, in the form of multi-filament tows, are woven into a cloth or, alternatively, carbon filaments may be sprayed from a spinneret to form a felt or mat. The woven cloth is then layered to form the desired thickness. In a 3D CFRC, the fiber bundles are usually mutually perpendicular.

The manufacture of carbon based composites begins with the production of the carbon fibers, which are long bundles of graphite plates with a crystal structure layered parallel to the fiber axis [2]. They are highly anisotropic and, for example, may have an elastic modulus in the fiber axis direction that is greater than 100 times the modulus perpendicular to the fiber axis. For commercial high performance CFRC, the fiber precursor material is generally either polyacrylonitrile (PAN) or mesophase pitch. The use of pitch

fibers would probably be a better choice for an application that is exposed to significant neutron irradiation such as the RCS control rods. PAN-based carbon fibers are far more resistant to compressive failure than their pitch-based counterparts. They are dominant in high strength, high temperature applications and represent ~90% of the total carbon fiber production. However, the PAN-based carbon fibers do not achieve tensile modulus and thermal conductivity values comparable to those of fibers produced from mesophase pitch, and the latter are used where those properties are important.

The processing of carbon fibers, whether from PAN- or pitch-based precursors, is quite similar [2]. Production of both of the fiber types involves spinning, oxidative stabilization in air at 200°C to 400°C and high temperature carbonization and graphitization.

In a typical process for PAN-based fibers, a PAN copolymer containing ~95% acrylonitrile is dissolved in one of various solvents (e.g., dimethylacetamide or nitric acid) to form a highly concentrated polymer solution (20 to 30% polymer by weight) and pumped through a wet-spinning system. The gel fiber that exits the spinning process undergoes a series of washing (in dilute solvent), drawing and drying steps. The as-spun fibers are then thermally stabilized under tension to preserve the molecular structure that is generated during drawing. This is normally done in air at 200 to 400°C and takes up to several hours. The heating rate is carefully controlled because the stabilization reactions are highly exothermic. The fibers are next heated slowly in an inert atmosphere to temperatures in the range 1000 to 1500°C. This drives out all non-carbon constituents and changes the fiber from a bundle of polymer chains into bundles of linked hexagonal graphite plates. This step is known as carbonization. Additional thermal treatment of PAN-based carbon fibers at temperatures >1700°C (“graphitization”) decreases their tensile strength, but the tensile modulus continues to rise with temperature. PAN based carbon fibers develop a fibrillar microstructure (see Figure 34) which contains regions of undulating ribbons. This structure is much more resistant to premature tensile failure resulting from microscopic flaws than microstructures with extended graphitic regions transverse to the fiber axis, such as those seen in mesophase pitch-based carbon fibers. Therefore, PAN-based fibers tend to develop exceptional tensile strengths.

The leading PAN-based fiber, T300, is widely used in the aerospace industry; primary suppliers are Toray and Cytec. A potential issue with these fibers is lot-to-lot variation (as much as 15%) in properties. Its price varies over the range 12 to \$80/lb, depending on specific requirements imposed by the buyer. Fibers with pedigree and QC consistent with the nuclear industry would be ~\$55/lb (CY 2002). This is still a low fraction of the cost of most finished CFRC materials.

Pitch-based carbon fibers are unique in that they can develop extended graphitic crystallinity during carbonization/graphitization. The mesophase pitches used for the production of high-modulus fibers are most commonly formed by the thermal polymerization of petroleum- or coal tar-based pitches. (Petroleum-based pitches now dominate because of environmental concerns relative to the coal-tar pitches.) The petroleum pitch is commonly formed as a by-product during cracking of the heavy oil fraction of crude oil [2]. A mesophase pitch is produced by heating the pitch in an inert atmosphere for an extended period of time at 400 to 550°C. The procedures used in the manufacture of carbon fibers from mesophase pitch are quite similar to those discussed in the paragraph above for PAN-based fibers. The four basic steps are melt-spinning, oxidative stabilization, carbonization and graphitization. In the first step, molten mesophase pitch is extruded through a multi-holed spinnerette. The as-spun fibers are then drawn to improve their axial orientation.

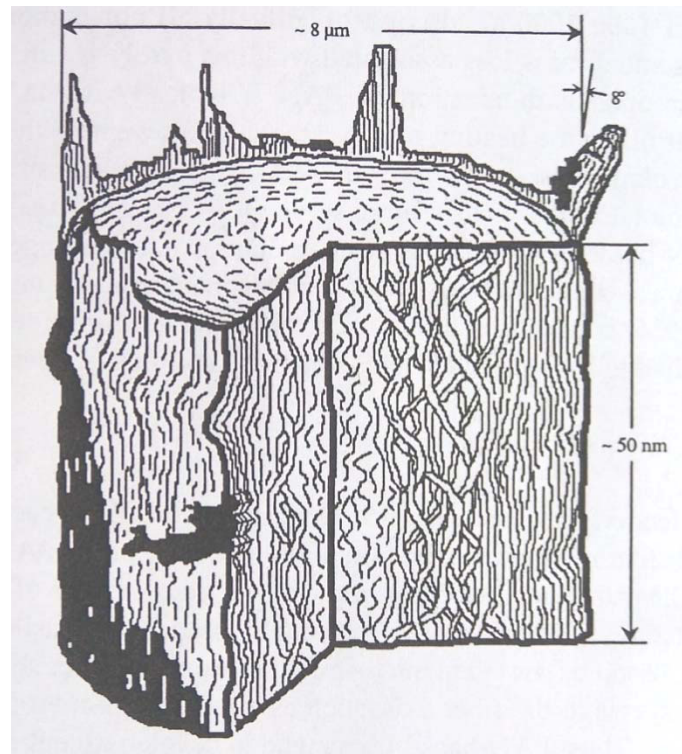


Figure 34 Fibrillar Texture of a Carbonized PAN Fiber [2]

At this stage, the as-spun mesophase pitch fiber is very weak and must be put through a series of heat treatments to develop its ultimate mechanical properties. As a first step, the fibers are oxidized/stabilized in air at around 300°C for periods of time from several minutes to several hours depending on fiber size, exact temperature, etc. This step is crucial in locking in the structure developed during the extrusion process. At this point, the carbon fibers can be carbonized; this is accomplished at temperatures in the range 1000°C to 1500°C in an inert atmosphere. The fibers may first be heated to and held at ~1000°C (precarbonization) to allow the majority of weight loss by the removal of CH₄, H₂, and CO₂. After carbonization, the fibers are heated to the graphitization temperature range (>1700°C) that is required to develop their high strength, high modulus properties. During graphitization, dislocations are removed from the carbon structure of the fibers and this eventually results in the formation of a three-dimensional graphite lattice.

The second phase in CFRC production is the creation of a carbon matrix around the fibers. The two most common methods of accomplishing this are chemical vapor deposition (CVD) and vacuum or pressure impregnation with resin or pitch. The usual commercial method for the production of CFRC items is resin- or pitch-impregnation of preforms that are built up from carbon fiber textiles (woven or non-woven) or yarns. Resin can be injected at temperatures as low as 65°C; pitch is typically injected at 300°C. A commonly used petroleum pitch is A-240; phenolic resins such as 91LD and SC1008 are aerospace qualified and readily available, but offer no advantage over pitches, except in a few special applications involving processing of complicated shapes.

In the CVD method, the preform (usually formed from several layers of woven carbon fabric in the desired final shape) is heated in a furnace pressurized with an organic gas such as methane or acetylene.

The gas decomposes under the high temperature and pressure conditions existing in the furnace and deposits layers of carbon onto the preform. As the gas must diffuse through the entire preform to make a uniform matrix, the process is very slow. It usually requires several weeks and numerous processing steps to make a single part and is expensive.

A typical production sequence involving impregnation begins with an initial impregnation under vacuum and is followed by carbonization of the impregnated part at 650°C to 1000°C to convert the organic matrix to an amorphous carbon material. The first carbonization cycle is done at atmospheric pressure to preclude damage to the fiber preform; carbon yield is ~50% of the volume of pitch or PAN resin injected. Subsequent impregnations and carbonizations may be done at high pressure to improve the carbon yield in each cycle to ~85%. Each impregnation and carbonization cycle is followed by a graphitization treatment at 2000 to 2800°C. The number of cycles required to produce high density material is typically three to five. As a general rule the thermal and mechanical properties of the material are found to improve with density; however, there is a trade-off between the properties obtained and the increased cost of multiple impregnation cycles. The final graphitization may be done at temperatures in the lower end of the graphitization temperature range to minimize cracking in the matrix and at the fiber-matrix interface. A typical CFRC will contain a volume fraction of fibers of from 40 to 50%. Additionally, the material will contain between 35 and 40% impregnant derived matrix graphite. The remainder of the composite volume is porosity distributed in the matrix and at the fiber/matrix interface.

The CFRC grades to be used for NNGP or DPP applications will be purified by means of halogen purification at high temperature. This ensures that the level of impurities available to catalyze an oxidation reaction is limited, and that the oxidation resistance of the CFRCs is suitable for the application of the material within the CSC. For a given level of impurities, the oxidation rate of the CFRC grades is less than that of the graphite grade used in the core

2.1.1.2 SiC/SiC Composites

Commercially available SiC fibers which can be used for nuclear applications are Hi-Nicalon™ Type-S (Nippon Carbon Co., Tokyo, Japan) and Tyranno™-SA3 (Ube Industries, Ltd., Ube, Japan). The other type of near-stoichiometric SiC fiber, Sylramic (Dow Corning, Midland, MI), is not appropriate as it contains boron as a part of sintering additives. Hi-Nicalon™ Type-S fiber appears to have the largest database on irradiated properties.

Comparing Hi-Nicalon™ Type-S and Tyranno™ SA3 fibers, the Type-S fiber CVI-SiC matrix composites generally exhibit slightly higher fracture energy and strain to failure than the SA3 fiber composites. On the other hand, the SA3 fiber is more attractive in terms of cost and stability at very high temperatures (>1400°C). Type-S and SA3 SiC fibers are compared in Table 9. Selection of SiC fiber for future NNGP potential composite applications should be carried out considering performance (primarily irradiation stability), cost, and long-range projected capacity of supply.

Table 9 Comparison of Three SiC Fibers Based on CY 2005 Information [3]

	Hi-Nicalon™	Hi-Nicalon™ Type-S	Tyranno™-SA3
Manufacturer Price	Nippon Carbon Co. (Tokyo, Japan) ~5k \$/kg	Nippon Carbon Co. (Tokyo, Japan) ~14k \$/kg	Ube Industries, Ltd. (Ube, Japan) ~5k \$/kg
Production Capacity (2005)	>100 kg/mo	30 kg/mo	20 kg/mo
Max. Temp. (in non-oxidizing conditions)	~1,400°C	~1,400°C	~1,800°C
Irradiation Stability	Poor	Proven (8dpa @300-800°C)	Proven (3dpa @600-950°C)

SiC composites normally require an interphase layer between the fiber and the matrix. Primary functions of the interphase layer are to:

- Transfer load between matrix and fibers
- Deflect matrix cracks
- Enable fiber pull-out
- Mitigate residual thermal stress.

Interphase layers are commonly applied between the SiC fibers and SiC matrices as coatings onto the fibers, namely Pyrolytic Carbon (PyC), PyC/SiC multilayer, and boron nitride (BN), are compared in Table 10. A BN layer is not appropriate for most nuclear applications due to the rapid burn-out of ¹⁰B during neutron irradiation. PyC/SiC multilayered interphase is preferred for nuclear applications over single-layered PyC interphase because of the better irradiation stability and oxidation resistance.

Table 10 Common Fiber Coatings for Interphase Layers in SiC/SiC Composites [3].

	Pyrolytic Carbon (PyC)	PyC/SiC Multilayer	Boron Nitride (incl. Multilayer)
Oxidation Resistance	Poor	Fair ~ Poor	Fair
Irradiation Stability	Fair	Good	Poor

Silicon carbide fibers, with diameters of around 15 μm , were first produced commercially in 1982 by Nippon Carbon. This industrial production was the direct result of research started in the 1970s and carried out by Professor Yajima and his team at the Tohoku University in Japan. The approach adopted to produce SiC fibers owed much to the experience gained from the development of carbon fibers and the spinning of polyacrylonitrile (PAN) precursor fibers. As noted previously, these fibers are stabilized by cross-linking and then pyrolyzed under controlled conditions to give carbon fibers. The starting polymer for producing SiC fibers, by necessity, needed to contain silicon and carbon atoms and the polycarbosilane (PCS), which was chosen as the starting material, comprised these elements arranged in a cyclic form consisting of six atoms, which suggested their arrangement in β -SiC. The synthesis of the PCS used dimethyldichlorosilane $(\text{CH}_3)_2\text{SiCl}_2$ which was converted into polydimethylsilane $[(\text{CH}_3)_2\text{Si}]_n$, by dechlorination with metal sodium and which in turn was converted into a polycarbosilane polymer by heating in an inert atmosphere at 400°C.[4]. The chemical composition of PCS can be simplified as $[\text{SiCH}_3\text{H}-\text{CH}_2]_n$.

The PCS obtained in this way could be melt-spun to give weak fibers. Stabilization was performed initially by cross-linking of the polymer by heating in air, just like the carbon fiber production route using PAN precursors. This was followed by heating in vacuum at temperatures, generally around 1200°C. This process allowed the first generation of small-diameter SiC fibers to be produced. The availability of these SiC fibers brought rapid interest from the aerospace and aero-engine industries as they offered the possibility of producing ceramic fiber reinforced carbon and ceramic matrix composites materials, capable of being used as structural materials at higher temperatures than those attainable with the best nickel based super-alloys. The attraction of silicon carbide is that it is a ceramic, which in bulk form, has a Young's modulus twice that of steel for less than half the density and can be used up to 1600°C. However, it was found that the characteristics of these first generation fibers were not those of bulk SiC. The fibers possessed a Young's modulus less than half that expected. The fibers were subject to creep at 1000°C and above and degraded above 1250°C. The understanding of the material science involved in the processes governing this behavior and the use of this knowledge to produce fibers with greatly enhanced properties have been the preoccupation of a number of laboratories across the world for the last quarter of a century. The result has been the development of three generations of fibers, the latest of which has produced fibers with properties approaching the limits of what is physically possible with silicon carbide. Details associated with these generations of fibers are given in Table 11.

Table 11 Details of Manufacture, Elemental Composition and Approximate Cost of Three Generations of SiC Based Fibers [4]

	Trade Mark	Manufacturer	Cross Link Method	Approximate Maximum Production Temperature	Elemental Composition (wt%)	Density (g/cc)	Average Diameter (μm)	Cost (US \$/kg)
First Generation	Nicalon 200	Nippon Carbon	Oxygen	1200°C	56Si + 32C + 12O	2.55	14	2000
	Tyranno LOX-M	Ube Ind.	Oxygen	1200°C	54Si + 32C + 12O + 2Ti	2.48	11	1250
Second Generation	Hi-Nicalon	Nippon Carbon	Electron Irradiation	1300°C	62.5Si + 37C + 0.5O	2.74	12	8000
	Tyranno LOX-E	Ube Ind.	Electron Irradiation	1300°C	55Si + 37.5 + 5.5O + 2Ti	2.39	11	N/A
	Tyranno ZM	Ube Ind.	Oxygen	1300°C	57Si + 34.5C + 7.5O + 1Zr	2.48	11	1500
	Tyranno ZE	Ube Ind.	Electron Irradiation	1300°C	58.5Si + 38.5C + 2O + 1Zr	2.55	11	N/A
Third Generation	Tyranno SA 1	Ube Ind.	Oxygen	>1700°C	68Si + 32C + 0.6Al	3.02	11	N/A
	Tyranno SA 3	Ube Ind.	Oxygen	>1700°C	68Si + 32C + 0.6Al	3.1	7.5	5000
	Sylramic	COI ceramics	Oxygen	>1700°C	67Si + 29C + 0.8O + 2.3B + 0.4N + 2.1Ti	3.05	10	10000
	Sylramic iBN	COI Ceramics	Oxygen	>1700°C	N/A	3.05	10	>10000
	Hi-Nicalon Type-S	Nippon Carbon	Electron Irradiation	>1500°C	69Si + 31C + 0.2O	3.05	12	13000

Cross linking the precursor fibers with different types of irradiation was introduced in Generation 2 fiber production. This allowed Si-Si and Si-C bonds to be formed. A number of different types of radiation were investigated by both fiber producers working in collaboration with the Japanese Atomic Energy Research Institute. Gamma irradiation was investigated but ultimately electron radiation in a helium atmosphere was used to make the second generation fibers. The cross-linking step was followed by heat treatment at 327°C for a short time to eliminate the remaining free radicals which were trapped in the irradiated precursor fiber [5]. The radiation cross-linking process, although costly, was successful in reducing the oxygen content of fibers produced from PCS precursors to 0.5 wt% and gave rise to the Hi-Nicalon fibers produced by Nippon Carbon.

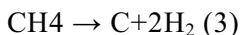
Nippon Carbon saw that to achieve near stoichiometry, the excess carbon in the Hi-Nicalon fiber had to be reduced. The radiation cured precursor route taken by Nippon Carbon to make the Hi-Nicalon fiber was used as an intermediary step to producing a near stoichiometric SiC fiber without the use of sintering aids. The Hi-Nicalon fiber was further heated to around 1500°C in a hydrogen rich atmosphere to reduce the excess carbon from a C/Si ratio of 1.39 to 1.05 for the near stoichiometric fiber, which was called Hi-Nicalon-Type-S [6].

In summary, the development of silicon carbide fibers with diameters of 15 μm or less has been stimulated by end users needs for fibers which show the characteristics of stoichiometric silicon carbide at high temperatures. The requirement was for fiber which would remain stable up to 1400°C in air. The first generation of fibers showed that filaments based on silicon carbide could be produced but it needed the efforts of research teams in a number of countries and the technology of the fibers manufacturers to improve the characteristics. These first generation fibers were limited to maximum temperatures of around 1000°C above which the fibers showed creep damage and ultimately decomposed. It was only when the vital role of oxygen in the fiber was recognized, which allowed an amorphous phase to be created, that the step towards making a second generation of fibers could be made. The use of electron irradiation for cross-linking the precursor fibers enabled the oxygen content to be controlled but only in those fibers which did not contain other species which contained oxygen. Chemical stability and creep resistance became the main aims of the research and much effort was put into understanding the mechanisms involved in each. The third generations of fibers to be produced were nearly stoichiometric in composition with the microstructure of granular silicon carbide and Young's moduli which were close to that of bulk silicon carbide. The creep and strength retention at high temperatures of the third generation of fibers also approach those of bulk silicon carbide. Even though further improvements to the fibers can be expected, it is clear that after a sustained effort over more thirty years, the third generation of small diameter SiC fibers now possesses characteristics which are close to being optimized and which are those required by industry. This has been possible through a fundamental understanding of the material science controlling the behavior of this class of filaments.

Chemical Vapor Infiltration (CVI) is currently used for fiber infiltration to produce selected nuclear grade SiC/SiC composites. The CVI process can produce a solid SiC form from a gas phase reactant at comparatively low temperature (1173–1373°K) without the use of sintering aids. Either methyltrichlorosilane (CH_3SiCl_3), or an ethyltrichlorosilane ($\text{C}_2\text{H}_5\text{SiCl}_3$) gas, combined with a hydrogen carrier gas, are common reactant gases. The CVI SiC material is typically synthesized by:



The product methane resulting from the ethyltrichlorosilane reaction in Equation (2) easily decomposes to free carbon with the generation of hydrogen as:



The free carbon can lead to undesirable carbon layers or carbon-rich phases when using ethyltrichlorosilane as a reactant gas. Other techniques can be used for fiber infiltration, however, CVI is inherently highly crystalline, high purity and stoichiometric, and provides a high theoretical density in the composite matrix which is critical for irradiation stability. However, this process limits the size of the component that can be fabricated.

2.1.2 Properties

The material properties of CFRC and SiC/SiC composites are strongly influenced by the fiber fraction, fiber type employed, fiber dimensions, fiber lay-up orientation and/or textile weave type (architecture), matrix material type or infiltration process, the individual properties of the fiber and matrix, details of the manufacturing process and the graphitization heat treatment temperature (CFRC).

In the case of CFRC materials, fiber properties depend on the precursor material (PAN or pitch), production processes including the tensioning step and the degree of graphitization. The matrix precursor

material and its manufacturing method also influence the properties of the finished composite. Although this may at first seem to present an overwhelming and confusing number of possibilities, it also allows the opportunity to select and tailor materials and processes to achieve a CFRC with physical and/or mechanical properties optimized for the intended application.

Some typical physical and mechanical values for CFRC materials are shown in Table 12 in relation to properties of “isotropic” graphite. The densities here are typical of CFRC materials with multiple (3 to 5) densification cycles; some commercial products with single densification cycles have densities as low as 1.35 g/cm³. Note that the thermal conductivity values given in the second row of the table for the isotropic graphite and the 3-D CFRC are essentially independent of orientation (i.e., the measurement direction). Values shown for the 1-D CFRC are for the direction parallel to the fibers; values in directions perpendicular to the fiber axis can be up to 25 times smaller. An excellent description of the effects of precursor materials and fabrication procedures on the thermal conductivity of 3-D CFRC materials can be found in Reference 7.

Table 12 Typical Unirradiated Properties of Graphite and CFRC Materials at Room Temperature [8]

Property	1-D CFRC (parallel to fibers)	3-D CFRC	Fine Grained Isotropic Graphite
Density [g/cm ³]	1.7 – 1.8	1.7 – 1.8	1.75 – 1.85
Thermal Conductivity [W/m.K]	400 - 600	100 - 200	90 - 200
Coefficient of Thermal Expansion [10 ⁻⁶ /K] (20-1000°C)	0.1 – 2.0; -0.10 MKC** [24]	0.1 – 0.2; 0.55-1.34*** [24]	2 - 5
Young’s Modulus [GPa]	150 – 250	75 - 125	10 - 15
Bending Strength [MPa]	50 - 150	176±20 [9]*	40 - 70
Tensile Strength [MPa]	300 - 900	150 - 400	40 - 60
Compressive Strength [MPa]	200 - 500	100 - 200	100 - 200
Fracture Toughness [MPa.m ^{1/2}]	2 – 3	4 - 6	<1

*Data for FMI-222, ultimate bend strength; **MKC, 1D CFRC material with pitch fibers parallel to the fiber plane; ***N11, N112 and FMI A27-130 parallel to the fiber plane

There are no data that could be located on the potential degradation of CFRC or SiC/SiC composites in high temperature impure helium similar to the coolant to be used in the NNGP; therefore, testing needs to be performed to determine corrosive effects, if any, under these conditions.

Typical unirradiated properties of selected second and third generation SiC fibers used in high performance composites are given in Table 13. Typical unirradiated properties of SiC matrix material and selected SiC Composites are given in Table 14.

Table 13 Unirradiated Properties of High Performance SiC Fibers [10]

SiC Fiber	C/Si Atomic Ratio	Oxygen Content (wt.%)	Tensile Strength (GPa)	Tensile Modulus (GPa)	Elongation (%)	Density (g/cm ³)	Diameter (μm)
Tyranno SA	1.07	<0.5	1.8	320	0.7	3.02	10
Hi-Nicalon Type S	1.05	0.2	2.6	420	0.6	3.1	12
Hi-Nicalon	1.39	0.5	2.8	270	1.0	2.74	14

Table 14 Unirradiated Properties of Monolithic SiC and Selected SiC Composites [11], [12], [13], [14], [15]

Property	Monolithic SiC, CVD	Selected SiC Composites
Density (g/cm ³)	3.215-3.219	2.61-2.87
Thermal Conductivity (W/m.K)	$K_0 = [-0.0003 + 1.05 \times 10^{-5} T]^{-1}$ (4)	15-40(1); 10-30(2); 3.8-16 [54]
Coefficient of Thermal Expansion (10 ⁻⁶ /K)	$CTE = -1.8276 + 0.0178T - 1.5544 \times 10^{-5} T^2 + 4.5246 \times 10^{-9} T^3$ (5)	NA
Dynamic Young's Modulus (GPa)	NA	218-338
Tensile Young's Modulus (Gpa)	460 (6)	174-369; 200-400(3)
Tensile Strength (MPa)	NA	78-366; 100-400(3)
Fracture Toughness (MPa.m ^{1/2})	2.0-5.2	NA
Proportional Limit Stress (PLS) (MPa)	NA	62-232
Fracture Strain (%)	NA	0.03-0.62
Matrix Micro-crack Stress (MPa)	NA	151-161; 150-250(3)
Ultimate Fracture Stress (MPa)	NA	267-515
Steady State Creep Rate (s ⁻¹)	$\sim 10^{-10}$ (1473°K)- 10^{-9} (1673°K) at a stress of 200MPa	NA

Notes: (1) 500°C; (2) 1000°C; (3) 500-1000°C; (4) Single crystal SiC from 300-1800°K; (5) 125-1273°K, at T>1273°K CTE=5.0x10⁻⁶/K; (6) CVD 100% dense polycrystalline SiC

2.1.2.1 Irradiation Effects

The irradiation behavior of CFRC depends largely on the way the fibers are arranged. A CFRC with 1D fibers experiences five to ten times more shrinkage in the “a” direction (parallel to the fibers) than “c” (perpendicular to the fibers), while a composite with a 2D weave of fibers might have about four times more shrinkage in the “a” direction than “c”. Three-dimensional fiber preforms result in the most isotropic, but also the most unpredictable, shrinkage. [16]

Reducing the density of a composite by increasing the fiber content can decrease the shrinkage of the material. Density can range widely and can be controlled by varying the components of the composite: the fibers, impregnants and dopants. In addition to composition, the density is a function of the type of matrix infiltration process, and the processing temperature and pressure

Pitch and mesophase matrix material has excellent irradiation stability compared to PAN- or resin-based matrix material [17, 18]. A pitch-based matrix is not only better because it is highly crystalline, but also because the crystals are arranged randomly. It also has gaps, cracks and microporosity between the crystals, which leave room for expansion of the crystals during irradiation, thus minimizing the overall effect of radiation induced strain [17].

The performance of the interface and the phases that are deposited to improve fiber/matrix adhesion can be critical to the irradiation behavior of SiC/SiC composites.

Selected post-irradiation properties of CFRCs and SiC/SiC composites are discussed below. Because CFRC material generally behaves in a similar manner to graphite under irradiation, the irradiation effects properties of nuclear graphite are discussed.

Dimensional Stability

In polycrystalline graphite, neutron irradiation initially causes volumetric shrinkage. On the crystallite scale, the irradiation behavior is quite anisotropic with vacancies forming voids, or micro-cracking at the crystallite boundaries, and new basal planes formed by interstitial agglomeration. [19, 20, 21, 22] This causes shrinkage in the <a> direction and growth perpendicular to the basal planes (<c> direction.) Initially, the <c> axis growth is accommodated by intrinsic misalignment of the basal planes and aligned porosity. However, at some (irradiation temperature dependent) dose, the ability to accommodate the <c> axis strain saturates. The newly forming basal planes then cause <c> swelling which combined with the ongoing <a> axis shrinkage causes the “turnaround” from macroscopic densification to swelling, leading to multiplication of the strain-induced cracks and severe degradation in the material strength. The point at which the volume returns to zero is typically taken as the useful lifetime for design applications.

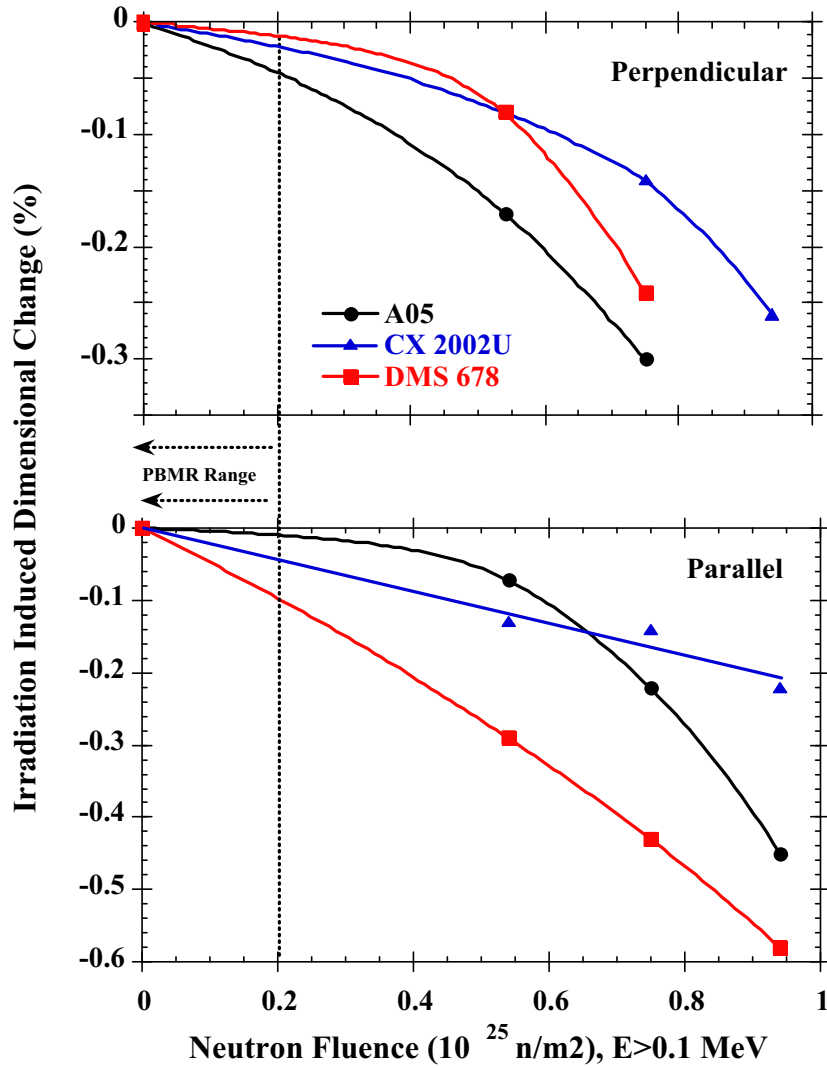
The microstructural processes determining the irradiation-induced dimensional changes in carbon fiber composite materials are not different than for graphite. However, because of the added architectural complexity of the composite, the dimensional stability of composites is more complex. Moreover, as the rate of dimensional changes is a function of the perfection of the graphite (crystallite size, micro porosity, etc) and because the composite matrix and fibers are microstructurally quite different, the irradiation stability is further complicated relative to typical nuclear graphite. Discussions of the effect of graphite fiber type and architecture on the macroscopic stability of composite under irradiation have been presented by Burchell [16] and Snead [23].

Figure 35 gives results on dimensional change from Bonal [24] plotted as a function of dose for three 2D CFRCs in directions parallel and perpendicular to the 2-D lay-up. Simple polynomial fits were applied to the data and an indication of the estimated dose ($\sim 2 \times 10^{20}$ n/cm², E>0.1 MeV) indicated by a dotted line is associated with the maximum fluence expected for the straps and tie rods for the NNGNP.

These materials are generally comparable to the SGL Grade 1502 YR material to be used for the DPP tie rods; however, these materials are probably not comparable to the SGL Grade 2002 YR material to be used for the DPP race track straps because the 2002 YR material is fabricated from 1D material. From this data it is apparent that the dimensional change for the 2-D PAN composites to be used by PBMR for the tie rods will be approximately, or less than, 0.1%. This indicates that little dimensional change would be expected for the NGNP tie rods if the 1502 YR material was used for the NGNP tie rods and the NGNP fluence estimate for the tie rods is close to the actual fluence.

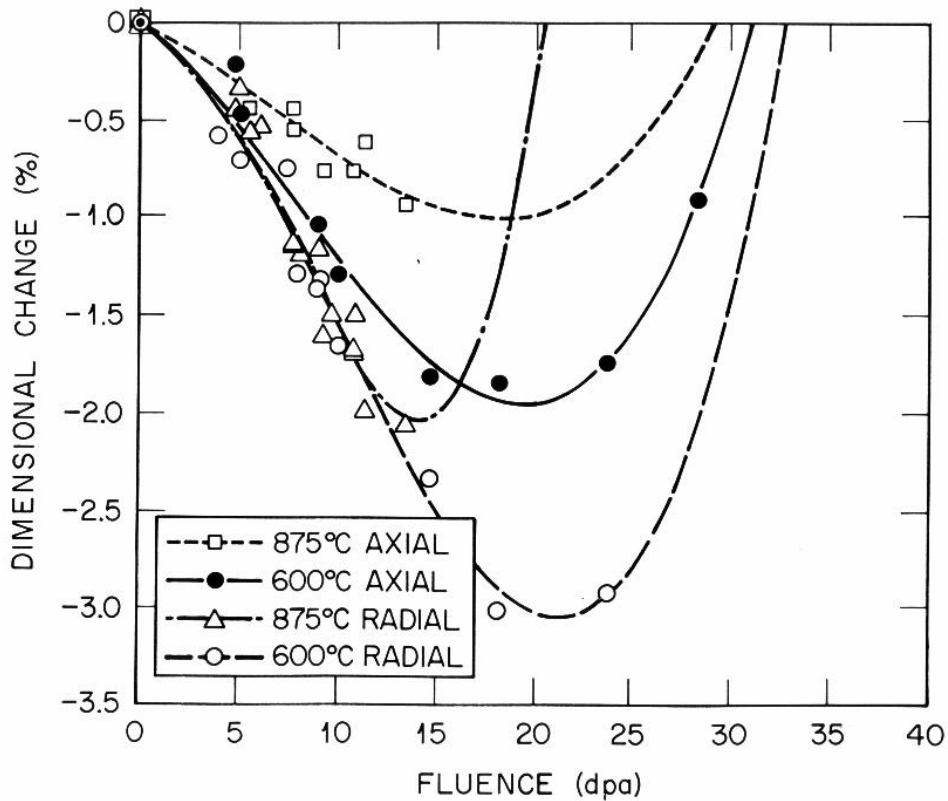
EOL fluence expected for CFRC components that would be potentially used in the RCS to replace Alloy 800H components is much higher (about $5 \times 10^{21} \text{ n/cm}^2$). This is off the scale for the data given in Figure 35; however, the general continuing trend for stable shrinkage can be seen in Figure 36 for GraphNOL N3M Graphite [25]. The data given in Figure 35 is in the region of $< 0.7 \text{ dpa}$ in Figure 36 for graphite. The projected EOL fluence for the straps and tie rods equals 0.15 dpa in Figure 36. The data indicates that stable shrinkage is expected for fluence levels up to at least 10 dpa which is about a factor of 66 greater than the EOL for the straps and tie rods and about a factor of 2 greater than the EOL for the RCS application. These conclusions assume that CFRC behaves in a similar way for dimension stability to graphite as a function of neutron irradiation. These conclusions agree with the discussion given in Sections 1.1.4, 1.2.4 and 1.4.2 for the use of CFRC components in the straps, tie rods and the RCS. This conclusion indicates that ideally CFRC would see stable shrinkage in this range of fluence; however, it will be seen based on the composite data given below, that composites are more complicated than graphite and swelling is dependent on fiber orientation.

CFRCs with fiber layouts in 1D, 2D and 3D orientations have been irradiated at the Oak Ridge National Laboratory (ORNL) and the results of the testing performed generally indicate the factors that affect swelling in these materials [26]. The 1D composite (UFC material) that was irradiated (see Figure 37) exhibited extremely anisotropic dimensional changes with rapid shrinkage in the fiber axis direction (length). This material used a PAN derived fiber and is generally similar to SGL Grade 2002YR material to be used for the race track strap DPP design. In the direction perpendicular to the fiber axis (diameter), the composite started shrinking at a dose of $< 1 \text{ dpa}$, followed by a reversal to expansion and returning to zero dimensional change at approximately 2.5 dpa . At this point, (following turnaround) the composite continued to expand at an increasing rate. However, as noted previously, the estimated fluence for this application is so small that little shrinkage would be expected assuming the estimated fluence is correct. The 2D composite (RFC random chopped fiber material) that was irradiated (see Figure 38) had the fiber axis in the direction of the specimen diameter. In the off-axis direction (length), the composite exhibited slight contraction followed by expansion. The composite returned to its original length at about 2 dpa . The diameter (fiber-axis) direction exhibited shrinkage, although the magnitude was much less than the 1D composite. The 3D PAN fiber composite exhibited (see Figure 39) isotropic behavior at damage doses up to approximately 2 dpa . At doses exceeding 2 dpa , the composite z-direction (specimen length) continued to display shrinkage, whereas the fiber x-y (specimen diameter) direction exhibited reversal and slight growth. Variables other than fiber distribution also affect CFRC swelling characteristics following irradiation. The effect of two of these variables (fiber type and graphitization temperature) for a 3D fiber lay-up CFRC is shown in Figure 40. The plot on the left directly compares the dimensional change of the pitch and PAN fiber composites at the same graphitization temperature (3100°C). This indicates, as previously noted, that if other variables are the same, the pitch fiber composite exhibits less dimensional change under irradiation. The plot on the right directly compares two PAN composites that were processed at different graphitization temperatures (3100°C versus 2650°C). The composite with the higher graphitization temperature shows slightly less dimensional change but both of these composites have more change than the pitch composite noted previously.



Note: The fluence conversion factor for the units used is 1E-4 times n/m² equals fluence as n/cm²

Figure 35 Irradiation-Induced Dimensional Change of Selected Carbon Fiber Composites [24, 27]



Note: The fluence conversion factor for the units used for graphite and CFRC is $\text{dpa}/7.3\text{E-}22$ equals fluence as n/cm^2 . Therefore, a fluence of $5\text{E}21\text{n}/\text{cm}^2$ = about 3.6 dpa.

Figure 36 Neutron Irradiation-Induced Dimensional Changes in GraphNOL N3M Graphite [25]

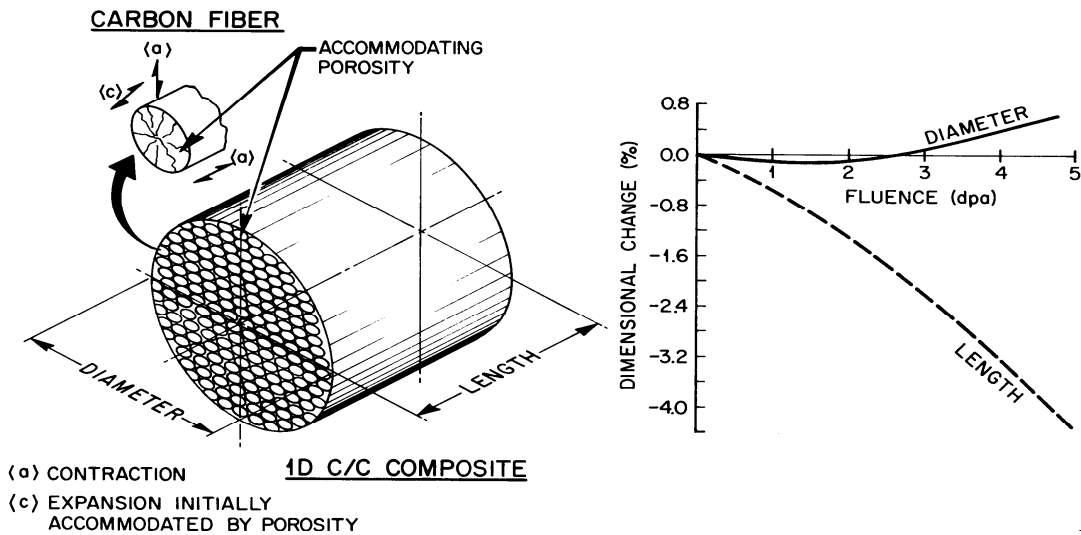


Figure 37 Microstructural Interpretation of Irradiation Induced Dimensional Changes in 1D CFRC composites [26].

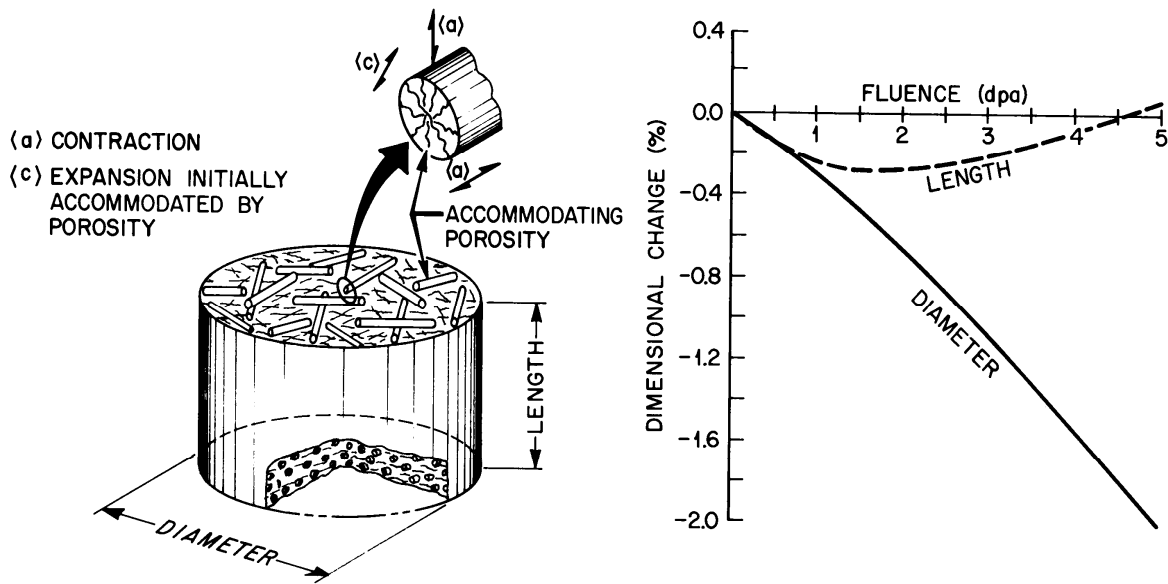


Figure 38 Microstructural Interpretation of Irradiation Induced Dimensional Changes in 2D CFRC composites [26]

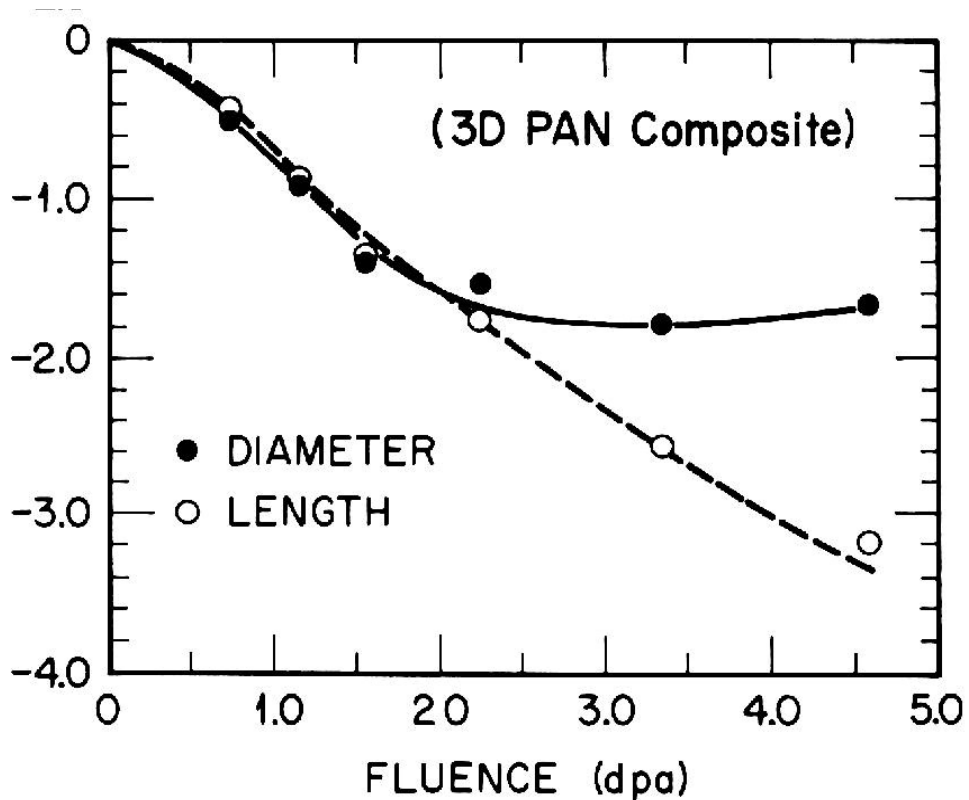


Figure 39 Dimensional Changes in 3D PAN CFRC [26]

In summary, the following factors in CFRCs tend to reduce irradiation induced dimension change:

- Fibers that are more highly graphitic perform better than those that are less graphitic
- Composites with a balanced lay-up generally perform better
- Composites with a high final heat treatment generally perform better

Irradiation induced dimensional changes in CFRCs can be explained by considering the following factors:

- The similarity to graphite single crystal dimensional changes
- A microstructural model of the carbon fiber used in the composite
- A knowledge of the composite architecture and the interactions of the fiber, fiber bundle, matrix and porosity of the composite

Specific swelling data for FMI-222 CFRC (Amoco P120 pitch fiber, balanced 3D weave with a pitch matrix, graphitized at 3100°C) is given in Table 15 following irradiation in HFIR at 4.1dpa, 7.3dpa and 9.5dpa. This material was intended to be the optimal CFRC to resist the effect of neutron irradiation damage. The material remained intact through 9.5dpa fluence; however, it was demonstrated that the FMI-222 CFRC undergoes significant dimensional instability under neutron irradiation at 800°C before 10dpa is reached. The deformation behavior appeared highly anisotropic and was strongly influenced by the state of mechanical constraint and or absolute dimensions. Therefore, it is anticipated that the deformation of reactor components made of the same material would be highly dependent on the component shape, size, mechanical constraint and or external stress state. The data suggests that for a straight cylindrical component with a relatively thin wall with 3D reinforcement architecture, such as a braided control rod sleeve, the component should contract in the axial and circumferential directions and increase wall thickness, with no external stress or mechanical stress or mechanical constraint applied. The contraction rate would be near constant at approximately 0.5%/dpa up to at least 10dpa, according to the present data. However, because of the variables involved in the prediction of CFRC irradiation behavior, qualification of a CFRC composite for the control rod application would require the assessment of the irradiation effects for the relevant specific architecture, geometry and mechanical conditions (if any) specific to the application. Swelling of this type could be a key issue for the control rod application unless this was carefully considered in the design.

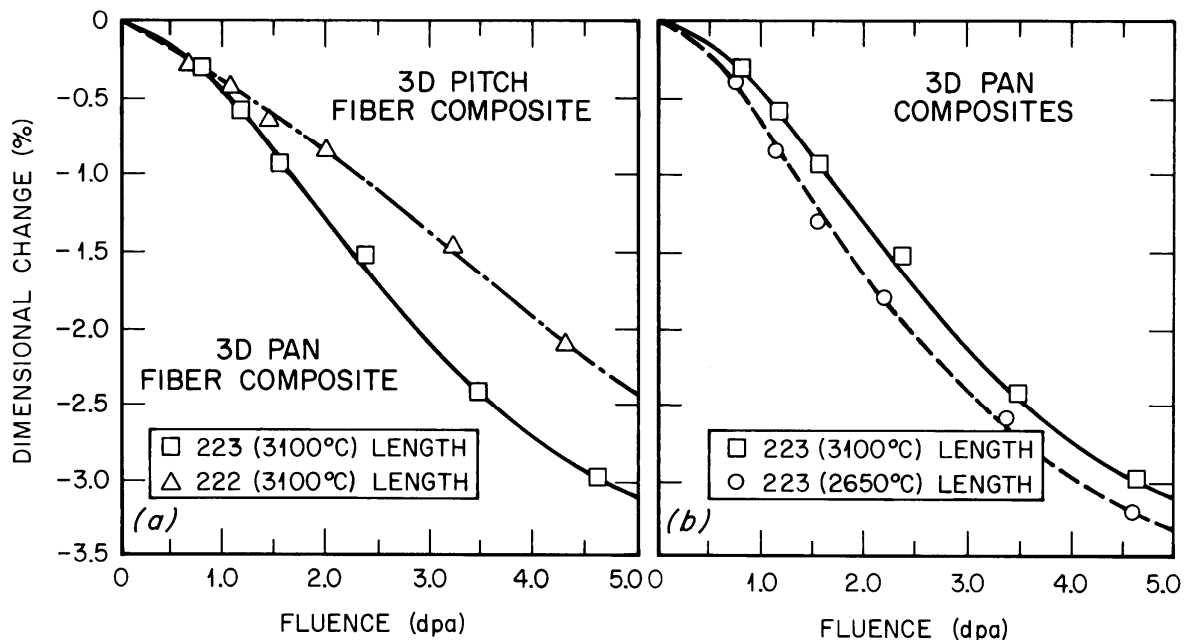


Figure 40 Effect of Fiber Type and Graphitization Temperature on Irradiation Induced Dimensional Changes in 3D CFRCs [26]

Table 15 Influences of Neutron Irradiation on Dimensions and Swelling of FMI-222 Graphite Composite [28]

	Length (mm)	Width (mm)	Height (mm)	Mass (gram)	Swelling (%)
Non-irradiated, As-machined	50.8 (0.01)	6.28(0.01)	2.87 (0.01)	1.79 (0.01)	NA
Non-irradiated, baked	50.8 (0.01)	6.29(0.01)	2.88 (0.01)	1.79 (0.00)	NA
Irradiated, 4.1 dpa	49.9 (0.01)	6.33 (0.02)	2.92 (0.02)	1.78 (0.00)	1.4 (0.6)
Irradiated, 7.3 dpa	49.4 (0.37)	6.46 (0.04)	2.98 (0.04)	1.78 (0.02)	5.4 (1.1)
Irradiated, 9.5 dpa	48.5 (0.56)	6.54 (0.04)	3.06 (0.04)	1.75 (0.00)	9.0 (2.1)

Note: Numbers in parentheses are standard deviations.

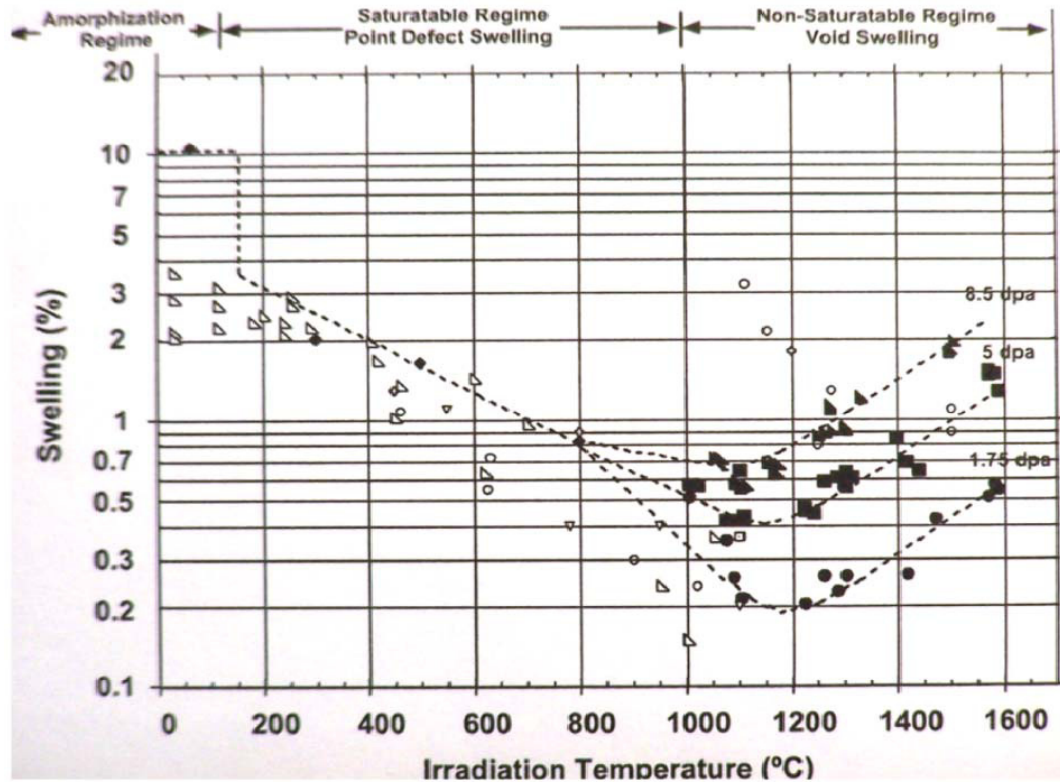


Figure 41 Irradiation-induced Swelling of SiC as a Function of Irradiation Temperature and Fluence [15]

Irradiation induced swelling of monolithic high density SiC is primarily a function of irradiation temperature and at high temperatures a function of fluence, as seen in Figure 41. Extended low temperature irradiation exposure in the amorphization range should be avoided because the long range crystal structure of the material is lost and the material becomes significantly less stable. This effect also occurs in SiC/SiC composite materials. For most temperatures of interest for the NNGP, irradiation induced swelling saturates at a low fluence and remains at 1% or less to fluences of at least 10 dpa. The Hi-Nicalon Type STM SiC/SiC composites show the same level of low swelling to a neutron irradiation exposure of 10 dpa and an irradiation temperature of 800°C to 1100°C [29]. Figure 42 gives irradiation induced swelling of Hi Nicalon fiber SiC/SiC composite material (second generation) as a function of irradiation dose and temperature. Figure 43 provides this same type of information for SiC/SiC composite materials using Hi Nicalon Type S fibers (third generation). As noted above, the swelling for both composite types saturate at low fluence and remain essentially unchanged out to high levels of fluence. The magnitude of the swelling is very similar for each with the Hi Nicalon composite having slightly less swelling saturation at elevated temperatures.

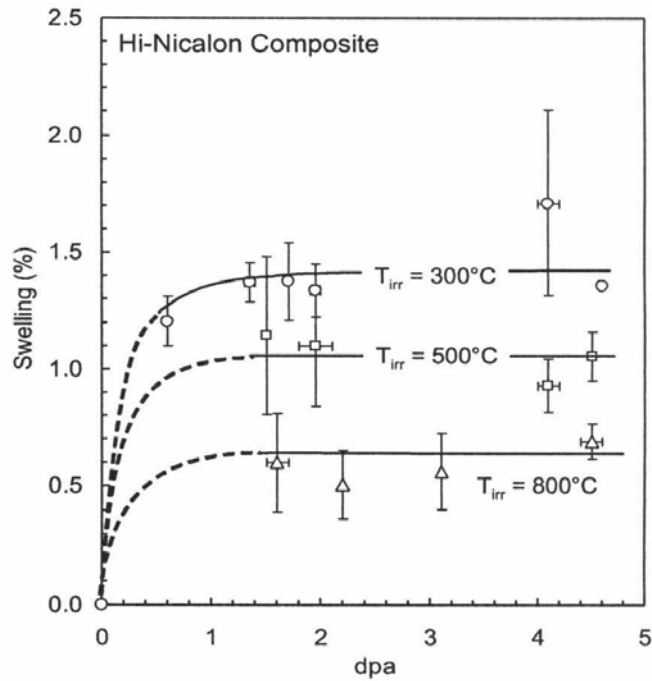


Figure 42 Irradiation-induced Swelling of Hi Nicalon Fiber SiC/SiC Composite Material as a Function of Irradiation Temperature and Fluence [55]

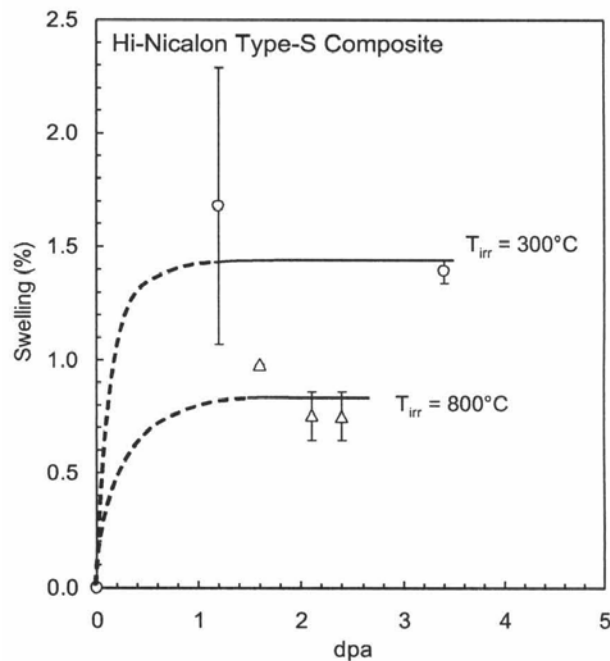


Figure 43 Irradiation-induced Swelling of Hi Nicalon Type S fiber SiC/SiC Composite Material as a Function of Irradiation Temperature and Fluence [55]

Strength

The effect of neutron irradiation on the strength, elastic modulus, and dimensional stability of graphite has been extensively studied and shown to be strongly inter-related. [20, 21, 22, 30] Upon neutron irradiation, polycrystalline graphite undergoes an increase in strength due to dislocation pinning caused by the produced defects. This effect occurs rapidly and largely saturates by a dose level of $\sim 1-3 \times 10^{25}$ n/m², $E > 0.1$ MeV. This dose for saturation defines the upper dose of what is referred to as Stage 1. The radiation effects for the estimated fluence for the NNGNP straps and Tie Rods belong in this initial stage. Above this Stage 1 dose a more gradual increase in strength occurs due to structural changes occurring within the graphite (Stage 2.) This Stage 2 increase continues until the graphite begins to swell and eventually loses mechanical integrity from extensive micro-cracking. The irradiation-induced increase in strength for graphite can be quite substantial. For example, nuclear graphite such as GraphNOL N3M [25], exhibits a peak increase in brittle-ring strength of up to 100%. A set of brittle-ring data is presented in Figure 44 for the nuclear grade GraphNOL N3M irradiated at 600 and 875°C [25]. This indicates that based on graphite data only, the strength of CFRCs would be expected to increase in a stable manner through the EOL fluence for the RCS.

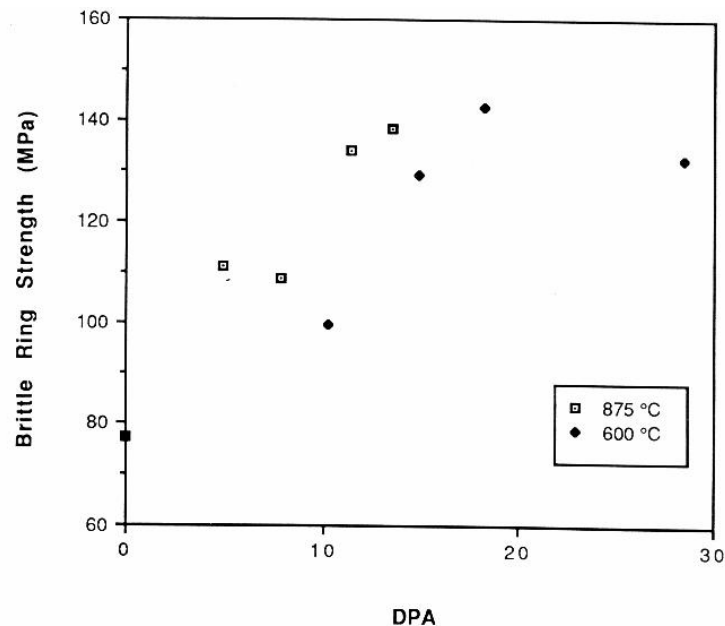


Figure 44 Neutron Irradiation-induced Strength Changes for GraphNOL N3M at Irradiation Temperatures 600 and 875°C [25]

The effect of neutron irradiation on the brittle ring strength of several types of CFRC materials as a function of fiber type and architecture compared to H-451 nuclear graphite in the fluence region from 0-3 dpa is given in Figure 45. The plot on the left compares the UFC CFRC (1D) with the RFC CFRC (2D) and H-451 graphite. The UFC material shows a slightly increasing strength as a function of irradiation but much lower than the RFC CFRC or the H-451 graphite. All of these materials show an increase in strength as a function of irradiation but the H-451 starts to decrease in strength after about 1 dpa. The plot on the right compares the brittle ring strength of two 3D CFRC materials in the same fluence range for two different graphitization temperatures. As noted previously, the FMI-222 is a pitch fiber, pitch matrix CFRC; whereas, the FMI-223 is PAN based. It can be seen that the FMI-222 material has a lower brittle ring strength compared to the FMI-223 material; however, the strength of the FMI-222 material increases as a function of fluence over the entire range up to 2 dpa; whereas, the FMI-223 material

increases initially but then decreases rapidly in strength after about 0.7 dpa and the two materials have a similar strength in the range of 2-2.5 dpa. The irradiation temperature for all specimens was 600°C.

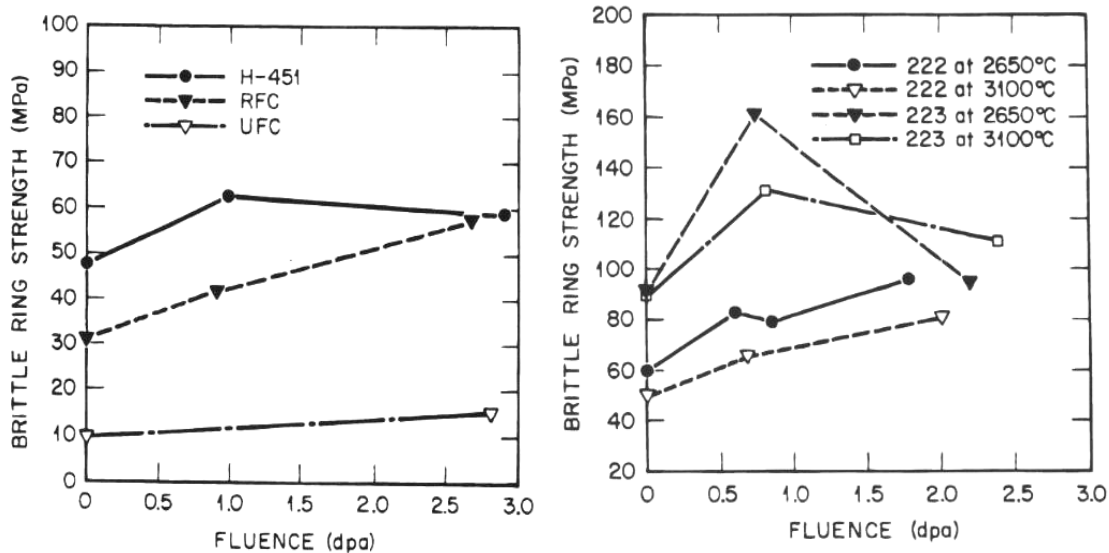


Figure 45 Strength Change versus Fluence in CFRC Materials as a Function of Fiber Type, Architecture and Graphitization Temperature. [31]

Actual strength and Young’s modulus data for FMI-222 irradiated in HFIR at 4.1 dpa, 7.3 dpa and 9.5 dpa at an irradiation temperature of 800°C is given in Table 16. Please note that even through the FMI-222 material was nominally the same in Figure 45 and Table 16, the actual specimens, the irradiation temperature and PIE test procedures were different due in part to the different time frames involved.

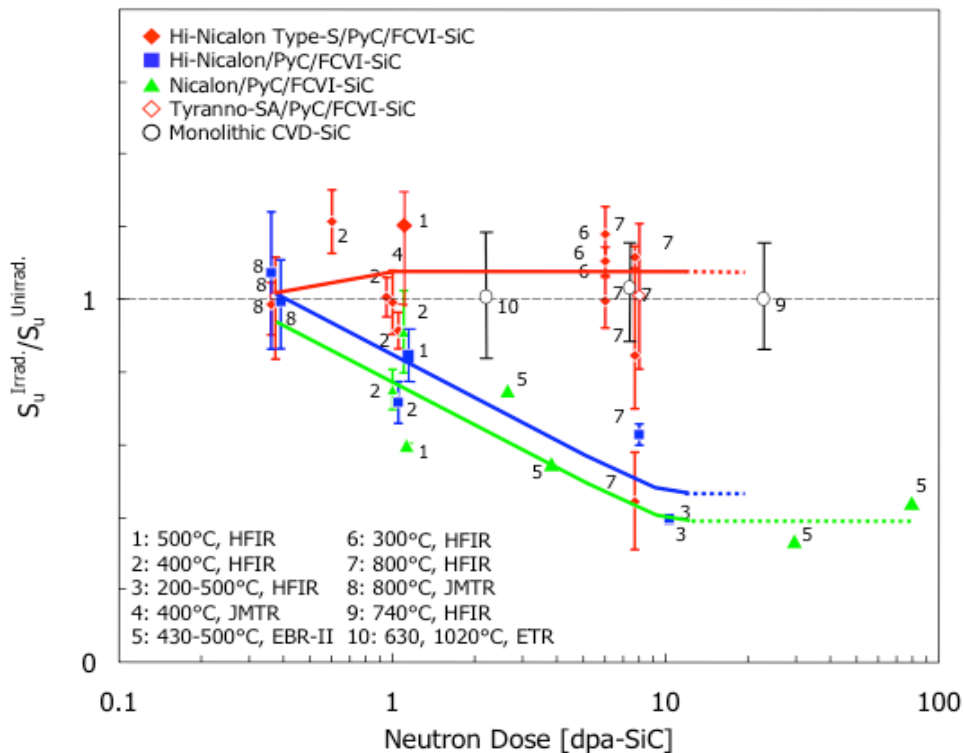
Table 16 Influence of Neutron Irradiation on Young’s Modulus and Flexural Strength of FMI-222 CFRC [28]

	Young’s Modulus	Flexural Stress (MPa)	
	GPa	Ultimate	Proportional Limit Stress (PLS)
Non-irradiated, As-machined	52.2 (7.3)	99.9 (12.8)	61.4 (11.1)
Non-irradiated, baked	51.0 (3.2)	103.2 (8.4)	67.3 (7.1)
Irradiated, 4.1 dpa	54.8 (3.5)	158.4 (13.4)	104.1 (5.4)
Irradiated, 7.3 dpa	57.8 (9.0)	146.4 (38.1)	134.4 (26.3)
Irradiated, 9.5 dpa	57.6 (5.5)	146.7 (33.1)	105.1 (25.0)

Note: Numbers in parentheses are standard deviations. PIE data was taken at room temperature

The pattern of mechanical behavior for monolithic SiC and composites fabricated using various SiC fibers is illustrated in Figure 46 at fluences up to 8 dpa. While the Hi-Nicalon Type-S fiber composites are slightly less stable than monolithic SiC they show a threshold behavior where the mechanical properties do not change significantly after about 1 dpa. This is in contrast to the curves plotted from composites made with Nicalon or Hi-Nicalon fibers, which exhibit irradiation induced strength degradation.

Actual post-irradiation strength data for Hi-Nicalon™ Type S SiC/SiC composite material irradiated to various fluences and at various temperatures is given in Table 17. A pyrolytic carbon coating was applied to the SiC fibers of the UD-HNLS/PyC material and multilayered pyrolytic carbon/SiC coatings were applied to the UD-HNLS/ML material to facilitate pseudo-ductile fracture behavior. The porosity of these materials ranges from 15-17% and the fiber volume fraction was 30 volume %. The fact that the ultimate tensile strength is greater following irradiation is primarily attributable to the coatings applied to the fibers. Prior efforts for coatings in many cases allowed fiber de-bonding from the matrix to occur which resulted in lower strengths following irradiation.



- 1,2: L.L. Snead, et al., J. Nucl. Mater., 283-287 (2000) 551-555. 8: T. Nozawa, et al., J. Nucl. Mater., (2002) to be published.
 3,4: T. Hinoki, et al., Mater. Trans., JIM, 43 [4] (2002) to be published. 9: R.J. Price, et al., J. Nucl. Mater., 108-109 (1982) 732-738.
 5: R.H. Jones, et al., 1st IEA-SiC/SiC (1996). 10: R.J. Price, J. Nucl. Mater. 33 (1969) 17-22.
 6,7: T. Hinoki, et al., J. Nucl. Mater., (2002) to be published.

Figure 46 The Irradiated-to-Non-irradiated Ultimate Strength Ratio ($S_U^{Irrad}/S_U^{Unirrad}$) Measured up to 8 dpa, Demonstrating the Irradiation Stability of Different SiC_f/SiC Composite Types Compared to Monolithic SiC [32].

Table 17 Summary of Room Temperature Strength Data of Hi-Nicalon™ Type S Fiber, CVI SiC/SiC Composites [13]

Sample	Young's Modulus (GPa)	Ultimate Tensile Stress (MPa)	PLS (MPa)	Elongation at Fracture (%)
UD-HNLS/PyC				
Non-irradiated	357 (30)	311 (60)	231 (42)	0.16 (0.06)
1.8 dpa at 380°C	354 (23)	366 (67)	197 (33)	0.40 (0.11)
7.7 dpa at 800°C	320 (11)	381 (26)	217 (36)	0.38 (0.02)
UD-HNLS/ML				
Non-irradiated	375 (18)	271 (49)	232 (45)	0.09 (0.03)
7.7 dpa at 800°C	356 (34)	302	186 (30)	0.12

Note: Numbers in parenthesis represent standard deviations.

The flexural stress and the proportional limit stress (PLS) are plotted as a function of neutron fluence and temperature for SiC/SiC composites using Hi Nicalon fibers and Hi Nicalon Type S fibers in Figure 47 and Figure 48, respectively. The composite material in Figure 47 has a significant decrease in strength levels up to 1 dpa and then the strength levels remain fairly constant out to high fluence levels. The composite material in Figure 48 show only a slight initial decrease in strength levels before the strength levels become essentially constant. The strength of neither material is significantly affected by irradiation temperature from 300-800°C.

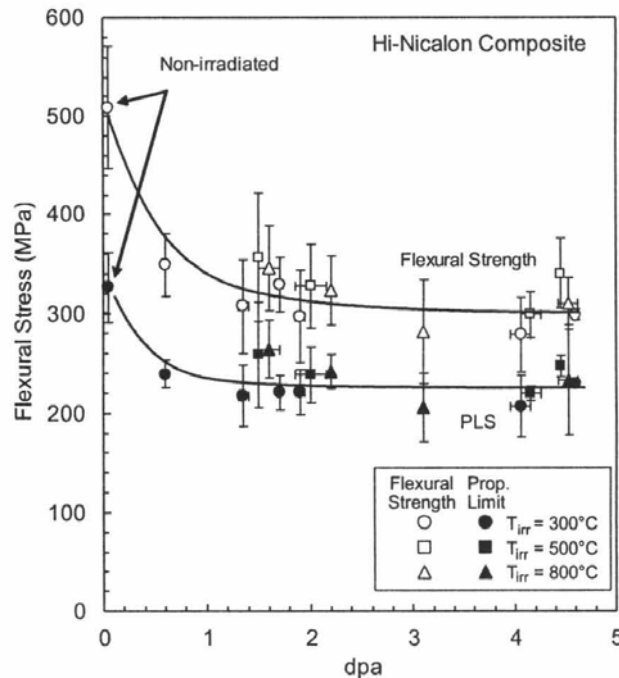


Figure 47 Irradiation-induced Strength Changes of Hi Nicalon fiber SiC/SiC Composite Material as a Function of Irradiation Temperature and Fluence [55]

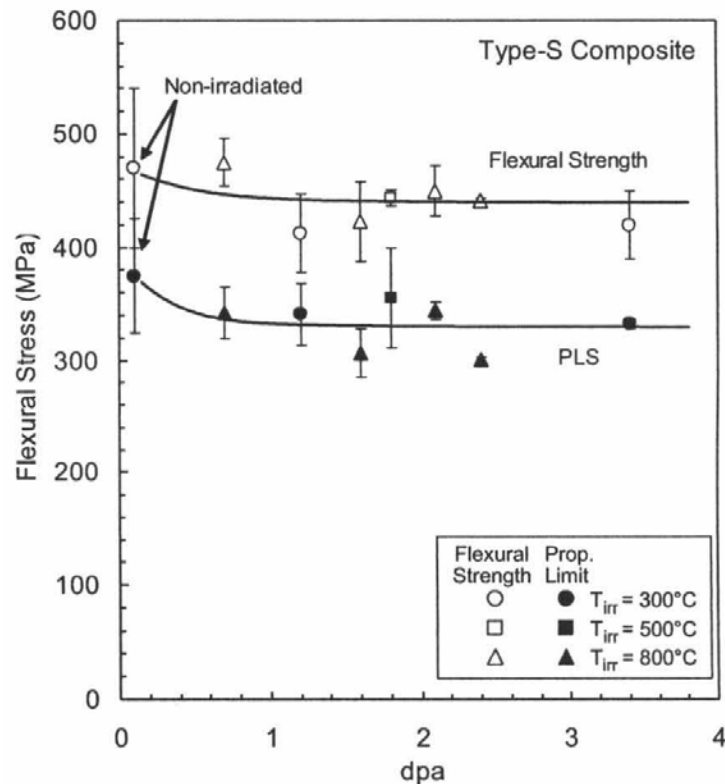


Figure 48 Irradiation-induced Strength Changes of Hi Nicalon Type S Fiber SiC/SiC Composite Material as a Function of Irradiation Temperature and Fluence [55]

Fracture Toughness

CFRCs are tough materials whose fracture mode is one of multiple cracking. For composite materials, the fracture toughness is often characterized in terms of the crack growth resistance, R . Depending upon the value of R , materials can be broadly classified as: (i) brittle ($R < \sim 10 \text{ J/m}^2$); (ii) semi-brittle ($\sim 10 < R < \sim 1000 \text{ J/m}^2$); or (iii) tough ($R > \sim 1000 \text{ J/m}^2$) [33]. Table 18 reports values of R for different types of carbon materials, including CFRCs. Graphites exhibit R -values of $100\text{-}300 \text{ J/m}^2$ and thus can be characterized as semi-brittle, whereas, CFRCs exhibit R -values $> 2500 \text{ J/m}^2$ in the plane of the reinforcement fiber. Lower values of R are observed for inter-laminar cracking for 2D CFRCs presumably because of the lack of fiber reinforcement in that direction. Multi-directional, balanced fiber CFRCs would be expected to exhibit R -values $> 2500 \text{ J/m}^2$ in all directions.

There have been a number of studies of the effects of neutron damage on the toughness of graphites. For example Delle et al [34] irradiated compact tension specimens of ATR-2E graphite in the Petten Reactor at irradiation temperatures of between 660 and 800°C and to a peak dose of $1.35 \times 10^{22} \text{ n/cm}^2$ [$E > 0.1 \text{ MeV}$]. Over this dose range graphite ATR-2E shrank, and approached turnaround. The value of K_{IC} varied linearly with the dimensional change over this dose range, increasing from a non-irradiated value of ~ 1.03 to $\sim 1.38 \text{ MPa}\cdot\text{m}^{1/2}$. The increase in toughness can presumably be attributed to the increase in strength and the closure of cracks in the graphite during the shrinkage stage of dimensional change.

Table 18 Crack Growth Resistance, R, of Selected Carbon Materials [33]

Material	Fracture Toughness, R (J/m ²)
Pyrolytic Graphite	37.8 ± 10
Porous Resin Carbons	50-138
Glassy Carbons	12-14
Coarse Grained Graphite	232-258
Nuclear Graphite	130-150
CFRC (satin weave, phenolic resin derived matrix)	~2500-5000
Bi-directional CFRC composite (woven fibers in CVI carbon matrix)	60-95 (Inter-laminar crack growth)
	~50,000 (crack growth perpendicular to laminate)

A comparison of fracture toughness values of graphite and various CFRC materials following irradiation at temperatures in the range of 650-1000°C at fluence values in the range 1.3-2.3x10²¹ (E>0.1 MeV) is given in Table 19. As indicated, the CFRC materials were several times tougher than nuclear graphite following irradiation and like graphite slightly increased in toughness following irradiation. Because the fluence was in the range of 0.9-1.7 dpa, it would be expected that at higher fluence levels (5-10 dpa) the fracture toughness would decrease.

The fracture toughness of monolithic SiC changes primarily as a function of irradiation temperature by factors of 0.8-1.6 times the unirradiated values given in Table 14 [15]. Essentially no data is available of the fracture toughness of SiC/SiC following irradiation.

Table 19 Effects of Neutron Irradiation on the Fracture toughness of Graphite and CRFC Materials [35]

Material	Fracture Toughness*, K _{1c} (MPa m ^{-1/2})	
	Pre-irradiation	Post-irradiation
Graphite IG-110	0.78	1.01
Graphite HCB-18	0.75	0.99
C/C A	2.96	3.65
C/C B	3.44	4.14
2D-C/C	5.26	5.77

Note: Irradiation exposure was between 1.1 and 1.9x10²¹ n/cm² (E>0.1 MeV)

Thermal Creep and Irradiation Creep

Steady state irradiation creep compliances of CVD SiC at fluences greater than 0.7 dpa have been estimated to be $2.7 (\pm 2.6) \times 10^{-7}$ and $1.5 (\pm 0.8) \times 10^{-6}$ (MPa dpa)⁻¹ at about 600-950°C and about 1080°C, respectively. Linear averaged creep compliances of $1-2 \times 10^{-6}$ (MPa dpa)⁻¹ were obtained for doses of 0.6-0.7 dpa in a temperature range of 400-1000°C [14]. Actual post-irradiation creep data for CVD SiC from bend test stress relaxation experiments is given in Table 20. The definition of irradiation creep is the difference in dimensional changes between a stressed and an unstressed sample irradiated under identical conditions. Irradiation creep is important for structural materials for nuclear services since it is a major contributor to the dimensional instability of irradiated materials at temperatures where thermal creep is negligible. However, studies on irradiation creep of SiC-based materials have so far been very limited.

No data was found for post-irradiation thermal creep of CFRC or SiC/SiC composite materials. Pre-irradiation tensile thermal creep testing has been performed on SGL 1501G CFRC material at 800°C in nitrogen atmosphere at 130 MPa for 100 hours. This material showed no significant creep strain under these conditions [36]. This material is very similar to SGL Grade 1502 YR and these materials are expected to have similar creep properties.

Table 20 CVD SiC Irradiation Creep Data from Bend Stress Relaxation Experiments [15]

Irradiation Temperature (°C)	Fluence (dpa)	Reactor	Initial/Final Bend Stress (MPa)	Initial/Final Bend Strain (x10 ⁻⁴)	Creep Strain (x10 ⁻⁴)	Bend Stress Relaxation (BSR) Ratio <i>m</i>	Average Creep Compliance x10 ⁻⁶ (MPa-dpa) ⁻¹
CVD SiC							
400	0.6	JMTR	82/60	1.80/1.39	0.41	0.77	0.97
600	0.2	JMTR	81/57	1.80/1.31	0.49	0.73	3.5
600	0.6	JMTR	81/46	1.80/1.05	0.75	0.58	2.0
640	3.7	HFIR	87/36	1.95/0.83	1.12	0.42	0.50
700	0.7	HFIR	102/72	2.27/1.64	0.63	0.72	1.1
750	0.6	JMTR	80/55	1.80/1.27	0.53	0.71	1.3
1030	0.7	HFIR	85/61	1.94/1.42	0.52	0.73	0.97
1080	4.2	HFIR	101/8	2.29/0.19	2.10	0.08	0.91
3C*-SiC							
640	3.7	HFIR	87/30	1.94/0.68	1.26	0.35	0.59
700	0.7	HFIR	102/90	2.27/2.06	0.21	0.87	0.34
1030	0.7	HFIR	86/57	1.94/1.31	0.63	0.67	1.2
1080	4.2	HFIR	101/1	2.29/0.02	2.27	0.01	1.1
*3C is one of several polytypes of the SiC bond							

Thermal Conductivity and Thermal Expansion

Changes seen in thermal conductivity in CFRC material as a function of temperature and neutron irradiation are given Figure 49. As noted, the thermal conductivity of unirradiated CFRC decreases as a function of temperature and irradiated thermal conductivity values are less than the unirradiated values. It should be noted as indicated previously in Table 12, values of thermal conductivity of CFRC can vary widely based on several variables.

No data were found for changes in thermal expansion properties for CFRC or SiC/SiC composite materials following irradiation.

The ratio of the irradiated to unirradiated thermal conductivity values (K_{irr}/K_0) for monolithic SiC and SiC/SiC composite materials evaluated at the irradiation temperature is given in Figure 50. The composite specimens were irradiated at about 335°C to 7.1 dpa. The curve for high purity CVD SiC represents a lower limit for SiC based materials with $K_{irr}/K_0 \sim 0.05$ at 200°C and only gradually increasing up to ~ 0.12 by 800°C. For irradiation temperatures above 800°C, an apparent transition occurs where the K_{irr}/K_0 curve turns upward with an increasing slope until at 1100°C the ratio is 0.6. The K_{irr}/K_0 ratio for the composite samples also increases with temperature and is greater than the CVD SiC. Based on the monolithic SiC thermal conductivity equation given in Table 14, unirradiated SiC at 800°C has a K_0 of 91.2 W/m K. This would yield a value of about 11 W/m K for irradiated SiC and a value of about 36.5 for the irradiated SiC/SiC composite samples. Therefore, as expected, the thermal conductivity of irradiated SiC/SiC composite material is lower than CFRC material at most temperatures of interest for the NNGP.

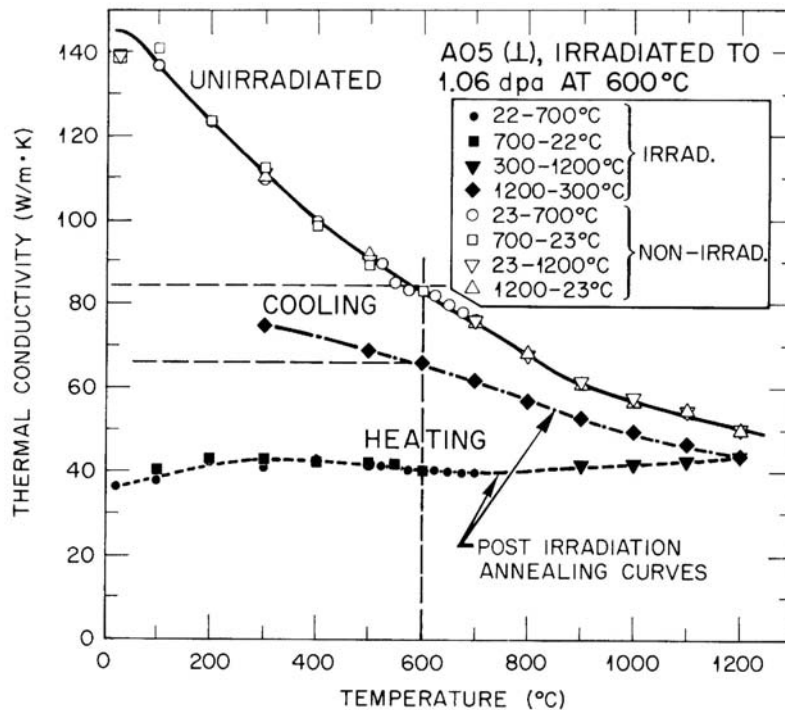


Figure 49 Thermal Conductivity Changes in CFRC Material as a Function of Temperature for Irradiated and Unirradiated Material [37]

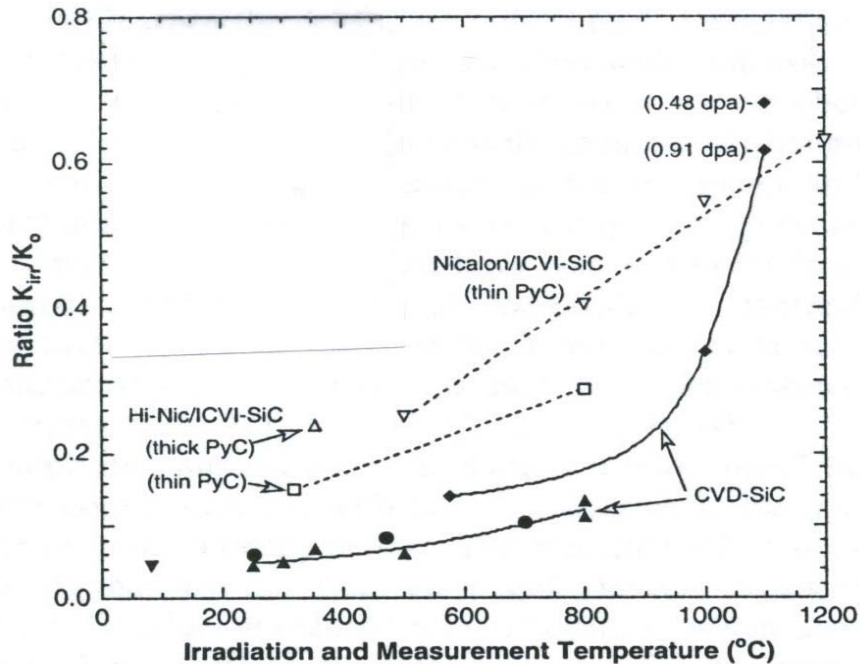


Figure 50 Ratio of Irradiated to Unirradiated Thermal Conductivity Values (K_{irr}/K_0) Measured at the Irradiation Temperature for High Purity CVD SiC and for Two Types of 2D SiC/SiC Composites [38]

Fatigue Properties

CFRC materials, of the type selected for the strap or tie rod applications, are only slightly degraded under dynamic loading conditions. Data are not available to evaluate the dynamic properties of SiC/SiC composites.

2.2 Structural Ceramics

It is not envisioned that structural ceramics including silicon carbide (SiC), Silicon Nitride (Si_3N_4) and Cordierite (magnesium aluminum silicate) would be used as a materials basis for any of the component applications noted. Therefore, with the exception of SiC properties data given previously, these materials are not addressed in this report. If the issue of a potential ceramic IHX A is investigated, then these materials and others would need to be investigated.

2.3 Insulation Products

These products are readily available in various forms and require only materials qualification for the specific component application. These materials are generally used in non-load bearing applications or in load bearing applications only in compression. Material choices include silica, alumina, or zirconia based insulation materials (including fused quartz insulation products) or baked carbon which can be fabricated in a wide range of forms.

It is expected that ASME codification for these materials for nuclear applications will not be required; however, it may need to be demonstrated that thermal stress in components made from these materials is not an issue, particularly where larger part sizes and more complicated geometries are involved.

Baked Carbon Insulation

NBC-07 baked carbon insulation material is formed by vibration molding and is manufactured from an isotropic pitch coke filler and coal tar pitch binder. The grain size of NBC-07 is identical to that used for NBG-18 thus qualifying NBC-07 as a medium-grain carbon. NBC-07 is manufactured from the same raw materials as NBG-18. It is pitch impregnated and re-baked once, following a similar processing route to NBG-18, except for a higher baking temperature of 1100°C. This carbon is the non-graphitized precursor to NBG-18 graphite.

This material will be used as an insulation layer in the BR of the DPP and should be usable for this application in the NGNP. The “against grain” orientation of this material is in the direction parallel to pressing of the billet during forming and the “with grain” orientation is in the direction perpendicular to the pressing direction. The physical properties of this material are given in Table 21.

Table 21 Selected Physical Properties of SGL NBC-07 Carbon Insulation Material [39]

Property	Units	Orientation	20°C	200°C	400°C	600°C	800°C	1000°C
Bulk Density	kg.m ⁻³	-	1740 ± 9	1740	1740	1740	1740	1740
Coefficient of Thermal Expansion* (CTE) (20°C – T)	10 ⁻⁶ K ⁻¹	With grain	Not Applicable	4.9 ± 0.1	See Figure 51			
		Against grain		5.0 ± 0.1				
		Combined		4.9 ± 0.1				
Isotropy Ratio	-	-	1.01 ± 0.01	Not Applicable				
Thermal Conductivity	800°C Bake W.m ⁻¹ .K ⁻¹	With grain	3.6 ± 0.07	TBD				
		Against grain	3.6 ± 0.09	TBD				
		Combined	3.6 ± 0.07	TBD				
	1050°C Bake W.m ⁻¹ .K ⁻¹	With grain	5.0 ± 0.1	See Figure 52				
		Against grain	4.9 ± 0.1					
		Combined	4.9 ± 0.1					
Emissivity	-	-	Not Applicable	0.78 ± 0.02				

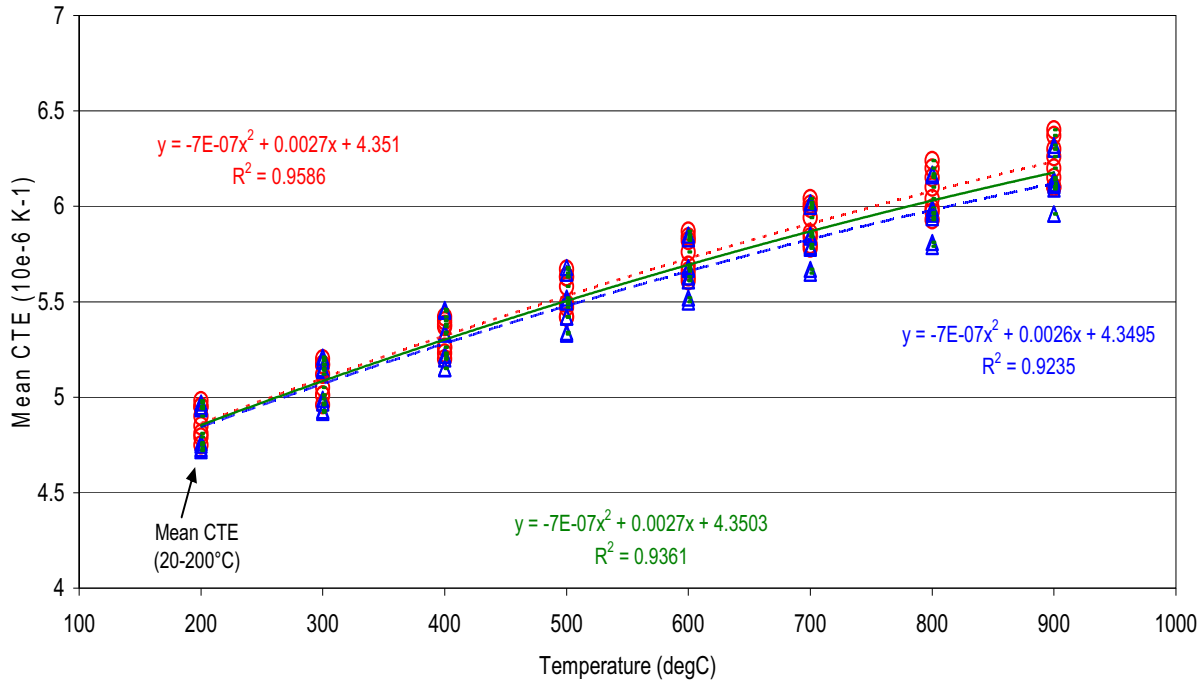


Figure 51 Mean Coefficient of Thermal Expansion (CTE) Plot for NBC-07 Baked Carbon Insulation [39]

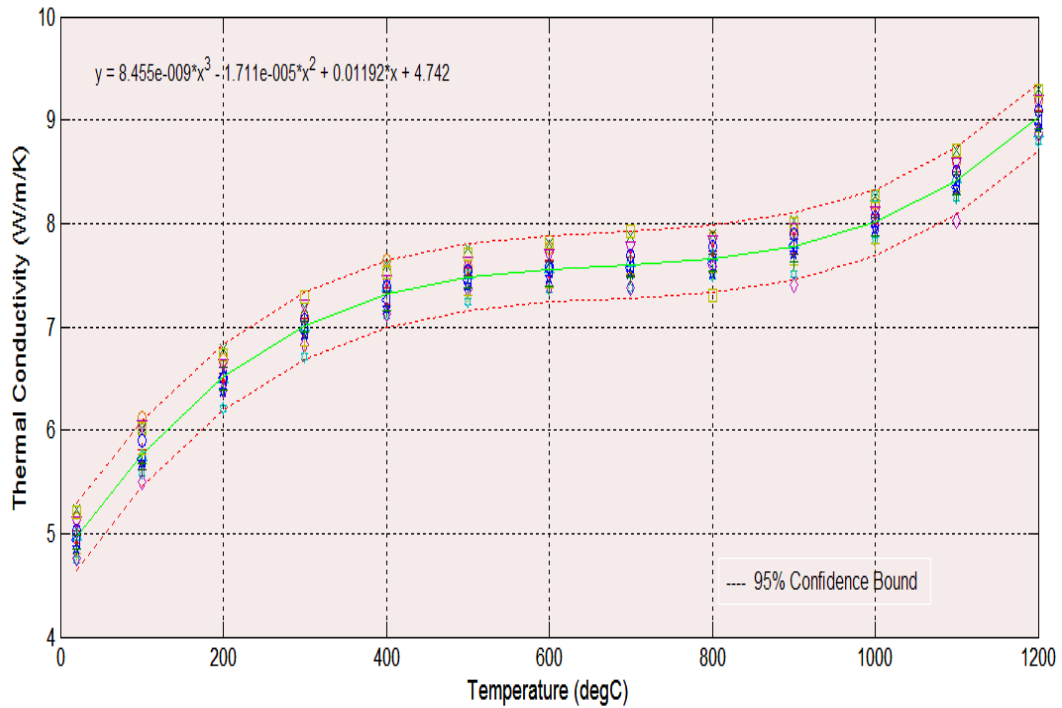


Figure 52 Thermal Conductivity of NBC-07 Baked Carbon Insulation [39]

The mechanical properties of the material are given in Table 22. Selected mechanical properties of the material following oxidization are given in Table 23.

Table 22 Selected Mechanical Properties of NBC-07 Baked Carbon Insulation Material [39]

Property	Units	Orientation	20°C
Tensile Strength	MPa	With grain	17.7 ± 1.2
		Against grain	18.0 ± 1.7
		Combined	17.8 ± 1.4
Compressive Strength	MPa	With grain	137.3 ± 6.7
		Against grain	139.7 ± 19.2
		Combined	138.5 ± 14.0
Flexural Strength (4-point)	MPa	With grain	25.0 ± 0.8
		Against grain	25.6 ± 1.3
		Combined	24.9 ± 1.7
Dynamic Elastic Modulus	GPa	With grain	15.7 ± 0.9
		Against grain	15.8 ± 0.4
		Combined	15.7 ± 0.7

Table 23 Selected Room Temperature Mechanical Properties of NBC-07 Baked Carbon Insulation Material Following Oxidation [39]

Property	Units	Orientation	0%	1%	3%	5%	7%	10%
Tensile Strength	MPa	With grain	17.7 ± 1.2	13.4	10.5	8.2	6.4	4.4
	MPa	Against grain	18.0 ± 1.7	13.4	10.5	8.2	6.4	4.4
Compressive Strength	MPa	With grain	137.3 ± 6.7	103.6	88.8	76.0	65.1	51.6
	MPa	Against grain	139.7±19.2	69.7	59.7	51.1	43.8	34.7

Note: The oxidized strength values were calculated using the same equation used to model the oxidized NBG-18 DPP core graphite strength

Fused Quartz Insulation Material

ZYAROCK is a slip-cast quartz material based on high grade fused quartz powder as the raw material. The slip-cast preform is sintered to form the final product form, which can be machined afterwards as may be required. ZYAROCK is similar to the GLASROCK material that was qualified for

use in the German HTR program and the MASROCK material that was used in the Ft. St Vrain HTGR in the US. It has very low thermal conductivity (<1.0 W/m/K) in the temperature range of interest for design (RT - 800°C). The use of quartz powder and a sintering process imparts some of the characteristics of fused quartz to ZYAROCK, e.g. very low CTE (<1.0x10⁻⁶ K⁻¹). The sintering process produces a permeable material with low tensile strength (<15 MPa). Selected properties of this insulation material are given in Table 24. A layer of quartz insulation material may be required in the bottom reflector region of the NNGP adjacent to the baked carbon layer to provide additional insulation to protect the metallic reactor support components.

Table 24 Key Properties of ZYAROCK Rigid Ceramic Insulation [40]

Property	Unit	Value
Density	kg/m ³	1950
Thermal Conductivity at RT	W.m ⁻¹ .K ⁻¹	0.64
Thermal Conductivity at 800°C	W.m ⁻¹ .K ⁻¹	0.55
CTE	10 ⁻⁶ K ⁻¹	0.6
Tensile Strength	MPa	15
Flexural Strength	MPa	27
Compressive Strength	MPa	50
Young's Modulus	GPa	20

OSC-2 is an opaque fused quartz based on electrically fused, high grade natural quartz powder as the raw material. The opacity of OSC-2 is induced via the manufacturing control which imparts controlled bubble content to the material. The OSC-2 material is similar to ZYAROCK but manufactured such that its key properties (specifically strength) are improved. A key difference is that the OSC material is fused as opposed to sintered, as is the case for ZYAROCK. The higher bubble content of OSC-2 needed for opacity lowers its ultimate strength from that of clear quartz, but imparts higher tensile strength than that of ZYAROCK. The OSC-2 material also has low thermal conductivity (<5W/m/K) in the NNGP temperature range of interest (RT - 800°C) but thermal conductivity is greater than ZYAROCK. Selected properties of this insulation material are given in Table 25.

Table 25 Key Properties of the OSC-2 Fused Quartz Insulation [41]

Property	Value
Density (kg/m ³)	2050
Thermal Conductivity (R.T) (W.m ⁻¹ .K ⁻¹)	1.25
Thermal Conductivity (800 °C) (W.m ⁻¹ .K ⁻¹)	2.19
CTE (10 ⁻⁶ K ⁻¹)	0.54

Property	Value
Tensile Strength (MPa)	20
Compressive Strength (MPa)	500
Young's Modulus (GPa)	72

Other Insulation Types

Other insulation types are discussed below that may be applicable for the HGD, IHX and COC applications. Several issues need to be considered for these applications, as noted below:

- Flexible insulation forms may be required due to the complex geometries associated with these components
- Flexible insulation forms are generally permeable by helium gas under pressure and, as a result, the thermal conductivity of the insulation increases as a function of the size of the gas molecule and the gas pressure
- The actual design of the COC and IHX has not been completed and design changes may be required for the HGD. Consequently, only estimates will be provided for the thickness and type of insulation required for the designs considered

Saffil insulation will be used in the HGD for the DPP design. Saffil insulation is available in a variety of forms and is 96% high purity polycrystalline fiber (Al_2O_3) that is manufactured by a unique process to control fiber diameter and non-fibrous material content. The maximum service temperature of this material in air is about 1540°C. This type of insulation material in blanket form has a thermal conductivity value that varies from 0.07 (315°C) to 0.2 (980°C) W/m K in air at normal atmospheric pressure; however, increased values would be expected in association with high pressure helium [42].

Another type of insulation which was considered for these applications is an aerogel insulation form available as a SiO_2 or Al_2O_3 based insulation material. This insulation material is described in ASTM C 1676-08, Standard Specification for Microporous Thermal Insulation. This insulation material has a thermal conductivity value that varies from about 0.028 (100°C) to 0.043 (800°C) W/m K in air at normal atmospheric pressure. The Al_2O_3 and SiO_2 based forms of this type of insulation have maximum temperature limits for long term exposure of 1150°C and 1000°C, respectively [43]. The most significant feature of aerogel insulation that imparts very low thermal conductivity values is its fine solid matrix with extremely fine pore size. Base-catalyzed tetraethoxysilane (TEOS) aerogel has a mean pore size of about 20nm. Such a small pore size greatly restricts the motion of gas molecules in the aerogel [44]. Figure 53 is a plot of estimated mean thermal conductivity of Microtherm silica based aerogel insulation as a function of temperature from 200-600°C. Table 26 compares thermal conductivity data for Microtherm and Saffil insulation types in air with estimated values for the Microtherm insulation based on Figure 53. Thermal conductivity of porous insulation increases as a function of mean temperature and helium pressure. If it is assumed that both insulation types increase at the same rate during exposure to high pressure helium at elevated temperature, it can be seen based on inspection of the estimated data given in Table 26 that the aerogel insulation is a factor of about 3-6 more effective than the Saffil based insulation for the same thickness of insulation, particularly at temperatures above 600°C, due to the difference in insulation type and the greater resistance to heat loss caused by radiative effects.

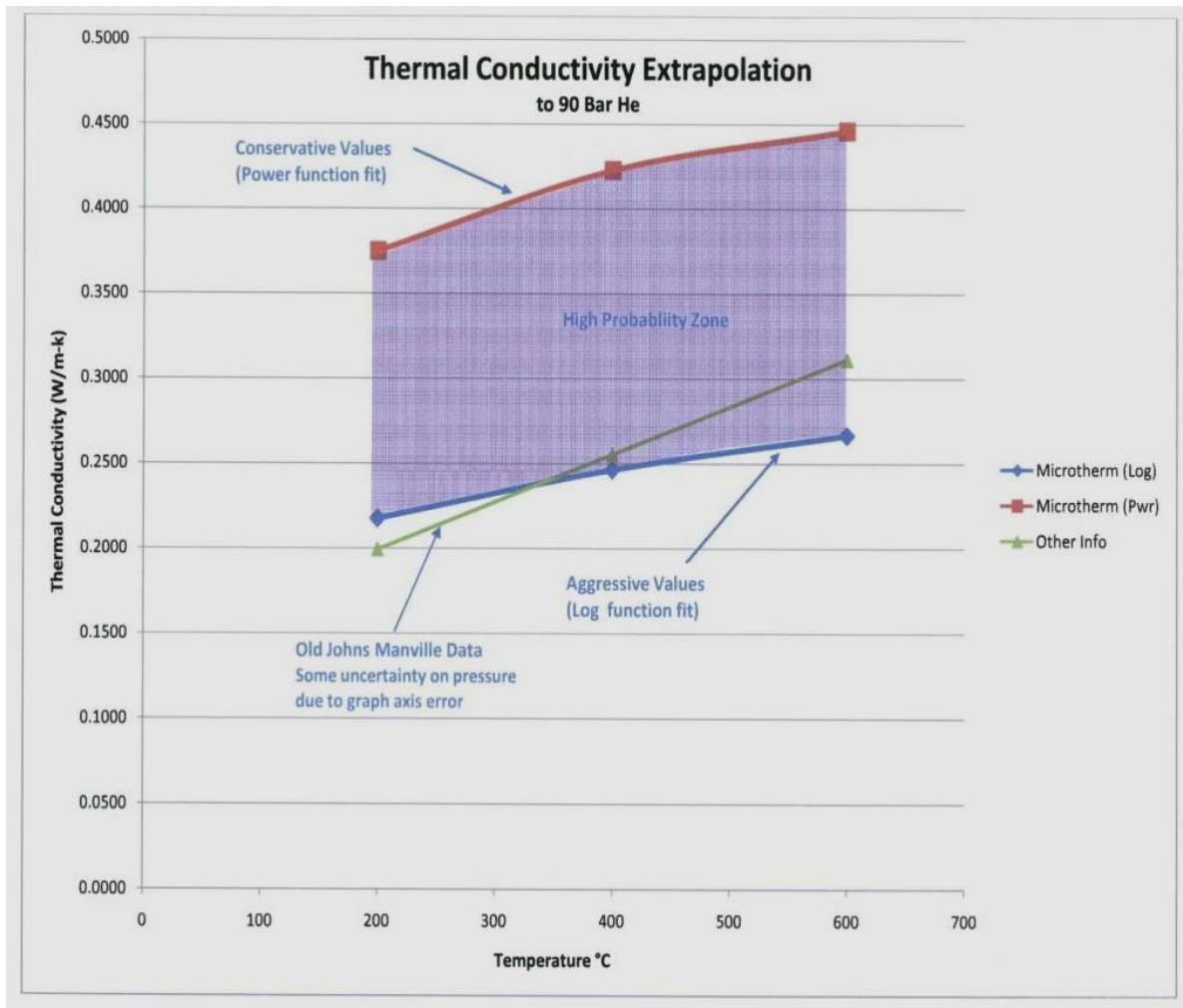


Figure 53 Mean Thermal Conductivity Data for Microtherm Aerogel Silica Insulation Estimated for a 90 bar Helium Environment [43]

Table 26 Mean Thermal Conductivity (TC) Data Comparing Microtherm and Saffil Insulation Types

Temperature, °C	TC of Microtherm Silica Insulation in Air (W/mK)	TC of Saffil Alumina Insulation in Air (W/mK)	Estimated TC of Microtherm Silica Insulation in He at 90 Bar (W/mK)
100	0.02		
315	0.02-0.03	0.07	0.2- 0.4
600	0.03		0.3- 0.4
800	0.03		
980		0.2	0.4- 0.5

2.4 Evaluation of Metallic Alloys for the RCS and HGD Liner Applications

A large number of alloys were evaluated previously for NNGP IHX fabrication applications [45]. Several alloys from this evaluation were considered to be potential alternatives to Alloy 800H for the COC and HGD liner applications and the RCS application. A discussion of these alloys and a comparison to Alloy 800H are given below.

Haynes 230 alloy is a nickel-chromium-tungsten alloy that has excellent high temperature mechanical properties and outstanding oxidization resistance. This alloy has excellent forming and welding characteristics and, due to good ductility, can also be formed by cold working. This alloy is furnished in the solution heat treated condition and is a solid solution high temperature alloy that contains about 57% nickel, about 22% chromium and about 14% tungsten. This alloy has excellent stability and resistance to grain coarsening following long time exposure at high temperatures and has a very low thermal expansion coefficient. This alloy does not precipitate embrittling second phases during high temperature exposure. Haynes 230 is available in a wide variety of product forms and specifications and is covered by ASME Section VIII, Division 1 up to 982°C. Post-irradiation properties are not available in the literature for this material; however, it is believed that this material would be embrittled by several potential mechanisms following irradiation [53]. Therefore, this material would not be suitable to potentially use for the RCS application. The high tungsten content in Alloy 230 is also undesirable for potential activation products in the oxide film; however, tungsten, due primarily to its isotopic composition is less likely to present a problem in this area.

Alloy X is a nickel-chromium-iron-molybdenum alloy that has moderately good high temperature mechanical properties and outstanding oxidization resistance. This alloy has excellent forming and welding characteristics and, due to good ductility, can also be formed by cold working. This alloy is furnished in the solution heat treated condition and is a solid solution high temperature alloy that contains about 47% nickel, about 22% chromium, about 18% iron and about 9% molybdenum. This alloy can precipitate embrittling second phases during high temperature exposure above 700°C. Alloy X is available in a wide variety of product forms and specifications and is covered by ASME Section VIII,

Division 1 up to 900°C. This alloy is very mature compared to Alloys 556, HR-120 and RA-330 and is slightly less mature compared to Alloys 617 and 800H. The Japanese conducted an extensive evaluation of Alloy X for application to the IHX of the HTTR demonstration that was subsequently constructed in Japan. In doing so, they developed an XR compositional variant of this alloy specifically designed to resist the oxidizing and carburizing effects of impure helium at high temperatures. Post-irradiation properties of Alloy X appear to be better than Alloys 230 and 617 but less than the post-irradiation properties of Alloy 800.

The influence of helium coolant on the chemical compatibility of structural materials that are planned for use in the NNGP is also of interest. Helium, because of its chemical inertness and attractive thermal properties, is used as a primary coolant in VHTRs. However, the primary coolant in an operating VHTR is expected to be contaminated by small amounts of gaseous impurities such as H₂, H₂O, CH₄, CO, CO₂ and O₂ from a variety of sources, such as reactions of ingressed water and oil with core graphite, and outgassing of reactor materials. These impurities are projected to be at ppm levels in the helium coolant, but the upper bound would strongly depend on the level of purification used for the helium supply and the leak tightness of the reactor system. These impurities probably do not have an effect on composites but are known to have an effect on the metallic alloys discussed at high temperature.

Figure 54 gives the summary results of a French helium corrosion study performed on Alloys 800H, 617, 230 and X at 950°C for 813 hours. In summary, Hastelloy X and XR are more stable than the other alloys, due to the improvement of the stability of surface oxide film which consists of MnCr₂O₄ and Cr₂O₃ layers.

The helium coolant in an operating VHTR makes a complete circuit from the graphite core to the heat exchangers or gas turbines and back to the core in several seconds. It is reported that the gas components in the coolant, via reaction with the graphite in the core and, to a limited extent, with themselves, will reach a steady state under this dynamic flow condition and may approach an equilibrium state with respect to the core [46]. Equilibrium between the surfaces of metallic components and the gaseous impurities in the primary coolant helium is not expected to occur under these very fast flow conditions. Therefore, the carbon activity and oxygen partial pressure in the helium coolant, under such non-equilibrium conditions, will be determined by individual reactions that predominate in the gas mixture.

From the structural materials standpoint, we are interested in reactions that can affect the corrosion loss and/or influence the mechanical integrity; reactions that can lead to processes such as oxidation, carburization, and decarburization are of interest. Carburization and decarburization processes are determined by the carbon activity in the gas mixture relative to that in the exposed metal surface. Similarly, the oxidation process is determined by the oxygen partial pressure in the environment relative to the stability of oxides of the constitutive elements that are present on the exposed metal surface. A detailed discussion on reactions between various gas species in helium and its influence on the thermodynamic activity of carbon and oxygen has been documented elsewhere [47].

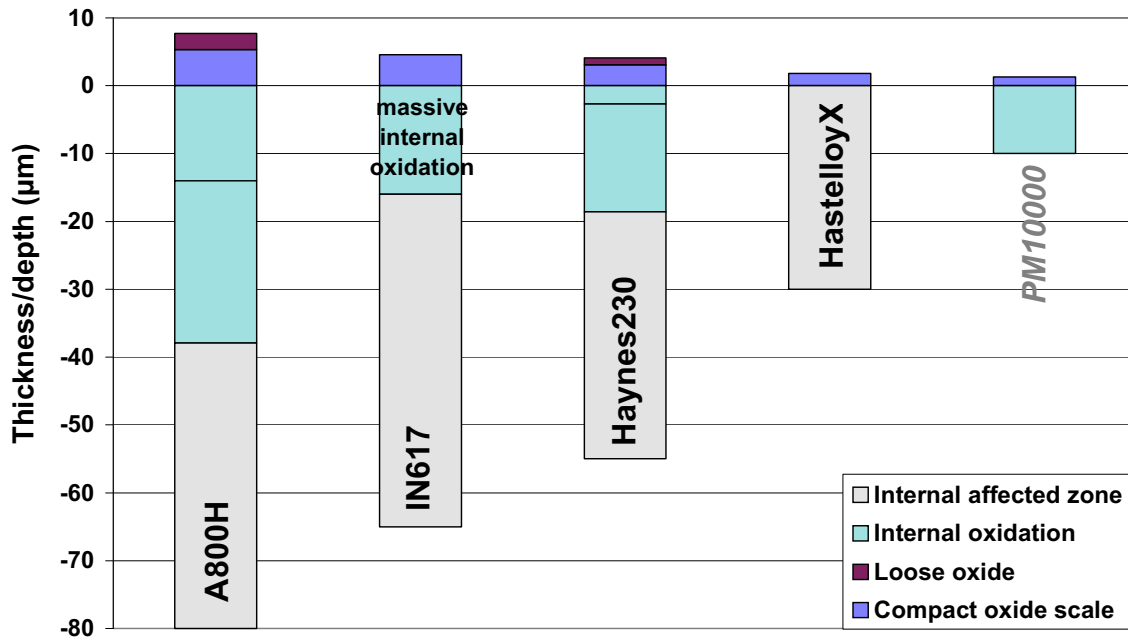


Figure 54 Summary of French He Test Data at 950°C and 813 Hours [48]

Alloy 617 is a nickel-chromium-cobalt-molybdenum alloy that has the highest high-temperature mechanical properties (compared to the other alloys evaluated) and outstanding oxidization resistance. This alloy was originally developed to optimize resistance to high temperature creep. This alloy has excellent forming and welding characteristics and, due to good ductility, can also be formed by cold working. This alloy is furnished in the solution heat treated condition and is a solid solution high temperature alloy that contains about 44% nickel, about 22% chromium, about 13% cobalt and about 9% molybdenum. This alloy has excellent stability and resistance to grain coarsening following long time exposure at high temperatures and has a low thermal expansion coefficient. This alloy does not precipitate embrittling second phases during high temperature exposure; however, the alloy does show some loss of fracture toughness as a function of aging time at high temperatures. Alloy 617 is available in a wide variety of product forms and specifications and is covered by ASME Section VIII, Division 1 up to 982°C. This alloy is the most mature of the alloys evaluated, with the exception of Alloy 800H, which has comparable maturity. Variability in high temperature mechanical properties for different heats of this alloy has been an issue in the past. This is due in part to the long history of this alloy, significant changes that have taken place over the years in melting practice and the relatively wide chemical specification range for this alloy. Alloy 617 has the highest cobalt content among the alloys. The high cobalt content is undesirable for any nuclear application because surface layers (oxides) that form on the surface of components made from these materials in the primary loop could become dislodged and form Co-60 by neutron activation following circulation in the reactor. Therefore, this material would not be suitable for the liner or the RCS application. Also, the post-irradiation properties of this material appear to be inferior to Alloy 800H.

Alloy 800H is an iron-nickel-chromium alloy that has fair high temperature mechanical properties and fair resistance to sulfidizing, carburizing and oxidizing environments. This alloy has excellent forming and welding characteristics and, due to good ductility, can also be formed by cold working. This

alloy is furnished in the solution heat treated condition and must be solution annealed at about 1093°C in order to obtain a stable austenitic structure. This alloy is a solid solution high temperature alloy that contains about 43% iron, about 33% nickel and about 22% chromium. Alloy 800H is available in a wide variety of product forms and specifications and is covered by ASME Section VIII, Division 1 up to 900°C. It is the only alloy in the group that is listed for use in ASME Section III, Subsection NH for a maximum temperature up to 760°C. This alloy has been tested for resistance to an impure helium environment at high temperatures. This alloy is the most mature of the alloys evaluated, with the exception of Alloy 617, which has comparable maturity. As noted previously, Alloy 800H is currently used for several components in the DPP design including the HGD liner and specific portions of the RCS system exposed to high temperatures and relatively high fluence. The HGD liner is not exposed to irradiation damage and only unirradiated high temperature properties, high temperature stability and corrosion resistance are relevant.

All austenitic alloys, including Alloy 800H experience irradiation induced ductility loss as a result of exposure to thermal neutrons at elevated temperature. The embrittlement worsens as either the exposure temperature or the fluence increases. Helium is produced by the nuclear transmutation reaction of thermal neutrons with the boron and nickel in the alloy. The bubbles grow and coalesce under tensile loads, and the result is intergranular cracking and low ductility. Because of the role of nickel in the production of helium, iron-based alloys experience less embrittlement than nickel-rich alloys, which explains why Alloy 800H performs better than many other high-temperature corrosion-resistant alloys during irradiation.

Fast neutrons result in atomic displacement damage, such as vacancies and interstitials. In metals these defects are annealed out, and the effect of fast neutrons on the material properties is negligible at high temperatures. For Alloy 800H this temperature range is between 250 to 600°C based on most studies performed.

In a classic German study on Alloy 800H [49], irradiation caused a large increase in yield strength and in the ultimate tensile strength when irradiated at 400°C, but there was no change in strength when irradiated at 600°C. Unirradiated control specimens were given the same thermal exposure as irradiated specimens before tests to eliminate the effects of thermal aging on the mechanical properties. In addition, some irradiated specimens were given simulated service exposure after irradiation. Annealing unirradiated Alloy 800H at temperatures above 500 – 600°C caused carbides to form, which resulted in strengthening. Irradiation also produced carbide precipitation and caused strengthening beginning at 400°C. Reduction in ductility is a consequence of increased strength. A decrease in ductility was observed at test temperatures above 400°C for either irradiation temperature, but there was no effect at lower test temperatures.

Tensile testing can be a means of evaluating materials before more complex testing is done, and there have been several tensile studies on irradiated Alloy 800H. For example, another German study [50] irradiated eight commercially available alloys at 375°C to a fluence of 1.1×10^{21} n/cm² (E>0.1 MeV). The ductility of Alloy 800H decreased after irradiation, but not as much as most of the alloys tested. Even in the embrittled state, it still had 15% elongation when tested at 700°C and about 3% elongation at 850°C.

In a Japanese study [51] with a maximum thermal fluence of 1.2×10^{21} n/cm² (E>0.1 MeV) and subsequent tensile testing at 700 – 1000°C and various strain rates, the tensile ductility and creep rate were reduced by about one order of magnitude for most of the alloys, but only by about half for Alloy 800H.

The thermal creep properties of Alloy 800H are seriously degraded by irradiation induced helium embrittlement, but again, Alloy 800H outperformed other alloys under consideration.

Alloy 800H has inherently high fracture toughness, comparable to those of austenitic stainless steels. As a result, elastic-plastic J_c methodology was used to characterize the ductile fracture behavior of the material at room temperature, 427°C, and 538°C. The J_c decreases with increasing temperature, as shown in Figure 55 for Alloy 800H. Irradiation at temperatures of 400 to 427°C and neutron exposures of 7 and 12 dpa, causes an order of magnitude reduction in J_c , as shown in Figure 55. The fracture properties for fluence levels of 7 and 12 dpa were very similar, so data for these exposures were plotted on a single curve. As a result, fracture toughness at higher neutron exposures is not expected to be worse. Note that 7 to 12 dpa corresponds to a fluence range of $2.2\text{-}3.4 \times 10^{22}$ n/cm² ($E > 0.1$ MeV), which is several times greater than the fast fluence predicted for the total 60 year lifetime of the control rod.

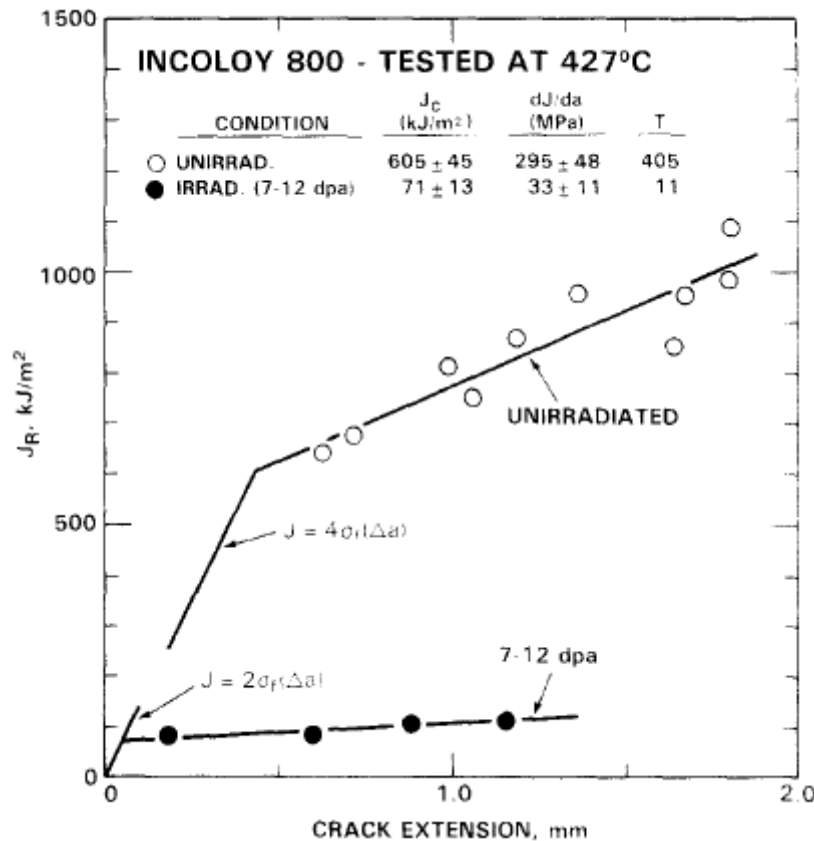


Figure 55 Ductile Fracture Behavior of Alloy 800 at 427°C [52].

2.5 Summary

In summary, several metallic alloys, composites and insulation materials were evaluated for the applications noted in the materials evaluations performed. The following factors are considered significant regarding these materials:

1. Materials evaluations have determined either specific materials or a general materials category (primarily CFRC) that are useable for the component applications noted.
2. Composites are several years from nuclear codification and can only be used in applications where design by test or analysis is appropriate for the application.
3. The composites evaluated have better high temperature properties above 1000°C than the metallic alloys evaluated. This could be important during off-normal events; however, at normal operating temperatures the properties of the highest temperature metallic alloys appear to be adequate for the RCS and liner applications; however, as noted above these materials are not considered to be optimum.
4. The composites can be engineered for specific applications (such as the tie rods and the straps).
5. The composites evaluated may be susceptible to corrosive attack by impure high temperature coolant under NNGNP conditions. There is a lack of data in this area for high temperature composites. The metallic alloys evaluated are either known to be subject to this type of attack to various degrees or it is suspected that they could be subject to this form of attack. This is important because all of the components evaluated must remain stable and able to perform their function over long time periods at elevated temperatures and it is known that this type of attack can potentially degrade the properties of the metallic alloys to various extents.
6. Pitch-based CFRC materials are better suited than PAN-based materials for use in components that are subjected to high neutron fluence; however, for components that have low or no neutron exposure, PAN-based CFRC composites have generally superior properties.
7. A primary issue for the application of CFRC components at higher levels of neutron exposure is swelling and eventual degradation of properties. This does not appear to be an issue for high performance SiC/SiC composite materials. This is important in the design of such a component to ensure that the function of the component could be maintained.
8. CFRC materials are more mature and versatile than high performance SiC/SiC composites. The only significant advantage that SiC/SiC composites have for the applications noted is higher resistance to neutron damage at higher fluence levels.
9. The use of baked carbon and or silica based insulation systems appears to be suitable for the lower reflector applications noted.
10. The use of high performance insulation material (as noted above) for the HGD and the IHX systems will be determined based on the evolution of design changes required for the HGD and the maturation of the IHX design. This study is limited to exploring potentially feasible concepts in these areas and a more extensive review to be performed during conceptual design will further define insulation and the associated design modifications required.
11. Alloy 230 appears to have adequate high temperature mechanical properties and helium corrosion resistance for the liner applications but, as noted above, is not considered optimum for these applications. This material is not suitable for the RCS application because this material appears to have poor post-irradiation properties.
12. Alloy 617 has the best overall strength at elevated temperature but is not suitable for either the liner applications or the RCS application because it has poor post-irradiation properties and contains a significant amount of cobalt.

13. Alloys X or XR are potentially viable for the liner applications because of their high resistance to helium corrosion and could represent a lower cost option, if needed. Post-irradiation properties may be unacceptable for the RCS application.
14. Alloy 800H may be a viable metallic alloy candidate for the RCS and liner applications; however, its mechanical properties near 1000°C and high temperature helium corrosion resistance are issues that would require further evaluation if this material is selected.
15. If a high temperature metallic alloy was used for the liner or RCS applications, the existing DPP design would not require modification to accommodate these materials.

2.6 References

1. Carbon Fiber Reinforced Carbon, product information, SLG Carbon Group
2. Carbon Materials for Advanced Technologies, edited by T. D. Burchell, Pergamon Press, 1999
3. Y. Katoh, et. al., Summary of SiC Tube Architecture and Fabrication, ORNL-GEN4/LTR-05-007 Draft, August 2005
4. A.R. Bunsell and A. Piant, A Review of the Development of Three Generations of Small Diameter SiC Fibers, *J. Materials Science* 41 (2006) Pages 823-839
5. M. Sugimoto et. al., *J. American Ceramics Society* 78 (1995) 1849
6. H. Ichikawa, et. al., High Temperature Matrix Composites II, edited by A.G. Evans and R. Naslain, *Ceramic Transactions* 58, ACS 1995, Page 65
7. Thermal Conductivity Databases of Various Structural Carbon-Carbon Composite Materials, NASA Technical Memorandum 4787, November 1997
8. "Evaluation of Materials Issues in the PBMR and GT-MHR", EPRI, Palo Alto, CA: 2002, 1007505
9. L.L.Snead, et. al., Strength of Neutron-Irradiated High-Quality 3D Carbon Fiber Composite, *J. Nuclear Materials* 321 (2003) Pages 165-169
10. Hinoki, et.al., The Effect of High Dose/High Temperature Irradiation on High Purity Fibers and Their SiC Composites, *J.Nuclear Materials* 307-311 (2002, Pages 1157-1162
11. T. Nozawa, et. al. (ORNL) and R. Shinavski (Hyper-Therm High Temperature Composites, Inc., Tensile Properties of Advanced SiC/SiC Composites for Nuclear Control Rod Applications, unpublished data
12. L.L. Snead, et. al., Evaluation of Neutron Irradiated Near-Stoichiometric SiC Fiber Composites, *J. Nuclear Materials*, 283-287 (2000) Pages 551-555
13. Y. Katoh, et. al., Effect of Neutron Irradiation on Tensile Properties of Unidirectional SiC Composites, *J. Nuclear Materials*, 367-370 (2007), Pages 774-779
14. Y. Katoh, et. al., Current Status and Critical Issues for Development of SiC Composites for Fusion Applications, *J. Nuclear Materials* 367-370 (2007), Pages 659-671
15. L.L. Snead, et. al., Handbook of SiC Properties for Fuel Performance Modeling, *J. Nuclear Materials*, 371 (2007), Pages 329-377
16. Burchell, T.D., et. al., *The effect of neutron irradiation on the structure and properties of carbon-carbon composite materials*. *J. Nucl. Mat.*, 1992. 191-194: p. 295-299
17. Klett, J.; Windes, W. E.; Lessing, P. *Next Generation Nuclear Plant Carbon Composites Vendor Survey*; Oak Ridge National Laboratory: Oak Ridge, May 25, 2005
18. Klett, J.; Windes, W. E.; Lessing, P. *Next Generation Nuclear Plant Carbon Composites Literature Review and Composite Acquisition*; ORNL-GEN4/LTR-05-008; Oak Ridge National Laboratory: Oak Ridge, August 15, 2005

19. Simmons, J.W.H., *Radiation Damage in Graphite*. 1965: Pergamon, New York, London.
20. Kelly, B.T., *Physics of Graphite*. 1981, London: Applied Science Publishers
21. Nightingale, R.E., *Nuclear Graphite*. 1962: Academic Press.
22. Burchell, T.D., *Fission Reactor Application of Carbon*, in *Carbon Materials for Advanced Technologies*, T.D. Burchell, Editor. 1999, Elsevier Science Ltd: Kidlington, Oxford, England. p. 429-478.
23. Snead, L.L., *Fusion Energy Application*, in *Carbon Materials for Advanced Technologies*, T.D. Burchell, Editor. 1999, Elsevier Science Ltd: Kidlington, Oxford, England. p. 389-427.
24. Bonal, J.P. and C.H. Wu, *Neutron Irradiation Effects on the Thermal Conductivity and Dimensional Stability of Carbon Fiber Composites at Diverter Conditions*. J. Nucl. Mat., 1996. 228: p. 155-161
25. Burchell T.D. et al. The effects of irradiation damage on the properties of GraphNOL N3M, J. Nuclear Material 170-181, pp205-208
26. Tim Burchell, Carbon-Carbon Composites for VHTR's (NGNP) – Current Status and Future Needs, Generation – IV International Forum, Materials and Components Provisional Management Board, NNC Ltd, Knutsford, UK, September 7-9, 2004
27. Assessment of the Effect of Neutron Irradiation on SGL Sigrabond Carbon Fiber-Reinforced Carbon Composite as Candidate Material for the PBMR, L.L. Snead, Revision 2, August 2005, Unpublished Report
28. Properties of Multilayered SiC/SiC and FMI-222 Graphite Composites after Medium-Dose Irradiation, Yutai Katoh and Lance L. Snead, ORNL/GEN4/LTR-08-003, April, 2008
29. Post Irradiation Evaluation of SiC/SiC and C/C Composites After 10 dpa Exposure, Yutai Katoh and Lance L. Snead, ORNL/TM-2006/556, September, 2006
30. Simmons, J.W.H., *Radiation Damage in Graphite*. International Series of Monographs in Nuclear Energy. Vol. 102. 1965: Pergamon Press.
31. Burchell, T., Radiation Damage in Carbon-Carbon Composites: Structure and Property Effects, Physica Scripta, Volume T64, Pages 17-25, 1996
32. Windes, W. E.; Lessing, P. A.; Katoh, Y.; Snead, L. L.; Lara-Curzio, E.; Klett, J.; Henager, C., Jr.; Shinavski, R. J. *Structural Ceramic Composites for Nuclear Applications*; DRAFT - INL/EXT-05-00652; Idaho National Laboratory: Idaho Falls, August 2005
33. McEnaney, B. and T. Mays, *Relationships between Microstructure and Mechanical Properties in Carbon-Carbon Composites*, in *Essentials of Carbon-Carbon Composites*, C.R. Thomas, Editor. 1993, Pub. Royal Society of Chemistry. p. 143-173.
34. Delle, W., et al. *Fracture Toughness of Fast Neutron Irradiated Graphite*. in *Contributions to the International Conference on Carbon. CARBON '88*. 1988. Germany.
35. Sato, et. al., Fusion Engineering and Design 13, Pages 159-176 (1990)
36. Creep Testing on C/C Composites for SGL Carbon Group, University of Bremen, SGL Report 02 2002, March 2002.
37. Burchell, Tim, MRS Bulletin XXII, Pages 29-35, 1997
38. Youngblood, G.E., et. al., Effects of Irradiation and Post-irradiation Annealing on the Thermal Conductivity/Diffusivity on Monolithic SiC and f-SiC/SiC Composites, J. Nuclear Materials. 329-333 (2004), Pages 507-512
39. PBMR Materials Datasheet 022141, NBC Baked Carbon Blocks, Revision 3, June 2008
40. PBMR Demonstration Plant Safety Analysis Report, Document Number, 001929-4 Rev 2B (Draft), Chapter 4, Reactor Unit and Fuel, 09/07
41. Saint Gobain OSC-2 Technical Data, 8/07.
42. ZIRCAR Technical Data , 8/08
43. Microtherm Technical Data, 8/08

44. Zeng, S. et. al., Transport Properties of Gas in Silica Aerogel, *J. of Non-Crystalline Solids*, 186 (1995), Pages 264-270
45. Special Study 20.3, High Temperature Process Heat Transfer and Transport, Document Number, NGNP-20-RPT-003, January 2007
46. Johnson, W.R. et. al., Interaction of Metals with Primary Coolant Impurities: Comparison of Steam-cycle and Advanced HTGRs, Specialist Meeting on High Temperature Metallic Materials for Application in Gas Cooled Reactors, Paper J1, 1981
47. Natesan K. et. al., Materials Behavior in HTGR Environments, NUREG/CR-6824 (ANL-02/37), 2003
48. Bulet H. et. al., French VHTR Near Term High Temperature Alloy Development Program, GIF Materials and Components Project Management Board, Paris, September 2005
49. Thiele, B. A.; Schubert, F.; Derz, H.; Pott, G., Influence of test temperature on post irradiation, high temperature tensile and creep properties of X8CrNiMoNb 16 16, X 10 NiCrAlTi 32 32 (Alloy 800 and NiCr22Fe18Mo (Hastelloy X)). *Journal of Nuclear Materials* 1990, 171, 94-102.
50. Thiele, B. A.; Diehl, H.; Ohly, W.; Weber, H., Investigations into the irradiation behavior of high-temperature alloys for high-temperature gas-cooled reactor applications. *Nuclear Technology* 1984, 66, 597-606
51. Watanabe, K.; Kondo, T.; Ogawa, Y., Postirradiation tensile and creep properties of heat-resistant alloys. *Nuclear Technology* 1984, 66, 630-638.
52. Mills, W. J., Fracture Toughness of Two Ni-Fe-Cr Alloys. *Engineering Fracture Mechanics* 1987, 26, (2), 223-238.
53. T. Angeliu, et. al, Assessing the Effects of Radiation Damage on Ni-base Alloys for the Prometheus Space Reactor System, LM-06K033, April, 2006
54. Yamada R., Mechanical and Thermal Properties of 2D and 3D SiC/SiC Composites, *J. Nuclear Materials* 283-287 (2000) 574-578
55. Newsome G., et al, Evaluation of Neutron Irradiated Silicon Carbide and Silicon Carbide Composites, *Journal of Nuclear Materials* 371 (2007), pages 76-89

3 DESIGN AND TECHNOLOGY DEVELOPMENT

This section comprises three main elements, as summarized below.

1. The identification of outstanding design issues associated with the applications discussed in Section 3.1. These are not DDNs, but are given to assist in the identification of design issues to be addressed during NNGP Conceptual Design.
2. Requirements for codification activities and a possible approach for implementation of these activities are given in Section 3.2. It is not currently possible to actually address these issues in terms of DDNs until the ASME has addressed the corresponding issues in further detail. It should be noted that codification is not considered necessary as a prerequisite for the NNGP demonstration plant; however, codification would be desirable in support of follow-on commercial plants.
3. DDNs identified as a result of this investigation are given in Section 3.3. The required DDNs are based on:
 - a. The potential need for post-irradiation examination data for the Tie Rod and Strap materials. In the case of the DPP, the fluences seen by the Tie Rods and Straps meet criteria for concluding that there is essentially no irradiation exposure. However, fluences in the NNGP will be higher and actual fluence accumulations calculated by modeling of the NNGP design may exceed the estimated values noted previously. If so, testing may be required to account for potential irradiation effects. (DDN COMP 01-01)
 - b. The actual materials selected in the future for the RCS application. The material options discussed previously include CFRC materials, SiC/SiC composite materials or a metallic alloy (Alloy 800H is the metallic alloy currently used in the DPP design). If one of these materials were selected, an irradiation program and post-irradiation examination would be required for the specific material selected. If Alloy 800H is retained, the irradiation program would not be required, but would be required if Alloy X or XR were selected. As noted in Section 2, the selection of Alloys 230 or 617 is not recommended for this application. (DDN COMP 01-02)
 - c. The actual materials selected for the COC and HGD liners. The material options discussed previously include CFRC materials and/or a metallic alloy (Alloy 800H is the metallic currently used in the DPP design). If CFRC was selected for the COC or HGD liner, a characterization program would need to be performed, based on the application requirements. If Alloy 800H, Alloy 230 or Alloy X were selected, the characterization program would not be required. As noted in Section 2, the selection of Alloy 617 is not recommended for this application. (DDN COMP 01-03)
 - d. The actual insulation materials selected for the HGD and other piping applications; the insulation selected for IHX A and B and the quartz insulation (if required) to supplement the baked carbon insulation in the Lower Reflector region below the core. Characterization of one or more of these materials would need to be performed, based on the application requirements. (DDN COMP 01-04)
 - e. It is estimated that about \$6.5M in funding and a schedule of 2-4 years would be required to accomplish the DDNs given, if all work was performed in parallel.

3.1 Design Needs

The following needs for further design development were identified from Section 1. In some cases, the results of this further design work will determine whether or not specific DDNs in Section 3.3 are required and, if so, will further define the associated requirements for those DDNs.

A. Core Restraint Straps

1. Review the current design of the core restraint strap developed for the DPP and determine if changes to the design are required for the NGNP
2. Modeling of the NGNP outer reflector region needs to be performed to validate the estimate of fluence for the straps.
3. Modeling of the outer reflector region needs to be performed to validate the temperature environment for both normal and off-normal operating conditions.
4. The DPP procedures and qualification information for the core restraint strap material needs to be reviewed; modified as required and validated for the NGNP design.

B. Tie Rods

1. Review the current design of the Tie Rods developed for the DPP and determine if changes to the design are required for the NGNP.
2. The surveillance, monitoring and inspection procedures were developed for the DPP design and these procedures need to be reviewed for the NGNP design.
3. Modeling of the NGNP upper reflector region needs to be performed to validate the estimate of fluence for the tie rods.
4. Modeling of the upper reflector region needs to be performed to validate the temperature environment for both normal and off-normal operating conditions.
5. The DPP procedures and qualification information for the Tie Rod material need to be reviewed; modified as required and validated for the NGNP design.

C. Hot Gas Duct Components

1. A review, potential modification and validation of the COC design are required for the NGNP.
2. The materials design basis for the CFRC liner and the metallic components of the COC needs to be validated for the NGNP design.
3. The piping system design needs to be reviewed and potentially modified for the NGNP.
4. The materials basis for the piping design needs to be reviewed and potentially modified for the NGNP.
5. Procedures for surveillance, inspection and monitoring of the COC and HGD for the DPP need to be reviewed and modified as required for the NGNP.
6. Modeling of the NGNP needs to be performed to determine the temperatures seen by the metallic components of the COC and the inner pressure pipe of the HGD.
7. Qualification procedures need to be developed for the NGNP COC and HGD.
8. An evaluation of the current PCDR piping design for the NGNP needs to be made to consider a specific off-normal event that has not been thoroughly evaluated. This off-normal event involves the loss of the secondary heat sink across IHX A and B due to loss of function in the secondary system. One of the issues to be considered that could directly affect the current

piping design is that helium cooling in the annulus from the circulator could increase in temperature up to some equilibrium level that could impact the integrity of the SA-533 pressure boundary piping.

D. Reactivity Control Components

1. A review of the adequacy of the Alloy 800H material for the control rods is required for the NGNP application and a recommendation made for alternate materials to be used in the NGNP design, if required.
2. Modeling is required of the ISR to determine the fluences seen by the control rods and chains for the NGNP application.
3. A modeling study to verify the temperature of the RCS control rods and chains needs to be performed for the NGNP design.
4. Qualification testing for RCS components has not been investigated for the NGNP design. Therefore, a study to determine qualification testing and procedures for these components is needed for the NGNP design.

E. Core Support/Core Barrel Interface Insulation

1. A temperature analysis study that models the upper and lower reflector regions of the NGNP design is required to determine the insulation requirements that will be needed to protect metallic support components.
2. A modeling study of the NGNP is required to determine the radiation exposure expected for Layers 1, 2 and 3 of the Lower Reflector region of the CSC.
3. Qualification procedures for the fused quartz material will need to be developed if required for the NGNP application.

F. High Temperature Section Insulation

1. A design study of the IHX systems is needed to evaluate the insulation required and to provide a more detailed conceptual design of the IHX systems for the NGNP.
2. A modeling study is required to evaluate the temperature distributions in IHX A and B.
3. A qualification plan is required for the insulation to be used in IHX A and B.

3.2 Codification Approach

The codification approach discussed in this section is directed at high temperature composite materials similar to the materials described in other portions of this report. This section does not address low temperature composites used for a variety of applications.

Establishing an ASME Code framework for the use of CFRC and/or SiC/SiC composites in a VHTR will require at a minimum the development of:

- Design codes, which list “rules” and guidelines for designing and testing composite components and incorporating them into advanced designs
- Design codes which regulate the certification procedures for processing materials, fabricating components, and assembling final designs
- Databases that provide statistically significant and complete material properties and performance.

Background

Currently, no internationally recognized nuclear design codes exist for composite materials or components. There is a lack of internationally accepted guidelines pertaining to the qualification of composite materials for nuclear applications. Coupled to this is a need to qualify commercially available composite manufacturing and processing techniques, particularly large-scale component fabrication and qualification techniques. Non-destructive techniques for composite materials and components also require significant development. The long-term, high temperature irradiation response of this class of materials entailing a wide range of properties such as strength, thermal properties, fatigue, and creep behavior remains largely unqualified. Grade-specific design data covering the full range of design data such as tensile, compressive, flexural and shear strength, thermal expansion and thermal conductivity, fracture toughness and oxidation resistance is lacking. There is also a need for standardization in Quality Assurance (QA) and test methods pertaining to the acquisition of this data. The current ASTM type test standards that exist for Ceramic Matrix Composites (CMC's) are given in Table 27, but further development is needed, particularly for more advanced CMC's, e.g. SiC-SiC composites. The steps in the ASTM and International Organization for Standardization (ISO) balloting processes are given in Figure 56.

A task group within ASTM Subcommittee C28.07 is planning to develop a specification for composite materials for gas reactor applications. Discussion is planned for their next meeting in January, 2009 in Daytona Beach.

Openly available databases must be developed for specific reproducible product forms for CMCs and CFRCs to produce valid, statistically-significant property and performance data using recognized, full-consensus standards. Most detailed databases that have been produced to date for specific materials in specific product forms are proprietary or not readily available. Limited standardization of these materials has been addressed in the following full-consensus standards:

- American Society for Testing and Materials (ASTM) Subcommittee C28.07 on Ceramic Matrix Composites
- Comité Européen de Normalisation (CEN) Subcommittee TC184/SC1 on Ceramic Composites
- International Organization for Standardization Technical Committee TC206 on Fine (Advanced, Technical) Ceramics.

In addition, other noteworthy, non full-consensus standards for CMCs have been developed by the NASA High Speed Research/Enabling Propulsion Program (HSR/EPM) in the United States and the Petroleum Energy Center (PEC) in Japan.

Table 27 Current ASTM Standards for the Mechanical evaluation of Fiber-reinforced Ceramic Matrix Composites]

C1275-00 (2005) e1 Standard Test Method for Monotonic Tensile Behavior of Continuous Fiber-Reinforced Advanced Ceramics with Solid Rectangular Cross-Section Test Specimens at Ambient Temperature

C1292-00(2005) Standard Test Method for Shear Strength of Continuous Fiber-Reinforced Advanced Ceramics at Ambient Temperatures

C1337-96(2005) Standard Test Method for Creep and Creep Rupture of Continuous Fiber-Reinforced Ceramic Composites under Tensile Loading at Elevated Temperatures

C1341-00(2005) Standard Test Method for Flexural Properties of Continuous Fiber-Reinforced Advanced Ceramic Composites

C1358-05 Standard Test Method for Monotonic Compressive Strength Testing of Continuous Fiber-Reinforced Advanced Ceramics with Solid Rectangular Cross-Section Test Specimens at Ambient Temperatures

C1359-05 Standard Test Method for Monotonic Tensile Strength Testing of Continuous Fiber-Reinforced Advanced Ceramics with Solid Rectangular Cross-Section Test Specimens at Elevated Temperatures

C1360-01 Standard Practice for Constant-Amplitude, Axial, Tension-Tension Cyclic Fatigue of Continuous Fiber-Reinforced Advanced Ceramics at Ambient Temperatures

C1425-05 Standard Test Method for Inter-laminar Shear Strength of 1-D and 2-D Continuous Fiber-Reinforced Advanced Ceramics at Elevated Temperatures

C1468-00 Standard Test Method for Trans-thickness Tensile Strength of Continuous Fiber-Reinforced Advanced Ceramics at Ambient Temperature

C1469-00(2005) Standard Test Method for Shear Strength of Joints of Advanced Ceramics at Ambient Temperature

C1557-03 e1 Standard Test Method for Tensile Strength and Young's Modulus of Fibers

ASTM (18 to 36 months)

New Work Item (Task group formed, title)

Subcommittee Ballot (Draft document submitted to subcommittee only)

Concurrent Main and Subcommittee Ballots (Refined document submitted to sub and main committees)

Society Review (Refined document available for society)

ASTM Standard

ISO

Stage 0 (preliminary stage): A study period is underway.

Stage 1 (proposal stage): An NP (New Project) is under consideration.

Stage 2 (preparatory stage): A WD (Working Draft) is under consideration.

Stage 3 (committee stage): A CD/FCD (Committee Draft/Final Committee Draft) is under consideration.

Stage 4 (approval stage): An FDIS (Final Draft International Standard) is under consideration.

Stage 5 (publication stage): An IS (International Standard) is being prepared for publication.

Figure 56 Steps in the ASTM and ISO standards balloting processes

The Department of Defense Handbook, Volume 17 on composite materials consists of five volumes. Volumes 1-3 cover polymer matrix composites, Volume 4 covers metal matrix composites and Volume 5 (which includes composite materials discussed in this report) covers ceramic matrix composites. It appears that the information in Volume 5 will directly support ASME codification activities. Volume 5 is organized into four parts:

- Part A Introduction and Guidelines, Pages 1-108
- Part B Design and Supportability, Pages 114-117
- Part C Testing, Pages 119-178
- Part D Data Requirements and Data Sets, Pages 180-233

Recommended Approach

In recent years, efforts have been initiated to develop design codes for composites within the ASME Boiler and Pressure Vessel Code (BPVC). In June 2008, a decision was made by the Subgroup on Nuclear Graphite to start an activity to codify the use of composites as core components. In addition to design rules, the BPVC also lists materials and materials specifications allowed for use in BPVC certified designs. Finally, detailed procedures for design, fabrication, and inspection of boilers, pressure vessels, and related components are spelled out in the Code. The Code is currently divided into ten sections and each section is comprised of several volumes of related information. It would be reasonable to initiate codification of composite materials by writing a draft code case initiated from within the Subgroup on Nuclear Graphite. This committee has been officially sanctioned by the Board of the ASME Boiler and Pressure Vessel Code and is a part of Section III (Nuclear). This Subgroup has concentrated its efforts to date on nuclear graphite; however, high temperature composites are a part of their charter.

This ASME Section III Subgroup has limited resources and codification of nuclear graphite is currently a priority; however, the creation of a new group within the committee to start work on VHTR composites is being discussed and a proposal to begin work on a code for composites was accepted at a recent Subgroup meeting in Japan. It is planned that an official proposal document including an initial proposed roster of experts that would be involved with composites will be submitted to the ASME Section III board for discussion at the BPVC meeting in November in Los Angeles.

A cost and schedule estimate for codification of ceramic composites is very speculative at this point. It is currently estimated that codification of these materials will take at least ten years but this could be reduced if a well coordinated effort was initiated. It is recommended that funding be provided to ASME to thoroughly investigate the codification issues involved, establish an initial set of high priority tasks, negotiate budgets for tasks developed and initiate bids for implementation of these tasks.

The primary reason why the codification effort has progressed very slowly in the past is lack of high level organizational support and lack of directed funding. Codification efforts for nuclear graphite have not received ASME funding in the past and this has resulted in a protracted schedule for this work. Implementation of the above approach could rapidly change this picture for composites.

As noted previously, codification is not believed to be required for the NNGNP Demonstration Plant component applications discussed in this report; but would facilitate the deployment of follow-on commercial plants. For the NNGNP Demonstration Plant, it is currently believed that codification would only need to be in place for critical core components, reactor support or pressure boundary applications; however, this cannot be fully validated prior to detailed licensing discussions with the NRC in support of NNGNP design.

Organization within the Code

The development of national design codes will recognize the maturation of composites and the need for designers to consider the unique properties and performance of these materials in their advanced designs from the outset. Two primary philosophies are followed in the BPVC: design by rule (i.e., what has worked in the past will work in the future) and design by analysis (i.e., application of sound engineering science). In addition to design rules, the BPVC also lists materials and materials specifications allowed for use in BPVC certified designs. Finally, detailed procedures for design, fabrication, and inspection of boilers, pressure vessels, and related components are spelled out in the Code.

Full consensus standards must first be developed to characterize materials. Databases must next be developed to produce valid, statistically-significant property and performance data using the recognized,

full-consensus standards. Various levels of significance are assigned to the information contained in the database, namely: screening, preliminary, and fully qualified. Design codes and life prediction methodologies must then be developed based on the unique design requirements of the materials and design applications. Inherent in the design codes are fully qualified materials properties and performance databases determined using full consensus standards. Life prediction methodologies are an integral part of these design codes. Finally, regulatory approval is achieved once the material, components, and design methodologies have been established, validated, and documented.

Design codes are widely-accepted general rules for the construction of components or systems with emphasis on safety. A main objective is reasonably long safe-life for the design while providing reasonably certain protection of life and property. While recognizing the needs of the users, manufacturers, and inspectors, the main premise of the codes is that safety of the design can never be compromised.

Design codes do not impose specific rules for design but allow flexibility for introducing new designs as required for performance, efficiency, usability, or manufacturability while still providing constraints for safety. This allows the design code to be wide ranging and links are incorporated between materials, general design (formulae, loads, allowable stresses, permitted details), fabrication methods, inspection, testing, certification, data reports, and quality control to ensure that the code has been followed. Thus, the code inherently contains many of the standards for materials testing, characterization, and quality control. Additionally, unlike standards that do not provide for compliance or accountability, codes require compliance through documentation, and certification through inspection and quality control.

The design approach that has been adopted by the Department of Defense for CMCs is documented in the Military Handbook 17, already mentioned above. For various reasons, this document will provide useful input to the codification effort being discussed, but the approach used in this handbook is not adequate for nuclear applications. However, the ASME Code, because of its direct application to pressurized equipment, is directly applicable. Two possible paths to codification could be considered:

- Development of a code case
- Development of a stand-alone section of the ASME Code

It is recommended that the first path be selected as a first step, because it requires less time, funding and effort and will meet the required nuclear codification needs for composites. It was also the path selected by the ASME Section III Nuclear Graphite Subgroup for the codification of nuclear graphite. The basic path that needs to be followed is the same one taken for nuclear graphite. An outline of the code case sections and appendices required for composites (based on the nuclear graphite code case being developed) is given below:

Article 1000: Introduction
Article 2000: Composite Materials Included in the Code Case
Article 3000: Design
Article 4000: Machining
Article 5000: Installation and Examination
Article 6000: Testing
Article 8000: Certification

Appendix 1 - Composites Material Specifications (Mandatory Appendix)
Appendix 2 - Guideline for Creation of a Composite Materials Datasheet (Mandatory Appendix)
Appendix 3 - Requirements for Generation of Design Data for Composite Materials (Mandatory Appendix)

- Appendix I - Composites as a Structural Material (Non-Mandatory Appendix)
- Appendix II - Irradiation Damage to Composites (Non-Mandatory Appendix)
- Appendix III - Environmental Effects on Composites (Non-Mandatory Appendix)
- Appendix IV - Recommended Practice for Design Practices with Composites (Non-Mandatory Appendix)
- Appendix V - Database for Selected Composites (Non-Mandatory Appendix)

3.3 Design Data Needs

The following DDNs have been identified as a result of the evaluations documented in Sections 1 and 2.

1. If modeling shows that the fluence given in Section 1 is significantly underestimated, a limited irradiation and post-irradiation examination program would be required to fully characterize SGL Sigrabond CFRC Grade 2002 YR and Grade 1502 YR or the specific materials selected for the Race Track Straps and Tie Rods and to verify the effect of the actual irradiation exposure on the materials selected (see DDN COMP 01-01).
2. The material options discussed previously for the RCS application include CFRC materials, SiC/SiC composite materials and metallic alloys, Alloy X or XR (Alloy 800H is the metallic alloy currently used in the DPP design). If one of these materials were selected (other than Alloy 800H), an irradiation program and post-irradiation examination would be required for the specific material selected. As noted in Section 2, the selection of Alloys 230 or 617 is not recommended for this application. (DDN COMP 01-02)
3. The material options discussed previously for the COC liner and the HGD liner include CFRC materials and metallic alloys, Alloy 230 and Alloy X (Alloy 800H is the metallic alloy currently used in the DPP design). If CFRC were selected, a characterization program based on the application requirements would need to be performed. If Alloy 800H, Alloy 230 or Alloy X were selected, this program would not be required. As noted in Section 2, the selection of Alloy 617 is not recommended for this application. (DDN COMP 01-03)
4. A program is required to characterize the actual insulation materials selected for the HGD and other piping applications; the insulation selected for IHX A and B and the quartz insulation (if required) to supplement the baked carbon insulation in the Lower Reflector region of the core. If the quartz insulation is needed, this would require a limited characterization program (DDN COMP 01-04).

DDNs corresponding to the above are provided in Appendices 1, 2, 3 and 4, respectively.

Appendix 1

DDN COMP-01-01 Characterize Race Track Strap and Tie Rod Materials

1. Assumptions

- a. The maximum calculated EOL fluence for the Tie Rods and/or the Race Track Straps to be used in the NGNP design is such that irradiation effects properties including swelling are required to be determined to fully characterize the materials to be used for the applications if, based on data obtained for similar materials in this report (Reference 26, Section 2), the maximum calculated EOL fluence levels is ≥ 0.2 dpa (carbon) or 3×10^{20} n/cm² (E > 0.1 MeV) for 1D CFRC material such as Grade 2002 YR and ≥ 0.5 dpa (carbon) or 5×10^{20} n/cm² (E > 0.1 MeV) for 2D CFRC material such as Grade 1502YR.
- b. The characterization data to be developed in support of the PBMR DPP will provide adequate characterization of the Race Track Strap and Tie Rod applications if irradiation effects data are not required.

2. Current Database Summary

The current and planned unirradiated databases for Sigrabond CFRC Grades 1502YR and 2002YR materials are adequate for the Race Track Strap and Tie Rod applications for the NGNP. If irradiation test data is required as noted above, new testing data would need to be generated.

3. Summary of Data Needed

If irradiation test data is required, adequate pre-characterization test data and post-irradiation test data on the specimens representative of the applications and the materials to be used is required. Irradiation test data for the specimens up to 1 dpa (carbon) or 1.4×10^{21} n/cm² (E > 0.1 MeV) in increments of 0.5 dpa (carbon) at irradiation temperatures of 600°C and 800°C is required. Pre-irradiation and post-irradiation test data required includes: Linear (parallel to length of racetrack and length of Tie Rod) shrinkage or swelling and, Density (CEN ENV 1389 (1994)), CTE (RT to 800°C, CEN ENV 1159-1 (1994)), Flexural Strength (3 point, RT, 600°C, 800°C ASTM C-1341-00 (2005)), Interlaminar Shear Strength (RT, ASTM C 1425-05), Thermal Creep (800°C and 1000°C, ASTM C 1337-96 (2005)), Tensile Strength (RT, 600°C, 800°C, ASTM C 1275-00 (2005) and ASTM C 1359-05).

Also, test data will be needed to determine susceptibility of these materials to corrosive attack in a high temperature impure helium environment of the type to be used in the NGNP.

4. Designer's Alternatives

Design's alternatives are to qualify other materials suitable for the applications if SGL Grades 1502YR and 2002YR materials are not used for the applications.

5. Selected Design Approach and Explanation

Selected design approach is to use the PBMR DPP design. This approach is used because alternate approaches would be less cost effective and could result in lower performance components.

6. Cost and Schedule Requirements

Test data, as noted above, is needed prior to NGNP Tie Rod and Strap qualification testing. It is estimated that this work would require about \$1.5M in funding and about two years to complete, if required.

7. Priority

Urgency (1-5):	2
Cost-Benefit (Low, Medium, High):	Medium
Uncertainty in Existing Data (Low, Medium, High):	Low
Importance of New Data (Low, Medium, High):	Medium

8. Fallback Position and Consequences Of Non-Execution

Assume that irradiation effects on materials properties are not significant and use DPP design and data.

9. References

- a. Material Qualification Plan, CFRC Plate, Document Number 030411, Revision 1, PBMR, July 2006
- b. Material Qualification Plan, CFRC Strap, Document Number 031327, Revision A, Draft, PBMR, August 2005
- c. CEN ENV 1389, Density of Continuous Fiber Reinforced Ceramic Composites
- d. CEN ENV 1159-1, Thermal Expansion of Continuous Fiber Reinforced Ceramic Composites
- e. ASTM C 1341-00, Standard Test Method for Flexural Properties of Continuous Fiber-Reinforced Advanced Ceramics (ambient and elevated temperatures)
- f. ASTM C 1425, Standard Test Method for Interlaminar Shear Strength of 1D and 2D Continuous Fiber reinforced Advanced Ceramics at Elevated Temperatures
- g. ASTM C1337-96, Standard Test Method for Creep and Creep Rupture of Continuous Fiber Reinforced Advanced Ceramics Under Tensile Loading
- h. ASTM C1275-00, Standard Test Method for Monotonic Tensile Strength Testing of Continuous Fiber Reinforced Advanced Ceramics with Solid Rectangular Cross Sections at Ambient Temperatures
- i. ASTM C1359-00, Standard Test Method for Monotonic Tensile Strength Testing of Continuous Fiber Reinforced Advanced Ceramics with Solid Rectangular Cross Sections at Elevated Temperatures

Appendix 2

DDN COMP-01-02 RCS Materials Characterization

1. Assumptions

- a. Any of the material options, including CFRC with a pitch fiber and a pitch base, Alloy 800H, Alloys X or XR or SiC/SiC composite material using Hi Nicalon Type S fiber and CVD infiltration are potentially suitable for the RCS application
- b. The limiting factors for candidate metallic alloys are the 1000°C estimated off normal maximum temperature, the post-irradiation mechanical properties and the resistance to high temperature helium corrosion
- c. The limiting factor for the CFRC material is the maximum estimated fluence
- d. The SiC/SiC material is not limited by any of these factors

2. Current Database Summary

In general, the database for Alloy 800H appears to be adequate; however, specific testing to further evaluate irradiated high temperature mechanical properties and helium corrosion may be required. Additional irradiated and unirradiated data may be required if Alloys X or XR were selected. Additional irradiated and unirradiated data would be required if CFRC or SiC/SiC composite materials were selected. Cost and schedule estimates for this DDN are based on the SiC/SiC and CFRC options.

3. Summary of Data Needed

For the CFRC or SiC/SiC composite materials selected, adequate pre-characterization test data and post-irradiation test data on specimens representative of the applications and the materials to be used is required. Irradiation test data for the specimens $\geq 7 \times 10^{21} \text{ n/cm}^2$ ($E > 0.1 \text{ MeV}$) in increments of 3.5×10^{21} at irradiation temperatures of 750°C and 1000°C is required. Pre-irradiation and post-irradiation test data required includes: Circumferential shrinkage or swelling following irradiation compared to pre-irradiation data, Density (CEN ENV 1389 (1994)), CTE (RT to 1000°C, CEN ENV 1159-1 (1994)), Flexural Strength (3 point, RT, 750°C, 1000°C ASTM C-1341-00 (2005)), Interlaminar Shear Strength (RT, ASTM C1425-05), Thermal Creep (750 and 1000°C, ASTM C 1337-96 (2005)), Tensile Strength (RT, 750°C, 1000°C, ASTM C 1275-00 (2005) and ASTM C 1359-05).

Also, test data will be needed for either material selected to determine susceptibility to corrosive attack in a high temperature impure helium environment of the type to be used in the NGNP.

4. Designer's Alternatives

Design's alternative is to use Alloy 800H for the RCS application based on PBMR and German qualification information.

5. Selected Design Approach and Explanation

The selected design approach is to use an alternate material for the NGNP RCS application (A Generation 3 SiC/SiC composite material is recommended). The approach selected uses a material that is more suitable for the NGNP application; however, it is anticipated that a redesign of the high fluence portion of the RCS would be required to accommodate either CFRC or SiC/SiC composite material if used for the application.

6. Cost and Schedule Requirements

Test data, as noted above, is needed prior to RCS testing for the NGNP. It is estimated that funding of about \$1.5M and a schedule of about 2 years would be required for this work.

7. Priority

Urgency (1-5):	1
Cost-Benefit (Low, Medium, High):	Medium
Uncertainty in Existing Data (Low, Medium, High):	High
Importance of New Data (Low, Medium, High):	High

8. Fallback Position and Consequences Of Non-Execution

Use Alloy 800H for the RCS application. It is anticipated that, if this alloy was selected, the service life of the RCS component would be reduced and replacement of the components would become more probable.

9. References

- a. CEN ENV 1389, Density of Continuous Fiber Reinforced Ceramic Composites
- b. CEN ENV 1159-1, Thermal Expansion of Continuous Fiber Reinforced Ceramic Composites
- c. ASTM C 1341-00, Standard Test Method for Flexural Properties of Continuous Fiber-Reinforced Advanced Ceramics (ambient and elevated temperatures)
- d. ASTM C 1425, Standard Test Method for Interlaminar Shear Strength of 1D and 2D Continuous Fiber reinforced Advanced Ceramics at Elevated Temperatures
- e. ASTM C1337-96, Standard Test Method for Creep and Creep Rupture of Continuous Fiber Reinforced Advanced Ceramics Under Tensile Loading
- f. ASTM C1275-00, Standard Test Method for Monotonic Tensile Strength Testing of Continuous Fiber Reinforced Advanced Ceramics with Solid Rectangular Cross Sections at Ambient Temperatures
- g. ASTM C1359-00, Standard Test Method for Monotonic Tensile Strength Testing of Continuous Fiber Reinforced Advanced Ceramics with Solid Rectangular Cross Sections at Elevated Temperatures

Appendix 3

DDN COMP-01-03 COC or HGD Liner

1. Assumptions

- a. Material options including CFRC with PAN fiber and a pitch base, Alloy 230, Alloy X or Alloy 800H are potentially suitable for the HGD liner applications. The COC liner will be some type of CFRC based on the DPP design.
- b. The limiting factor for the metallic alloys is the long term 950°C normal temperature exposure and corrosion from helium impurities
- c. The CFRC material is not believed to be limited by either factor; however, the degree of susceptibility to high temperature helium corrosion needs to be established.
- d. SiC/SiC composite materials could be used for this application; however, the cost would be much higher and this material is not required for this application because these liners are not irradiated.

2. Current Database Summary

The databases for Alloy 800H, Alloy X and Alloy 230 are adequate. Additional unirradiated data is required for the specific CFRC material selected.

3. Summary of Data Needed

For the CFRC material selected, test data on specimens representative of the applications and the materials to be used is required. The data required includes: Density (CEN ENV 1389 (1994)), CTE (RT to 1000°C, CEN ENV 1159-1 (1994)), Flexural Strength (3 point, RT, 1000°C ASTM C-1341-00 (2005)), Interlaminar Shear Strength (RT, 1000°C ASTM 1425-05), Thermal Creep (1000°C, ASTM C 1337-96 (2005)), Tensile Strength (RT, 1000°C, ASTM C 1275-00 (2005) and ASTM C 1359-05).

Also, test data will be needed to determine susceptibility to corrosive attack in a high temperature impure helium environment of the type to be used in the NGNP.

4. Designer's Alternatives

Design's alternative is to use Alloy 800H for the HGD liners based on PBMR and German qualification information.

5. Selected Design Approach and Explanation

Selected design approach is to use an alternate to the DPP design approach (a CFRC material is recommended for the HGD liner). The approach selected uses a material that is more suitable for the NGNP application; however, the use of CFRC for the HGD may require a design modification.

6. Cost and Schedule Requirements

Test data, as noted above, is needed prior to COC or HGD testing for the NGNP. It is estimated that funding of about \$500K and about a two-year schedule would be required for this work. It is estimated that an additional \$500K of funding and about a two-year schedule would be required to perform high temperature helium environment testing for all materials used in DDN COMP 01-01, 02 and 03.

7. Priority

Urgency (1-5):	1
Cost-Benefit (Low, Medium, High):	High
Uncertainty in Existing Data (Low, Medium, High):	Medium
Importance of New Data (Low, Medium, High):	High

8. Fallback Position and Consequences Of Non-Execution

Use Alloy 800H for the COC or HGD applications. It is anticipated that if this alloy was selected the service life of these component would be reduced and replacement of the components would become more probable.

9. References

- a. CEN ENV 1389, Density of Continuous Fiber Reinforced Ceramic Composites
- b. CEN ENV 1159-1, Thermal Expansion of Continuous Fiber Reinforced Ceramic Composites
- c. ASTM C 1341-00, Standard Test Method for Flexural Properties of Continuous Fiber-Reinforced Advanced Ceramics (ambient and elevated temperatures)
- d. ASTM C 1425, Standard Test Method for Interlaminar Shear Strength of 1D and 2D Continuous Fiber reinforced Advanced Ceramics at Elevated Temperatures
- e. ASTM C1337-96, Standard Test Method for Creep and Creep Rupture of Continuous Fiber Reinforced Advanced Ceramics Under Tensile Loading
- f. ASTM C1275-00, Standard Test Method for Monotonic Tensile Strength Testing of Continuous Fiber Reinforced Advanced Ceramics with Solid Rectangular Cross Sections at Ambient Temperatures
- g. ASTM C1359-00, Standard Test Method for Monotonic Tensile Strength Testing of Continuous Fiber Reinforced Advanced Ceramics with Solid Rectangular Cross Sections at Elevated Temperatures

Appendix 4

DDN COMP-01-04 Insulation Materials

1. Assumptions

- a. Silica or alumina aerogel insulation will be used for all or part of the HGD and IHX insulation
- b. Aerogel insulation may allow the use of passive insulation as an alternative to active cooling in the primary and/or secondary heat transport circuits.
- c. Quartz insulation will be used to supplement the baked carbon insulation used in the lower reflector as required based on NNGP design requirements.
- d. NBC-07 baked carbon insulation will be the primary insulation used in the lower reflector

2. Current Database Summary

The NBC-07 baked carbon database to be developed by PBMR for the DPP will be adequate. Additional unirradiated data is required for the specific quartz and aerogel insulation materials selected.

3. Summary of Data Needed

For the aerogel insulation material selected, test data on specimens representative of the insulation materials to be used for the piping, COC and the IHX applications is required. Test data are required to validate the thermal conductivity of the insulation in 90 bar helium at 200°C, 400°C, 600°C, 800°C, and 1000°C (ASTM C 680 and C 177). It is required that this test also include a determination of thermal conductivity of the insulation in helium following a rapid depressurization cycle from 90bar helium to atmospheric pressure that would be representative of a worst case pipe break off-normal event. This is required to verify that the distribution of small porosity in the aerogel type insulation is not disrupted by this type of event. Test data are also required to validate the dimensional stability of the material at 1000°C for 1 day, 2 days and 7 days (ASTM C 356). It is anticipated that the dimensions of the solid specimens used will initially change and then stabilize for the 2 and 7 day tests. Also, characterization of moisture content and determination of the amount of moisture removed from the insulation material during a heat-up cycle similar that that envisioned for the NNGP is required.

The data requirements for the quartz insulation selected are the same as that obtained for the baked carbon given in Reference 39, Section 2, except that post-irradiation properties based on irradiation \geq about $1E20$ n/cm² ($E > 0.1$ MeV) is required because data for low level irradiation properties only exists for clear fused quartz and not for the type of quartz to be used for insulation materials, if required.

4. Designer's Alternatives

Design's alternative for the aerogel insulation material is to use active cooling in conjunction with a conventional insulation material, such as Saffil, in a manner that is similar to the DPP design. There are no designer alternatives to the use of baked carbon or quartz insulation materials.

5. Selected Design Approach and Explanation

The selected approach is to use an alternate to the DPP design approach for the piping and COC insulation (an aerogel insulation product is recommended). The approach selected uses materials that are more suitable for the NGNP application. The selected design approach for the Lower Reflector insulation is to use the DPP design approach, supplemented by the use of quartz insulation, as necessary. This approach is considered to be suitable for the NGNP design. The selected approach for the IHX design has no precedent in the DPP design. The approach selected (an aerogel insulation product is recommended) is considered to be suitable for the NGNP design.

6. Cost and Schedule Requirements

Test data, as noted above, are needed prior to COC, HGD or IHX testing. It is estimated that funding of about \$2.5M and a schedule of about one year would be required for this work if all tasks were performed in parallel.

7. Priority

- | | |
|--|------|
| a. Urgency (1-5): | 1 |
| b. Cost-Benefit (Low, Medium, High): | High |
| c. Uncertainty in Existing Data (Low, Medium, High): | High |
| d. Importance of New Data (Low, Medium, High): | High |

8. Fallback Position and Consequences Of Non-Execution

Use Saffil insulation in conjunction with active cooling for the piping, IHX and COC applications. There is no fallback position for the Lower Reflector insulation noted. The consequence of using the Saffil insulation material is implementing designs for the piping, IHX and COC applications that would allow a lower performance insulation to be used.

9. References

- ASTM C680-04, Standard Practice for Estimate of the Heat Gain or Loss and the Surface Temperatures of Insulated Flat, Cylindrical and Spherical Systems by Use of Computer Programs
- ASTM C177-04, Standard Test Method for Steady State Heat Flux Measurements and Thermal Transmission Properties by Means of the Guarded Hot Plate Apparatus
- ASTM C356-03, Standard Test Method for Linear Shrinkage of Preformed High Temperature Thermal Insulation Subjected to Soaking Heat

BIBLIOGRAPHY

None. References are provided in individual sections.

DEFINITIONS

None

REQUIREMENTS

None

LIST OF ASSUMPTIONS

The following assumption served as a basis for this report:

1. Except as otherwise noted, the work within this report is based upon the functions, requirements, configuration and operating parameters recommended in the PBMR NGNP Preconceptual Design Report (NGNP PCDR, Section 4, Nuclear Heat Supply System, Revision 0, NGNP-04-RPT-01, May 2007 and NGNP PCDR, Section 6, Heat Transport System, Revision 0, NGNP-06-RPT-01, May 2007), as supplemented by the NGNP IHX and Heat Transport System Conceptual Design Study Report, (NGNP-HTS-RPT, TI001, Rev. 0, April 2008).

APPENDIX 1: 90% REVIEW VIEWGRAPHS

Composites Special Study
Conceptual Design Studies FY 08-2
Next Generation Nuclear Plant

90% Review Meeting with BEA

WBS Element Code Level: NHS.000.S15

Washington DC
02 October 2008

NGNP TEAM 



Project Team

- **George Hayner, Scott Penfield, Phil Rittenhouse, Fred Silady, and Dan Mears - Technology Insights**
- **Mark Mitchell, Steven Pieterse, Ruttie Nel, Shahed Fazluddin and Pieter Venter - Pebble Bed Modular Reactor (Proprietary) Ltd.**
- **Sten Caspersson, Alan Spring and Chris Hoffman – Westinghouse Electric Company**
- **Jan van Ravenswaay and Johan Markgraaff-M-Tech Industrial (Pty) Ltd.**

Key Milestones

1-1	Release to Start Work	5 May 08
1-3	Identify Components for Further Evaluation	13 Jun 08
1-4	Materials Survey	18 Jul 08
2-1	Recommended Operating Conditions	18 Jul 08
2-2	Required Materials Properties	22 Aug 08
2-3	Anticipated Codification Requirements	05 Sep 08
3-1	Development Requirements Cost & Schedule	10 Oct 08
4-1	Report Annotated Outline	30 May 08
4-2	50% Review	23 Jul 08
4-3	90% Review	02 Oct 08
4-4	Final Report	31 Oct 08

Purpose

- The purpose of this study is to identify the potential applications and design requirements for ceramic and ceramic composites in the HTGR primary system. Note: ceramic and ceramic composites refer to non-graphite materials
- Identify components that are anticipated to be fabricated from ceramic and ceramic composites along with the operating conditions for normal and off-normal conditions (i.e., stress, temperature, fluence, environmental conditions, etc.)
- Activities necessary to codify these materials (e.g., in ASME and ASTM codes) will be identified
- Identify any additional work anticipated to be required to support NRC licensing of the Nuclear Heat Supply System (NHSS).
- The objective of initiating operation of NGNP in 2021 shall be a factor in conducting this study

PBMR NGNP (a) (Indirect) vs PBMR DPP (Direct) - Operating Conditions (b)

Parameter	Normal Operation		DLOFC		PLOFC ^c	
	NGNP	DPP	NGNP	DPP	NGNP	DPP
RIT (°C)	350	500	-	-	-	-
ROT (°C)	950	900	-	-	-	-
Tmax, CB (°C)	350 (d)	414 (b)	466-634 (d)	579 (48h) (b)	565 (b)	482 (b)
Tmax, RPV (°C)	308 (d)	324 (b)	328-452 (d)	419 (56h) (b)	401 (56h) (b)	373 (48h) (b)
He Mass Flow (kg.s ⁻¹)	160	192	-	-	-	-
Thermal Power (MW)	500	400	-	-	-	-

^a 25% increase in power level, hence 25% higher flux level assumed for NGNP compared to DPP

^b Based on Case 5, NGNP Special Study 20.2: Prototype Power Level Study, NGNP-20-RPT-002, 26-01-07

^c Indirect cycle NGNP design, hence operating pressure in system assumed to remain constant at 9 MPa

^d Reactor Parametric NGNP Special Study, NGNP-NHS 90 PAR, August, 2008

Note: CB and RPV temperatures are only indicative and should not be used as absolute values

Composite Components in PBMR NGNP - Operating Conditions*

Component	Temp. (°C)		Max. Fast Neutron Fluence [n.cm ⁻² (E > 0.1 MeV)]
	Normal	DBE	
Core Circumferential Support – Lateral Restraint Straps	550	750	DPP limiting fluence = 1x10 ²⁰ n/cm ² Est. NNGNP fluence ≈ 2x10 ²⁰ n/cm ² **
Upper Reflector - Tie Rod Support; RSS tubes/insulation	550	650	DPP limiting fluence = 1x10 ²⁰ n/cm ² Est. NNGNP fluence ≈ 2x10 ²⁰ n/cm ² **
Hot Gas Duct – Inner Liner Core Outlet Connection Liner	950	<950	Not Applicable
RCS Control Rod – Control Rod Sheath; Secondary shock absorber	750	1000	DPP max fluence = 2.7x10 ²¹ n/cm ² Est. NNGNP fluence ≈ 5x10 ²¹ n/cm ² ***
Core Support/Core Barrel – Insulation	700	<700	Probably not significant
IHX High Temperature Section - Insulation	TBD	TBD	Not Applicable

*Assumption: DPP+50°C for NNGNP temp's, (DPP+25%)x1.5 for NNGNP fluences (60 yrs)

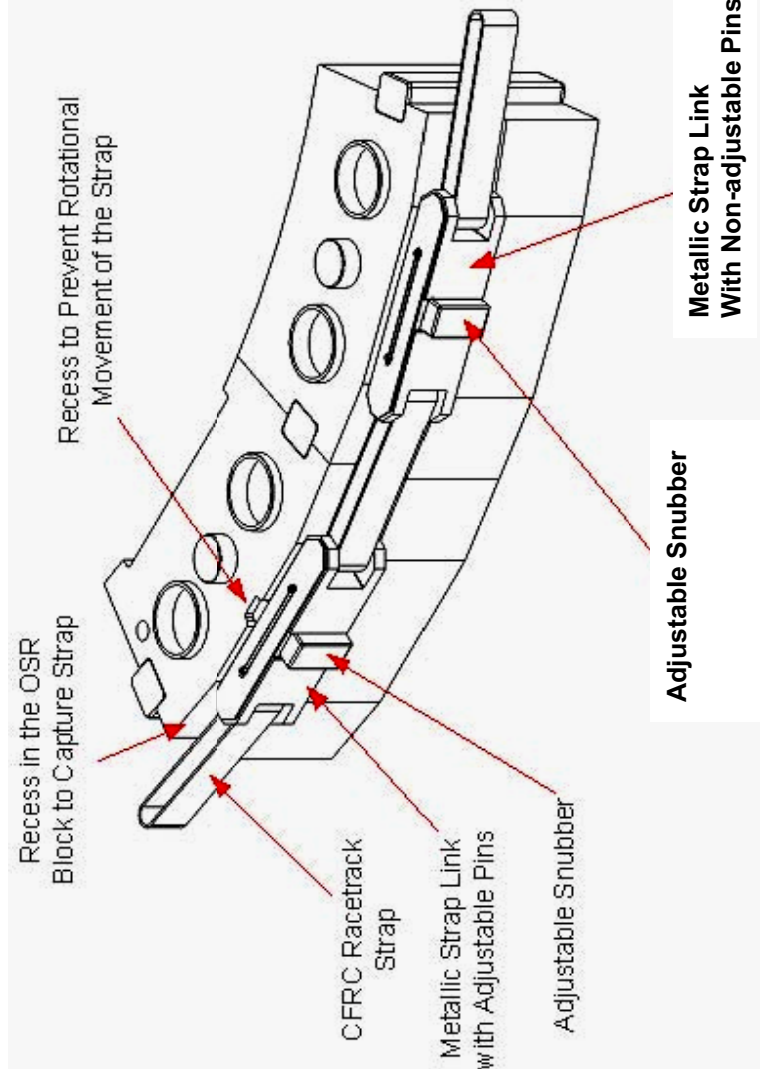
** 0.1 dpa; *** 3.6 dpa

Identification of Components

- **Core Circumferential Support Components**
 - **Strap Assembly with Carbon Fiber Reinforced Carbon (CFRC) Components**
- **Upper Reflector Support Components**
 - **CFRC Tie Rods; RSS Interface Tubes**
- **Hot Gas Duct Components**
 - **Hot Gas Duct, Including Liner and Insulation**
 - **Core Outlet Connection (COC) CFRC Liner**
- **Reactivity Control Components**
 - **Control Rods, Cladding Tubes and Joints; RCS Secondary Shock Absorber**
- **Core Support/Core Barrel Interface Insulation**
 - **Bottom Reflector (BR) Insulation; RSS Interface Insulation**
- **High Temperature Section Insulation**
 - **IHX A and B Insulation**

Core Lateral Restraint Strap Design

- Mating Components in the strap assembly are Fabricated from Type 316 SS
- The strap is used to ensure that the core is circumferentially constrained under all operating conditions
- PBMR has a completed design for the Straps for the DPP and a testing program will be performed on the Straps prior to installation
- The CFRC straps are designed for flexural strength and slight negative thermal expansion properties.
- The proper function of the CFRC Racetrack Strap in the NGNP design requires that the neutron fluence remains low.



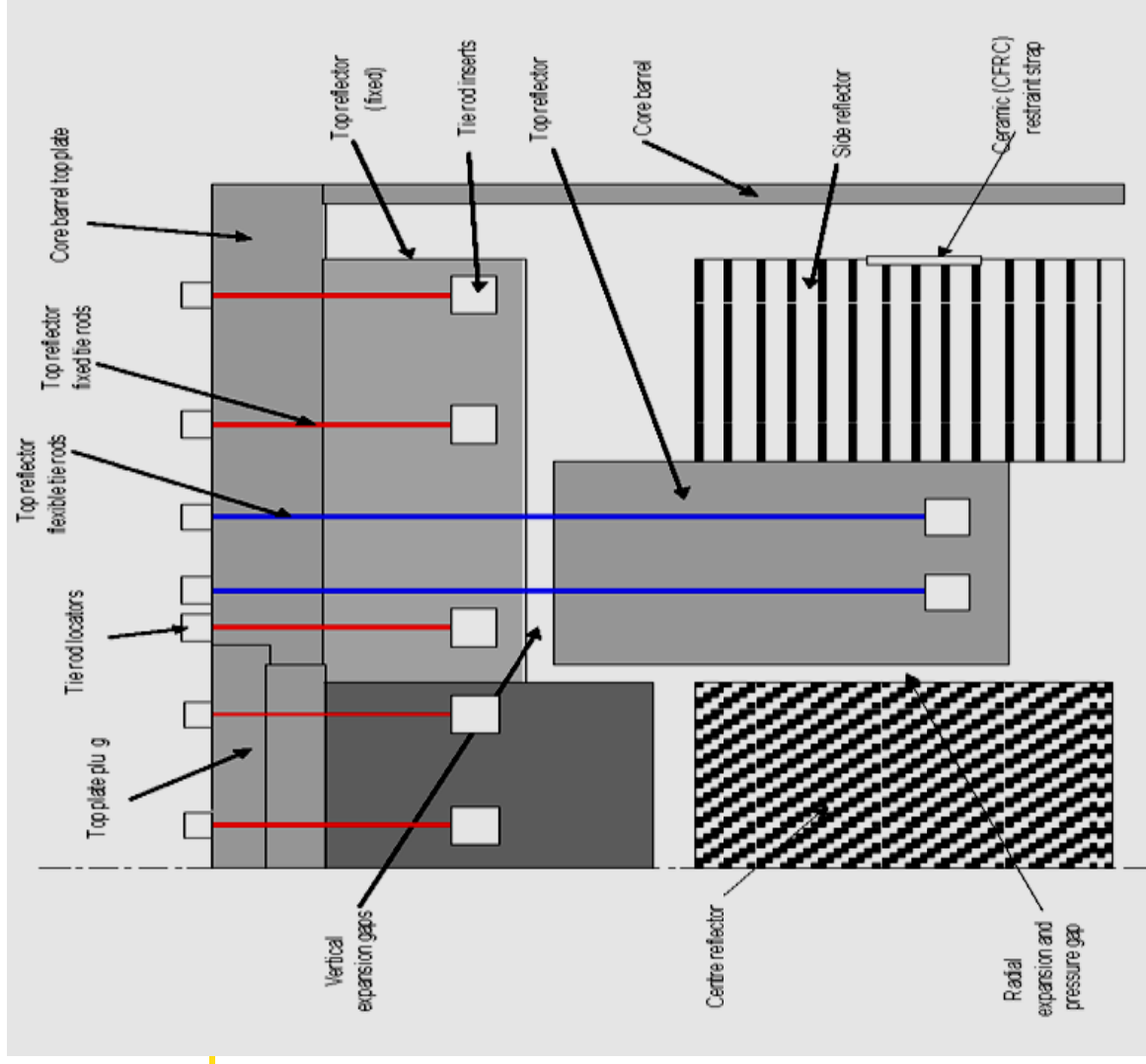
Conclusions Related to Strap Assembly

- **Lateral Restraint Strap Assembly**
 - DPP design appears applicable to NGNP
 - Design complete for DPP
- **The CFRC Racetrack Straps**
 - Fabricated using SGL Sigrabond 2002 YR comprising polyacrylonitrile (PAN) fiber impregnated with coal tar pitch
 - Unidirectional filament wound in a racetrack layout in the loading direction
- **DPP design needs to be reviewed for the NGNP**
 - Determine required changes to the design
 - Modeling of the NGNP outer reflector region to validate estimate of fluence

Conclusions Related to Strap Assembly (cont)

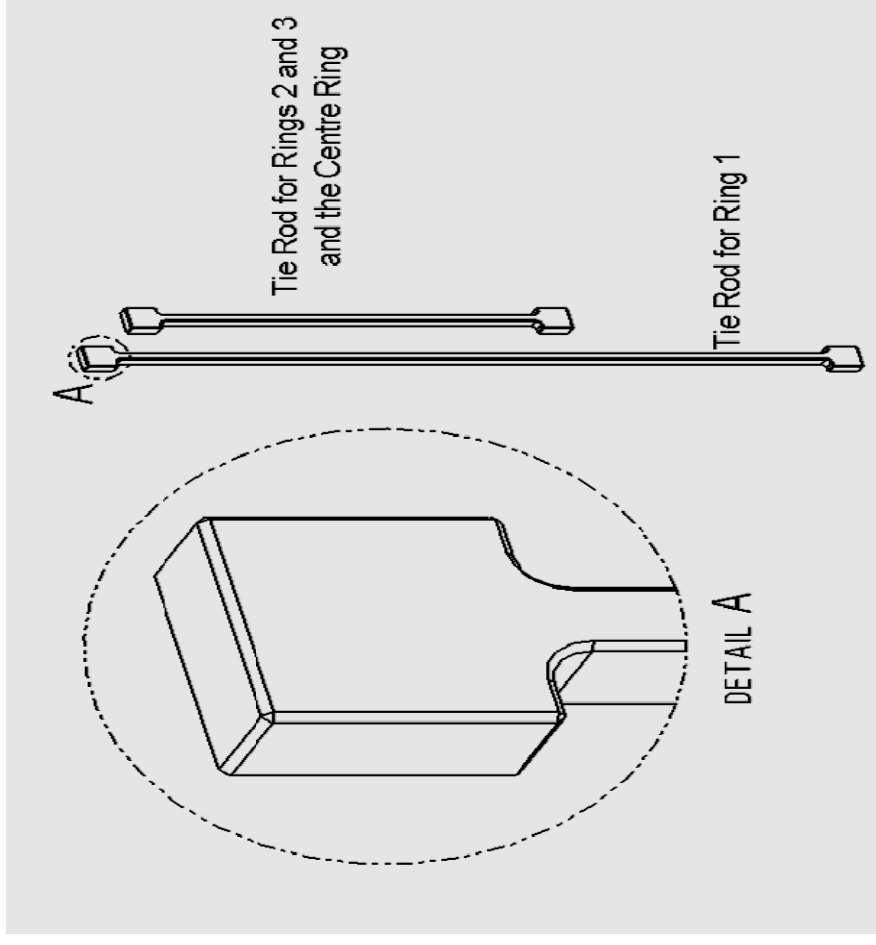
- Irradiation program
 - Required if maximum calculated End of Life (EOL) fluence level is ≥ 0.2 dpa (carbon) or 3×10^{20} n/cm² (E > 0.1 MeV)
 - This is considered unlikely based on the estimated fluence
- 1D CFRP material susceptible to shrinkage in the axis of the racetrack
 - Could cause problems with the function of the strap assembly, if excessive.
- DPP procedures and qualification
 - Need to be reviewed and or modified for the NGNP design.
- Also, test data will be needed to determine susceptibility to corrosive attack in a high temperature impure helium environment of the type to be used in the NGNP.

CFRC Upper Reflector Tie Rods



Upper Reflector Tie Rod Design

- Tie Rods used to support Upper Reflector Blocks from Top Plate
- PBMR has a completed design for the Tie Rods for the DPP
- Testing program will be performed by PBMR on Tie Rods prior to installation
- Tie Rods designed to enhance tensile strength and fracture toughness and have insignificant creep
- 20 Short Tie Rods used to support the Upper Reflector Center Ring
- 60 Long Tie Rods and 72 Short Tie Rods used to support Rings 2 and 3 and 3



Conclusions Related to Tie Rod Assembly

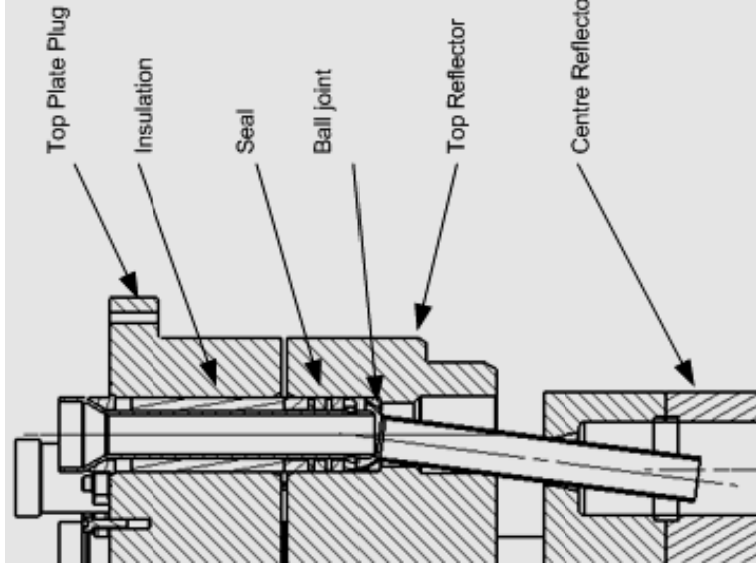
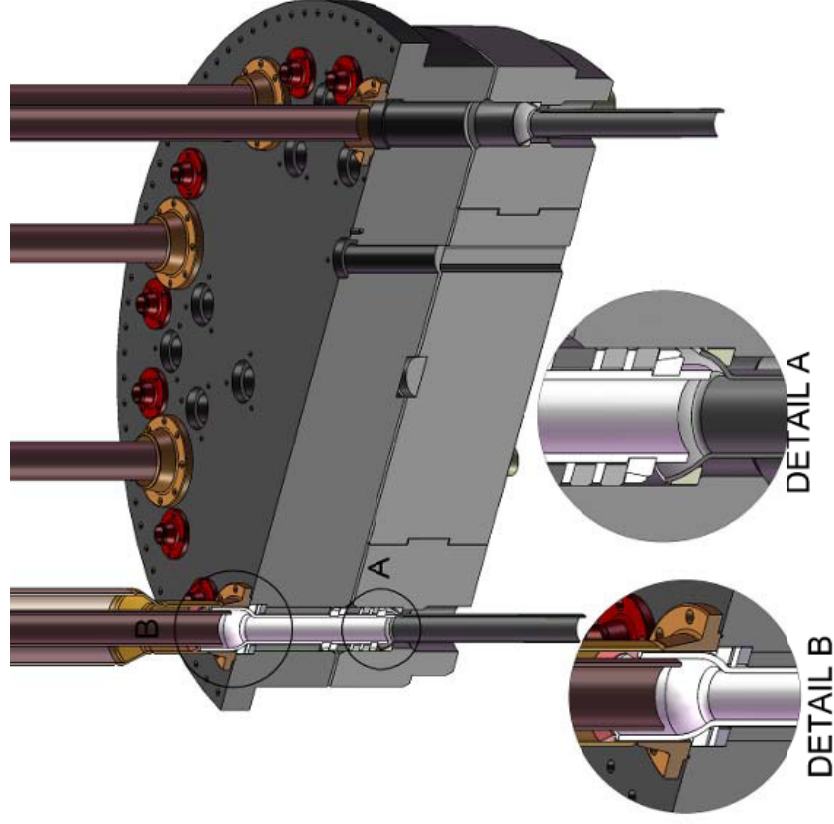
- Tie Rod Assembly
 - DPP design appears applicable to NGNP
 - Design complete for DPP
- Tie Rods
 - Fabricated using SGL Sigrabond 1502 YR comprising 2D polyacrylonitrile (PAN) fiber mat impregnated with coal tar pitch
- DPP design needs to be reviewed for the NGNP
 - Determine required changes to the design
 - Modeling of the NGNP upper reflector region to validate estimate of fluence

Conclusions Related to Tie Rod Assembly (cont)

- Irradiation Program
 - Required if maximum calculated End of Life (EOL) fluence level is ≥ 0.5 dpa (carbon) or 7×10^{20} n/cm² ($E > 0.1$ MeV)
 - This is considered unlikely based on the estimated fluence of 2×10^{20} n/cm² ($E > 0.1$ MeV) which is equal to about 0.1 dpa
 - 2D CFRC material is less susceptible to shrinkage in the axis of the Tie Rods
- DPP procedures and qualification
 - Needs to be reviewed and or modified for the NGNP design
- Also, test data will be needed to determine susceptibility to corrosive attack in a high temperature impure helium environment of the type to be used in the NGNP.

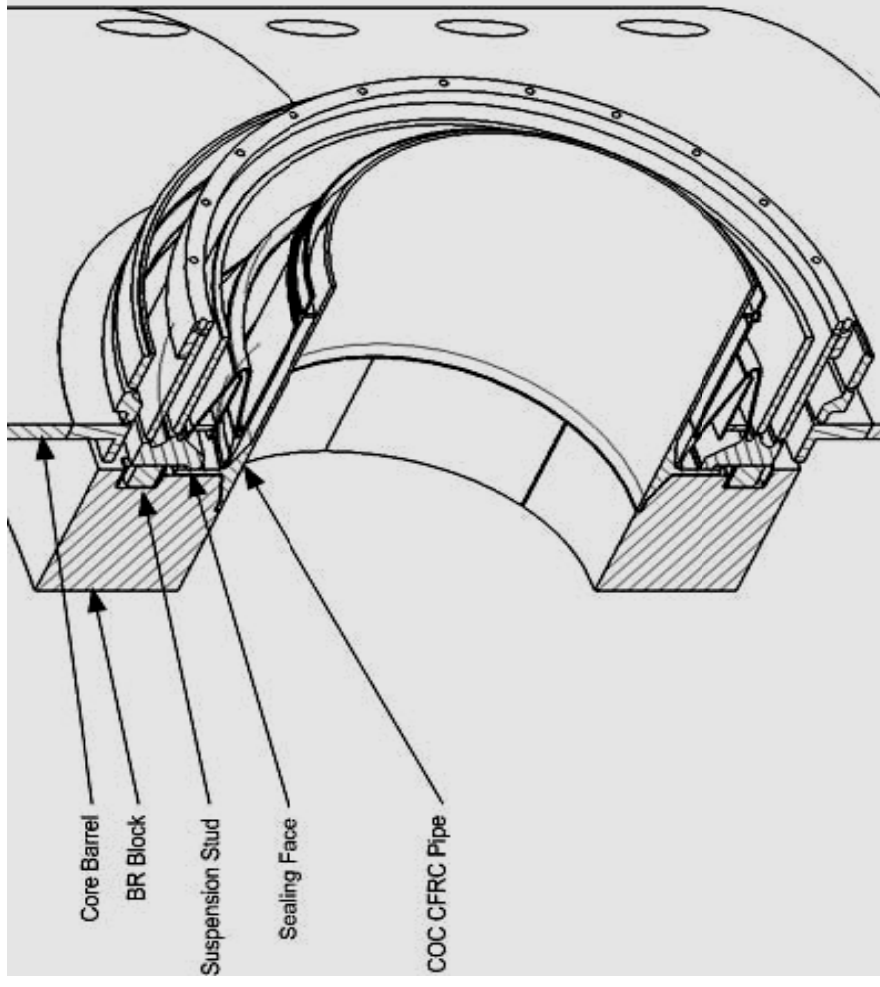
CFRC Tubes (Sigrabond 1502 YR) RSS System Interface Between Top Reflector and Center Reflector

CFRC Tubes used at Reserve Shutdown System (RSS) Interface showing purpose of Ball Joint



Detail of Core Outlet Connection Assembly

- The COC connects to HGD
- Contains a CFRC Liner as the first barrier
- Selected primarily because of thermal mixing issues
- It is believed that a high temperature metallic alloy could be susceptible to the initiation of surface cracks under these conditions.
- PBMR has a conceptual design for the COC for the DPP and a contract for detail design is being negotiated.



Conclusions Associated with the Core Outlet Connection

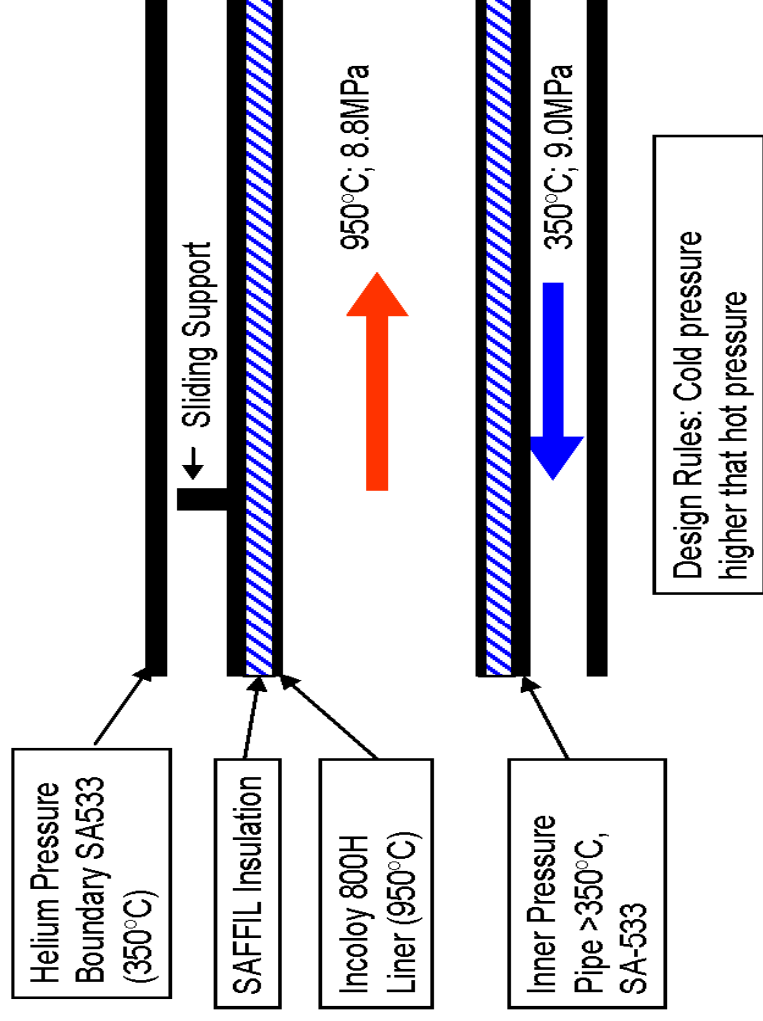
- **COC is being designed for the DPP**
- **COC appears to be applicable to the NGNP design.**
- **Materials used in DPP design may need to be modified for the NGNP.**
- **Modeling of DPP COC design needs to be performed for NGNP to better understand materials issues.**
- **A review and potential modification and or validation of design are required for the NGNP.**

Conclusions Associated with the COC (cont)

- Design bases for CFRC liner and metallic components
 - Require validation for the NGNP design
 - Test data representative of the CFRC selected is required including helium environmental testing
- Procedures for surveillance, inspection and monitoring of the COC need to be reviewed and modified as required for the NGNP.
- Qualification procedures need to be developed for the NGNP COC application.

DPP Hot Gas Duct Design Showing NGNP Temperatures

- DPP design currently uses Alloy 800H liner
 - Probably not acceptable for NNGNP design
- Inner Pressure Pipe will probably exceed the normal operational limit using this design for NNGNP
- HPB Pipe will be close to this limit using this design
- Therefore, design change probably needed



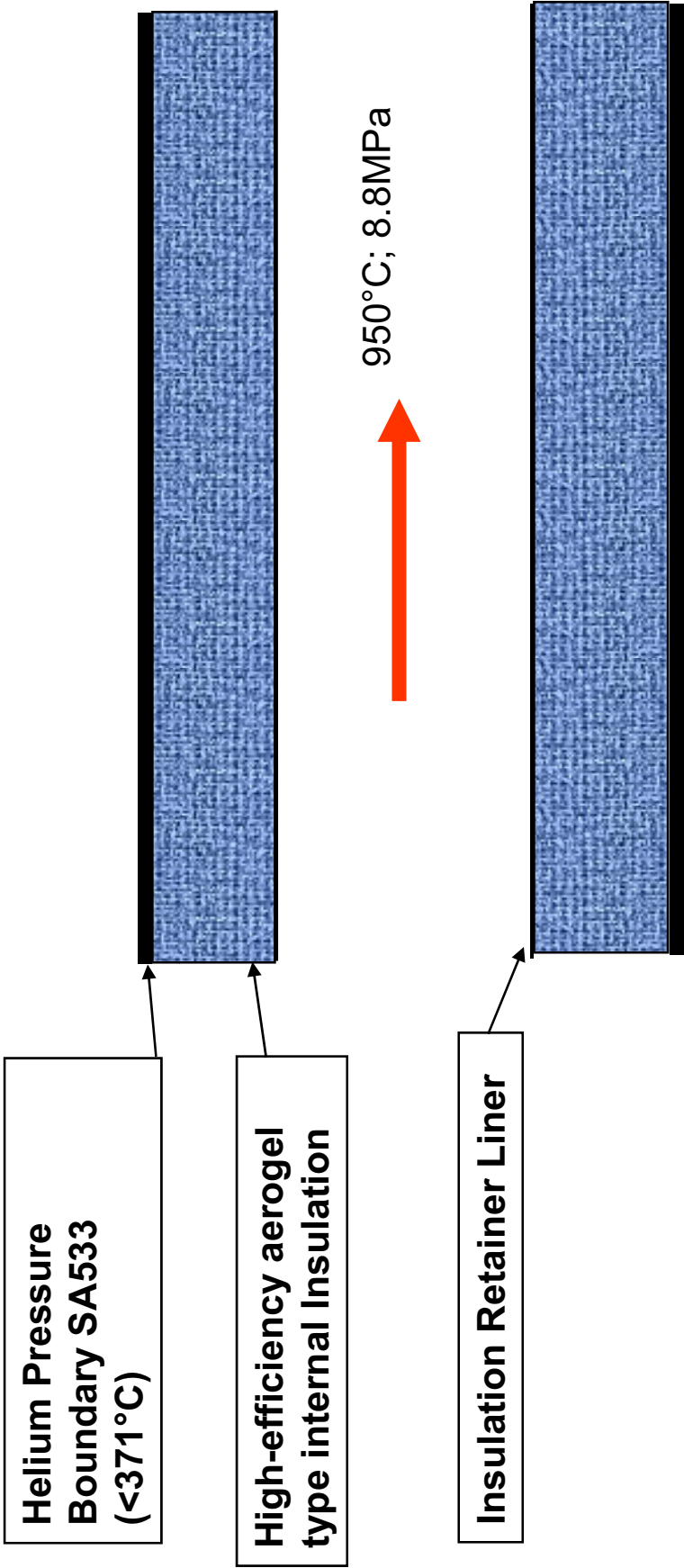
Summary of HGD Design Issues

Key Attributes of the HGD Design for the DPP

Key Differences in NNGNP HGD Design

- Source of piping annulus cooling gas is HP compressor outlet @ ~110C.
- This is a low enough temperature to ensure that the temperature limits of the SA 533 pipe material will not be exceeded with the current insulation system and design
- Cooling and flow are inherently linked in the DPP design
 - Cooling gas at the highest pressure in the cycle
 - Loss of cooling inherently shuts down circulation in the Brayton cycle which causes a loss of circulation in the pipe and allows a temperature equilibrium in the pipe to develop
- Reactor Outlet: 950°C
- Cooling source is circulator outlet @350°C
- Circulation and cooling are not inherently linked
 - Potential for high-temperature PHTS transient with loss of heat removal via IHX + failure to trip PHTS circulator
 - Need for helium pressure boundary (HPB) insulation (internal and/or external)
 - Need to protect HPB from excessive temperatures
 - Need to reduce HPB external surface to reasonable temperature (e.g., ≤100°C)
 - Need to avoid excessive heat losses

Possible Passive Insulation Design for NGNP Hot Gas Duct



Tentative Passive Insulation Assessment

Pros

- Eliminates transient concerns
- Easy to manufacture and install
- Less Expensive
- Repairs to pipe conceptually possible
- Based on preliminary heat flow calculations performed by Microtherm, 450mm radial thickness of aerogel insulation with a liner would result in a surface temperature of < 100C on the outside of the HPB with no annulus cooling

Cons

- Passive Insulation Design has not been evaluated for response to off-normal or postulated events
 - Validation of a new design may require extensive effort
 - DPP design has been extensively evaluated and validated over many years for all postulated events
 - DPP design has been found acceptable

Conclusions Associated with the Hot Gas Duct

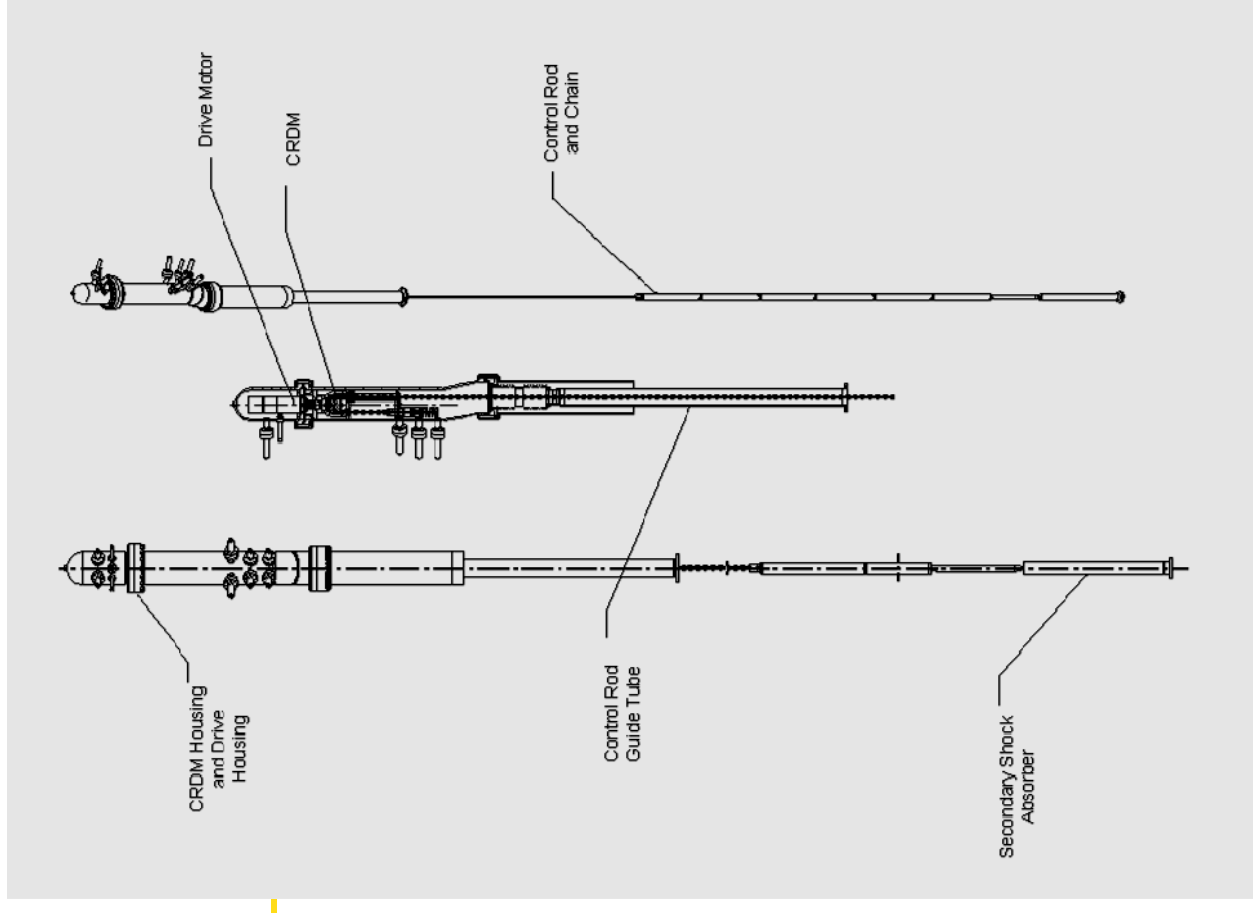
- It is almost certain that the NGNP Hot Gas Duct (HGD) will require a liner with higher temperature capability than the Alloy 800H liner used in the DPP design.
- It is recommended that the liner be fabricated using a Polyacrylonitrile (PAN) fiber-based CFRC material
 - To ensure optimum performance for the life of the plant
 - Representative test data is required for the CFRC material selected including environmental test data in helium.
- It is recommended that a passive insulation system using high performance aerogel based on silica or alumina be considered for the PHTS HGD application.
- PCRD selection of passive insulation for high-temperature sections of SHTS is supported by the results of this study
- Other Hot Gas Duct design changes will likely be required for the NGNP due to the higher annulus cooling gas temperature
- Modeling of the NGNP needs to be performed to determine the temperatures seen by the inner pressure pipe and the HPB for the PCDR design

Conclusions Associated with the Hot Gas Duct (cont)

- Review and Evaluation Required for NGNP
 - Materials basis for the PCDR piping design
 - Evaluation of current DPP piping design to consider a specific off-normal event (noted previously) that has not been thoroughly evaluated
 - Procedures for surveillance, inspection and monitoring of the HGD for the DPP
- Qualification procedures need to be developed for the HGD.

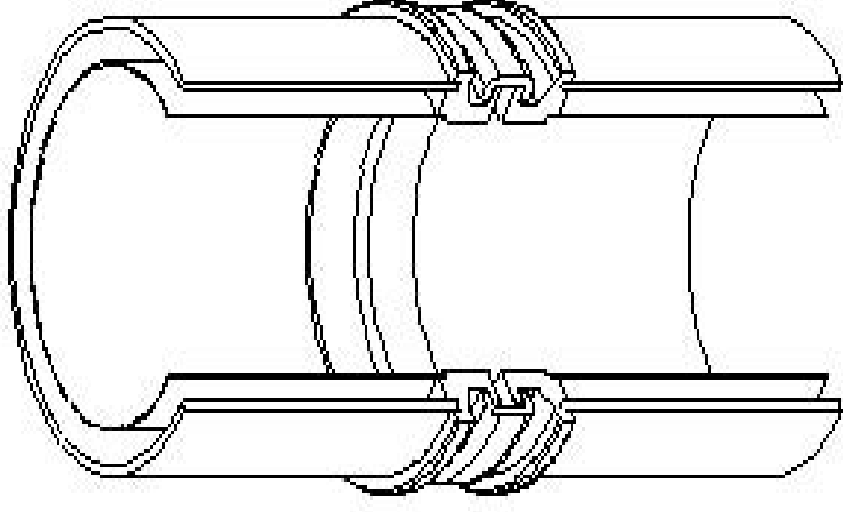
Control Rods

- Reactivity Control System (RCS) used to control reactivity in the core, to quickly shut the reactor down and to keep it in a shutdown mode
- RCS consists of 24 identical control rods.
 - Control rods are one group of 12
 - Shutdown rods are one group of 12
- Each rod has six segments containing absorber material (sintered B₄C rings between two coaxial cladding tubes separated by joints)
- DPP design uses Alloy 800H for cladding, joints and secondary shock absorber
- Chain lowers and raises the control rods through segmented graphite liners in the Inner Side Reflector (ISR)
- During SCRAM event, control rods drop by gravity but are limited by the characteristics of the drive and the shock is absorbed by secondary shock absorber



DPP Control Rod Details

- Alloy 800H used in the DPP design for the cladding, joint and secondary shock absorber.
- This material is probably marginally acceptable but not optimal for the NNGNP application because:
 - Component replacements would be anticipated caused by the higher temperature and fluence exposure inherent to the NNGNP design.



Conclusions Associated with the Control Rods

- Composite material would be more optimal for the RCS cladding and joint
 - Redesign would be required
 - This could represent a potential product improvement option for the DPP
- If CFRC or SiC/SiC composite materials were selected:
 - Adequate pre-characterization test data and post-irradiation test data on representative specimens is required
 - Irradiation test data for the specimens $\geq 7 \times 10^{21} \text{ n/cm}^2$ ($E > 0.1 \text{ MeV}$) in increments of $3.5 \times 10^{21} \text{ n/cm}^2$ ($E > 0.1 \text{ MeV}$) at irradiation temperatures of 750°C and 1000°C would be needed.
 - The maximum fluence estimate is $5 \times 10^{21} \text{ n/cm}^2$ ($E > 0.1 \text{ MeV}$)
- This is needed because all designs are potentially affected by dimensional changes and stability of the material used.

Conclusions Associated with the Control Rods (cont)

- It is recommended that a SiC/SiC composite using a high performance generation three design be used for this application because:
 - It is anticipated that a lifetime component would result
 - Material would be less affected by the fluence or the exposure temperature
- Modeling
 - Required for Inner Side Reflector (ISR) to determine the fluences and temperatures seen by the control rods and chains for the NGNP application
- A study to determine qualification testing and procedures for these components is needed for the NGNP design.
- Also, test data will be needed to determine susceptibility to corrosive attack in a high temperature impure helium environment of the type to be used in the NGNP if a composite is selected.

Reactor Core Insulation

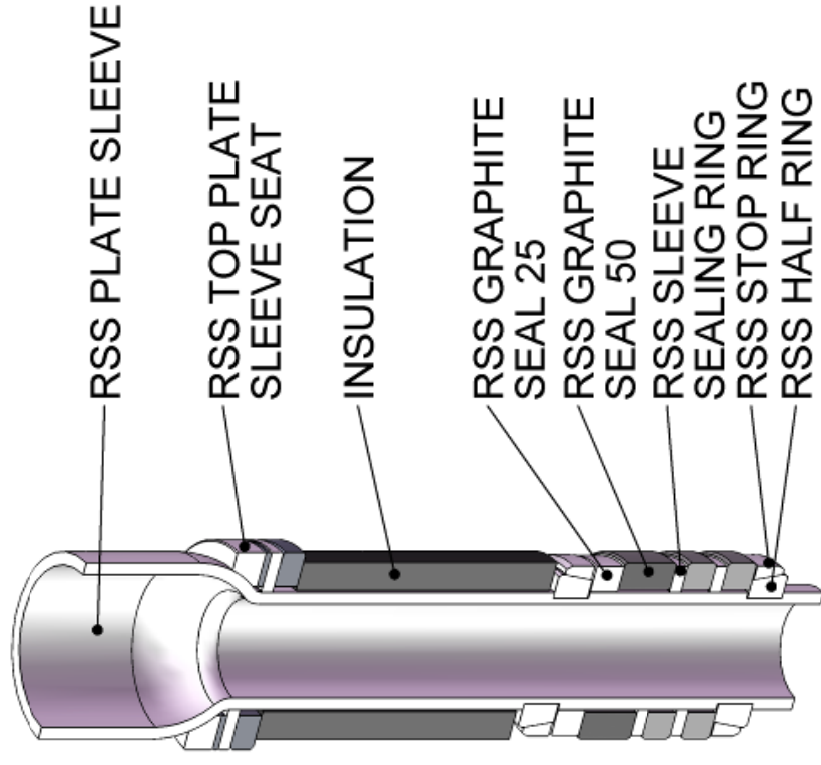
- Layers 1, 2 and 3 in the Bottom Reflector will be insulation layers rather than graphite layers in the NGNP design
- These layers are designed to protect the metallic components that support the core and the core barrel from excessive temperatures
- Baked carbon insulation is used in the DPP design for these layers
- Enhanced insulation will likely be required in one of these layers of the Bottom Reflector (BR) assembly in the NGNP due to the higher outlet temperature.

Conclusions Associated with Core Insulation in the Lower Reflector

- It is recommended that a machinable quartz insulation product be used for this application, if required
 - Data requirements if quartz insulation is needed are the same as that obtained for the baked carbon except that limited post-irradiation testing is needed.
- Modeling Study Needed
 - Temperature analysis study that models the upper and lower reflector regions of the NGNP design
 - Radiation exposure expected for Layers 1, 2 and 3 of the Lower Reflector region of the CSC
 - Determination of insulation requirements
- Qualification procedures for the fused or sintered quartz material will need to be developed if required for the NGNP application.

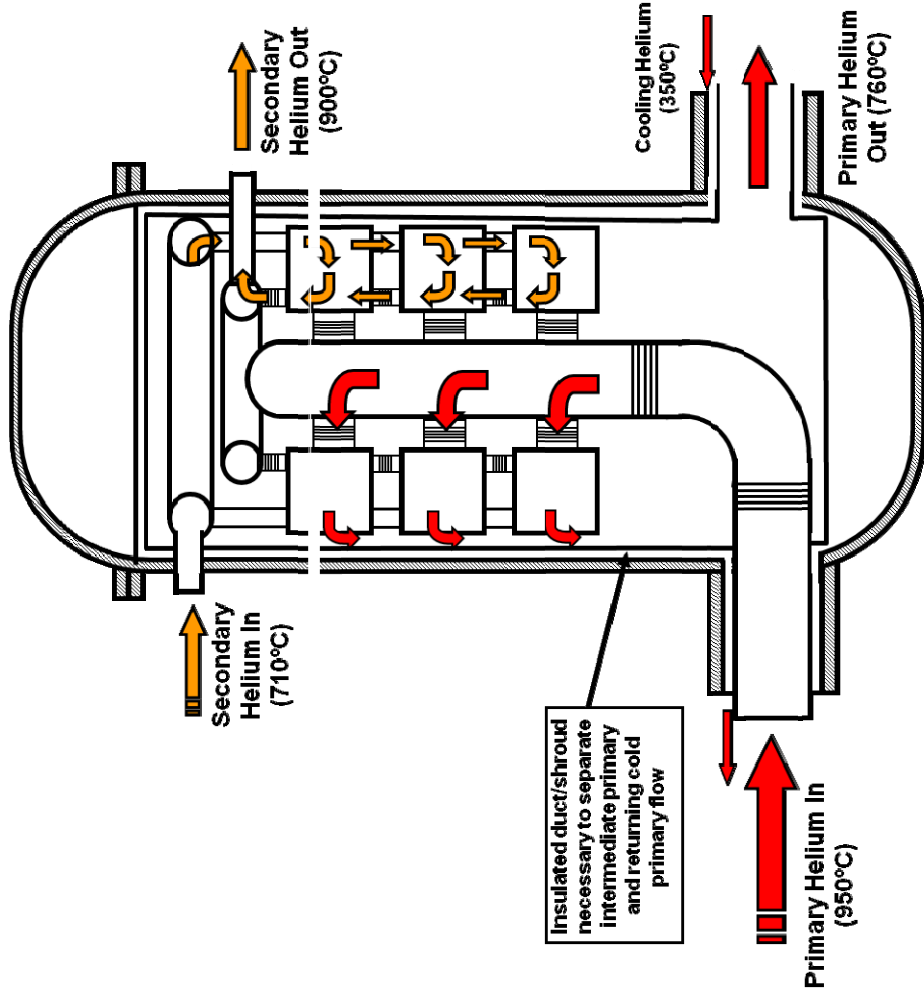
RSS Graphite Felt Insulation at Interface Between Top and Center Reflector

- Sigratherm RFA-FF rigid graphite felt is used as insulation adjacent to RSS Interface between Top and Center Reflector to protect against high temperature streaming
- This insulation material should be usable for the NGNP application
- Qualification procedures and test data will be developed by PBMR and should be reviewed for the NGNP



PCDR IHX Concept

- It is recommended that a high performance aerogel insulation system, based on silica or alumina be considered for the IHX application
- Design study of the IHX systems needed
 - To evaluate insulation required
 - To provide a more detailed conceptual design for the IHX systems
- Modeling study needed
 - To evaluate the temperature distributions in IHX A and B
- A qualification plan is required for the insulation to be used
- Test data is required
 - For insulation system selected to evaluate properties of the material in high pressure helium under various conditions
 - To validate the stability of the material for the IHX and piping applications



Materials Evaluation

- Ceramic Matrix Composites (CMCs) including CFRC and SiC/SiC were evaluated
 - **Manufacturing**
 - **Properties**
 - **Irradiation Effects**
 - **Specific Applications**
- **Insulation Products**
 - **Review of Applicable Products**
- Selected high temperature metallic alloys including Alloy 800H were evaluated for comparisons, where applicable
- Other structural ceramics or composites were not evaluated in detail because they are not applicable for the applications identified.

Comparison of General Properties of Three Structural Material Classes Evaluated

High Temperature Metallic Alloys	CFRC	SiC/SiC Composites
Less specific strength and rigidity at temperatures $\geq 900\text{C}$	High specific strength and rigidity at temperatures $\geq 900\text{C}$	High specific strength and rigidity at temperatures $\geq 900\text{C}$
Higher density and no porosity	Lower density and some open porosity	Lower density and some open porosity
Higher thermal expansion	Lower thermal expansion	Lower thermal expansion
Less resistance to thermal shock (cracking can be initiated)	Extremely high resistance to thermal shock	Little data on resistance to thermal shock
Essentially no anisotropy	Anisotropic. Selected properties have different values for orientations parallel and perpendicular to the fiber or layer	Anisotropic. Selected properties have different values for orientations parallel and perpendicular to the fiber or layer
Susceptible to high temperature impure He corrosion	Suspected to be susceptible to high temperature impure He corrosion; however, data not available	Suspected to be susceptible to high temperature impure He corrosion; however, data not available

Comparison of General Properties of Three Structural Material Classes Evaluated (cont)

High Temperature Metallic Alloys	CFRC	SiC/SiC Composites
Plastic fracture behavior	Pseudoplastic fracture behavior with little elongation	Pseudoplastic fracture behavior with little elongation
Physical and mechanical properties set by alloy selected or processing parameters	Tailorable physical and mechanical properties without making composition changes	Tailorable physical and mechanical properties without making composition changes
Irradiation Properties	Irradiation Properties	Irradiation Properties
Alloys containing Ni show loss of ductility and fracture toughness	CFRC starts to show indications of degradation at low irradiation doses (<0.5 dpa). In general, as irradiation continues, dimensional changes, increases in strength and decreases in thermal conductivity continues to turnaround.	With specific fiber types and consolidation processes, SiC/SiC composites show little swelling or volume expansion under irradiation up to 10dpa and other properties show little change.
Irradiation temperatures and other factors affect behavior	Following turnaround, the properties rapidly deteriorate.	No turnaround effect.

Other Factors Associated with the Three Structural Material Classes Evaluated

High Temperature Metallic Alloys	CFRC	SiC/SiC Composites
Materials are readily available	Materials are less available than metallic alloys but more available than SiC/SiC composites	Materials are less available
Least expensive material cost	Intermediate material cost	Most expensive material cost
Materials are mature and have ASME Code listings	Materials are less mature and are not listed in the ASME Code	Materials are least mature
Versatile engineering materials	Versatile engineering materials	Versatile engineering materials

Other Factors Associated with the Three Structural Material Classes Evaluated (cont)

High Temperature Metallic Alloys	CFRC	SiC/SiC Composites
<p>Properties are a function of the alloy</p>	<p>Properties are a function of the fibers, fiber fraction, architecture and consolidation process.</p>	<p>Properties are a function of the fibers, fiber fraction, architecture and consolidation process.</p>
	<p>PAN fibers provide better overall properties</p>	<p>Hi Nicalon Type S fibers with CVD consolidation appears to provide the best properties for the RCS application</p>
<p>Manufacturing processes are well established</p>	<p>Pitch fibers provide better resistance to irradiation induced dimension changes</p>	<p>Manufacturing processes are complex, least established and require interphase layer between fiber and matrix</p>

Selected Physical Properties of the Three Structural Material Classes Evaluated

Physical Properties	Metallic Alloys	CFRC		SiC/SiC Composites
Thermal Conductivity [W/m.K]	At 900C	100-200.	3D, Independent of orientation	4-40
	26.4 (Alloy 230)	60-600	1D, parallel to fibers,	Function of temperature, grain size and crystal structure of matrix material
	27.2 (Alloy X)	Values perpendicular to fibers can be 25x lower	Decreases as a function of temperature.	Lower at all temperatures following irradiation
	30.8 (Alloy 800H)	Decreases at all temperatures following irradiation	0-5	Strong function of temperature
Mean Coefficient of Thermal Expansion [10 ⁻⁶ /K] (20-1000°C)	16.1 (Alloy 230);	-0.1-2.0 (1D)		Data for SiC, no available data for composites).
	16.6 (Alloy X);	0.1-1.3 (3D)		No change expected following irradiation.
	14.4 (Alloy 800H)			
	No data on irradiation effects			

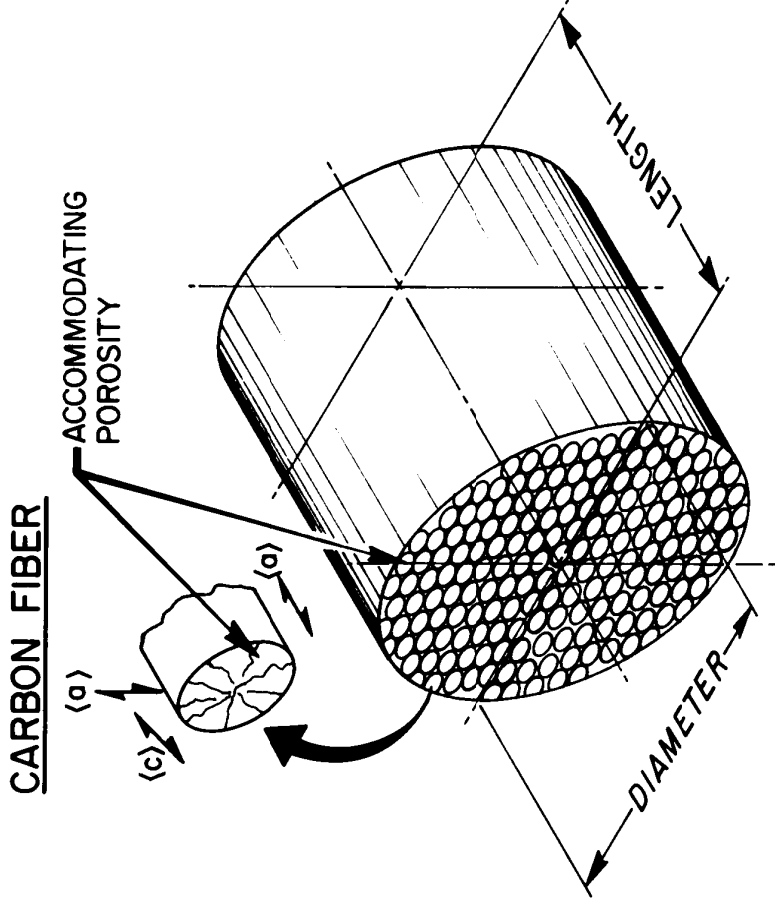
Selected Physical Properties of the Three Structural Material Classes Evaluated (cont)

Physical Properties	High Temperature Metallic Alloys	CFRC	SiC/SiC Composites
Density [g/cm ³]	8.83 (Alloy 230) 8.22 (Alloy X) 7.94 (Alloy 800H)	1.7-1.8	2.6-2.9
Density [g/cm ³] Irradiation Effects	Density is reduced at all temperatures	Density is reduced at all temperatures	Density is reduced at all temperatures
Melting Range (°C)	1300-1370 (Alloy 230) 1260-1355 (Alloy X) 1357-1385 (Alloy 800H)	About 3550	About 2700

Selected Mechanical Properties of the Three Material Structural Classes Evaluated

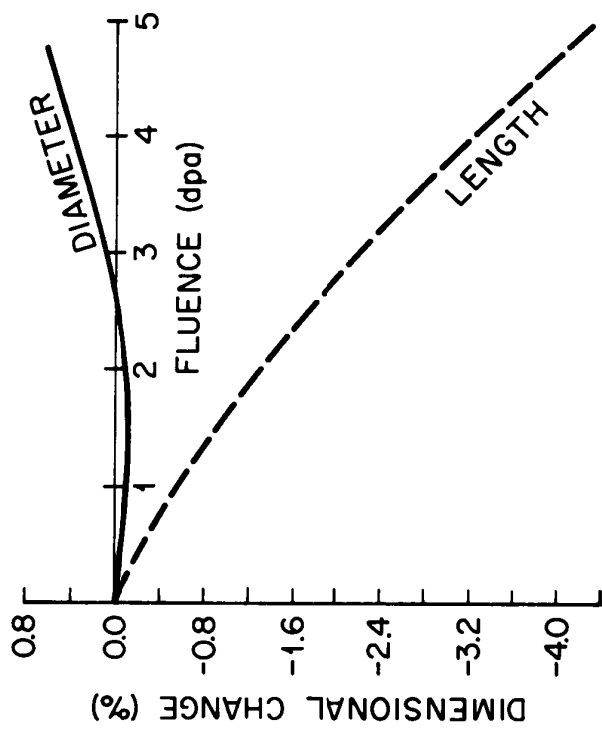
Mechanical Properties	Metallic Alloys	CFRC	SiC/SiC Composites
Young's Modulus (GPa)	At 800°C	150-250 (1D)	174-400
	19 (Alloy 800H)	75-125 (3D)	Decreases slightly at >1000°C
	23 (Alloy 230)	Decreases slightly at >1000°C	Generally unaffected by irradiation
	20.7 (Alloy X)	Increases slightly following irradiation	
Tensile Strength (MPa)	No data on effect of irradiation		
	At 982°C.	300-900 (1D)	78-400
	172 (Alloy 230)	150-400 (3D)	Decreases at >1000°C
	255 (Alloy X)		
	70 (Alloy 800H)	Decreases at >1000°C, Increases significantly following irradiation	Increases initially following irradiation
Total Elongation at Fracture (%)	At 870°C.	<1	0.03-0.62
	34 (Alloy 230)	Little change from irradiation up to 5 dpa	Little change from irradiation up to 10 dpa
	26 (Alloy X)		
	Decreases significantly following irradiation		

Irradiation Induced Dimensional Change for a 1D CFRC Material (Burchell, 2004)

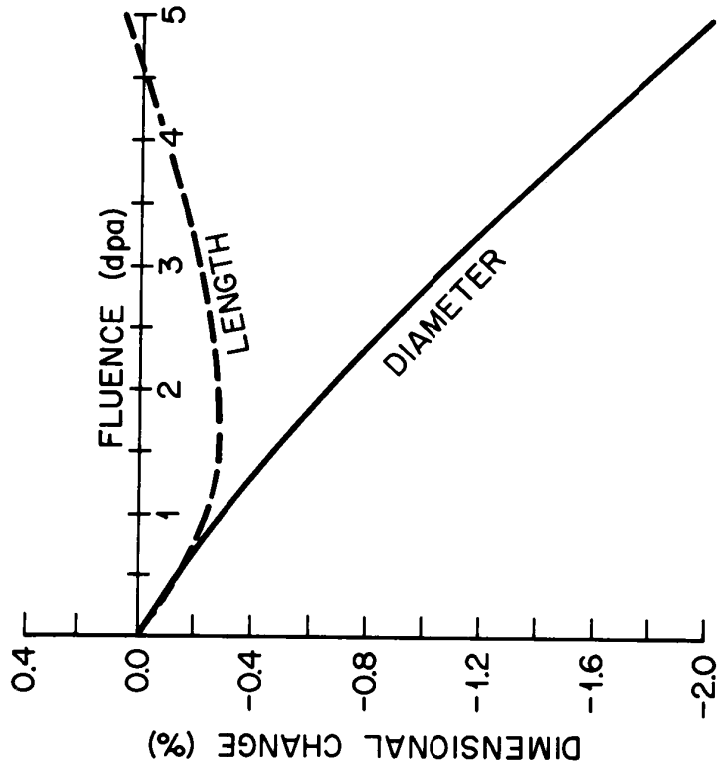
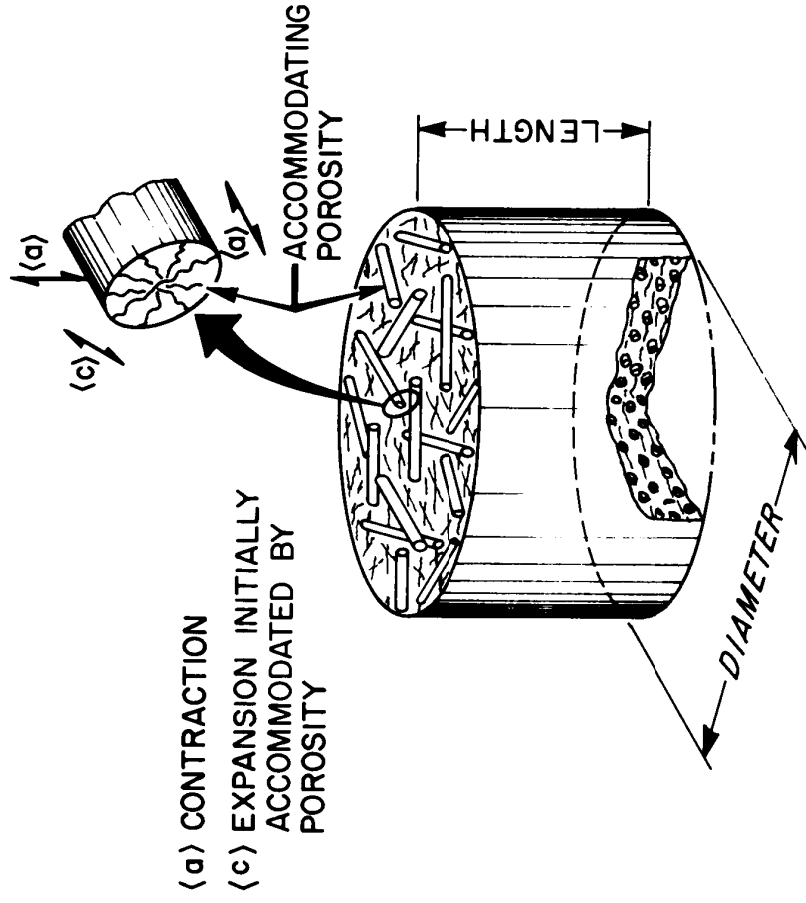


1D C/C COMPOSITE

- (a) CONTRACTION
- (c) EXPANSION INITIALLY ACCOMMODATED BY POROSITY

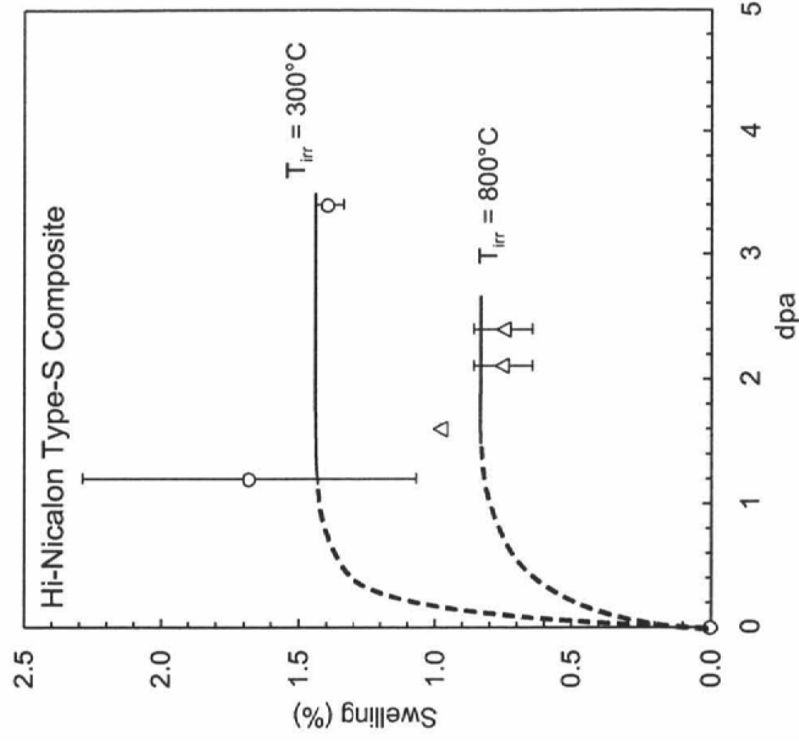


Irradiation Induced Dimensional Change for a 2D CFRC Material (Burchell, 2004)

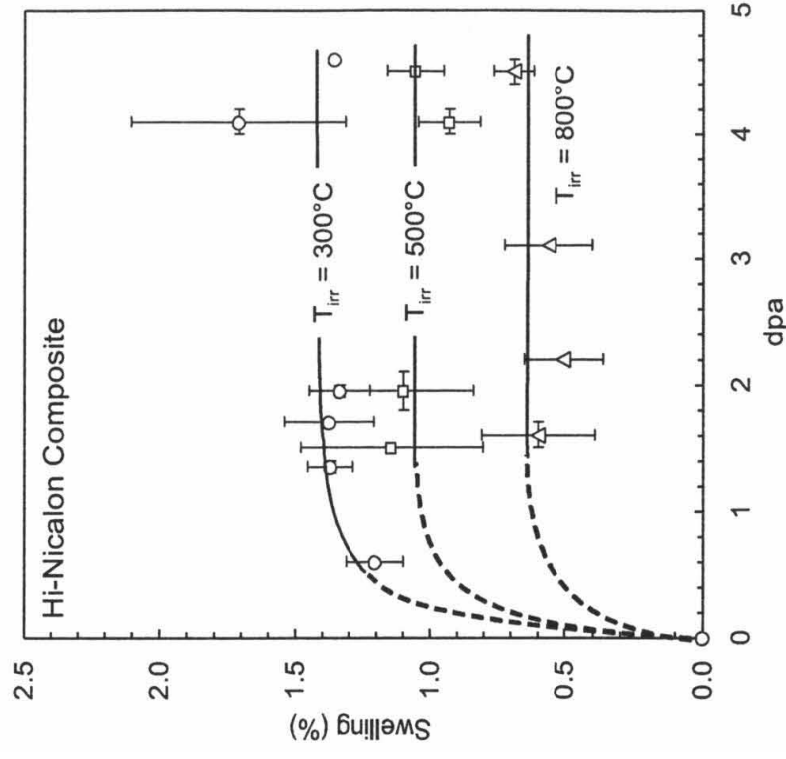


Irradiation Induced Swelling in SiC/SiC Composite Materials (Newsome, et al, 2007)

Swelling of Hi Nicalon Type S Fiber Composite as a Function of Irradiation



Swelling of Hi Nicalon Fiber Composite as a Function of Irradiation



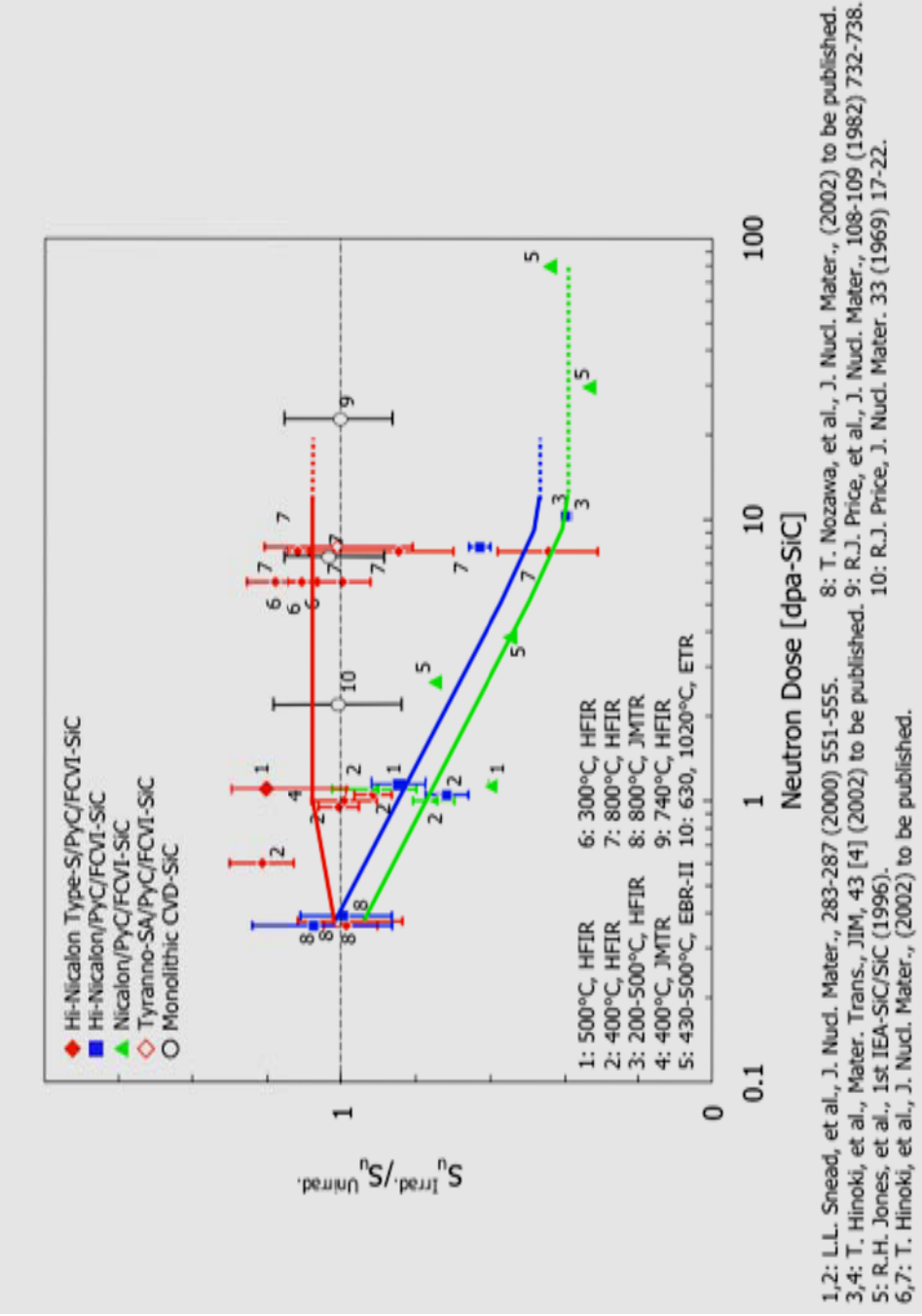
Properties of CFRC – SGL Sigrabond Grade 2002 YR

Property	Unit	Value
Density	kg/m ³	1340 ± 30
Thermal Conductivity (RT)	W/mK	Per 3.8 ± 0.17 Par 66.0 ± 6.1
CTE (20 °C to 200 °C)	10 ⁻⁶ /K	Par -0.03 ± 0.17
Flexural Strength (3-point)	MPa	Par 207.7 ± 0.5
Flexural Elastic Modulus	GPa	Par 154.4 ± 0.4

Properties of CFRC – SGL Sigrabond Grade 1502 YR

Property	Unit	Value
Density	kg/m ³	1560 ± 20
Thermal Conductivity (RT)	W/mK	Per 7.6 ± 1.7 Par 58.5 ± 1.7
CTE (20 °C to 200 °C)	10 ⁻⁶ /K	Per 8.14 ± 0.10 Par -0.26 ± 0.05
Tensile Strength	MPa	Par 488.8 ± 23.5
Tensile Young's Modulus	GPa	Par 108.3 ± 1.6
Thermal Creep		Insignificant

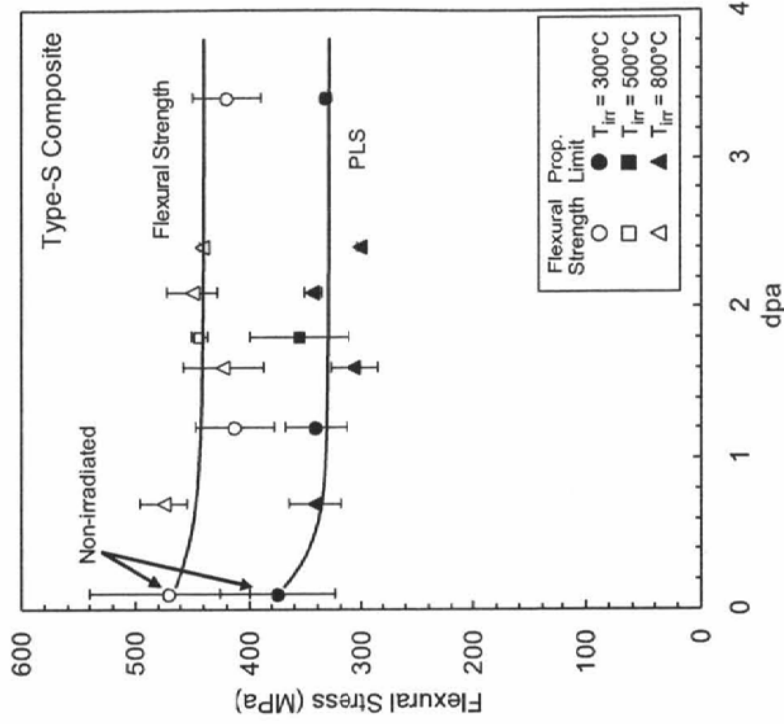
Ratio of Irradiated Tensile Strength to Unirradiated Tensile Strength as a Function of Irradiation Exposures for Various SiC/SiC Composites (Snead, et al 2007)



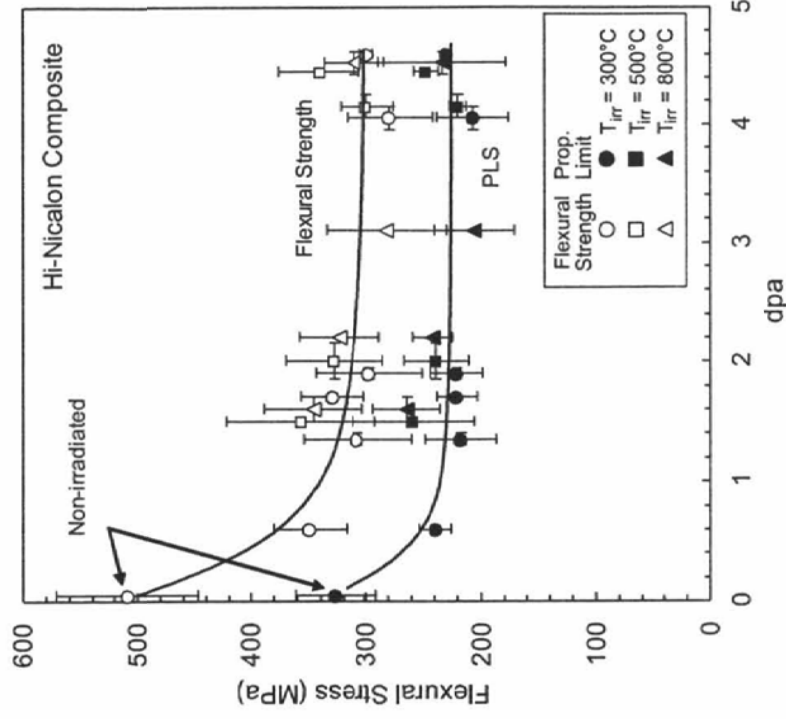
1,2: L.L. Snead, et al., J. Nucl. Mater., 283-287 (2000) 551-555. 8: T. Nozawa, et al., J. Nucl. Mater., (2002) to be published.
 3,4: T. Hinoki, et al., Mater. Trans., JIM, 43 [4] (2002) to be published. 9: R.J. Price, et al., J. Nucl. Mater., 108-109 (1982) 732-738.
 5: R.H. Jones, et al., 1st IEA-SiC/SiC (1996).
 6,7: T. Hinoki, et al., J. Nucl. Mater., (2002) to be published. 10: R.J. Price, J. Nucl. Mater. 33 (1969) 17-22.

Irradiation Induced Mechanical Property Changes in SiC/SiC Composite Materials (Newsome, et al, 2007)

Flexural Strength and PLS for Hi Nicalon Type S Composite as a Function of Irradiation



Flexural Strength and PLS for Hi Nicalon Composite as a Function of Irradiation

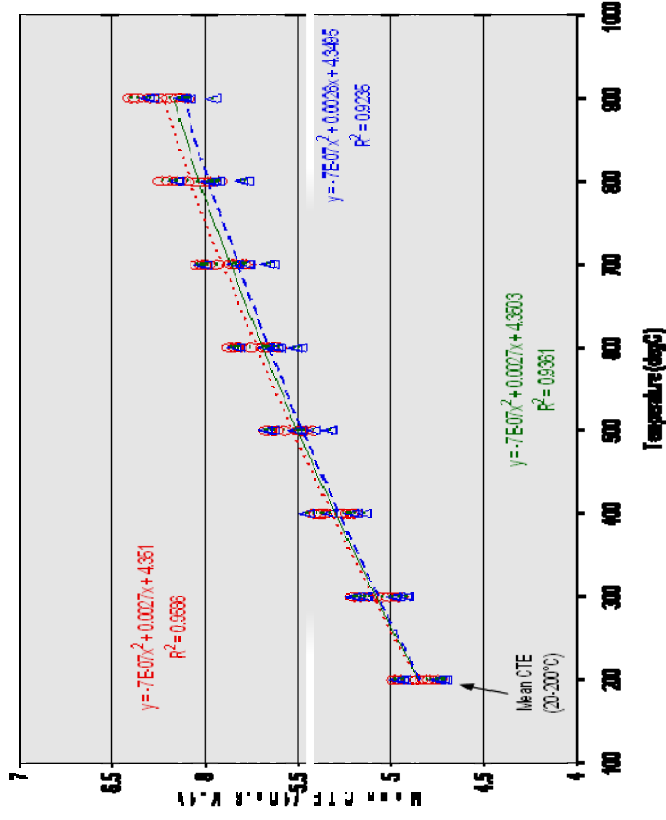


Selected Properties of NBC-07 Baked Carbon Insulation

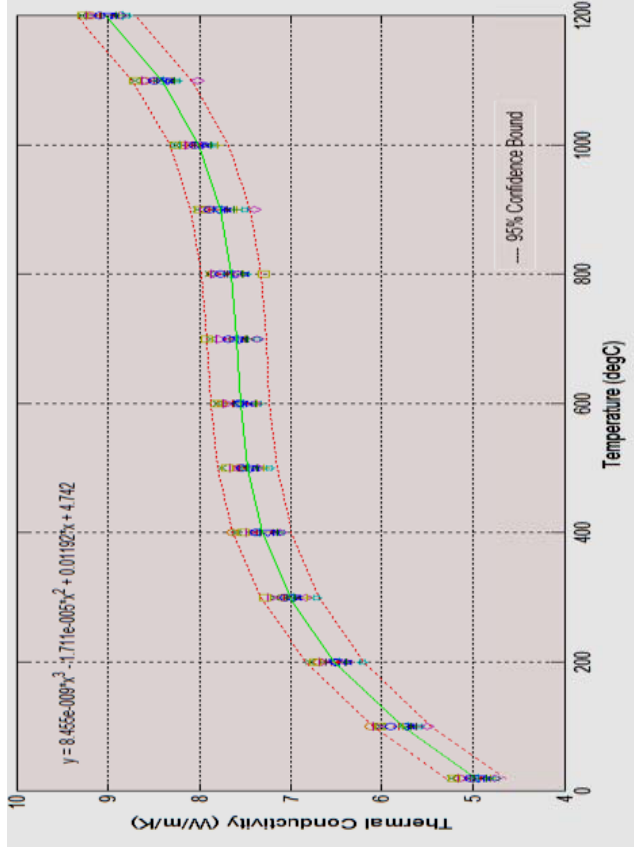
Property	Unit	Value With grain (wg) Against grain (ag)
Density	kg/m ³	1740
Thermal Conductivity (800C bake) RT	W.m ⁻¹ .K ⁻¹	3.6 (wg) 3.6 (ag)
Thermal Conductivity (1050C bake) RT	W.m ⁻¹ .K ⁻¹	5.0 (wg) 4.9 (ag)
Coefficient of Thermal Expansion (200C)	10 ⁻⁶ K ⁻¹	4.9 (wg) 5.0 (ag)
Isotropy Ratio	NA	1.01
Compressive Strength (RT)	MPa	17.7 (wg) 18.0 (ag)
Flexural Strength (four point) (RT)	MPa	25.0 (wg) 25.6 (ag)

NBC-07 Baked Carbon Selected Physical Properties vs Temperature

Mean Coefficient of Thermal Expansion



Thermal Conductivity



Selected Properties of Quartz Insulation Materials

Sintered Quartz Insulation

Property	Unit	Value
Density	kg/m ³	1950
Thermal Conductivity at RT	W.m ⁻¹ .K ⁻¹	0.64
Thermal Conductivity at 800°C	W.m ⁻¹ .K ⁻¹	0.55
CTE	10 ⁻⁶ K ⁻¹	0.6
Flexural Strength	MPa	27
Compressive Strength	MPa	50

Fused Quartz Insulation

Property	Unit	Value
Density	kg/m ³	2050
Thermal Conductivity (R.T)	W.m ⁻¹ .K ⁻¹	1.25
Thermal Conductivity (800 °C)	W.m ⁻¹ .K ⁻¹	2.19
CTE (10 ⁻⁶ K ⁻¹)	10 ⁻⁶ K ⁻¹	0.54
Compressive Strength (MPa)	MPa	500

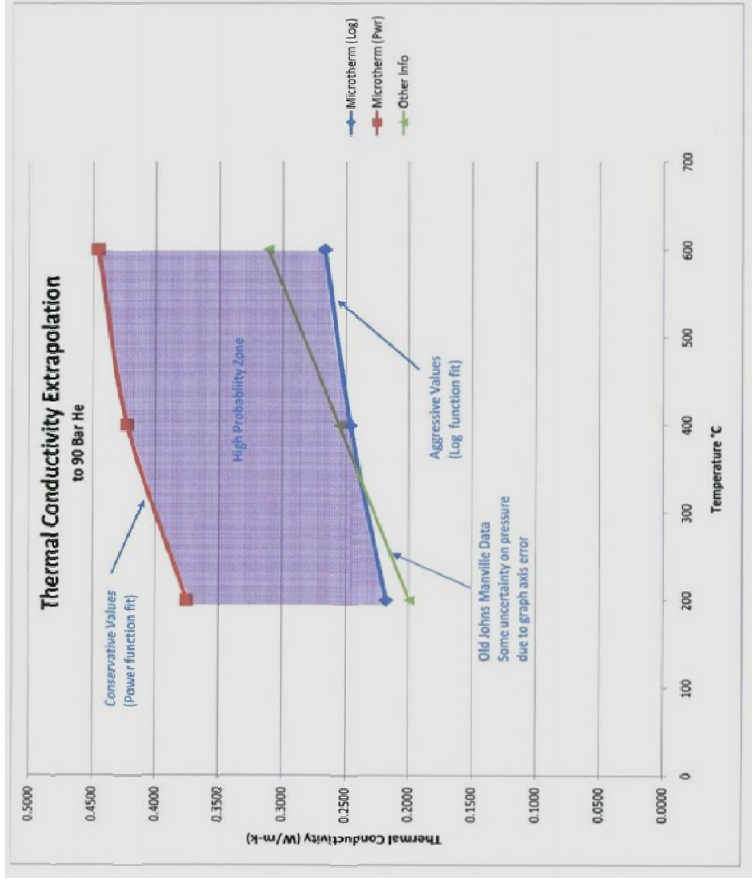
General Information Regarding Insulation for HGD, COC and IHX Applications

- Flexible insulation forms will probably be required
- Insulation is permeable by helium gas under pressure
- Thermal Conductivity of insulation increases as a function of mean temperature and helium pressure
- Saffil insulation is used in DPP design of COC and HGD and is based on a 96% high purity alumina fiber which is available in a variety of forms with a maximum temperature rating of 1540C
- Microtherm insulation is an aerogel type insulation with a very small mean pore size available as an alumina or silica based material in a variety of forms and has a maximum temperature exposure rating of 1150C (alumina based) and 1000C (silica based)
- Aerogel type insulation is a factor of about 3-6 more effective than Saffil based on the same thickness of insulation particularly at temperatures above 600C due to the difference in insulation type and greater resistance to heat loss caused by radiative effects

Thermal Conductivity (TC) for Insulation Products Evaluated based on Manufacturer Data

Mean TC Data of Microtherm Aerogel Insulation Estimated for 90 Bar Helium Environment

Mean TC Data Comparing Microtherm and Saffil Insulation Types



Temperature, C	TC of Microtherm Silica Insulation in Air (W/mK)	TC of Saffil Alumina Insulation in Air (W/mK)	Estimated TC of Microtherm Silica Insulation in He at 90 Bar (W/mK)
100	0.02		
315	0.02-0.03	0.07	0.2-0.4
600	0.03		0.3-0.4
800	0.03		
980		0.2	0.4-0.5

Approach for Codification of Composites

- The approach should be based on the initial development of an ASME Code Case rather than development of a stand-alone section of the Code.
 - The approach used should be similar to the approach used for development of the nuclear graphite Code Case.
 - ASME Standards Technology LLC could be an implementing organization
 - Approach taken should be similar to the initial tasks performed to strengthen Section III, Subsection NH
- The development of a Code Case for composites is within the Section III assigned charter for the Sub-Group for Nuclear Graphite and this effort has already been initiated
 - Composites activities have been limited to date due to lack of resources and a higher priority effort leading to the codification of graphite
 - Resources will become available after the graphite code case is drafted
- Key decisions that have been made within the ASME and ASTM have already initiated the composite codification effort
- The key factors required to further develop and simulate this effort is predictable funding and a consensus from stakeholders that this effort is required to further develop HTGRs

List of Design Data Needs (DDNs)

- **DDN COMP-01-01** Characterize Race Track Strap and Tie Rod Materials
 - Performance of DDN is contingent on results of modeling studies except He environmental testing
 - The need for testing is considered unlikely based on the current fluence estimates
 - He environmental testing required if composite materials are selected
 - The DDN, if performed, would include the following pre-irradiation and post-irradiation (1 dpa ($E>0.1$ MeV) or $1.4E21$ n/cm² ($E>0.1$ MeV) in 0.5 dpa increments) test results as noted below:
 - Dimensional changes
 - Density changes following irradiation (CEN ENV 1389)
 - CTE (RT to 800°C, CEN ENV 1159-1)
 - Flexural Strength (3 point, RT, 600°C, 800°C ASTM C-1341-00)
 - Interlaminar Shear Strength (RT, ASTM C 1425-05)
 - Thermal Creep (800°C, ASTM C 1337-96)
 - Tensile Strength (RT, 600°C, 800°C, ASTM C 1275-00 and ASTM C 1359-05).

List of DDNs (cont)

- **DDN COMP-01-02 RCS Materials Characterization**
 - This DDN does not currently include test data for metallic alloy options, if selected
 - He environmental testing is required if composite materials are selected
 - If CFRC or SiC/SiC composite materials are selected, pre-irradiation and post-irradiation test data would be required as noted below at $7E21$ n/cm² ($E > 0.1$ MeV) in increments of $3.5E21$ n/cm² ($E > 0.1$ MeV):
 - Dimensional changes
 - Density changes following irradiation (CEN ENV 1389)
 - CTE (RT to 800°C, CEN ENV 1159-1)
 - Flexural Strength (3 point, RT, 600°C, 800°C ASTM C-1341-00)
 - Interlaminar Shear Strength (RT, ASTM C 1425-05)
 - Thermal Creep (800°C, ASTM C 1337-96)
 - Tensile Strength (RT, 600°C, 800°C, ASTM C 1275-00 and ASTM C 1359-05).

List of DDNs (cont)

- **DDN COMP-01-03 COC or HGD Liner**
 - This DDN does not currently include test data for metallic alloy options, if selected
 - If CFRC material is selected, unirradiated test data would be required for the COC and HGD liner materials as noted below:
 - Density (CEN ENV 1389)
 - CTE (RT to 1000°C, CEN ENV 1159-1)
 - Flexural Strength (3 point, RT, 1000°C ASTM C-1341-00)
 - Interlaminar Shear Strength (RT, 1000°C ASTM C 1425-05)
 - Creep (1000°C, ASTM C 1337-96)
 - Tensile Strength (RT, 1000°C, ASTM C 1275-00 and ASTM C 1359-05).
 - He environmental testing

List of DDNs (cont)

- **DDN COMP-01-04 Insulation Materials**
 - This DDN does not provide any test data needs for Saffil insulation if selected for the HGD and IHX
 - This DDN assumes that quartz insulation will be used to supplement baked carbon insulation in the lower reflector region
 - This DDN assumes that NBC-07 will be the primary insulation used in the lower reflector region
 - Quartz insulation test data requirements similar to baked carbon except that limited post-irradiation testing is required
 - For aerogel type insulation, test data representative of the insulation to be used is required as noted below:
 - Test data are required to validate the TC of the insulation material in 90 bar helium at 200C, 400C, 600C, 800C and 1000C (ASTM C680 and C177)
 - Test data noted above should include the effect of a rapid depressurization cycle from 90 bar to atmospheric pressure
 - Test data is required to validate the stability of the material at 1000C for times up to seven days (ASTM C 356)
 - Test data for the quartz insulation should be the same as that provided by PBMR for the baked carbon material

DDN Cost and Schedule Estimates

DDN	Ball Park Cost (\$K)	Ball Park Schedule (Years)
COMP 01-01	1500	2
COMP 01-02	1500 (SiC/SiC or CFRC)	2
COMP 01-03	500	2
COMP 01-04 (aerogel)	2000	1
COMP 01-04 (quartz)	500	1
He Environmental Testing (DDNs 01, 02, 03)	500	2
Totals	6500	2-4

Comparison of NNGNP Options Relative to DPP Reactor Unit

Plant	DPP (base)	750C NNGNP	950C NNGNP	Comments
Key Parameters: RIT/ROT, C Power, MWt Design Life, years	490/900 400 40	280/750 500 60	350/950 500 60	
Core Lateral Support Strap	CFRC/SS316	No Change	No Change	For NNGNP, need to confirm negligible fluence for longer life (no changes expected)
Upper Reflector Tie Rods	CFRC	No Change	No Change	For NNGNP, need to confirm negligible fluence for longer life (no changes expected)
SAS Channel Interface Tubes	CFRC	No Change	No Change	For NNGNP, need to confirm negligible fluence for longer life (no changes expected)
Core Outlet Connection	CFRC	No Change	No Change	For NNGNP, need to confirm negligible fluence for longer life (no changes expected)
Lower Reflector Insulation	Baked Carbon	No Change	Add Fused Quartz [TBC]	At 950C, additional insulation may be required between outlet plenum, Core Barrel bottom
Reactivity Control System Components	800H	[TBD]	[TBD]	Increased DLOFC at higher power level likely to require higher temperature/ fluence components (CFRC or SiC/SiC). Would also increase useful life of RCS components (Potential product improvement for DPP)

Comparison of NNGNP Options Relative to DPP HTS/IHX

Plant	DPP (base)	750C NNGNP	950C NNGNP	Comments
Key Parameters: RIT/ROT, C Power, MWt Design Life, years	490/900 400 40	280/750 500 60	350/950 500 60	
Hot Gas Duct (Active Cooling) Liner Inner Pressure Pipe HGD Insulation HPB Insulation	800H SA-533 (Equiv) Saffil (Al ₂ O ₃) None	No Change No Change No Change ^[1] [TBD] ^[2]	CFRC or I-617 ^[3] 316SS ^[3] No Change ^[1] [TBD] ^[2]	[1] Advanced aerogel insulation may provide efficiency advantage, particularly at higher temperatures [2] Internal HPB insulation or additional protection features may be required to mitigate transients [3] At 950C, higher RIT/ROT expected to require liner & inner pressure pipe materials changes
Hot Gas Duct (Passive Insulation) Liner HGD Insulation HPB Insulation	N/A	800H Aerogel None	CFRC or I-617 ^[3] Aerogel None	Replaces inner HGD assembly and active cooling provisions with insulation/liner on HPB. Eliminates transient issues and offers significant economic advantages. Unproven relative to present DPP active cooling approach.
IHX Internal Insulation	Not Required (No IHX)	SiO ₂ or Al ₂ O ₃ (e.g., Kaowool, Saffil, aerogel)	SiO ₂ or Al ₂ O ₃ (e.g., Kaowool, Saffil, aerogel)	Single IHX section, lower RIT in 750C NNGNP simplifies insulation design relative to 950C/2-stage IHX design. Increased incentive for advanced insulation (aerogel) at higher temperatures.